SELF-PROTECTION AND PARTNER-PROTECTION FOR NEW VEHICLES (UNECE R94 AMENDMENT)

Cyril Chauvel
Gérard Faverjon
Nicolas Bertholon
Laboratory of Accidentology, Biomechanics and Human Behavior
PEUGEOT CITROËN RENAULT,
France
Sophie Cuny
European Center of Safety Studies and Risk Analysis
CEESAR
France
Pascal Delannoy
Safran Engineering, SAFRAN Group - UTAC Passive Safety Department
France
Paper number 11.0209

ABSTRACT

This work aims at bringing evidence for mass incompatibility in frontal impact for cars built according to the UNECE R94 regulation. French national injury accidents database census for years 2005 to 2008 were used for the analysis. The heterogeneity of frontal self-protection among cars of different masses is investigated, as well as the partner protection parameter offered by these cars. The last part of the analysis deals with the estimation of the benefit, in terms of fatal and severe injuries avoided, if crashworthiness was harmonized for the whole fleet of vehicle. This calculation is done for France and is extended to all Europe.

INTRODUCTION

About 42 000 people die each year in Europe due to road traffic accidents. In France there were 2 446 fatalities in cars and 1 290 involved in car to car or car to vehicle accident. This figure represents more than half of people that die in a car collision. Our approach has been for many years to study real world accidents and try to understand what were and are the mechanisms of injury causation. Accident studies during the last twenty-five years clearly showed that car-to-car head-on collision is a major impact configuration to take into account in order to improve safety on the roads. With the new self-protection regulation, all cars offer equivalent behaviour against a fixed obstacle. Therefore, in the future, it is expected that the main progress will have to be made in car-to-car compatibility.

Over the past ten years, vehicle stiffness has been increased a lot. We also have a better understanding of the front-end design energy absorption. Front-end design is at the cross road of numerous contradictory constraints: self-protection of occupants, protection of vulnerable users such as pedestrians, reparability, styling, aerodynamics, engine cooling and so on. Therefore, each manufacturer has developed its own solution to solve the difficult equation that resulted in a wide variety of front-end designs, structure and stiffness regardless of the overall mass of the vehicle. Solutions however have been optimized for meeting R94 regulation but not in car-to-car configuration.

This work aims at bringing evidence of the impact of UNECE R94 regulation on car designs and the need to amend and improve it to answer new compatibility requirements. The heterogeneity of frontal self-protection level among cars of different masses is investigated, as well as the partner protection parameter offered by these cars. The last part of the analysis deals with the estimation of the benefit, in terms of fatal and severe injuries avoided, if crashworthiness test severity was harmonized for the whole fleet of vehicle. The calculation is based on French accident data and is extended to all Europe.

RELEVEVANCE OF THE FRONTAL IMPACT IN THE FRENCH NATIONAL STATISTICS

The relative magnitude of frontal impacted car is revealed through the French national statistics of road accidents (BAAC database - year 2007). Figure 1 describes the proportion of accident types for fatally injured car occupants. Single vehicle crashes and car-to-car accidents represent the most important part of the accident types (respectively 47% and 30%)

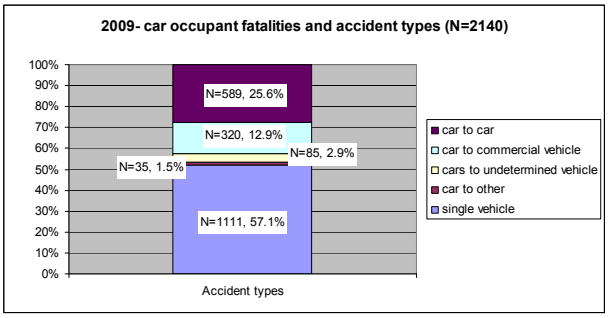

Figure 1. Car occupant fatalities and accident types.

Figure 2 has a look on the main impact for single vehicle crashes and car to other vehicle accidents. It is noticeable that frontal impact is not of the same importance for single vehicle crashes and for car-to-car accidents. Frontal impact in car to vehicle accidents represents 32.2% of all the car occupant fatalities, whereas single vehicle frontal impact stands for 15.3% of these fatalities.

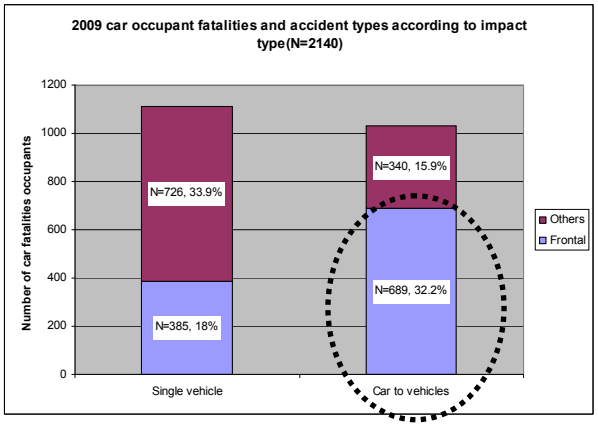

Figure 2. Car occupant fatalities and accident type according to impact types.

The 32.2% fatalities occurring in frontal impact enlightens the accidentological importance of this configuration.

METHOD AND DATA SOURCES

Definition of self-protection, partner protection and severity rate.

Compatibility can be described as the capacity of two vehicles to distribute in a balanced way the energy (proportionally to its mass) of an impact to offer to their occupants the same chances of survival. In this study, it will be evaluated as the proportion of fatal and serious injuries observed in the considered car model (internal injuries) and called Severity Rate (SR) Compatibility mixes two features: self-protection (SP) and partner protection (PP). Self-protection or crashworthiness is the capacity offered by a car to protect its own occupants (1).

$$SR(protection) = \frac{(Fatalities + Severe_injuries)_{int}}{(Fatalities + Severe_inj + Slight_inj + Not_inj)_{int}} \quad (1).$$

On the other side, partner protection or aggressivity characterizes the propensity of a vehicle to create or not injuries in the vehicle it impacts. In this survey, it will be evaluated as the proportion of fatal and serious injuries observed in the impacted vehicle by the considered car model (external injuries) (2).

$$SR(partner) = \frac{(Fatalities + Severe_injuries)_{ext}}{(Fatalities + Severe_inj + Slight_inj + Not_inj)_{ext}} \quad (2).$$

Safety benefits calculation.

The benefit of having an homogenous fleet in term of frontal protection is estimated by calculating the reduction number of fatal and severe injuries expected if all cars come up with the severity rate of the most crashworthy vehicle in frontal impact.

One might expect that introducing the Progressive Deformable Barrier (PDB) within the test of frontal impact regulation will harmonize the severity of the impact, whatever the mass of the vehicle. This harmonization should lead to an hamonization of the frontal impact protection offered by the new vehicle, whaterver their massses. This hypothesis will support the safety benefit estimation of the introduction of the PDB in the frontal test regulation. If frontal protection is set at the same level among all vehicles of different mass, the result should be observed in accidents : under this assumption, severity rates for car occupants are expected to be identical among all classes of vehicle masses.

At first, a target population is choosen to represent the level of frontal protection to be reached by all vehicle. The class of vehicle performing best in frontal impact is determined on the basis of accidental data as the group of vehicle for whom the severity rate is the lower one in frontal impact. This severity rate is set to be the objective to achieve an harmonization in term of frontal protection among all vehicle. Once the target severity rate is defined, it is applied on the effective of the other classes of vehicle. A new number of severe and fatal injuries is then calculated for each class of vehicle under the asumption that all vehicles have the same severity rate. The difference betwwen the observed number of severe and fatal injuries and the number expected under the hypothesis of identical frontal protection represents the estimated number of casualties that could be avoided in case of harmonised frontal protection. This number is then

extrapolated to the whole number of severe and fatal injuries for car passengers occuring in France.

Data sources and cases selection

National data base French national injury accidents database census (BAAC - Bulletin d'Analyse d'Accident Corporel) for years 2005 to 2008 has been used for the analysis. This is an disaggregated database which records only accidents with at least one injuries involved into the accident. Injury severity is assigned as follow : fatal injuries are considered up to 30 days after the accident, injuries are classified as serious injuries if the occupants stay more than 24 hours at the hospital, and slight injuries if they stay then 24 hours in the hospital. Uninjured occupants involved in an accident making at least one injuries also have to be recorded in the database. The national census also describes the circumstances of each accident through a series of descriptive variables.

Cars designed according to UNECE 94 regulation were selected in the database. Cars have been considered in compliance with this regulation if they have been designed since the year 2000 or if they were registered since 2004. Among these new cars, only those with a frontal impact against another car were taken into account. Accident involving high goods vehicle, pedestrian or two wheelers were excluded from the analysis as the frontal impact severity for the car could be either to high or to low in these configuration. Single vehicle crashes were also not analysed there. Belted driver and belted front right passenger cars were included in the sample. As the analysis deals with protection, it requires that restraint status of the occupants is comparable and optimal, so no unrestraint occupant, nor rear seat passenger were used for this study (and no child occupants). Cars were selected if their mass could have been identified and classified among 6 classes, defined as follows : [<950], [950-1149], [1150-1349], [1350-1549], [1550-1749], [>1750].

The Polk database It contains data regarding the european fleet. Number of vehicles per mark, model and year of registration are avalaible for 23 out of the 27 of the European Community (Bulgaria, Romania, Malta, Cyprus are missing). The database has been implemented with information regarding the compliance of the models with the ECE R94 regulation, and with the mass of the models. The mass distribution of the vehicles among the European fleet is then readily available to be compared with the repartition among the French fleet. Data on the year 2007 is used for the analysis.

RESULT

Sample description

In the national census year 2005-2008, 2 871 belted front occupant of cars designed according ECE R94 were identified (figure 3). The selected cases are frontal impact type against another car.

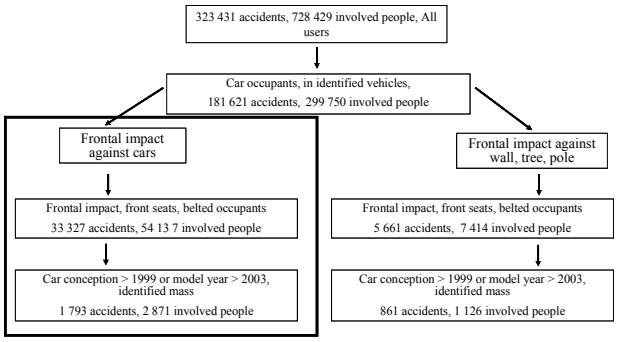

Figure 3. Selection process of the sample.

Table 1 below describes the vehicle mass distribution and the main segment associated with the mass.

Table 1.
Vehicle mass distribution.

Mean mass of the vehicle	Segment	Nb of occupant
<950 kg	Super mini	97
950-1149 kg	Super mini et Small family cars	839
1150-1349 kg	Small et Large family cars	1026
1350-1549 kg	Large family cars et executive cars	638
1550-1749 kg	Large family cars, executive cars, Small et large MPV	170
1750 kg and more	Large MPV, off road cars	101
Total		2871

Heterogeneity of frontal self-protection among cars of different masses

Figure 4 shows the severity rates for belted frontal car occupants having a frontal impact against another car. Confidence intervals at the 95% level are also reported on the graph. Both cars in the selected accidents have been designed according to ECE R94 regulation. The figures show that severity rates decrease as weight of the cars increase.

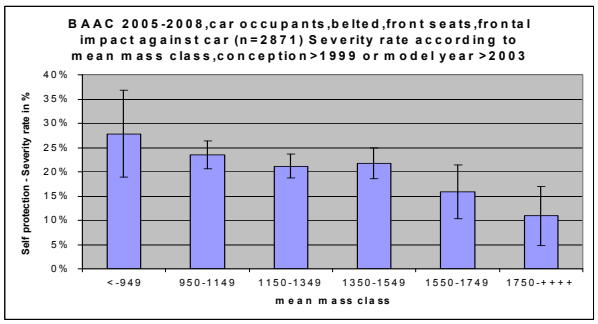

Figure 4. Severity rate in frontal impact according to the mass of the vehicle. Vehicle designed since 2000 or registered since 2004.

Cars weighting more than 1750 kg display the lowest severity rate for their front occupant, whereas light cars weighting les than 950 kg present the highest severity rate. Confidence intervals allow to assess that severity rate for front occupants is statistically better for car weighting 1750kg and over compared to cars of the following categories : less than 950kg, 950-1149 kg, 1150-1349 kg and 1350-1549kg. This illustrates a discrepancy between frontal protections offered by cars of different masses.

Partner protection parameter offered by these cars. Self-Protection vs. Partner-Protection.

In taking into account injuries caused in the opposite vehicle hit by the studied vehicle, the notion of partner is introduced. A focus is made on how frontal protection varies with the mass of the focus vehicle. Head on collisions are selected from the initial sample of 2 871 front occupant of new cars. The sample related to partner protection ends up with 1 875 belted front occupant involved in an head collision, both cars being in compliance with ECE R94 regulation.

Table 2.
Vehicle mass distribution. Head on collision.

Mean mass of the vehicle	Segment	Nb of occupant
<950 kg	Super mini	70
950-1149 kg	Super mini et Small family cars	561
1150-1349 kg	Small et Large family cars	659
1350-1549 kg	Large family cars et executive cars	419
1550-1749 kg	Large family cars, executive cars, Small et large MPV	110
1750 kg et plus	Large MPV, off road cars	56
Total		1875

The distribution of the mass in this sub sample is presented in the table 2.
Severity rate for self and partner are calculated as noted in equation 1 and 2, according to the mass of the focus vehicle and presented in figure 5 below.

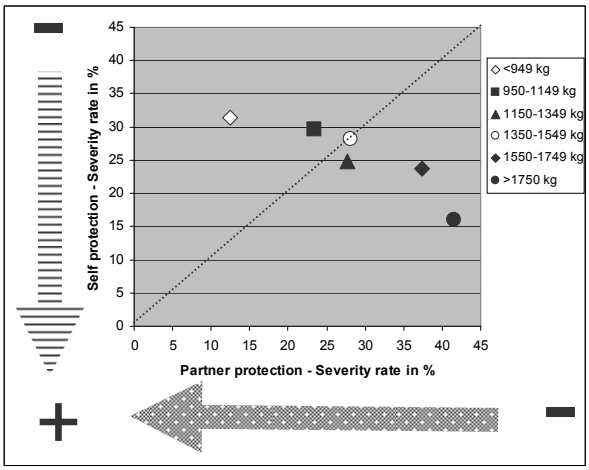

Figure 5. Self-Protection and Partner Protection according to the mass of the vehicle Vehicles designed since 2000 or registered since 2004.

Figure 5 enlightens heterogeneity in partner protection bring by vehicles designed according ECE R94 regulation. The line on the graph represents cases for which self-protection and partner protection are identical. Vehicles ranging from 950 to 1549 kg are relatively close to this configuration. Heaviest vehicles (above 1550 kg) show high level of crashworthiness and weak performance regarding partner protection, whereas vehicles under 950 kg present a smaller self-protection level associated with a small percentage of casualties in the opposite car.

UNECE R94 AMENDMENT PRESENTATION

According to figure 4 and figure 5 the present demand on self-protection is increasing the local strength and global force deformation of all cars and conducts to an inhomogeneous fleet.
The design of a large car makes it stiffer than a small one in order to compensate the mass. Furthermore, the current frontal offset test is more severe for heavy vehicles because of the specific barrier used.

With self-protection offset test regulations and ratings, all cars offer equivalent behaviour against a rigid obstacle. Solutions have been optimized against a rigid wall or soft obstacle but not in car-to-car configuration, accident data shows clearly this lack of consideration.

Problem raised with the current regulation R94

Current ODB barrier was developed fifteen years ago and adapted to car designs (geometry and force

deformation) from 90's. Since then, introduction of regulation, ratings, insurance test and recently pedestrian have modified a lot car front design in terms of stiffness and geometry to achieve that requirements. The current barrier is becoming more and more obsolete regarding to new generations of vehicles.

Instability and bottoming out of the barrier

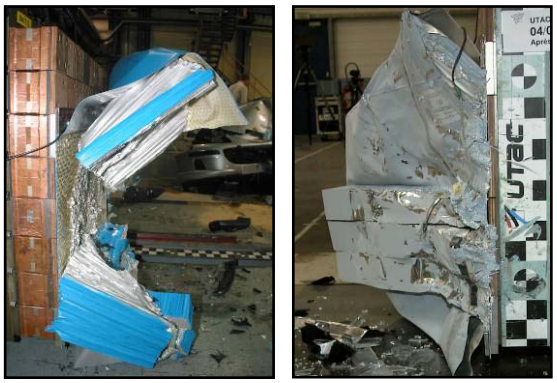

Figure 6. Current ODB barrier instability and bottoming out.

Since this time, vehicles were reinforced and became stiffer. The stiffer front end leads to unstable behavior of the barrier that creates serious problems in the design of vehicles. Today, all vehicles bottoms out the barrier (figure 6) that leads same amount of energy absorbed by the barrier. Usually this is achieved through different load paths, which absorb energy and transmit the load from the front to the occupant compartment.

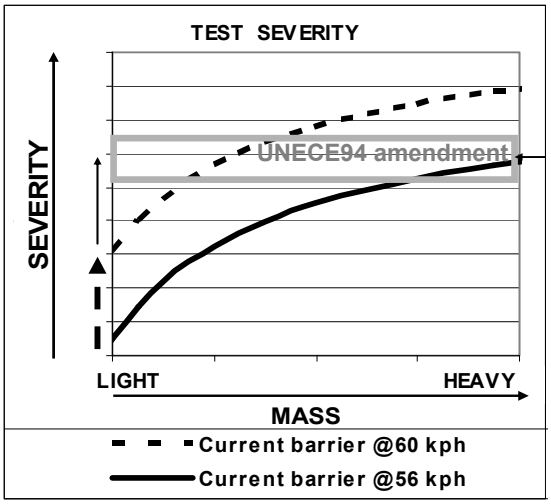

Figure 7. Theoretical Test severity depends on the vehicle mass. Need to harmonize this phenomenon with introduction of new barrier.

These load paths are designed and tuned against two types of obstacles: full width rigid barrier or soft deformable barrier. This means that the front-end design is not controlled by the barrier stiffness because the structure collapses with the help of the rigid wall behind the barrier. In all cases, the obstacle is far from representing a car front unit. That is why structural behaviour in car-to-car accidents is different. So in order to reach the same level of self-protection, design against deformable barrier with bottoming out heavy cars is designed stiffer (figures 7 and 8). The result is that heavy cars cannot be made compatible, in term of stiffness, with small ones.

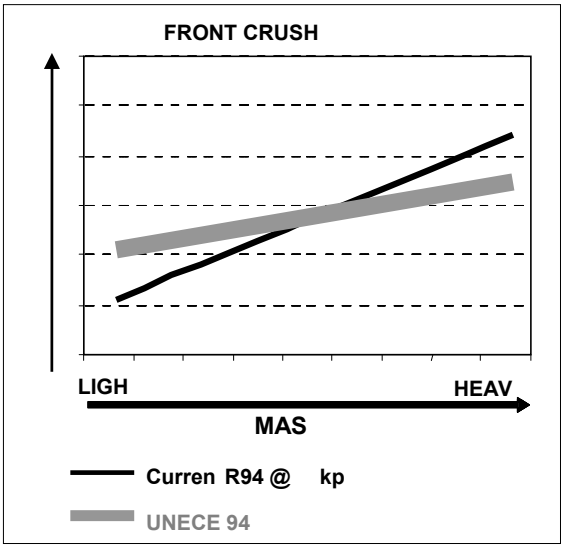

Figure 8. Front end force more homogenous among different vehicle mass with UNECE 94 amendment

The energy absorbed by the barrier does not depend on the vehicle mass. Severity for the vehicle structure rises up with the mass. Figure 8 clearly shows this unequal energy distribution. The fraction of energy absorbed in the barrier is roughly the same regardless of the car mass resulting in a higher fraction of energy to be absorbed by the large vehicle than by the small one. For a light car, energy in the barrier represents 40% of the total kinetic energy but only 10% for a heavy one (figure 9).

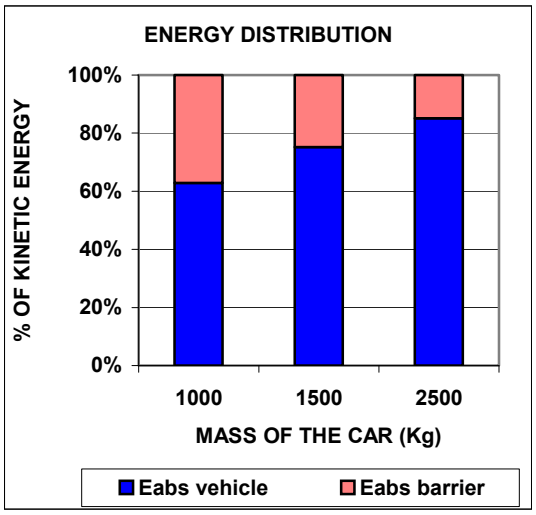

Figure 9. Severity situation with current barrier, percentages of kinetic energy absorbed.

UNECE R94 test procedure

Moreover, it is yet required to improve light cars compartment's strength without increasing heavy cars' one and to limit vehicle front units' aggressiveness. In other words, it is necessary to assess the possibility to check and improve partner protection with regards to self-protection. To achieve this new requirement, an amendment of UNECE R94 test procedure was proposed in 2007, based on PDB barrier, in order to check both parts of compatibility (structural interactions -partner- and compartment strength -self).

Details of the procedure are fully explained in document ECE/TRANS/WP.29/GRSP/2007/17 published at May 2007 GRSP. Test configuration is not so far from current regulation but some essential changes must be included.

- Test speed: 60 km/h
- Overlap: 50 %
- Barrier: PDB

Figure 10. PDB test configuration (UNECE 94 amendment).

Compatibility is a mix between self-protection and partner protection and cannot be separate for investigation because both act simultaneously.
Compartment strength is an answer for the first one, homogeneous front end is an answer for the second to improve structural interaction.

Barrier used

It is a progressive increase in stiffness in the depth, and two height dependant stiffness's, which contribute to its name: PDB as Progressive Deformable Barrier. Its dimensions and stiffness make the bottoming-out phenomenon very unlikely.

New test speed

To answer the question of improving compartment strength of the light car, it was necessary to increase the test speed to reach compartment deformation. 60 km/h seams reasonable.

Self-protection

Car design for frontal crash must limit passenger compartment intrusion and generate acceptable deceleration from the occupant point of view. Higher acceleration pulse combine with higher intrusion level allows getting closer to real life accident where both parameters are responsible for fatal injuries and injured.
Compartment intrusion was shown as the most important parameters in car-to-car head on collision, so this parameter must be put under control. This parameter is directly linked to the force generated by the compartment. A harmonisation among fleet masses is possible (figure 9 grey line).

Partner protection

UNECE R94 amendment protocol allows checking also partner protection. In addition to test all vehicles at a more or less constant equivalent energy speed (EES), the barrier used (PDB) gives the ability to check the front unit aggressiveness.

The current barrier deformation does not contribute to improve partner protection. No chance to detect front unit homogeneity, all vehicle deformations are completely flat smoothed by the rigid wall (figure 11).

Figure 11. Front deformation against current ODB barrier.

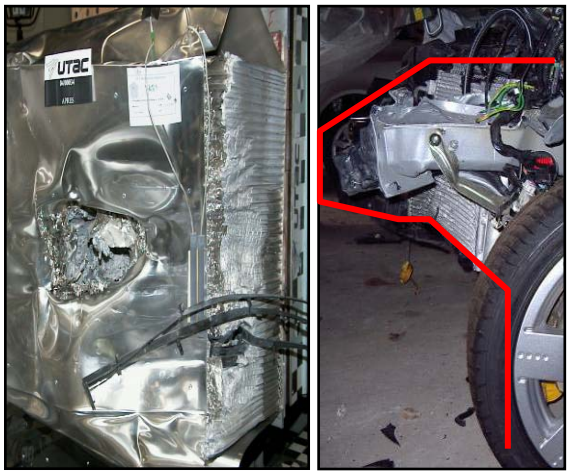

Figure 12. Front deformation of same car against PDB barrier.

Barrier analysis

The UNECE R94 procedure puts under control the energy absorbed by vehicle, the barrier is supposed to represent the vehicle we want to protect.

Inhomogeneous front-end example Stiff longitudinal with weak crossbeam penetrates the barrier. Forces are badly distributed. Cross member is not able to spread the force coming from the longitudinal. The surface in front of the load path is not in line with its stiffness. Deformation is inhomogeneous (figure 13).

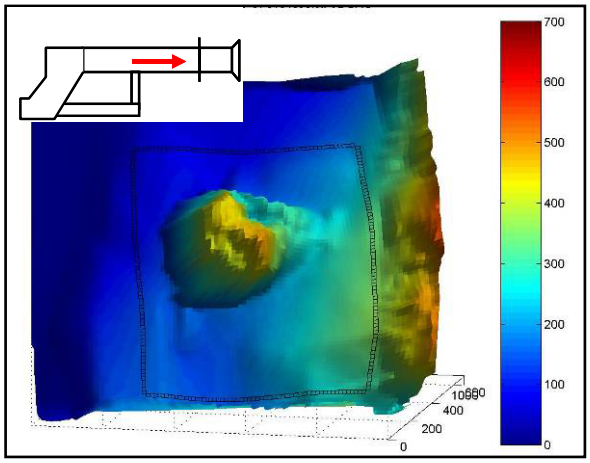

Figure 13. PDB deformation corresponding to inhomogeneous front end.

Homogeneous front-end example High forces generated by longitudinal and subframe is well distributed on a large surface. No over crushed between upper and lower load paths. Deformation is homogeneous (figure 14).

The PDB barrier is able to detect local stiffness but also transversal and horizontal links among load paths. The barrier records front cross member, lower cradle subframe, pendants linking position and stiffness that improve vehicles compatibility.

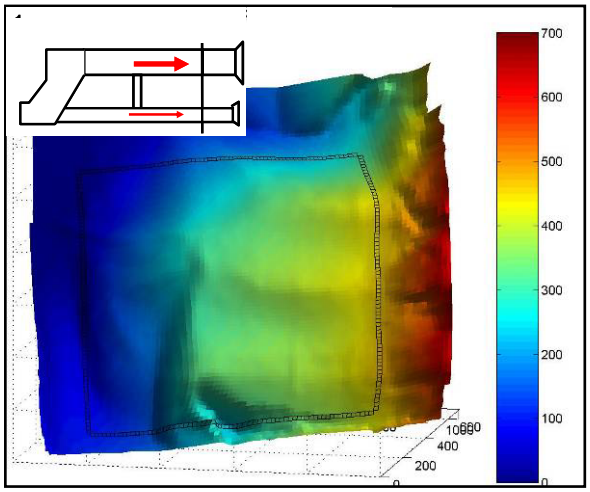

Figure 14. PDB deformation corresponding to homogeneous front end.

Conclusion of the UNECE R94 introduction

Harmonisation of offset test severity is considered by several passive safety experts as the main priority, the most effective way and probably the first step towards compatibility, to change the trend of inhomogeneous fleet showed by accident data. The UNECE R94 amendment is a good opportunity to solve problems of current regulation.

This amendment is closer and more representative of real world accident and will improve the current incompatibility.

The development of future vehicles with respect to these targets would result in a compatible fleet that gives clear answers to accident data presented before.

SAFETY BENEFIT CALCULATION

Since vehicles designed according the latest regulation exhibit unequal crashworthiness and aggressivity characteristics, it is of interest to evaluate the benefit of bringing cars at the same level of frontal protection. For this evaluation, it is assumed that all cars would have the same level of frontal protection as the more crashworthy vehicles. In this case, the target population is represented by cars weighting 1750 kg and above, which show a severity rate for self-protection of 16.07%. Severity rate of belted front occupants involved in head on collision between two newly designed cars are presented in table 3. Knowing the effective of each mass class, the number of severe and fatal injuries expected under the hypothesis if equal severity rate among cars of different mass is calculated in table 3.

Table 3.

Frontal protection harmonization based on the heaviest vehicle. Severe and fatal injuries expected.

Mean mass of the vehicle	Observed SR	Target SR	Number of severe and fatal injuries expected with the target SR=16,07%
<950 kg	31,4%	16,07%	11
950-1149 kg	29,6%	16,07%	90
1150-1349 kg	24,9%	16,07%	106
1350-1549 kg	28,2%	16,07%	67
1550-1749 kg	23,6%	16,07%	18
> 1750 kg	16,07%	16,07%	9
Total	26,9%		301

If crashworthiness turns out to be identical within the all new vehicles, 301 instead of 505 severe and fatal injuries would be observed for belted front occupant of new cars in head on collision. That is a 40.3% reduction. Given that severely or fatally injured belted front occupant involved in head on collision represent 17% of the totality of the severe and fatal injuries in France, the overall safety benefit of harmonization of the frontal protection is evaluates at 7% (40.3% x 17%), as summarized in table 4.

Table 4.
Safety benefit evaluation.

	Head on collisions	All impacts
	Victims reduction on pertinent accidents (front occupant, belted, head on collision between two cars of conception > 1999 or model year > 2003)	Victims reduction extrapolated to the whole set of car occupants
Reduction in fatalities and severe injuries (SR)	40.3%	7.0%

Provided that in 2007, 18 950 car occupants have been severely injured or killed, the safety benefit of such a harmonization would lead to 1 327 avoided casualties.

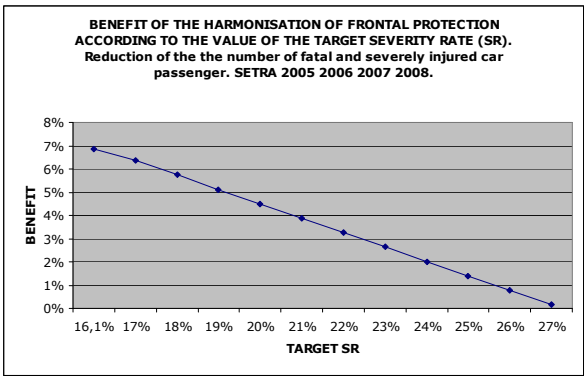

Figure 15. Benefit of the harmonization of frontal protection according to the value of the target severity rate.

If we estimate the benefit for several levels of harmonization, we obtain the figure 15. On this figure, we note that the benefit became null for a self-protection level of 27%. This figure corresponds to mass vehicle class of about 1350kg (table 3).

Extension to European data

Because regulations are done on a European level, it is crucial to obtain estimated benefice of safety measure not only for France but also for the whole Europe. As no European data on mass, year of registration or year of conception for crashed cars is available, fleet data will be analyzed. For that purpose, the Polk database which gathered information for 23 out of 27 of the European country is used. The goal is to make a link between the characteristic of the French fleet and the characteristics of the European fleet. Distributions of the mass of the vehicle among the French fleet as well as the percentage of cars in compliance with the ECE R94 regulation are available. The figures for the European fleet were obtained from the Polk data base and are presented in tables 5. Information was available for more than 95% of the vehicles.

Table 5.
Percentage of the fleet compliant with R94.

	France	Europe
Fleet designed according to R94 (%)	33.9%	35%
Fleet not designed according to R94 (%)	66.1%	65%

The figures make clear that the percentage of the fleet in compliance with ECE R94 is nearly identical in

France and in Europe: in France 33.9% of the car fleet is designed according to the latest frontal regulation whereas the percentage for Europe is estimated at 35%. If looking at the distribution of the mass within the fleet, one can say that they are quite similar for the total fleet, for car in compliance with ECE R94 regulation and also for older cars (not ECE R94 compliant).

When we have a look at the distribution of car fleets within the European countries (table 6), we can notice that five countries (France, UK, Germany, Italy and Spain) represent more than 70% of the European fleet.

Table 6.
Distribution of car fleets regarding the different countries in Europe.

Country	Number	%	Cumulative %
Germany	41,183,594	18.8%	18.8%
Italy	31,414,905	14.4%	33.2%
France	30,700,623	14.1%	47.3%
United King	30,257,323	13.8%	61.1%
Spain	21,760,174	10.0%	**71.1%**
Poland	13,393,451	6.1%	77.2%
Netherlands	7,509,649	3.4%	80.7%
Belgium	5,006,294	2.3%	82.9%
Greece	4,805,156	2.2%	85.1%
Portugal	4,379,071	2.0%	87.1%
Czech Repub	4,285,465	2.0%	89.1%
Sweden	4,249,344	1.9%	91.1%
Austria	4,245,583	1.9%	93.0%
Hungary	3,012,165	1.4%	94.4%
Finland	2,553,556	1.2%	95.5%
Denmark	2,060,418	0.9%	96.5%
Ireland	1,899,639	0.9%	97.4%
Lithuania	1,592,051	0.7%	98.1%
Slovakia	1,433,926	0.7%	98.7%
Slovenia	1,029,342	0.5%	99.2%
Latvia	869,656	0.4%	99.6%
Estonia	523,766	0.2%	99.9%
Luxembourg	321,538	0.1%	100.0%
Total	218,486,689	100.0%	

Assuming that types of crashes are nearly the same in all these countries, and as the fleet are identical in France and Europe, it is estimated that the Safety Benefit Estimation of frontal protection harmonization expected in Europe would be of the same extend of the one observed in France : 7% of avoided severe and fatal injuries.

With this assumption, the number of fatalities and severe injuries reduction in Europe is calculable. For that, the CARE database for year 2005 is used. 20 countries (missing Germany, Lithuania, Slovakia Slovenia, Latvia, Cyprus and Bulgaria) are available. It represents 95 659 fatalities and severe injuries in cars. The result will be then, after multiplication with the 7% safety benefit, of 6 696 severe and fatal car occupants injuries avoided in case of frontal protection harmonization, for these 20 countries.

LIMITS

As we may observed in many safety studies, result limitations often come from available data. Either data are in-depth data with high quality coding but not representative, either they are available at a macro level (i.e. national or international level) with lower quality but representative from a country. In our survey, we rather chose to use French national data to have a consequent sample and less dispersion for the safety benefit calculation. The Europe extension study shows again the limit of available data. In that case, it was necessary to use fleet data rather than safety data. Another limitation concerns the national data years used. Only years after 2005 were taking into account due to the count changes for severe injured and fatalities.

We observe that compatibility represents a significant stake and that the potential of improvement is important. Only a few new systems launched on the market nowadays can afford an equivalent safety potential of 7 % (level of self-protection and partner-protection align on the best mass class). However, the result depends on the severity rate target we would like to obtain. Benefit is null for intermediate class mass of vehicles.

Finally, this calculation concerns only head-on car-to-car collisions and it is also necessary to add the possible benefit for an improvement of the compatibility between car-to-light truck or car-to-heavy truck collisions.

CONCLUSION

A comprehensive accident study for frontal impact was performed to help prioritize frontal impact scenarios for casualty reduction and potential future changes to frontal impact legislation, namely Regulation 94. This study consisted of the following parts:

- quantification of associated French target populations for potential changes to frontal impact legislation;

- focus on self-protection and determination of severity proportion for different mass of vehicles;
- focus on self-protection versus partner protection;
- an example of safety benefit calculation that could be expected for France and for Europe.

According to our accident analysis, improving compatibility is a first priority to reduce the number of road accident victims. The regulation way is the most appropriate to switch towards a homogeneous fleet. The development of future vehicles with respect to these targets would result in a compatible fleet of new vehicles. Based on these remarks, the updated of the R94 regulation must include its capacity to verify the behaviour of new vehicles in regard to the partner protection targets (to be less aggressive) and one the other hand the new R94 must be more homogenous in terms of test severity for all class mass to avoid that heavy vehicles continue to be stiffer than light ones.

A new deformable element, more realistic, associated to a new test speed should be introduce. The R94 will become closer to real life accident and will solve a large part of compatibility problems. The introduction of these improvements will design new vehicles better in terms of:

- partner protection: vehicles should have an homogeneous front end and absorb a certain amount of energy before reaching self-protection force
- self-protection: vehicle should have a certain compartment crush force capacity and stability.

According to these improvements and with the amendment introduction, the estimated gains could reach 6 696 fatalities and serious injured in Europe.

REFERENCES

[1] European transport policy for 2010: time to decide. COM (2001) 370 final.

[2] Informal document No. GRSP-41-25, 41st GRSP, 7-11 May 2007,

[3] Improvement of Vehicle Crash Compatibility through the Development of Crash Test Procedures (VC-COMPAT) - Final Report, GRD2/2001/50083, 15/02/2007

[4] EEVC WG Final Report to EEVC Steering Committee, May 2007, www.eevc.org

[5] Design Considerations for a Compatibility Test Procedure, Stephen Summers, William T. Hollowell, Aloke Prasad, Society of Automotive Engineers Paper No. 2002-02B-169. March 2002,

[6] Australian Research To Support The Ihra Vehicle Compatibility Working Group, K A Seyer, C A Newland and M B Terrell, ESV 2003 Paper No: 274

[7] The Development of a Load Sensing Trolley for Frontal Off-set Testing, Marian Bosch-Rekveldt, Ton Versmissen, Cor van der Zweep. Herman Mooi, Steve McEvoy, ICRASH 2006 Paper 71

[8] NHTSA's Recent Compatibility Test Program, Stephen Summers & Aloke Prasad, 19th ESV Conference 2005, Paper No. 278

[9] Feasible steps towards improved crash compatibility, Henchen Dietmar, Schwarz Thomas, Thomas Gareth, Zobel Robert, SAE transactions ISSN 0096-736X 2004, vol. 113, nº 6 (1304 p.)

[10] ESV Washington DC 2005, P.Delannoy, T.Martin, P.Castaing

[11] UNECE 94 Amendment ECE/TRANS/WP.29/GRSP/2007/17 –

PRIORITIES FOR THE ASSESSMENT OF FRONTAL IMPACT COMPATIBILITY

Dr. Sean O'Brien
Volkswagen AG
Germany
Paper Number 11-0295

ABSTRACT

Vehicle-to-vehicle crash compatibility is a complex subject that has been extensively researched during the last 40 years. For the purposes of this paper, compatibility is defined as the optimisation of vehicle design to help minimise the number of injuries and fatalities that occur in collisions between passenger vehicles. For the evaluation of compatibility in these collisions, the criteria of self-protection and partner-protection are considered together in a measure of 'total safety'. It is also shown that separate evaluations of self-protection and partner-protection should not be used to guide regulatory policy on passenger vehicle to passenger vehicle compatibility because they are less effective at bringing about reductions in the total number of injuries and fatalities in passenger vehicle to passenger vehicle collisions.

Front-to-front passenger vehicle collisions from the German In-Depth Accident Survey (GIDAS) relational database are evaluated, and it is shown that, in a collision between two vehicles with unequal masses, the driver of the lighter vehicle typically experiences a higher risk of injury than the driver of the heavier vehicle. However, by analysing these accidents at the collision level, it is shown that the 'total safety' of front-to-front collisions between passenger vehicles in the German fleet is independent of the mass ratio of the involved vehicles. In other words, the 'total safety' of a collision between a heavier passenger vehicle and a lighter passenger vehicle is equivalent to the 'total safety' of a collision between two equally massive vehicles. It is therefore concluded that mass-dependent criteria cannot be justified as the principal evaluative measure in future regulations that aim to address compatibility in front-to-front collisions between passenger vehicles.

Structural homogeneity is analysed using collision simulations between a mid-sized passenger car and a larger Sports Utility Vehicle (SUV). Vertical and horizontal structural homogeneity are analysed separately by using homogeneous 'shields' as substitutes for the bumper crossbeam structure. The simulations show that the vertical alignment of primary structures and improved vertical homogeneity result in improved compatibility. If vertical homogeneity is achieved, horizontal homogeneity between the main load paths does not provide additional benefit and hence this should not be prioritised in a compatibility assessment. The assessment of horizontal homogeneity is only relevant for small overlap collisions outboard of the vehicles' longitudinals.

Finally, the ability of various barriers and test procedures to evaluate compatibility is discussed. It is concluded that vertical alignment may be evaluated by measuring load cell wall forces and that low speed tests may be used to improve homogeneity.

INTRODUCTION

Research on collisions between small and large passenger vehicles was well underway in the early 1970s [2], and, by 1973, it had been recognised that the compatibility of a vehicle is a product of its self-protection, which describes the functions of its design that protect its own occupants, and its partner-protection, which describes the functions of its design that protect other road users in the event of a collision [3]. By 1974, it had also been found that the outcome of a vehicle-to-vehicle collision is influenced by the vehicles' mass ratio, their force-deformation characteristics, and the architecture of the energy absorbing structures [4]. By the beginning of the 1980s, constructive measures to improve compatibility had already been proposed, including lateral connections between the longitudinals, changes to deformation force levels in the crumple zone, and increased structural support in the passenger compartment [5].

Compatibility research in Europe is currently being led by the Frontal Impact and Compatibility Assessment Research (FIMCAR) project. The FIMCAR project has the objective to "propose an assessment approach for frontal impact integrating self and partner protection" [6]. To this end, it has prioritised the evaluation of structural alignment, load spreading, energy absorption management, compartment integrity in single vehicle collisions, and restraint system capacity. The consortium has stated its intention to propose a combination of a full-width and an offset test, and it is also considering a mobile offset barrier as an alternative to the fixed mobile barrier [7].

The Japanese compatibility working group has focussed their research on mismatches in front rail height and determined that height mismatches greater than 100 mm can lead to override/underride and increase the risk of occupant injury. The working group has developed several metrics for

the evaluation of front rail height using the Full Width Rigid Barrier (FWRB) [8], which have also formed the basis of similar activities in the FIMCAR project [9].

In the USA, the Insurance Institute for Highway Safety (IIHS) is developing a test procedure to address small overlap collisions [10], and the National Highway Traffic Safety Administration (NHTSA) is investigating test procedures to address small overlap and oblique offset collisions [11]. However, neither organisation is directly addressing compatibility in these activities.

The objective of this paper is to build upon this broad base of research and identify priorities for the assessment of compatibility in the current and future vehicle fleets.

DEFINITION OF COMPATIBILITY

Many measures of passenger vehicle safety tend to focus on self-protection, and hence a particular passenger vehicle design may be considered "safe" for its own occupants even though it could theoretically pose a higher risk of injury to the occupants of a passenger vehicle that it collides with. The sole evaluation of self-protection is relevant for single vehicle collisions, but, in studies of vehicle-to-vehicle compatibility, the evaluation of partner-protection is also common. This results in the complexity of having two measures of vehicle safety, which are independent and applicable to different portions of accident environment, and hence this approach "may not be ideal from the perspective of trying to steer the vehicle fleet as a whole in the direction of optimum safety" [12, p3]. Therefore, similar to the approach taken in [12], the applicability of a 'total safety' measure of compatibility is discussed below.

The accident environment is complex, and collision characteristics such as speed, direction, and overlap all contribute to the risk of injury to a vehicle occupant. For a vehicle to be considered "safe", it does not have to provide the same level of self-protection in all collision configurations, but it should be designed to help minimise the risk of injury to its occupants across the range of likely collision events. Similarly, for a passenger vehicle to be considered compatible, it does not necessarily have to provide the same level of self-protection and partner-protection in collisions with all other passenger vehicles, but it should be designed to help minimise the risk of injury to all involved persons across the range of likely collision partners.

Based on this broad view of compatibility, the evaluation of a compatible collision or a compatible vehicle requires detailed knowledge of the entire accident environment. For example, reduced risk in an infrequent collision type could result in increased risk in another, more frequent collision configuration and hence an overall increase in the total number of injuries and fatalities. However, knowledge of the accident environment is retrospective and limited in scope. For the design of new vehicles that will operate in a future accident environment, it may therefore be impossible to accurately evaluate their compatibility using this approach.

Even without perfect knowledge of the entire accident environment, it is possible to select a frequently occurring collision configuration and use it to provide a partial evaluation of the compatibility of different vehicle designs. This approach is already used in regulations and consumer testing and is the state-of-the-art method for evaluating safety. In the discussion below, the effects of speed, overlap, etc. are hence ignored, and it is assumed that the vehicle designs are the only significant variable that affects a collision outcome. The discussion below refers to the risk of fatality, but it may also be interpreted in terms of injuries since, as described in the Abbreviated Injury Scale (AIS) in [13], the severity of an injury can be rated according to its survivability.

If, for any particular passenger vehicle, a "safe" frontal collision is considered to be one in which there is ρ risk of a fatality occurring then, for a front-to-front collision involving two identical passenger vehicles, the outcome can be considered compatible if the risk of a fatality occurring is ρ in each vehicle and hence $2\times\rho$ overall. However, for a vehicle-to-vehicle collision involving non-identical vehicles, the risks of fatality for each vehicle's occupants are likely to be different. In this case, there are two possible approaches: an evaluation at the vehicle level and an evaluation at the collision level.

If, under this premise, the evaluation is performed at the vehicle level, the outcome can only be considered equivalent to the example above if the occupants of the first vehicle and the occupants of the second vehicle each have a ρ risk of fatality. If all likely combinations of passenger vehicles are considered, the theoretical optimum for compatibility would only be achieved if all vehicles had equal self-protection and equal partner-protection In contrast, if the evaluation is performed at the collision level, the outcome can be considered equivalent to the example above if the risk of a fatality occurring is $2\times\rho$ overall. When considered across all likely combinations of passenger vehicles, this would be achieved if the combination of self-protection and partner-protection, i.e. the 'total safety', were equal.

Let us assume that one or more regulatory test procedures is defined so that all new passenger vehicles have collisions that are considered compatible when evaluated at either the vehicle level or the collision level. In either case, the risk of a fatality occurring in any front-to-front collision would be same: $2\times\rho$, and hence the total number of fatalities that would occur in the entire accident environment would also be the same. In contrast, the cost of the vehicles designed to satisfy the two possible sets of test procedures would be different, since equal 'total safety' provides for more freedom of design. Furthermore, the goal of equal self-protection and equal partner-protection may be unreasonable, since some vehicles would need to reduce their partner protection to satisfy the requirements whilst others would need to reduce their self-protection. The additional costs would also not bring about a reduction in the total number of injuries and fatalities, and hence this approach would be inappropriate for regulation. If resources are available, it would be more appropriate to apply a 'total safety' approach to passenger vehicle to passenger vehicle collisions and then use the additional resources to reduce the total risk of fatalities across all collisions to a value less than ρ.

PRIORITIES FOR COMPATIBILITY

In the previous section, it is shown that the compatibility of a vehicle design may be evaluated by measuring the 'total safety' for all occupants involved in a collision. In terms of injury risk, the important physical properties of any collision are the interface force and the structural interaction. The former dictates the deceleration and deformation of a vehicle whereas the latter dictates the efficiency with which it is deformed and hence the degree to which its structure can protect its occupants. Correspondingly, the critical physical properties of a vehicle's design are the relationship between force and deformation, which may also be referred to as its stiffness, as well as the structural geometry and mechanics of the vehicle's deformation. The mass of the vehicle also has an effect since, as described by Newton's second law of motion, for any given force, the deceleration of a vehicle is inversely proportional to its mass.

In this section, the effects of vehicle mass ratios and structural homogeneity are investigated in front-to-front collisions and evaluated according to the definition of compatibility from the previous section. Vehicle stiffness is not investigated as an independent variable in this paper, since previous studies have shown a strong relationship between vehicle stiffness and mass [14].

Vehicle mass

The effect of vehicle mass on occupant protection is a frequent topic of discussion in safety related publications. Depending on the perceptions of the author, the focus may be directed towards either the "aggressiveness" of larger, heavier passenger vehicles (for example, [15]) or the "inferior" safety of smaller, lighter passenger vehicles (for example, [16]). However, the evaluation of collisions based on risk ratios, which describe the relative risk of injury in two colliding vehicles, has also been criticised because it does not distinguish between positive and negative behaviour. For example, in [17] it is shown that the perceived 'inferior' safety of lighter vehicles may in fact be attributed to their high level of partner protection and the correspondingly low level of injuries and fatalities that occur in the vehicles with which they collide.

In Figure 1, the cumulative distribution of belted drivers is shown for front-to-front collisions between passenger vehicles. The independent variable in this figure is the mass ratio of the driver's vehicle compared to the collision partner's vehicle. For the hypothetical case of a collision between a 1500 kg vehicle and a 1200 kg vehicle, the driver of the first vehicle would be plotted with a vehicle mass ratio of 1:0.8, and the driver of the second vehicle would be plotted with a vehicle mass ratio of 1:1.25. The mass ratios are calculated from the estimated total vehicle mass, which includes the mass of the occupants and payload and hence reflects the true mass, momentum, and kinetic energy at the time of the collision.

The data are taken from the GIDAS relational database and only include matched pairs of drivers. The data are limited to cases where both vehicle masses are known, the MAIS of both drivers is known, both drivers were belted, both vehicles were manufactured between 1981 and 2005, the direction of force on both vehicles indicates a frontal impact (VDI1 = 11, 12 or 1), and the location of damage on both vehicles indicates a frontal impact (VDI2 = 1).

In Figure 1, it can be seen that 23% of all belted drivers experience front-to-front collisions where their vehicle has a mass ratio of less than 1:0.8 and, since the distribution is based on matching pairs, 23% experience a mass ratio of more than 1:1.25. However, it can also be seen that the mass ratios less than 1:0.8 account for only 13% of MAIS 2+ injuries and 7% of MAIS 3+ injuries whereas the mass ratios greater than 1:1.25 account for 33% of MAIS 2+ injuries and 42% of MAIS 3+ injuries.

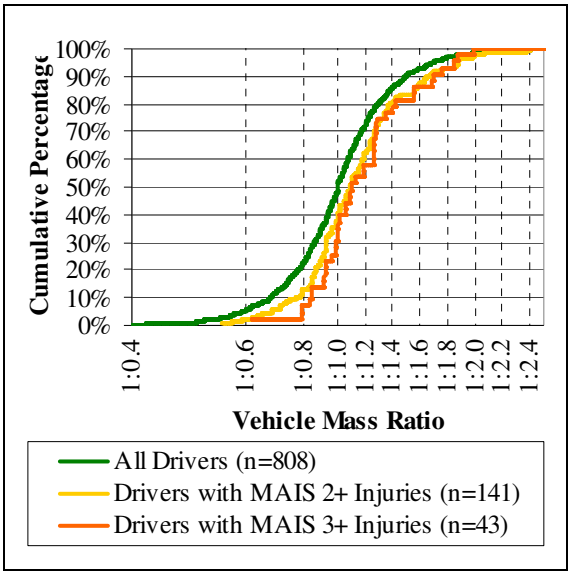

Figure 1. Vehicle mass ratio: cumulative distribution of belted passenger vehicle drivers involved in front-to-front collisions with other passenger vehicles.

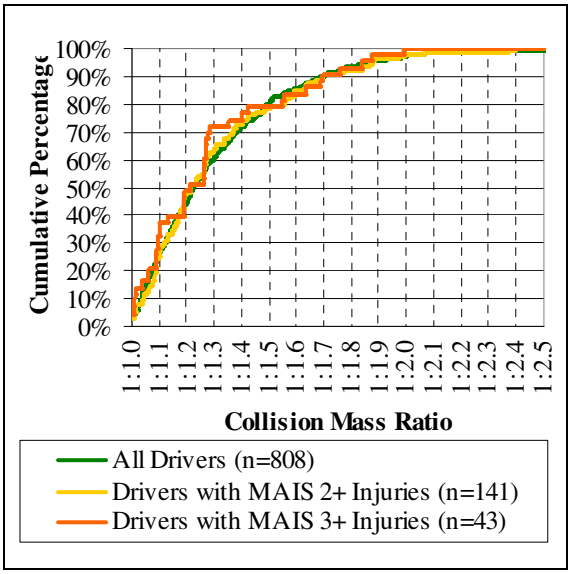

Figure 2. Collision mass ratio: cumulative distribution of belted passenger vehicle drivers involved in front-to-front collisions with other passenger vehicles.

Using a Kolmogorov-Smirnov test, it can be shown that the difference between the distribution of all drivers and the distribution of drivers with MAIS 2+ injuries is statistically significant ($p = 0.015$). This result reflects observations from numerous other accident analyses and indicates that the drivers of lighter vehicles are more frequently injured in front-to-front collisions than the drivers of heavier vehicles. However, as discussed at the beginning of this section, mass is not the only factor that influences injury risk. A higher MAIS is recorded for the driver of the heavier vehicle in 20% of the cases included in Figure 1.

The results derived from Figure 1 are interesting, but they represent a vehicle based approach to the evaluation of the collision outcomes. The definition of compatibility at the beginning of this paper promotes a collision based approach to ensure that actions are taken that maximise the benefit across the entire accident environment. By considering the data at the collision level, it is possible to determine whether collisions between vehicles with unequal masses are responsible for a disproportionately high number of injuries when compared to collisions between vehicles with equal masses. Under the null hypothesis, which is that collisions between vehicles with unequal masses are equivalent to collisions between vehicles with equal masses, it may be concluded that higher mass ratios do not represent a higher risk of injury to the community as a whole, even if, as shown in Figure 1, they represent an increased risk of injury to one of the involved individuals.

In Figure 2, the data from Figure 1 are distributed according to the collision mass ratio, which is the ratio of the lighter vehicle's mass compared to that of the heavier vehicle. Hence, for the hypothetical collision between the 1200 kg and 1500 kg vehicles discussed above, <u>both</u> of the drivers would be plotted with a collision mass ratio of 1:1.25. It is critical to note that both drivers are plotted in Figure 2 for each collision. The data could also be plotted according to the maximum MAIS for both drivers combined, but this would not reflect the fact that MAIS scale defines injuries according to their survivability and that the risk of a fatality occurring in a collision is greater when both of the drivers are injured.

The results in Figure 2 show a clear similarity between the distribution of all drivers and the distribution of drivers with MAIS 2+ injuries. However, due to the relatively small number of drivers with MAIS 3+ injuries, it is not clear whether higher collision mass ratios result in a higher, lower, or equivalent risk of injury.

The differences between the distribution of all drivers and the distribution of drivers with MAIS 2+ injuries are not significant (Kolmogorov-Smirnov test, $p = 0.801$). The lack of a significant difference cannot be taken as proof of the null hypothesis. However, the data in Figure 2 appears to support the conclusion that the total risk of injury to all occupants in a collision is independent of the relationship between the masses of the vehicles involved. Therefore, from a societal perspective, there is no justification for a mass-dependent assessment of compatibility in front-to-front collisions between passenger vehicles.

Structural homogeneity

Homogeneity can be defined by addressing the way a structure either applies forces or the way it reacts forces. A deformable honeycomb element is an example of a structure that applies forces homogeneously (i.e. it has a constant stiffness distribution), whereas a rigid wall is an example of a structure that reacts to forces homogeneously (i.e. its behaviour under loading is independent of the distribution of the forces that are applied to it). A vehicle structure that reacts homogeneously to different loading conditions is more robust, and hence this definition is used as the basis for the discussion in this section.

To investigate the effects of vertical structural homogeneity and horizontal structural homogeneity as independent variables, simulation models have been developed with homogeneous 'shields' as substitutes for the bumper crossbeam structure. The vertically homogeneous shield is designed to be rigid in the vertical direction but flexible in the horizontal direction. In contrast, the horizontally homogeneous shield is designed to be rigid in the horizontal direction and flexible in the vertical direction. Figure 3 shows the two types of shields and the way that they deform in a collision with a Full Width Deformable Barrier (FWDB).

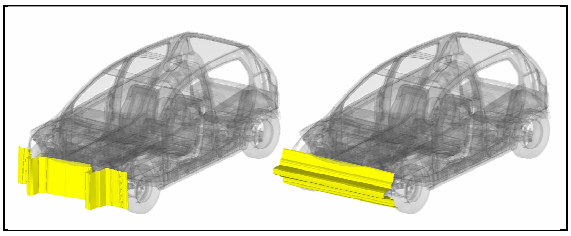

Figure 3. Typical deformation behaviour of the vertically homogeneous shield (left) and the horizontally homogeneous shield (right).

The shields are modelled using a thin mono-directional ply structure and are similar in mass to the bumper crossbeam structures that they replace. Translation and rotation of each shield is controlled within the vehicle's local coordinate system. Vertical and lateral translation is fixed, but movement in the collision direction is free. All rotations are fixed except for those about the axis parallel to the direction of homogeneity and, for the horizontally homogeneous shield, rotations about the vertical axis. The shields are 250 mm in height and are positioned to cover a zone between 330 mm and 580 mm of ground clearance.

To investigate the effects of the shields, a series of front-to-front collision simulations has been performed with models of a mid-sized passenger car and a large SUV. Severable variables have been investigated, including various overlap conditions, changes in vehicle ride height, and changes to the sizes of the homogeneous shields, and the most significant results are described below. The simulations have all been performed with a mass ratio of 1:1.9, collinear velocity vectors, and an approach speed of 112 km/h. In addition to the vertically homogeneous shields and the horizontally homogeneous shields, basis simulations have also been performed with 'inhomogeneous' models without bumper crossbeams.

The results of the simulations have been evaluated using a method described in [1], which uses measurements of compartment deformation to predict the 'total safety' for both vehicles' occupants. This method applies the collision based approach to the evaluation of compatibility that is recommended earlier in this paper. However, a weakness of this method is that it does not directly evaluate changes in the compartment deceleration, nor does it consider either vehicle's restraint system. A more detailed description of the evaluation method is not possible within the constraints of this paper, and hence the following discussion is restricted to a description of the vehicle deformations that have been most influential in the evaluation. In most cases, these differences have been measured in the passenger car, although the deformations of both vehicles have been evaluated equally.

The first significant conclusion from the simulations is that vertical homogeneity further improves the interaction between structures under dynamic loading even when initial, geometrical alignment of the structures is provided. At the nominal ride heights, the car longitudinal is lower than the SUV longitudinal, but the two structures overlap by more than 50% of their respective heights. In upper diagram in Figure 4, it can be seen that the geometrical alignment of the longitudinals results in the interaction and deformation of both structures. However, the car has a moderate degree of dive, which results in loading of the car upper longitudinal and deformation of its compartment at the upper A-pillar and instrument panel crossbeam. In the lower diagram in Figure 4, it can be seen that the addition of the vertically homogeneous shields reduces the dive of the car and the deformation of the upper longitudinal, which results in a 29% reduction in the compartment deformations in the car.

The second significant conclusion is that a horizontally homogeneous structure has limited effectiveness when the main load paths of the vehicles are not in vertical alignment. To investigate this, the SUV and its driving surface have been raised by 125 mm in the simulations. In

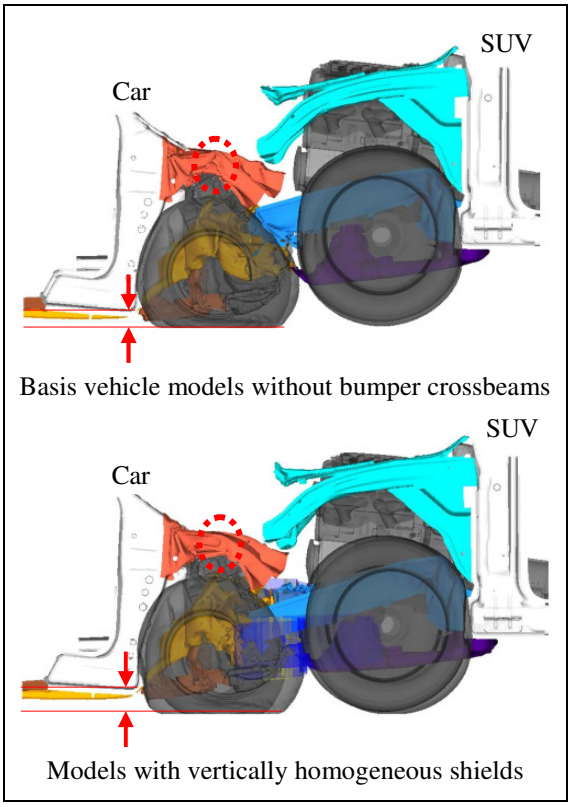

Figure 4. Front-to-front collision with 100% overlap. Side view after 70 ms.

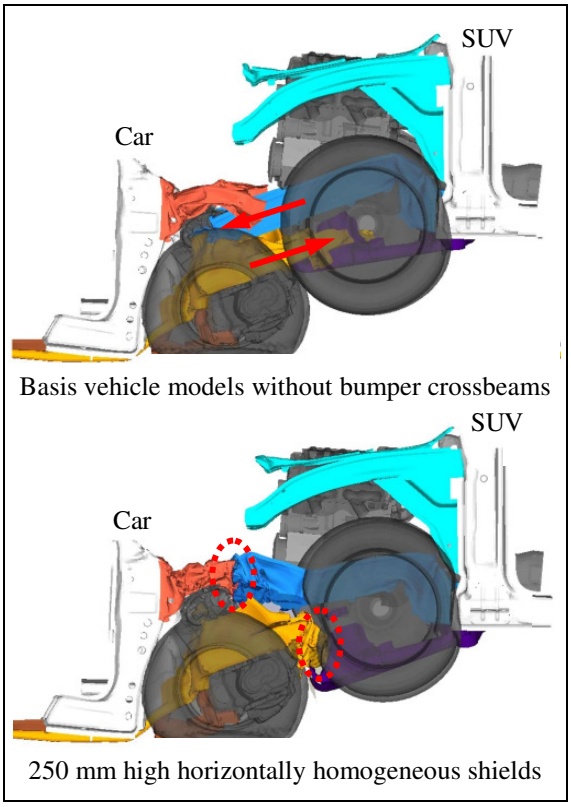

Figure 5. Front-to-front collision with 100% overlap and 125 mm raised SUV driving surface. Side view after 70 ms.

the upper diagram in Figure 5, it can be seen that the main load paths of the vehicles do not interact and they remain largely undeformed. In the lower diagram in Figure 5, it can be seen that the horizontally homogeneous shield improves the structural interaction and the primary load paths of each vehicle interact with the secondary load paths of the other vehicle. This results in a 20% reduction in the compartment deformations in the car, but override/underride still occurs, and the resulting deformations are still four times higher than those observed in the simulation with the SUV at its nominal ride height.

The third significant conclusion is that horizontal homogeneity is only marginally more effective than vertical homogeneity in partial overlap collisions. This result challenges conventional wisdom, since it is often argued that crossbeam structures are necessary to prevent the 'fork effect'. However, although the upper diagram in Figure 6 confirms that horizontal homogeneity indeed prevents the fork effect, the lower diagram in Figure 6 shows that vertical homogeneity is equally effective at achieving this goal. The vertically homogeneous shields do not increase the interaction between the primary load paths of the vehicles, which have a lateral offset, but they enable the left SUV longitudinal to interact with the engine and gearbox of the car and they also enable the left car longitudinal to interact more effectively with the engine subframe of the SUV. The compartment deformations in the car are slightly lower in the simulation with the horizontally homogeneous shields, but the effect on any occupants would be marginal.

Figure 5 and Figure 6 provide an interesting contrast, since the former shows that horizontal homogeneity is ineffective in cases of vertical offset, whereas the latter shows that vertical homogeneity is still effective in cases of lateral offset. In both cases, the loads from the primary load paths are supported by secondary load paths in the collision partner vehicle. The critical difference between these two cases is that the former still results in override/underride, which places additional loading on the passenger compartment and increases the risk of occupant injury.

The final conclusion from the collision simulations is that horizontal homogeneity is beneficial in low overlap collisions, but only if it extends beyond the width of the longitudinals. Low overlap collisions have been investigated with 33% overlap between the vehicles. In this configuration, there is no interaction between the longitudinals of the basis vehicle models. As shown in the upper diagram in Figure 7, the car longitudinal is supported by the left wheel of the SUV, which is able to support the forces necessary to deform it. In contrast, the SUV

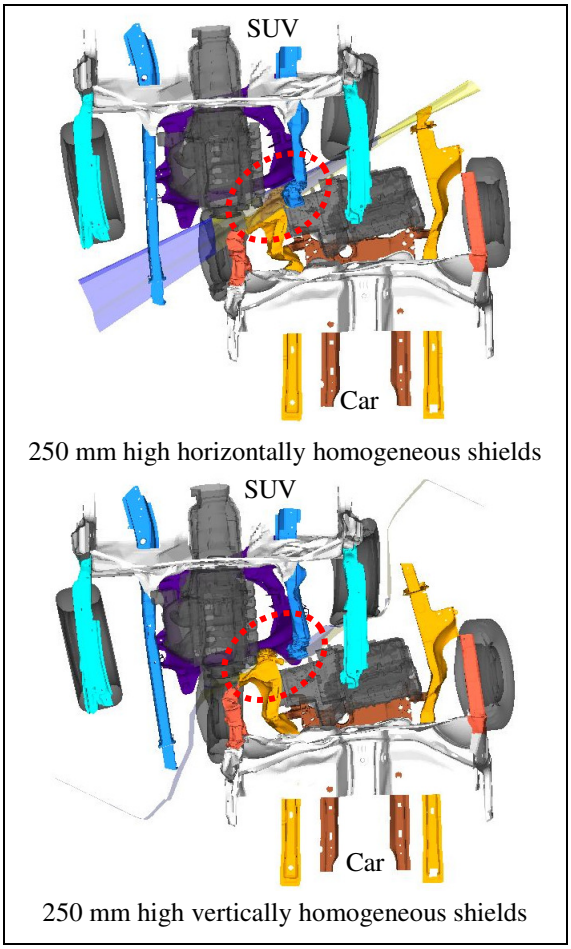

Figure 6. Front-to-front collision with 66% overlap. Modified vehicle models with. Top view after 75 ms.

longitudinal remains undeformed whilst directly loading the A-pillar of the car. With the addition of a wide, horizontally homogeneous shield, which is shown in the middle diagram in Figure 7, loads are transferred between the two vehicles' longitudinals, and they are both deformed to a greater degree. However, this is only possible because the horizontally homogeneous shields overlap. In the lower diagram in Figure 7, the shields only cover the region between each vehicle's longitudinals and hence they do not interact in a low overlap collision. The SUV longitudinal remains effectively undeformed, and although the horizontally homogeneous shield averts the direct interaction between the SUV longitudinal and the A-pillar of the car that occurred in the basis simulation, the load path including the car longitudinal and the wheel of the SUV is more heavily loaded. Due to a lack of deformation in the SUV longitudinal, the collision energy is dissipated by increased deformation in passenger compartment of the car and, to a lesser degree, the footwell of the SUV.

The first priorities for improved compatibility are hence the vertical alignment of primary structures

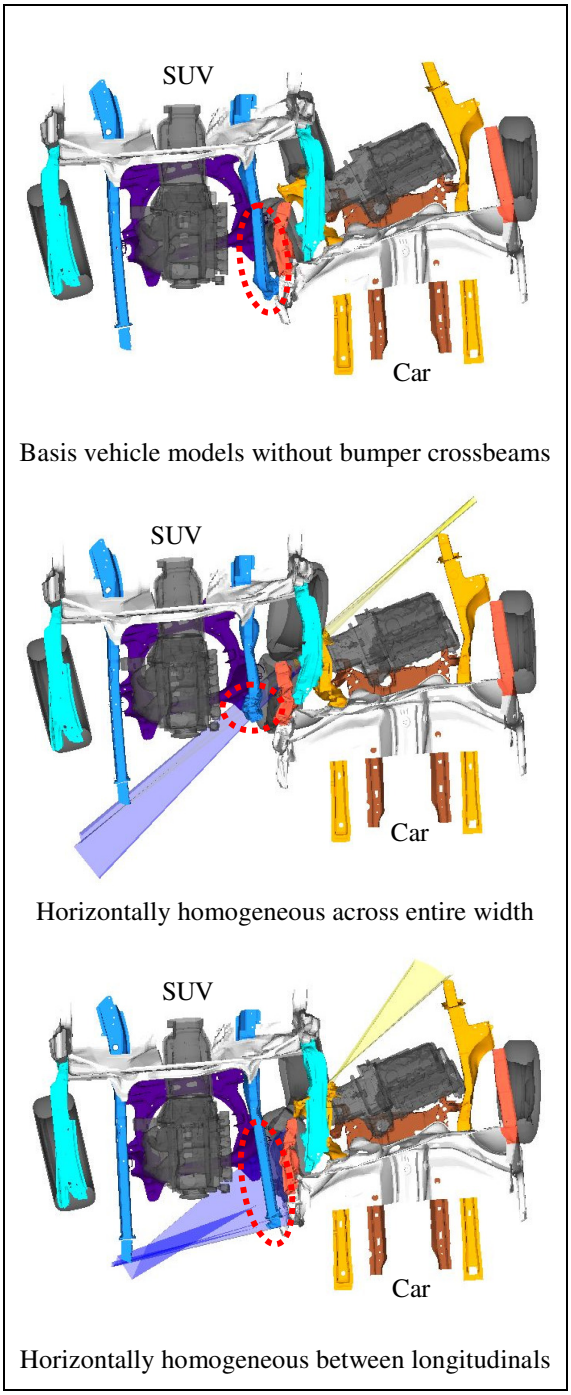

Figure 7. Front-to-front collision with 33% overlap. Top view after 85 ms.

and improved vertical homogeneity. If vertical homogeneity is achieved, horizontal homogeneity between the main load paths does not provide additional benefit and hence this should not be prioritised in a compatibility assessment. The assessment of horizontal homogeneity is only relevant for small overlap collisions outboard of the vehicles' longitudinals.

The validity of the conclusions above is limited by the underlying characteristics of the car and SUV

models, which are not inhomogeneous and have certainly influenced the outcome of the simulations. However, given that the designs of the car and SUV are typical for modern vehicles, it is reasonable to generalise the conclusions to other vehicle types.

ASSESSMENT OF COMAPTIBILITY

In the preceding sections, it is shown that the priorities for the assessment of frontal impact compatibility are vertical alignment of primary structures, improved vertical homogeneity, and improved horizontal homogeneity outboard of the longitudinals. Design characteristics related to vehicle mass and horizontal homogeneity between the longitudinals should not be prioritised for evaluation. In this section, the assessment of compatibility using various barriers and test procedures is discussed.

Offset Deformable Barrier (ODB)

The ODB is used worldwide in regulation and consumer information programs. Tests using the ODB place high demands on the vehicle structure, and the strength of the passenger compartment is a key factor in meeting the requirements [18]. The ODB is sometimes criticised for having a mass-dependent test severity, but the accident statistics in Figure 2 do not reflect any negative consequences to support this criticism.

Research has shown that load cell wall measurements from ODB tests may be inappropriate for the evaluation of vertical force distributions [19]. This was attributed to interaction between the load cell wall edge and the engine and crossbeam, but at that time the evaluation of structures was based on the peak forces measured throughout the entire impact. Recent research in Japan [8] and Europe [9] has focussed on solving similar force measurement problems with the FWRB by only assessing the initial part of the collision. Even if this were implemented for the ODB, the measured force distribution may still be affected by the transfer of shear forces within the aluminium honeycomb that makes up the barrier. However, the honeycomb used in the main block of the ODB has a stiffness of 0.34 MPa, and load spreading has typically only been observed with stiffer honeycombs such as the 1.71 MPa rear layer of the FWDB [14].

The offset nature of the test ensures that the horizontal connections between main load paths are stable, but further assessment of horizontal homogeneity does not appear feasible with the existing barrier design.

Full width barrier

Full width barrier tests are used in many vehicle regulations worldwide, but Europe is notable for having abolished the full width test when the ODB was introduced. Full width tests apply loading to both longitudinals of a vehicle, which maximises the effective stiffness of the front-end and hence places higher demands on the restraint system.

As mentioned in the introduction, research in Japan and Europe has led to the development of several metrics for the evaluation of vertical structural alignment. However, as shown in Figure 4, vertical homogeneity can further improve the interaction between structures even when initial, geometrical alignment of the structures is provided. Neither the FWRB nor the FWDB can assess the way that a vehicle structure reacts to inhomogeneous loading because they are both flat and homogeneous themselves. The FWRB is only capable of applying forces normal to the barrier face, and although the deformable element in the FWDB can induce some shear forces within the vehicle structure, the load cells behind the deformable element are unable to directly evaluate this. The situation is similar for horizontal homogeneity: the FWDB can induce shear forces in the vehicle structure and hence detect a horizontal spreading of loads, but this evaluation is only valid within the 300 mm depth of the deformable element. Once the FWDB is bottomed out, or in any test with the FWRB, no further evaluation of homogeneity is possible.

Full width tests encourage optimisation of the vehicle stiffness to minimise the severity of the pulse. For high speed collisions, it has been shown that minimal occupant loading is achieved with high initial stiffness levels in the vehicle front-end. As the collision velocity increases, so too does the stiffness level required to achieve minimal occupant loading. In contrast, at lower collision velocities, it is preferable to have lower front-end stiffness [20]. With current technology, the stiffness of a vehicle front-end cannot be modified with respect to the collision severity, and hence a compromise must be found that provides the optimum protection across all likely collision velocities. A high severity full width test that is not representative of the accident environment may have negative effects on the total number of casualties and should therefore be avoided.

Progressive Deformable Barrier (PDB)

The PDB has a deep deformable element that may be used to evaluate the stiffness distribution of a vehicle front-end. Various metrics have been

developed that evaluate the deformation of the barrier face. However, to enable an assessment of deformation, the design of the barrier compromises many other aspects of robust test design.

The PDB is larger than the ODB, which helps to avoid vehicles bottoming out the barrier. This is a fundamental design aspect, because barrier deformations cannot be used to delineate between vehicle structures once the maximum degree of barrier deformation is reached. However, the deformation of the barrier dissipates a part of the collision energy and hence reduces the quantity of energy that must be dissipated by the vehicle itself. A crash test barrier has the primary purpose of guiding the design of new vehicles, but the PDB would allow new vehicles to be designed so that more energy was deformed by the barrier and less by the vehicle itself. The bottoming out of the ODB limits the quantity of energy that can be dissipated by the barrier and hence ensures that current vehicle designs are capable of dissipating collision energy in the accident environment. The requirements of the ODB test also ensure that current vehicles deform in PDB tests. However, simulations with modified vehicles [21] and concept tests [22] have shown that a new generation of vehicles could be designed to exploit this aspect of the PDB design. The combination of FWRB and PDB tests has been suggested as a way to limit this behaviour, since the vehicle must dissipate all of its energy in the rigid barrier test. However, a full width test is less severe for the structure because the entire front-end is loaded. Furthermore, as discussed above, a high severity full width test encourages high initial stiffness levels, which would enable further exploitation of the PDB deformation.

The dissipation of energy in a crash test barrier creates a divergence between impact speed and front-end deformation. In real accidents, this may result in suboptimal performance of the vehicle structure and the restraint system. For the ODB, a test speed of 56 km/h corresponds to an Energy Equivalent Speed (EES) of 50 km/h, i.e. it represents a front-to-front collision at 50 km/h [23]. For the PDB, this EES is achieved by at a test speed of 60 km/h. The depth and stiffness of the PDB may also create a divergence between the vehicle front-end stiffness and the compartment decelerations. Even after major modifications are made to a vehicle structure or front-end package, it has been shown that the compartment decelerations observed in PDB tests remain similar [24]. As a consequence, restraint systems that are designed to perform well in a PDB test may or may not perform appropriately in real accidents.

Current proposals for the evaluation of the PDB deformation are focussed on crossbeam stiffness and the presence of lower load paths. Neither of these design characteristics is considered in this paper to be a high priority for the evaluation of compatibility.

Mobile Deformable Barrier (MDB)

A MDB has the appearance of an ideal compatibility test, but an appropriate evaluation of the results is impracticable. According to the collision based approach to the evaluation of a compatible collision, it would be inappropriate to require all vehicles to provide the same occupant protection in a MDB test. Instead, the occupant protection in the test vehicle and the hypothetical risk to the occupants of the MDB would need to be evaluated together. Pass/fail criteria would then apply to the combined score and not to the individual parts. Although this is theoretically possible, it would be extremely difficult to validate an occupant injury risk curve for a MDB with the same accuracy as is currently expected for crash test dummies.

Small overlap barrier

The IIHS is developing a small overlap barrier that directly loads the structure outboard of the vehicle longitudinals. The test configuration may be capable of improving horizontal homogeneity in this part of the structure, but the IIHS assessment is limited to dummy measures and compartment deformation [10]. The very high test severity used in the research program heavily loads the passenger compartment, but it is too severe to demonstrate the benefits of homogeneous structures that are further forward in the front-end. Ideally, new test procedures should be representative of the accident environment and encourage the design features that provide the most benefit.

The specifications of the IIHS small overlap test are, at the time of writing, not finalised, and hence a full evaluation is not possible in this paper. The potential for a lower severity small overlap test to improve horizontal homogeneity outboard of the longitudinals may warrant further investigation.

Low speed bumper tests

Low speed tests are not able to determine the behaviour of structures that only deform in high speed collisions, and they are hence often neglected in discussions of compatibility test procedures. However, the structures loaded in low speed collisions must be supported by those that are also

deformed in high speed collisions, and hence low speed tests play a significant role in determining the design of an entire vehicle. For example, the Part 581 bumper tests in the USA indirectly encourage all passenger car longitudinals to be at a similar height. Two classes of vehicles that are typically not subjected to these tests, light trucks in the USA and minicars in Japan, have been identified as having poor vertical alignment with the passenger car fleet [24]. The new RCAR bumper tests are more stringent than the Part 581 bumper tests and specifically address the dynamic performance of a vehicle and its ability to prevent override and underride. The RCAR bumper tests are therefore the only current or proposed evaluation of vertical homogeneity.

CONCLUSIONS

Priorities for the assessment of frontal impact compatibility are vertical alignment of primary structures, improved vertical homogeneity, and improved horizontal homogeneity outboard of the longitudinals. Design characteristics related to vehicle mass and horizontal homogeneity between the longitudinals should not be prioritised for evaluation. Further improvements in vehicle safety can be also be achieved by focussing on improved self-protection for all vehicles, which is applicable in all collision types.

Vertical alignment may be evaluated by measuring load cell forces in either the ODB or the full width test procedures. Other options exist, but these two tests are already established in worldwide regulations. Vertical homogeneity is currently being addressed by the RCAR bumper test, and further research is warranted to determine if alternative low speed tests can bring about improved horizontal homogeneity outboard of the vehicle longitudinals.

ACKNOWLEDGEMENTS

Much of the research described in this paper was performed within a doctoral research program that was jointly supervised by Associate Professor Sylvester Abanteriba (RMIT University) and Professor Robert Zobel (Volkswagen AG). The full results of that program are published in [1] and can be accessed from the RMIT University Library.

REFERENCES

[1] O'Brien, S. (2010), Measurement and assessment of passenger vehicle compatibility in front and side collisions, Doctoral thesis, RMIT University, Melbourne. (http://researchbank.rmit.edu.au/view/rmit:9477)

[2] Severy, D. M., Brink, H. M. & Blaisdell, D. M. (1971), Smaller vehicle versus larger vehicle collisions, in S. H. Backaitis, ed., 'Vehicle Compatibility in Automotive Crashes', Society of Automotive Engineers, Warrendale, pp. 285–335.

[3] Appel, H. (1973), Aggressivität von Fahrzeugen als Teilproblem der passiven Sicherheit, in 'Jahrestagung Fahrzeugtechnik', Stuttgart.

[4] Seiffert, U., Hamilton, J. & Boersch, F. (1974), Compatibility of traffic participants, in 'Third International Conference on Automotive Safety', Vol. 1, San Francisco.

[5] Danner, M., Appel, H. & Schimkat, H. (1980), Entwicklung kompatibler Fahrzeuge, Technical report, HUK-Verband, TU-Berlin, Volkswagenwerk AG, Wolfsburg.

[6] Johannsen, H. (2011), 'Home', Frontal Impact and Compatibility Research Consortium, Berlin. (http://www.fimcar.eu, accessed 23rd February 2011).

[7] Thomson, R. (2011), FIMCAR Priorities and Strategies for Selecting Test Procedures, in 'First FIMCAR Workshop', FIMCAR, Brussels.

[8] Yonezawa, H., Mizuno, K., Hirasawa, T., Kanoshima, H., Ichikawa, H., Yamada, S., Koga, H., Yamaguchi, A., Arai, Y. & Kikuchi, A. (2009), Summary of activities of the compatibility working group in Japan, in '21st International Technical Conference on the Enhanced Safety of Vehicles', Stuttgart.

[9] Adolph, T., & Edwards, M. (2011), FIMCAR Full Frontal Test Procedure, in 'First FIMCAR Workshop', FIMCAR, Brussels.

[10] Sherwood, C. (2011), An update on the IIHS small overlap frontal crash research program, in 'SAE Government/Industry Meeting', Washington, DC.

[11] Saunders, J. (2011), Update on NHTSA small overlap/oblique testing, in 'SAE Government/Industry Meeting', Washington, DC.

[12] Newstead, S., Watson, L. & Cameron, M. (2008), An index for total secondary safety of light passenger vehicles estimated from police reported crash data, Technical Report 273, Monash University Accident Research Centre, Clayton.

[13] Gennarelli, T. A. & Wodzin, E., eds (2005), Abbreviated Injury Scale 2005, Association

for the Advancement of Automotive Medicine (AAAM), Barrington.

[14] Edwards, M. J., Davies, H., Thompson, A. & Hobbs, A. (2003), 'Development of test procedures and performance criteria to improve compatibility in car frontal collisions', Proceedings of the Institution of Mechanical Engineers 217(4), pp. 233–245.

[15] Brieter, K. (2008), 'David gegen Goliath', ADAC Motorwelt 8/2008, pp. 22–23.

[16] IIHS (2009), 'Car size, weight and safety', Insurance Institute for Highway Safety: Status Report 44(4), pp. 1–7.

[17] Dreyer, W., Richter, B. & Zobel, R. (1981), Handling, braking, and crash compatibility aspects of small, front-wheel drive vehicles, in 'SAE Passenger Car Meeting', Society of Automotive Engineers, Dearborn, Michigan.

[18] Edwards, M. J., Hynd, D., Thompson, A., Carroll, J., & Visvikis, C. (2009), Technical Assistance and Economic Analysis in the Field of Legislation Pertinent to the Issue of Automotive Safety: Provision of information and services on the subject of the tests, procedures and benefits of the requirements for the development of legislation on Frontal Impact Protection, Client Project Report CPR 403, Transport Research Laboratory, Wockingham.

[19] Edwards, M., Benedetto, A., Castaing, P., Davies, H., Faerber, E., Fails, A., Martin, T., Schaefer, R. & Thompson, A. (2002), A study to improve the crash compatibility between cars in frontal impact, Technical Report Contract Reference: E3-3 B2702/SI2.318663/2001 TRL, European Commission Directorate-General for Energy and Transport, Brussels.

[20] Witteman, W. (1999), Improved vehicle crashworthiness design by control of the energy absorption for different collision situations, Doctoral thesis, Eindhoven University, The Netherlands.

[21] O'Brien, S., Zobel, R. & Schwarz, T. (2007), Assessment of compatibility for both self- and partner-protection, in 'VDI Fahrzeug- und Verkehrstechnik Tagung Innovativer Kfz-Insassen und Partnerschutz', Berlin.

[22] Lorenz, B. (2008), Mobile progressive deformable barrier and mobile rigid barrier tests – MPDB and MRB, in 'Minutes of 3rd meeting of the Informal Group on Frontal Impact – 9th December 2008', Document FI-03-10, UN-ECE Working Party on Passive Safety, Paris.

[23] Lowne, R. W. (1994), EEVC working group 11 report on the development of a front impact test procedure, in '14th International Technical Conference on the Enhanced Safety of Vehicles', Munich.

[24] VDA (2008), Detailed discussion of the VDA position on the proposal for draft amendments to UN-ECE R94, in 'Minutes of 3rd meeting of the Informal Group on Frontal Impact – 9th December 2008', Document FI-03-09, UN-ECE Working Party on Passive Safety, Paris.

FIMCAR – FRONTAL IMPACT AND COMPATIBILITY ASSESSMENT RESEARCH: STRATEGY AND FIRST RESULTS FOR FUTURE FRONTAL IMPACT ASSESSMENT

Heiko Johannsen
Technische Universität Berlin
Thorsten Adolph
Bundesanstalt für Straßenwesen
Germany
Robert Thomson
VTI
Sweden
Mervyn Edwards
TRL
United Kingdom
Ignacio Lázaro
APPLUS IDIADA
Spain
Ton Versmissen
TNO
The Netherlands
Paper Number 11-0286

ABSTRACT

For the assessment of vehicle safety in frontal collisions, the crash compatibility between the colliding vehicles is crucial. Compatibility compromises both the self protection and the partner protection properties of vehicles.

For the accident data analysis, the CCIS (GB) and GIDAS (DE) in-depth data bases were used. Selection criteria were frontal car accidents with car in compliance with ECE R94. For this study belted adult occupants in the front seats sustaining MAIS 2+ injuries were studied. Following this analysis FIMCAR concluded that the following compatibility issues are relevant:

- Poor structural interaction (especially low overlap and over/underriding)
- Compartment strength
- Frontal force mismatch with lower priority than poor structural interaction

In addition injuries arising from the acceleration loading of the occupant are present in a significant portion of frontal crashes.

Based on the findings of the accident analysis the aims that shall be addressed by the proposed assessment approach were defined and priorities were allocated to them. The aims and priorities shall help to decide on suitable test procedures and appropriate metrics. In general it is anticipated that a full overlap and off-set test procedure is the most appropriate set of tests to assess a vehicle's frontal impact self and partner protection.

INTRODUCTION

For the assessment of vehicle safety in frontal collisions, the crash compatibility between the colliding vehicles is crucial. Compatibility compromises both the self protection and the partner protection properties of vehicles. Although compatibility has received worldwide attention for many years, no final assessment approach has been defined. FIMCAR (Frontal Impact and Compatibility Assessment Research) is a research project started in October 2009 to address compatibility test procedures and is co-funded by the European Commission within the 7th Framework Programme. The aim of the project is to answer the remaining open questions identified in earlier projects (such as understanding the advantages and disadvantages of force based metrics and barrier deformation based metrics, confirmation of specific compatibility issues like structural interaction, investigation of force matching) and to finalise the test procedures required to assess compatibility. Within the project the research activities focus on car-to-car frontal impact accidents. However, other configurations such as lateral impact, car-to-HGV accidents etc. will be considered to ensure that changes made to cars to improve their compatibility in frontal impacts are not detrimental for other impact types. The FIMCAR project is harmonising its activities with the GRSP informal group on frontal impact

and cooperating with EUCAR to address relevant stakeholders.

ACCIDENT ANALYSIS

Over the past twelve years, since the introduction of the European frontal impact legislation and Euro NCAP, the frontal impact crashworthiness of cars has improved significantly.

The objectives of the accident analysis were:

- To determine if compatibility issues identified in previous studies [1, 2] are still relevant in the current vehicle fleet.
    - structural interaction
    - frontal force matching
    - compartment strength (in particular for light cars)
- To determine the current nature of occupant injuries and injury mechanisms

The analysis was performed in two parts. Firstly, an overall analysis was performed, using data that could be analysed statistically, to investigate compartment strength issues, occupant injury patterns and injury mechanisms. Secondly, a detailed case analysis was performed, using all data available including photographic evidence, to investigate structural interaction and frontal force / compartment strength matching issues.

To ensure that the results of the work were relevant to the current fleet only cars which were compliant with UNECE R94 or had an equivalent safety level (i.e. new cars) were selected for the analysis.

Data Sample

The accident data bases used for this study were:

- UK Cooperative Crash Injury Study (CCIS)
- German In-Depth Accident Survey (GIDAS)

The following criteria were used to select the data samples used in this study:

- Car involved in significant frontal impact
- UNECE Regulation 94 compliant or equivalent safety level.
- Front seat adult occupants (i.e. over 12 years old).

The resulting data sample sizes are shown (Table 1). The reason that CCIS had more cases of interest than GIDAS is that CCIS uses a stratified accident sampling procedure which favours accidents in which there were fatal or serious injuries. The GIDAS sampling procedure is designed to produce a sample representative of the national data. Also, it should be noted that for an accident to be included in the CCIS study a newer car (not older than 7 years at the time of the accident) must have been involved. The result of this is that the CCIS data sample does not represent the national data precisely. The main bias is that older occupants are over-represented slightly.

Table 1.
Number of occupants in CCIS and GIDAS data samples

Database	Fatal	MAIS2+ Survived	MAIS 1
CCIS	83	466	1236
GIDAS	16	155	701

The following additional criteria were used to refine the data sample for the majority of the analyses:

- Occupant belted
- Occupant sustained a MAIS 2+ injury

Overall Analysis

The overall characteristics of the data sets were investigated. The key finding from this work, for both CCIS and GIDAS data sets, was that there was a high proportion of fatal and MAIS 2+survived injuries in accidents with high overlap, i.e. >75% (Figure 1).

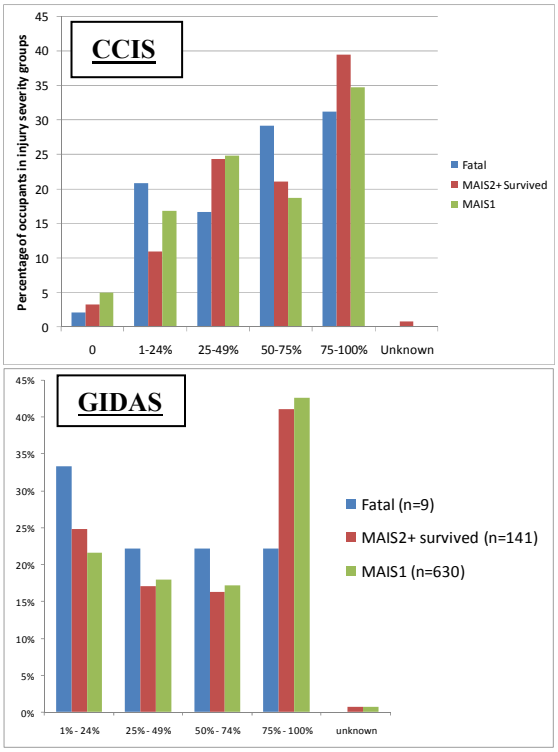

Figure 1. Injury distribution by overlap for belted occupants (Note: in CCIS narrow object impacts (poles and trees) are included in the '0' category whereas in GIDAS they are included in the '1-24%' category)**.**

For the GIDAS data there is a higher proportion of fatal and MAIS 2+ survived injuries for low

overlap impacts (1-24%). However, the overlap definition in GIDAS refers to the amount of direct contact on the vehicle front, regardless of location. Thus many of the cases in the low overlap (1-24%) category are impacts with narrow objects such as trees. These impacts could be at the centre of the car.

Injury mechanisms and patterns were examined to investigate compartment strength issues. In both CCIS and GIDAS the accident investigators attribute each injury a causation code. For example, an occurrence of multiple rib fractures may be attributed a code relating to the seat belt, whilst a fracture to the tibia or fibula may be attributed to contact with the facia. For this investigation the causation codes were grouped into the six categories below:

- 'Restraint': relating to seatbelts and airbags, mainly caused by acceleration loading
- 'Contact no intrusion': relating to contact with an interior component of the occupant compartment with investigators determined had not intruded.
- 'Contact with intrusion': as above but the structure contacted has intruded.
- 'Non-contact': for injuries where no contact with any component was made, e.g. whiplash.
- 'Other object': relating to contact with another object inside or outside the vehicle such as unrestrained loads or an external object such as a tree.
- 'Unknown': cause could not be determined.

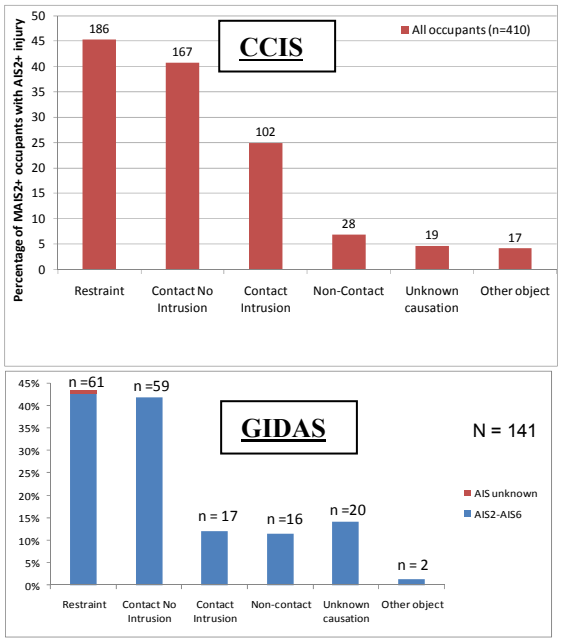

Figure 2. Percentage of belted MAIS 2+ injured occupants with AIS 2+ injury attributed to injury causation category.

The percentage of belted MAIS 2+ injured occupants who had an AIS 2+ associated with each of the categories above was determined (Figure 2). The proportion of occupants with injuries categorised as 'contact with intrusion' can be used to give an indication of the size of the compartment strength problems because reduction of the intrusion would likely help mitigate these injuries. The percentage of MAIS 2+ occupants who had an AIS 2+ injury caused by 'contact with intrusion' was 25% for CCIS and 12% for GIDAS. Note: for CCIS this reduces to 16% if intrusion of less than 10 cm is classified as 'no intrusion'.

Further analysis was performed with the CCIS data to investigate the cause of the most severe injury received by the occupant, see Figure 3. This showed that for 22% of occupants, the most severe injury was attributed to 'contact with intrusion'. When this is compared with the 25% above it can be concluded that in the majority of cases when an occupant receives an AIS 2+ injury related to 'contact with intrusion' it is the most severe injury.

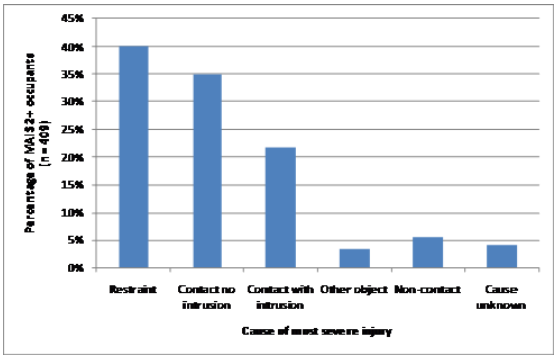

Figure 3. Cause of most severe injury for belted MAIS 2+ occupants in CCIS data set (Note: a small number of occupants are counted twice as they have two most severe injuries by more than one cause).

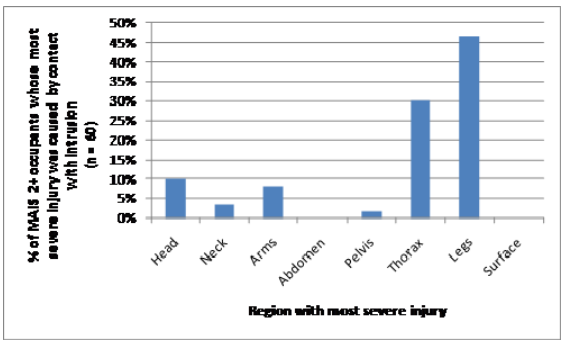

Figure 4. Distribution of 'most severe' injury by body region for MAIS 2+ belted occupants with their most severe injury caused by contact with intrusion.

For CCIS additional analysis was performed to investigate the injury patterns for injuries with

specific causes. It was found that for occupants whose most severe injury was caused by 'contact with intrusion,' the injury was mainly to the legs with some to the thorax (Figure 4).

For occupants whose 'most severe' injury was attributed to the 'restraint system', the injury was mainly to the thorax (62%) with some to the arms (21%) (clavicle fractures). Similarly for occupants whose most severe injury was attributed to 'contact no intrusion' the injury was mainly to the legs (42%) with some to the arms (30%) and thorax (12%).

Further analysis was performed to investigate the nature of the injuries received by the occupant overall. It was found that the body region most frequently injured at the AIS 2+ level was the thorax for both CCIS and GIDAS (Figure 5).

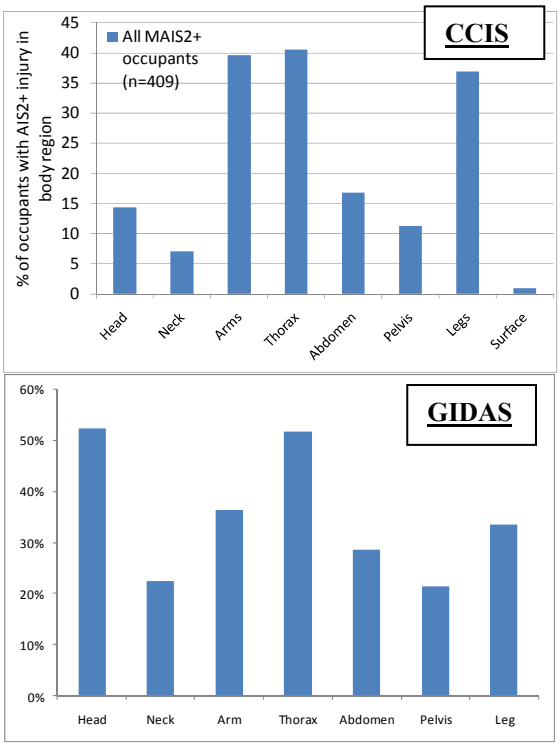

Figure 5. Percentage of belted MAIS 2+ injured occupants with AIS 2+ injury to body region.

For CCIS this was closely followed by arm and leg injuries. For GIDAS this was closely followed by head, arm and leg injuries. It should be noted that for fatally injured occupants the CCIS analysis showed a high frequency of head injury. The arm injuries were often clavicle fractures.

Other analysis found that:

- As the overlap of the accidents increased the proportion of injuries attributed to the 'restraint system' increased and the proportion caused by 'contact with intrusion' decreased.
- A higher proportion of older occupants sustained fatal and MAIS 2+ injuries compared with other occupants indicating that they have a greater risk of injury. This was particularly the case for elderly occupants (> 60 years old).
- Casualties in collisions with HGVs and objects sustained a higher proportion of fatal and MAIS 2+ injuries compared with other collisions such as car-to-car. This indicates the more injurious nature of HGV and object type collisions.

Detailed case analysis

In order to understand whether compatibility issues such as structural interaction and frontal force / compartment strength matching were still present in the current vehicle fleet, a detailed case analysis was necessary. This was because these types of compatibility problems can only be identified through a detailed analysis which includes examination of photographic evidence of both vehicles.

The analysis was performed using CCIS data only because it was only for this data set that there were a sufficient number of relevant cases. The analysis was performed at an occupant level and divided into two parts, an analysis of fatal cases and an analysis of MAIS 2+ survived cases. For each part of the analysis, cases were divided into ones where intrusion was present and ones where intrusion was not present. The main reason for this was that it was only for the cases where there was intrusion present in at least one vehicle that it could be determined definitely whether or not a frontal force / compartment strength problem was present. This is because for cases with no intrusion in either vehicle it is known that the vehicles have absorbed the impact energy in their frontal structures. Hence the frontal force and compartment strength levels were not exceeded at least for that particular accident case. Similar arguments apply for structural interaction. When there is compartment intrusion it can be argued that improved structural interaction could increase the energy absorption efficiency of the front-end structures and consequently reduce the intrusion. When there is no intrusion, improved structural interaction will change the compartment deceleration pulse but it cannot be determined definitely if this would help mitigate occupant injury.

The results of the fatal and the MAIS 2+ survived analyses are shown in Figure 6 and Figure 7 respectively. For fatal casualties, structural interaction problems were identified in 19 out of 48 cases (40 %). However, it is only in 12 of these cases where there was intrusion (25%) that it can be said definitely that improved structural

interaction would have improved the safety performance of the car. Frontal force / compartment strength problems were identified in 4 cases (8%) which indicates that this is much less of an issue then structural interaction. However, it should be noted that poor structural interaction may mask frontal force / compartment strength matching problems. It is interesting to note the high proportion of high severity cases for which the vehicle's deformation was so great that it masked any compatibility issue that may have been present.

For MAIS 2+ survived casualties structural interaction problems were identified in 36 out of 100 cases (36 %). However, only 12 of these cases (12%) were in the presence of intrusion. As for the fatal cases, few frontal force / compartment strength problems were identified.

In summary this indicates that structural interaction is still a major problem and frontal force / compartment strength is much less of an issue. However, it should be noted that poor structural interaction may mask frontal force / compartment strength matching problems. The main structural interaction problems were determined to be override and low overlap.

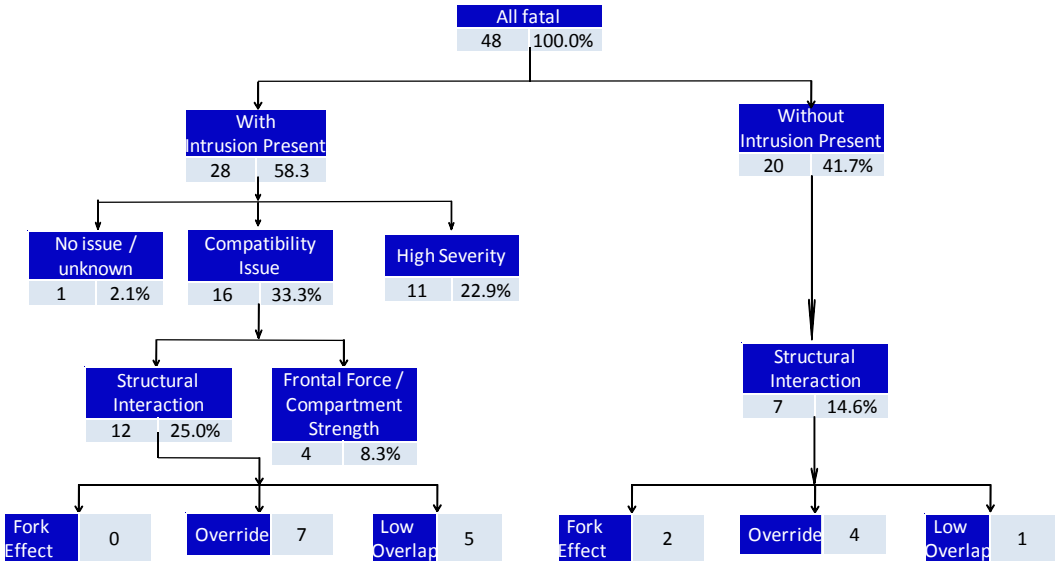

Figure 6. Identification of compatibility issues for fatal cases.

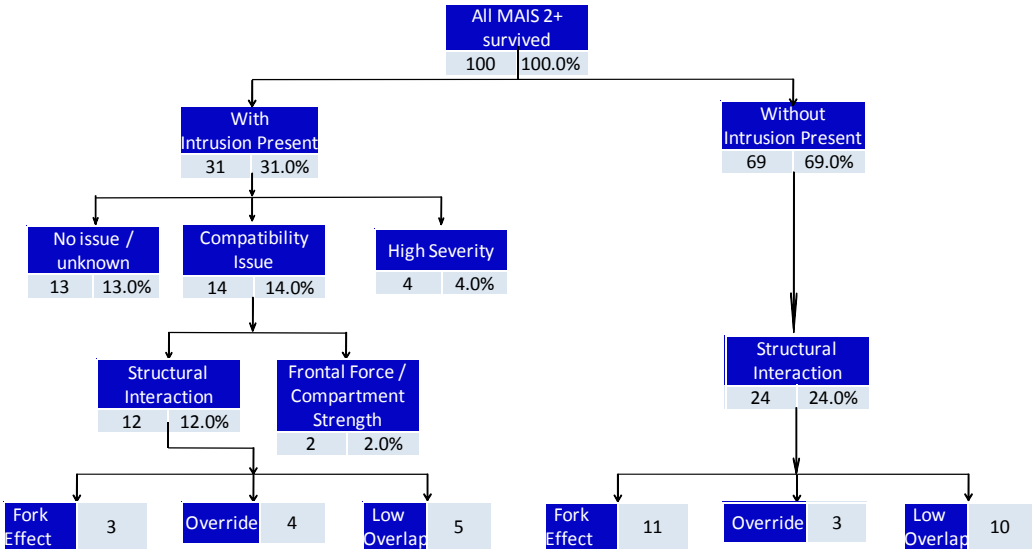

Figure 7. Identification of compatibility issues for MAIS 2+ survived cases.

Conclusions from Accident Analysis

- Poor structural interaction between vehicles, in particular low overlap and over/underriding of car fronts, has been identified as an issue in the current vehicle fleet.
  - Identified in 40% of fatal and 36% of MAIS 2+ injured cases. However, only in 25% of fatal and 12% of MAIS 2+ cases there was intrusion present and thus it can be said definitely that improved structural interaction would have improved the safety performance of the car.
- Frontal force / compartment strength mismatch between cars in the current fleet appears* to be less of an issue than poor structural interaction. *Note: structural interaction problems could be masking frontal force / compartment mismatch problems.
- Compartment strength of vehicles is still an issue in the current vehicle fleet especially in accidents with heavy good vehicles and objects.
  - Proportion of belted MAIS 2+ injured occupants with AIS 2+ injuries caused by 'contact with intrusion' CCIS 25%, GIDAS 12%.
  - When an occupant sustains an injury caused by 'contact with intrusion' in the majority of cases it is the most severe injury, often a leg or thorax injury but sometimes a head or arm injury.
- High proportion of fatal and MAIS2+ injuries in accidents with high overlap (>75%)
  - Proportion of injuries related to the 'restraint' increased with overlap whereas proportion of injuries caused by 'contact with intrusion' decreased.

FIMCAR PRIORITIES AND STRATEGIES

The general aim of FIMCAR is to develop a frontal impact assessment approach addressing self and partner protection in order to decrease the injury risks in single and multiple vehicle accidents. For compatibility it is expected that compatible vehicles will deform in a stable manner allowing the deformation zones to be exploited even when different vehicle sizes and masses are involved.

An assessment approach consists of one or more assessment procedures. For the FIMCAR project it is likely that the assessment approach consists of a full overlap and an off-set assessment procedure according to the decisions of previous research (i.e., VC-Compat [1] and EEVC WG15 [2], IHRA [3]).

The FIMCAR members reviewed the previous research and updated the results with the recent accident analysis. As a result the priorities of the project were to address structural interaction, high overlap collision types, and the risk of injuries arising from acceleration loading.

In order to address the under/over riding aspect of structural interaction structural alignment is considered as an important parameter. To address structural interaction a common interaction zone is needed. The US voluntary commitment for the common vertical interaction zone is considered as the base line. When looking at the accident case with over riding involving two identical vehicles load spreading, related to the vertical arrangement of the loadpaths, is also important. Load spreading in the horizontal direction is also an important factor for addressing small overlap cases. Strong cross beams help provide good interaction in accidents with narrow objects and cross beams extending outboard from longitudinal members can improve structural interactions in cases with small overlap at the corners.

Energy absorption management is needed for two purposes:

- To ensure that the impact energy is absorbed in the car's front-end structures without significant compartment intrusion
- To control the occupant compartment deceleration pulse.

The compartment integrity for single vehicle accidents and car-to-car accidents needs to remain in the current level. However, it is still unclear whether ECE R94 or Euro NCAP or both contribute to the current level of compartment integrity. It is likely that both contribute as ECE R94 tests the heaviest model of car whilst Euro NCAP tests the best-selling model but at a higher speed. According to the data analysed to date, there was no overrepresentation of intrusion cases with smaller vehicles. Thus it is not deemed critical to pay special attention on increasing compartment integrity for smaller cars, particularly if it creates additional test requirements.

In order to address the acceleration type injury issue a full overlap test in order to assess restraint capacity is proposed. In addition the combination of full frontal and off-set tests is meant to create two different pulses.

In summary the FIMCAR assessment approach shall aim at:

- Detecting appropriate structures in the common interaction zone
- Promoting good load spreading by larger force transmitting elements in the interaction zone and multiple load paths
- Keeping the compartment integrity at least at the current level

- Promoting favourable compartment deceleration pulses in vehicle-to-vehicle accidents
- Producing a more severe occupant restraint system test
- Presenting a variety of pulses for restraint system testing and triggering of safety devices

For the evaluation of the different test candidates, amongst others, the following criteria will be used:

- Do the proposed metrics address the compatibility issues described above?
- Are appropriate pass / fail thresholds defined?
- Does the assessment result reflect real world performance?

ANALYSED TEST PROCEDURES

The previous work in compatibility has identified the need for both a full width and an offset test procedure. In FIMCAR full width, offset and offset Mobile Deformable Barrier (MDB) test and assessment procedures are being developed.

Full Frontal Test Procedures

In this chapter an overview of the status of current work to develop a full frontal test procedure is described. The main aim of this work is to develop a test procedure which can control a vehicle's structural alignment and to provide a severe deceleration pulse for the assessment of the restraint system.

Two types of full width test are being investigated a Full Width Rigid Barrier (FWRB) test and a Full Width Deformable Barrier (FWDB) test. For both tests, the use of Load Cell Wall (LCW) data to control the structural interaction characteristics of a vehicle by controlling the measured force distribution is being investigated. The current defacto standard for a LCW is one that consists of 125 mm square elements with the bottom row mounted with an 80 mm ground clearance (Figure 8).

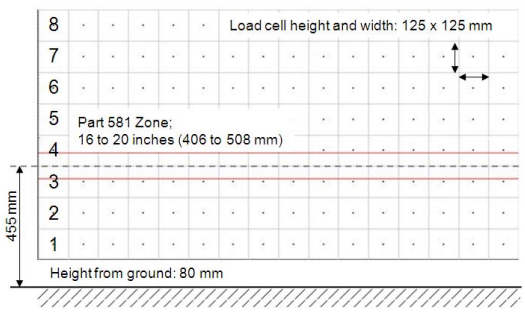

Figure 8. Overview of the specifications of the LCW (rows, columns, height of ground, Part 581 zone).

The FWRB test is conducted in many countries (USA, Canada, Japan, etc.) for both regulation and consumer testing programs. Test speeds range from 50 to 56 km/h. Instrumented Hybrid III dummies are typically used to measure occupant response.

The FWDB test has a 300 mm deformable element [4]. This barrier is currently only used in research applications and is not part of a regulation or consumer test procedure. Tests are conducted with Hybrid III dummies to assess occupant injury risk. Although essentially the same test configuration as the FWRB, the additional honeycomb is included to attenuate the initial contact with the barrier and introduce more shear forces within the vehicle structure. Past research shows that the deformable element reduces the influence of small, stiff structures such as protruding bolts, and the drive-train loads on the barrier.

The FWRB has several advantages over the FWDB such as the LCW measures vehicles forces directly, i.e. they are not filtered by a deformable element. Probably, the main advantage is that the FWRB is effectively already a defacto worldwide standard test. In contrast to this the FWDB has advantages over the FWRB test. These include that the FWDB is more representative of real world accident especially in initial stage of impact which is important for sensing of the crash for restraint system triggering. The engine dump loading is also attenuated, so it is easier to make an assessment of vehicle structural loading. Furthermore, the deformable face can help detect Secondary Energy Absorbing Structures (SEAS) and hence assess them because the deformable face 'reaches' into the vehicle and allows these structures to load the wall even though they may not be in direct contact with it. In addition items such as protruding bolts and towing eyes are less likely to influence LCW measurements. There is also the possibility to assess horizontal structures (bumper beams). On the other hand the possible risk of load spreading due to deformable face can be counted as a disadvantage.

For both the FWRB and FWDB tests metrics to assess a vehicle's ability to apply loads in a common interaction zone are being developed. The main aim of these metrics is to enforce vertical structural alignment because this is a first basic step to increase the compatibility of car crash outcomes. After a common interaction zone is defined, issues such as horizontal distribution or frontal force can be addressed.

The concept on which this development is based incorporates aspects of the US voluntary commitment for the improvement of the geometric frontal impact compatibility of Light Trucks and Vans (LTVs) [5];and the current investigations by

Japan [6]. The concept was decided following the review of metrics developed previously, e.g. AHOF, homogeneity criterion. The aim of the US voluntary commitment is to ensure that LTVs have structure in alignment with a common interaction zone from 16 to 20 inches (406 – 508 mm), further named as "Part 581 zone") measured vertically from the ground (Figure 8) to enable better interaction with cars. Current investigations by Japan are researching the feasibility of metrics which assess the forces measured in rows 3 and 4 of the load cell wall.

Metrics for FWRB tests Test data from JNCAP, NHTSA and previous European projects were used to develop the metric proposals. A total of 54 vehicles which were previously tested in a full width test at a speed of 56 km/h were used. The structural geometrical information for these vehicles was available, although some of the results had to be adjusted to account for the different LCW ground clearances.

The approach for development was that the metric should be able to identify vehicles which had structures which were in a vertical alignment with the 'Part 581 zone' and those which did not. The level of vertical geometric alignment was assessed based on the two parts of Option 1 of the US voluntary commitment [5] as shown in Figure 9.

Next metrics and associated performance limits were developed based on the LCW force measured in rows 3 and 4 to give the best correlation possible with the assessment of the vehicle made using the US voluntary agreement approach 'Option 1' (PEAS alignment).

OPTION 1a: The light truck's primary frontal energy absorbing structure shall overlap at least 50 percent of the 'Part 581 zone'.

OPTION 1b: AND at least 50 percent of the light truck's primary frontal energy-absorbing structure shall overlap the Part 581 zone.

OPTION 2: If a light truck does not meet the criteria of Option 1, there must be a secondary energy absorbing structure (SEAS), connected to the primary structure, whose lower edge shall be no higher than the bottom of the Part 581 bumper zone.

Figure 9. Options from the US voluntary commitment explained [5].

To ensure that the metrics assessed the vehicle's structure only and not 'engine dump' loading, LCW data before the time when the engine loads the wall should be used. To fulfil this requirement, the metrics proposed were based on the loads measured in rows 3 and 4 of the LCW before the time when the LCW total force was 200 kN. For virtually all cars this approach ensured that there was little/no engine loading on the wall in the period of the impact that the metric assessed. In addition, this approach ensured that the metric developed was mass independent because all cars put at least 200 kN total load on the wall.

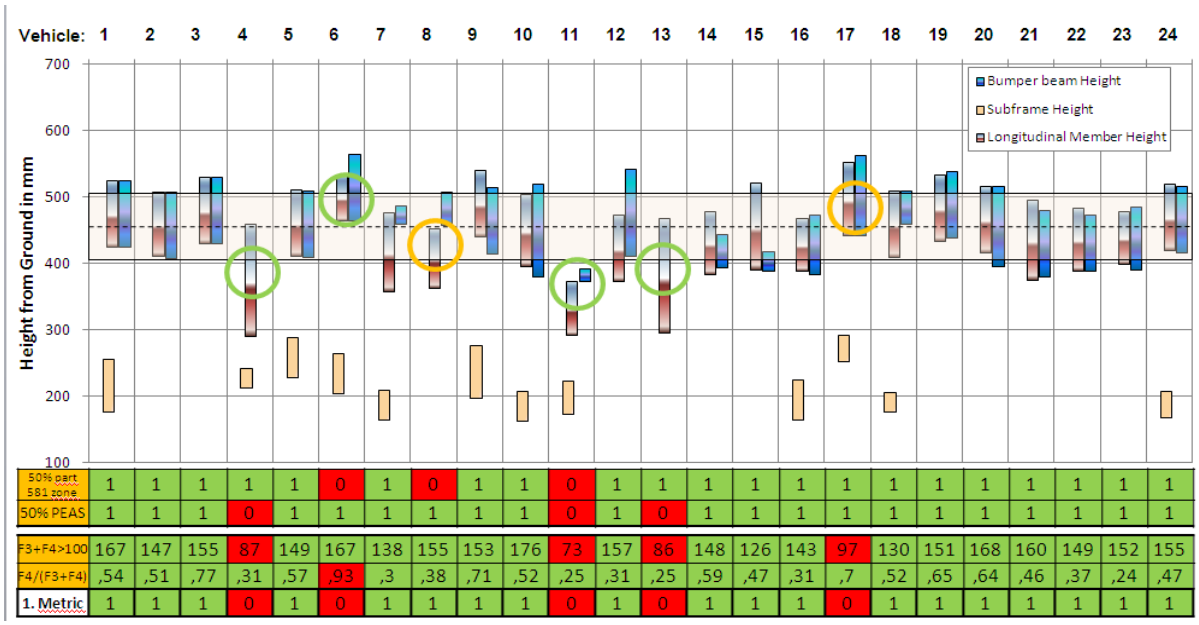

Figure 10. Geometry of longitudinal member, bumper beam and subframe height, geometrical assessment according to US voluntary commitment and FWRB metric assessment for 24 different vehicles.

The process for metric development is illustrated in Figure 10. The geometry of the longitudinal member, bumper beam and subframe height is shown for 24 vehicles in combination with a geometric assessment according to Option 1a (labeled as "50% part 581 zone") and Option 1b (labeled as "50% PEAS") of the US voluntary commitment. The values for the proposed FIMCAR metrics are shown (sum force of rows 3 and 4 shall exceed 100 kN before the time when the total LCW force is 200 kN, labeled "F3 + F4 > 100" and sum force of row 4 divided by the sum force of rows 3 and 4 shall be between 0.2 and 0.8 labeled as "F4/(F3+F4)"). It is seen that there was agreement between the geometric assessment and the metric assessment for all vehicles apart from vehicles 8 and 17 (marked with a yellow circle). However, these vehicles were borderline cases so it was deemed acceptable that there was not agreement in these cases.

Further analysis showed that the proposed metric was able to identify, in general, vehicle structures which had PEAS in alignment with the Part 581 zone and those that did not. However, some issues were identified which require further investigation. These included that some of the tested vehicles were borderline in terms of the geometric vertical alignment performance and may fail, depending on impact accuracy. Furthermore front end items which were felt to have little influence on crash compatibility such as the towing hook may partially influence the results.

Proposals for metrics which reflect Option 2 of the US voluntary commitment (to assess SEAS) still need to be developed but some possibilities are shown in Figure 11. These include an Over-Ride Barrier (ORB) test, evaluation of LCW force values at a later stage of the impact or an assessment from the off-set procedure. However, another important point is if the second stage should be offered just for vehicles with high PEAS (e.g. off-road vehicles) or for all vehicles, i.e. should there be an eligibility assessment for the second stage.

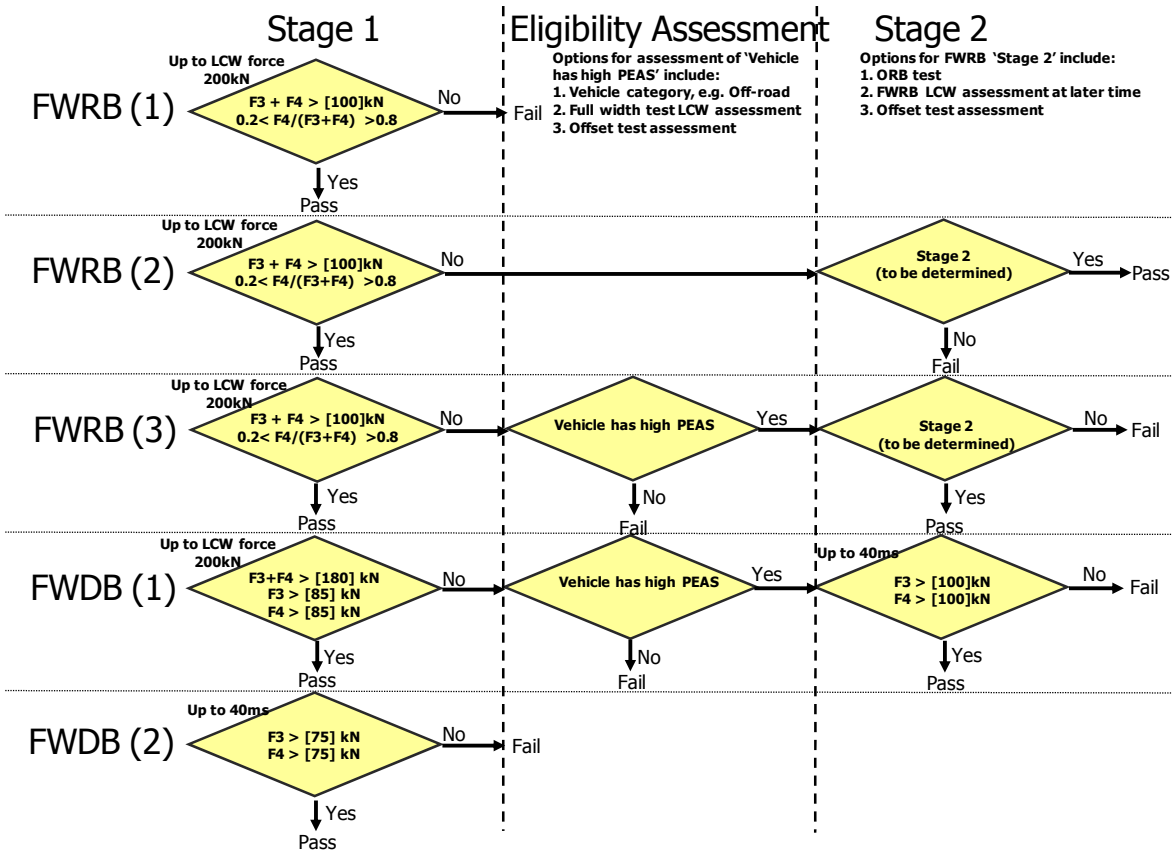

Figure 11. Draft metrics for the FWRB and the FWDB test procedures.

Metrics for FWDB tests Data from VC-Compat, APROSYS, ACEA, BASt, DfT FWDB tests and associated structural geometric information were used to develop the metric (in total 17 tests). In general, the same approach was used as for the FWRB metrics. However, the advantage with the FWDB test is the attenuation of engine dump. Therefore metrics that assessed the vehicle at later stages of the impact could be developed (e.g. up to a time when the total LCW force is 400 kN or up to 40 ms).

Two different proposals for metrics have been made for the FWDB test (Figure 11). The first FWDB (1) consists of a two stage approach. In the first stage, up to the time when the total load cell wall experiences 400 kN, minimum forces of 180 kN are required to be measured in rows 3(F3) and 4 (F4). Additionally, a minimum force requirement of 85 kN in each of row 3 (F3) and 4 (F4) is required to assess the load distribution between rows 3 and 4. In the second stage, up to an impact time of 40 ms, the forces in rows 3 (F3) and 4 (F4) should be greater than 100 kN. This stage was developed to reflect the requirements of the US voluntary agreement 'Option 2' and check that if a vehicle's main structures are not in alignment with the Part 581 zone, then a secondary structure is. It still has to be decided whether or not an eligibility assessment should be required for stage 2. Possibilities for an eligibility assessment include a restriction that only categories of vehicles with high PEAS, e.g. off-road vehicles, should be eligible for a stage 2 assessment. An eligibility assessment would ensure that a standard car would have to align its PEAS (main structure) to meet the requirements of the metric and could not meet the requirements with a low PEAS which could lead to it been over-ridden in an accident.

The second proposed metric, FWDB (2), has just one stage, which assesses up to an impact time of 40 ms. For both these metrics a high correlation with the geometric assessment was reached in the development process.

Load Cell Wall (LCW) specification and certification To use a LCW in a regulatory procedure specification and certification procedures are needed to ensure the LCW used is appropriate.

A collection of the specification data of LCWs used around the world has been performed to give an overview of the current status. From this minimum performance specifications will be defined. Examples these are overload capacity, off-axis error, non-linearity, hysteresis, cross axis sensitivity as well as resonant frequency and frequency response. Further specifications, e.g. the determination of cross talk or the evaluation of wall flatness, are under discussion.

Calibration and certification methods will be based on existing protocols such as SAE J25-70 for load cell calibration. A static calibration method at the centre of the load cell to assess mean axis sensitivity, non-linearity and hysteresis will be proposed. In addition, the off-axis loading error will be assessed (Figure 12). However, at this stage it is considered unlikely that a dynamic test will be necessary.

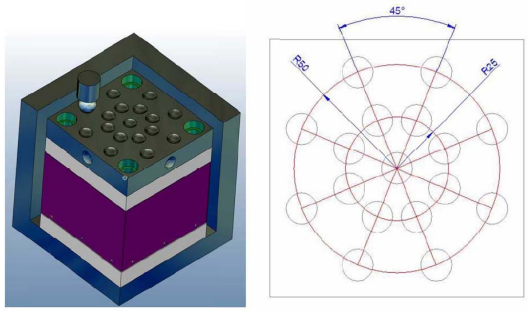

Figure 12. Off-axis loading of a load cell.

Further investigations to complete the specification and certification procedures are ongoing. These will include investigation of issues such as whether or not the overall flatness of the LCW should be specified and if so what the limits should be.

Conclusion of Full Width Test Procedure
Based on the concept of 'force in a common interaction zone' initial proposals for metrics to control a vehicle's structural alignment have been developed for both the FWRB and FWDB tests. However, further work is required to develop these metrics further to choose the most appropriate one. This includes the choice of type of test, i.e. with a rigid or deformable face. In addition the test speed needs to be determined.

Work to develop a specification and certification procedure for a LCW suitable for regulatory purposes has begun.

Off-set Test Procedure

The main objectives of the off-set test procedure are to address structural alignment, load spreading issues, compartment integrity and the restraint system issues (different test pulses).

The current ECE R94 barrier face and the PDB (Progressive Deformable Barrier) as proposed by France in previous projects were the main candidates. Previous research indicated that load cell measurements in off-set tests do not result in appropriate assessment of the load distribution. Following that the decision was taken to

concentrate on the PDB and to assess barrier face deformation.

The test severity needs to be defined taking into account sufficient compartment strength requirements. The best way to assess test severity for this aim is to use the deformation energy expressed by EES (energy equivalent speed). The proposed test procedure shall ensure a level of EES comparable to the today's EES level (observed in ECE R94 and Euro NCAP test conditions), therefore the PDB test speed is fixed at 60 km/h. The details of the test procedure are described in [7].

The PDB test is a 50 percent overlap off-set test which uses measurements from a progressive deformable barrier to assess car's compatibility in terms of partner and self protection [8]. This barrier is currently only used in research applications and is not part of a regulation or consumer test procedure.

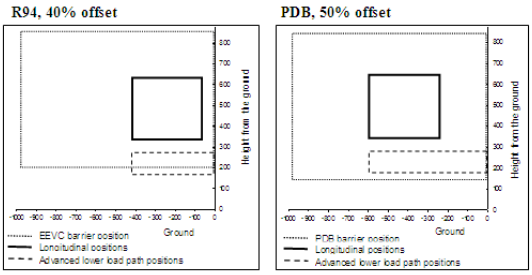

Figure 13. R94 and PDB geometrical comparison.

The 50 percent overlap and the barrier characteristics allow the PDB to identity the main structures involved in the frontal crash. Geometrical data from previous European research projects shown that the main structures of the vehicles will interact with the PDB. Figure 13 shows the interaction areas for the PEAS and SEAS in both, R94 and PDB barriers.

The barrier stiffness increases with depth and has upper and lower load levels to represent an actual car structure. The progressive stiffness of the barrier has been designed so that the Equivalent Energy Speed (EES) for the vehicle should be independent of the vehicle's mass. The use of a PDB barrier should thus harmonise the test severity among vehicles of different masses by encouraging lighter vehicles to be stronger without increasing the force levels of large vehicles.

The key data used in a PDB test is the post-crash deformations of the barrier. A 3-D image of the barrier is recorded in the computer and the depth and distribution of the deformations are used to assess the vehicle's compatibility characteristics.

Metrics assessing the depth and distribution of the barrier deflections are under development in FIMCAR. Instrumented HIII dummies are used to record the risk for occupant injuries.

The barrier is divided in the following three zones, each with a defined objective for evaluation.

i) Upper [from 820 to 600 mm to the ground]: Area above the PEAS and SEAS structures. No significant longitudinal deformations are allowed in the zone.

ii) Middle [from 600 to 350 mm to the ground]: Area for the location of the PEAS. Deformations of the barrier are required in this zone. Promoting the homogeneous deformations and controlling the longitudinal ones.

iii) Lower [from 350 to 180 mm to the ground]: Area for the location of the SEAS. Deformations also allowed in this area. Promoting the homogeneous deformations of the zone and controlling the longitudinal ones.

The analysis within each zone does not consider the total width of the barrier, the extremities of the barrier are excluded. The zone width covers 150 mm from the barrier edge to a distance equal to the half of the vehicle width minus 100 mm (Figure 14).

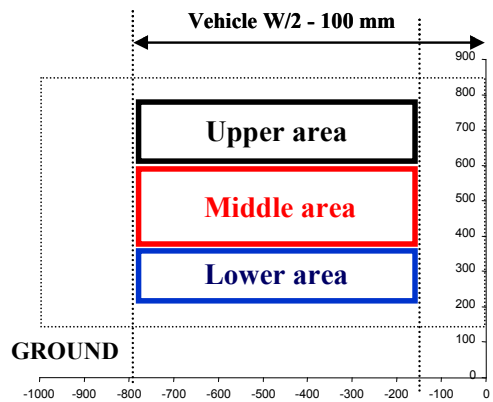

Figure 14. Barrier areas.

The zones defined ensure the evaluation of the front structure over a wide range, taking into account compatibility issues such as small overlap. The following two criteria are obtained from the barrier digitalization. These parameters will be used to evaluate the partner protection of the vehicle. Longitudinal deformation (*d*): Robust statistics characterizing the deformation of the considered zone, taking a q-th percentile of the barrier longitudinal deformation (i.e. 99th percentile of the deformations).

i) Homogeneity (*H*): Estimation of the total amount of variation of an image, mathematically defined as the average length of contour lines of the image.

In a first stage the map (image) is filtered by an additional low-pass filter. Then, the map is normalized, so all images have the same dimension and only vertical and horizontal deformations are taken into account.

The gradient of the length is given the magnitude of change of slope. *H* is proportional to the sum of lengths of the gradient of the map at all points.

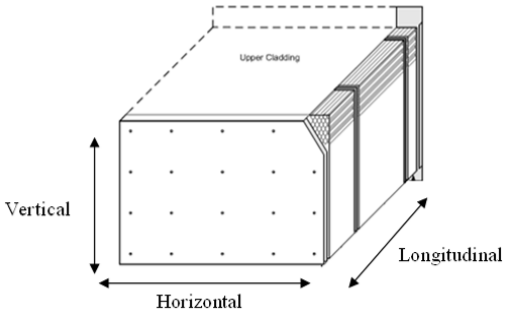

Figure 15. Barrier axis definition.

The metric The off-set test assessment procedure was supported by a database of 37 PDB_60 tests. The barrier deformations of these tests were analysed and taken as a reference for the further metric investigations.

The database is the result of previous research projects, e.g. VC Compat. In a first stage, the barriers were classified following a subjective approach, gathering the barriers that suggest a good performance in compatibility in a first group (G1), the barriers that suggested a bad compatibility performance in a separate group (G3) and finally the barriers between G1 and G3 were classified in G2.

In a second stage, the barriers in each group (G1, G2 and G3) were classified from best to worst performance also using subjective criteria.

The subjective classification described above was used as guidance for an initial stage of the development of the metric, a good correlation between the subjective classification and the initial proposals for metric (objective method) gives a good starting point for the development of the metric.

The proposed metric will give a single score (*S*), the score being the result of a formula which combines the longitudinal deformation and homogeneity assessments for the lower, middle and upper areas, d_U, d_M, H_M, d_L, and H_L.

$$S = f(d_U, d_M, H_M, d_L, H_L)$$

Figure 16. Scoring formula.

d_i (i=U, M and L) and H_j (j= M and L) scores will be calculated from the longitudinal deformation and the homogeneity criteria respectively. A sliding scale system of points scoring will be used to calculate points for each measured criterion. This involves two limits for each parameter, a more demanding limit (*higher performance*), and a less demanding limit (*lower performance*).

The proposed limits to be used in the metric were also derived from the database tests, taking the objective classification as a reference.

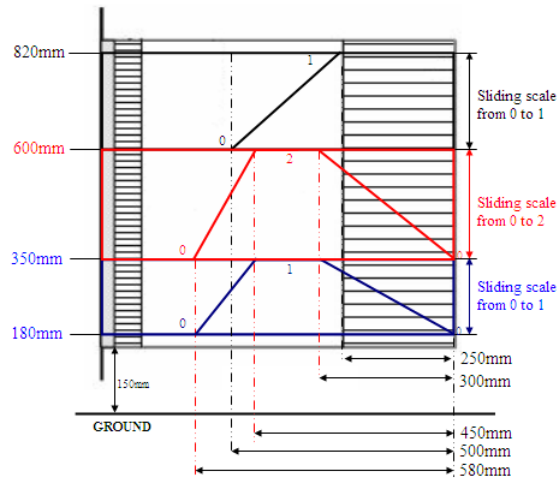

Figure 17. Longitudinal deformation limits.

The score, including "weighting factors" for the different sub-scores, will be developed following the priorities to evaluate the frontal compatibility.

The main structures to contribute in the frontal crash are the PEAS, therefore d_M and H_M scores are considered to have a larger weight factor than the d_L and H_L, scores of the zone where the SEAS are located. Finally, the contribution of the d_U score will depend on the level of relevance that will be considered for issues like over/under ride or eventually the aggressivity of the vehicle in a frontal/side crash.

Figure 18 shows an example of scoring formula that has been investigated in FIMCAR project, in this particular case the scores of the middle zone are sliding from 0 to 2 points and for the upper and lower from 0 to 1 point.

$$S = d_U + d_M + H_M + d_L + H_L$$

Figure 18. Example of scoring formula.

In the formula, the maximum score is 7 points and the two scores of the middle area represent the 57% of the total, lower area 29% and upper area 14%.

Scoring concepts like capping limits may be considered in the metric in order to address some relevant issues detected in compatibility. Exceeding a capping limit could indicate an unacceptable high risk of a specific issue in compatibility (i.e. over/under ride) which may lead to the loss of points for that part of the score.

Conclusion of Off-set Test Procedure The fundamentals of the assessment method using the PDB_60 off-set test have been defined. Different metrics have been investigated for assessing compatibility issues. The investigated metrics have shown a good correlation with a subjective assessment. The metric needs to be further developed and validated using the upcoming tests that will be performed in FIMCAR project.

During the testing activities of the project, the test severity will also be investigated and validated.

MDB Test Procedure

The main aims of the MDB (moveable deformable barrier) test procedure are to address structural alignment, load spreading issues, compartment integrity and the restraint system issues (different test pulses and increased challenge for lighter cars). Except for the increased challenge for lighter cars these aims are the same aims as for the off-set test procedure using a static barrier.

Although in principle MDB tests with off-set and full width are possible, FIMCAR decided early in the process to develop an off-set MDB test only. The deformable barrier face was selected based on a theoretical review of existing off-set barrier faces. The PDB was chosen because it offered the best possibilities. The Moving Progressive Deformable Barrier (MPDB) was originally tested in Australia and has been further developed in the Netherlands [9].

As for the PDB, the MPDB test severity needs to be defined taking into account sufficient compartment strength requirements. The best way to assess test severity for this aim is to use the deformation energy expressed by EES (energy equivalent speed). However, the test severity in an MDB test is defined by the closing speed of trolley and test car and the weight relationship between both. In the initial step barrier mass was fixed at 1,500 kg and the closing speed was fixed at 100 km/h.

The mass of the trolley is based on a Swedish data showing the cumulative distribution of the vehicle fleet of Sweden in 2008 and the EU in 2005 [10].Both distributions are in-line and give an average vehicle mass of 1500kg. This is also backed up by the AE-MDB (Advanced European Moving Deformable Barrier) side impact trolley mass, which is also set to 1500kg [11].

The impact speed, angle and overlap are based on real word accident data and existing test procedures.

The baseline situation for the current R94 is a frontal car-to-car collision with both vehicles travelling at 50 km/h with an overlap of 50% and an impact angle of 0 degrees. To best represent this baseline situation, the single vehicle-to-barrier test was derived and set to 56 km/h, an overlap of 40% with an impact angle of zero degrees.

Figure 20 shows the closing speed of front-to-front car collisions based on recent accident data. A closing speed of 100km/h, in-line with the baseline test, will cover 90% of the frontal car-to-car collisions in terms of speed [Data from GIDAS, accidents from the Hannover and Dresden area in between 1999 to 2009 with no restriction on car model/age. Only front to front car to car crashes are included where the direction of force during the collision is in between 11, 12 and 1 o'clock. MAIS has been calculated on the basis of the maximum MAIS of all occupants of the subject car. Both cars are within 600 to 3500 kg curb weight and all collisions have closing speeds below 150 km/h].

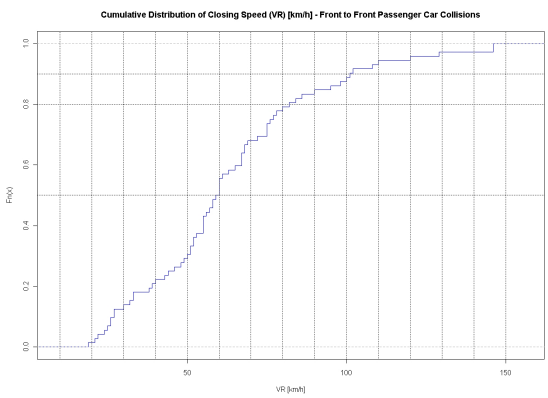

Figure 19. Cumulative distribution of closing speed in front to front collisions.

The combination of MDB mass and closing speed was confirmed by a test with an Opel Astra to represent a desired severity level, expressed in

EES, in mid-size cars. Currently, investigations, tests and simulations for heavy and light cars are ongoing in order to check whether or not the self protection level is sufficient for heavy cars and test severity is not too high for light cars, respectively.

Figure 20. MPDB test with Heavy Vehicle.

The needs to change the test parameters, such as trolley mass or closing speed for light or heavy vehicles to adjust the severity are part of the investigations.

The MPDB will have identical assessment procedures as the PDB with the difference of impact severity related to vehicle mass. A heavy (2300 kg) vehicle experienced a crash of similar severity as the R94 test while a 1400 kg vehicle experienced a much higher test severity, approaching Euro NCAP levels.

The main compatibility assessment will be the PDB deformation, the potential metric will be identical to the PDB metric. Investigations are on-going to develop additional metrics based on typical MPD parameters such as the trolley acceleration.

CONCLUSIONS / OUTLOOK

The FIMCAR project is developing a verification procedure to guide the final selection of test procedures. This program will specify the types of testing, simulation, and/or analysis that confirm the test procedures address specific aspects of compatibility. These procedures will be applied in the final year of the project to both select the candidates and finalize their assessment criteria.

The current proposal from FIMCAR is that a full width and offset test procedure will be developed together as a compatibility assessment approach. There is no clear answer yet as to which full width and offset candidate is best.

For the full width test promising metrics are available for both FWRB and FWDB to control structural alignment, which is the first and basic step towards compatibility. Next steps will be to decide on performance limits, validate with real world accident data and crash tests, confirm test severity and estimate the benefit. The development of LCW specification and certification procedure is ongoing.

For the off-set test in principle a stationary PDB or an MPDB test are possible. Metric development for the PDB for the assessment of aggressive structures is promising. In case metric development for the PDB is not successful, the current ODB used in ECE Regulation 94 is a fall back solution. The final FIMCAR assessment approach proposal is expected to be published in Autumn 2012.

ACKNOWLEDGEMENTS

The paper is written on behalf of the members of the FIMCAR project. The FIMCAR project is co-funded by the European Commission under the 7th Framework Programme (Grant Agreement no. 234216). The members of the FIMCAR consortium are: Technische Universität Berlin, Bundesanstalt für Straßenwesen. Chalmers tekniska hoegskola AB, Centro Recerche Fiat S.C.p.A., Daimler AG, FIAT Group Automobiles Spa, Humanetics GmbH, IAT Ingenieurgesellschaft für Automobiltechnik mbH, IDIADA Automotive Technology SA, Adam Opel GmbH, Peugeot Citroën Automobiles SA, Renault s.a.s, TNO, TRL Limited, UTAC, Volvo Car Corporation, Volkswagen AG, TÜV Rheinland TNO Automotive International BV.

Further information is available at the FIMCAR web site www.fimcar.eu.

This paper used accident data from the United Kingdom Co-operative Crash Injury Study (CCIS) collected during the period 2000-2009. CCIS was managed by TRL Limited, on behalf of the DfT (Transport Technology and Standards Division) who funded the project along with Autoliv, Ford Motor Company, Nissan Motor Company and Toyota Motor Europe. Previous sponsors of CCIS have included Daimler Chrysler, LAB, Rover Group Ltd, Visteon, Volvo Car Corporation, Daewoo Motor Company Ltd and Honda R&D Europe (UK) Ltd. Data was collected by teams from the Birmingham Automotive Safety Centre of the University of Birmingham; the Transport Safety Research Centre at Loughborough University; TRL Limited and the Vehicle & Operator Services Agency of the DfT.

Further information on CCIS can be found at http://www.ukccis.org

The FIMCAR development of FWRB metrics was supported by JMLIT and Nagoya University by offering test data combined with the corresponding geometrical data of the respective cars. Members of the FIMCAR project want to thank JMLIT and Nagoya University for their contribution.

REFERENCES

1 Edwards, M. & de Coo, P.
Final Report: Improvement of Vehicle Crash Compatibility through the Development of Crash Test Procedures, European Commission 5th Framework Project GRD2/2001/50083, 2007

2 EEVC Working Group 15, Car Crash Compatibility and Frontal Impact Enhanced European Vehicle-safety Committee, www.eevc.org, 2007

3 O'Reilly, P. Status Report of IHRA Compatibility and Frontal Impact Working Group Proceedings of the Enhanced Vehicle Safety Conference, No. 03- 402, 2003

4 Edwards M et al. (2003). 'Development of Test Procedures and Performance Criteria to Improve Compatibility in Car Frontal Impacts', Proceesings of the 18th ESV Conference, Nagoya, Japan, 2003.

5 Barbat, S., "Status Of Enhanced Front-To-Front Vehicle Compatibility Technical Working, Group Research And Commitments", 19th ESV conference Proceedings Paper Number 05-463, 2005

6 Yonezawa, H.; Mizuno, K.; Hirasawa, T.; Kanoshima, H.; Ichikawa, H.; Yamada, S.; Koga, H.; Yamaguchi, A.; Arai, Y.; Kikuchi, A.: Summary of Activities of the Compatibility Working Group in Japan (2009); ESV Conference 2009

7 Dellannoy, P.; Martin, T.; Meyerson, S.; Summers, L.; Wiacek, C.: 'PDB Barrier Face Evaluation by DSCR and NHTSA's Joint Research Program, ESV Conference 2007

8 Delannoy, P.; Faure, J.; Coulombier, D.; Zeitouni, R. & Martin, T. New Barrier Test and Assessment Protocol to Control Compatibility SAE Annual Conference, 2004

9 Schram, R. The Development of a mobile deformable test procedure. Proceedings of the Enhanced Vehicle Safety Conference, No. 07- 327, 2007

10 Sveriges officiella statistic (SIKA)

11 The development of an advanced European mobile deformable barrier face (AE-MDB); J.D. Ellway on behalf of EEVC WG13; paper number 05-0239

ACCURACY OF AHOF400 WITH A MOMENT-MEASURING LOAD CELL BARRIER

John Brewer
Volpe National Transportation Systems Center
United States Department of Transportation
United States
Sanjay Patel
Stephen Summers
Aloke Prasad
National Highway Traffic Safety Administration (NHTSA)
United States Department of Transportation
United States
Pradeep Mohan
National Crash Analysis Center
The George Washington University
United States
Paper Number 11-0335

ABSTRACT

Several performance measures derived from rigid barrier crash testing have been proposed to assess vehicle-to-vehicle crash compatibility. One such measure, the Average Height of Force 400 (AHOF400) [1], has been proposed to estimate the height of a vehicle's primary energy absorbing structures. Previous studies have shown that the difference in AHOF measures is a significant predictor of crash partner fatality in vehicle to vehicle crashes. However, the single axis 250x250 mm and 125x125 mm size of the load cells limited the accuracy of these performance measures. The National Highway Traffic Safety Administration (NHTSA) recently purchased an advanced load cell barrier using 125 x 125 mm load cells (in a 9x16 load cell array) that measure compressive force and moments. Simulation studies predicted this should significantly improve the AHOF accuracy. This test program will evaluate this prediction. Previous studies suggest that single axis load cell measurements may not provide sufficient accuracy. This paper will evaluate the results using a rigid barrier that measures vertical and lateral moments in addition to longitudinal force. The results will be evaluated against vehicle geometry measurements. Six crash tests were conducted using an advanced load cell barrier with vertical and lateral moment capability. The test results are compared with previous single axis 125 x 125 mm rigid barrier tests. The additional accuracy resulting from the moment data is assessed. The benefits of the advanced load cell barrier in terms of amplifying and enabling compatibility criteria are discussed.

INTRODUCTION

The National Highway Traffic Safety Administration (NHTSA) regularly conducts crash tests of vehicles into a rigid load cell barrier. The load distribution on the load cells during the crash test provides information on the structural load paths that develop and decay during the event. In particular, the average height of force (AHOF) and the load transferred into the 49 CFR Part 581 bumper height zone can be important indicators of how effectively front end structures would manage load interaction with a crash partner. The Part 581 bumper zone is 16-20 inches (406-508 mm) above the ground as established by NHTSA federal regulation.

Traditional barrier load cells are square faceplates supported from a rigid wall through a device for measuring applied load. An inherent drawback to this approach is that the analyst is forced to assume the load is applied through the center of the cell when in fact it could be distributed in an arbitrary manner across the surface. The load distribution may well be nearly uniform across the surface of the load cell, but there is the theoretical possibility that the load is concentrated at one edge of the load cell, resulting in an error between the actual and assumed position of as much as one half of the load cell dimension [2].

In order to minimize this error, NHTSA, in conjunction with the Volpe National Transportation Systems Center (Volpe Center), developed a prototype barrier that uses 125x125 mm load cells which can also measure the moment applied about the y- (transverse) and z-axes (vertical) of the load cells mounted in the vertical y-z plane. The ability to measure the moment should reduce or eliminate the error in height of force (HOF) calculations. The

additional data from advanced load cells will also increase the resolution of force distribution plots.

Six crash tests using the advanced high resolution barrier were conducted at the Transportation Research Center (TRC) of Ohio. The data from these tests are in the NHTSA crash test database as tests 6945 (2003 Honda Odyssey), 6946 (2005 Honda Odyssey), 6947 (2006 Ford F-250), 6948 (2007 Chevrolet Silverado), 6982 (2006 Honda Ridgeline), and 6983 (2002 Ford Focus). This paper assesses the results of these tests and the effect of the enhanced data on compatibility metrics.

EMPLOYING ADDITIONAL DATA IN ANALYSES

For ease of visualization and calculation, the distributed loads on a load cell surface are usually characterized by a point load of equivalent magnitude located at the center of the cell. The data from each advanced load cell are characterized by one force and two moments (F, M_y, M_z) as depicted in Figure 1. A straightforward approach to visualizing the implication of this additional data is to break the load down into an equivalent set of four point loads that yield the same total force and moment, as shown in Figure 2.

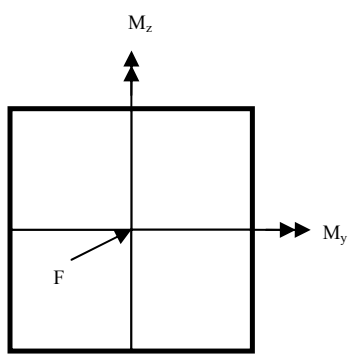

Figure 1. Load data available for advanced load cells.

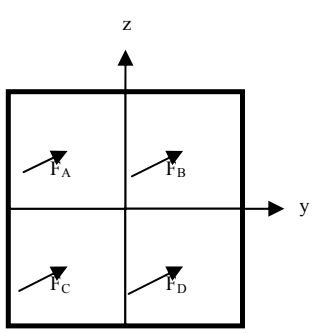

Figure 2. Equivalent force and moment through multiple loads.

It can be shown that for a square load cell of width W, the forces needed to replicate the same total force and moments would be:

$$F_A = \frac{F}{4} - \frac{M_y}{W} - \frac{M_z}{W} \quad (1a)$$

$$F_B = \frac{F}{4} - \frac{M_y}{W} + \frac{M_z}{W} \quad (1b)$$

$$F_C = \frac{F}{4} + \frac{M_y}{W} - \frac{M_z}{W} \quad (1c)$$

$$F_D = \frac{F}{4} + \frac{M_y}{W} + \frac{M_z}{W} \quad (1d)$$

This representation of one force and two moments by four forces effectively doubles the resolution of the equivalent point loads in both dimensions (See Figure 3) which can yield important additional detail. This also provides a more accurate average height of force calculation than the force data alone.

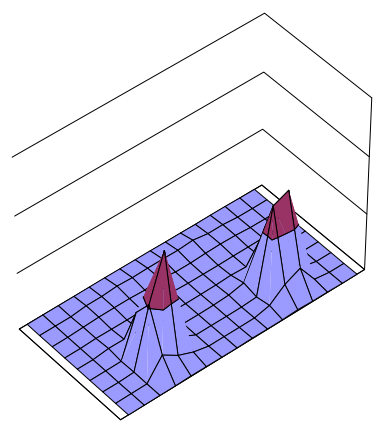

(a) Load data only - 125x125 mm resolution.

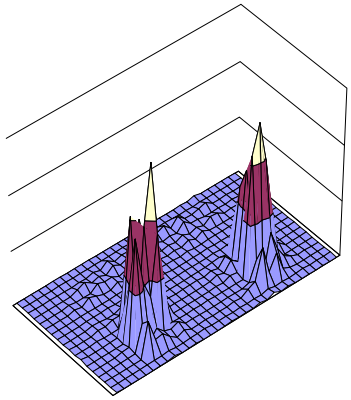

(b) Load and moment data - 62.5x62.5 mm interpreted resolution.
Figure 3. Point load distribution at maximum total load for test 6947.

The addition of moment information to the load cell data gives an indication of the distribution of forces across the load cell. Of course, with only two quantities of data about the distribution in, say, the z-direction (that is, F and M_y), the best that can be asserted is a linear estimate of the force distribution. Nonetheless, given this formulation, a better estimate of the force in a specific subsection of a load cell can be made. In particular, an improved estimate of the force in the Part 581 bumper interaction zone (from 16-20 inches above the surface) can be made.

In load cell barriers with 125 x 125 mm cell dimensions, the rows of load cells are typically arrayed such that the boundary between the third and fourth row from the floor runs along the centerline of the Part 581 zone. The linear force estimate enables some of the compatibility criteria that depend on the sum of forces in the nominal[1] third and fourth rows of load cells ("F3" and "F4") to be adjusted for the Part 581 zone itself.

It can be shown that the equation for the linear approximation of force per unit height (as a function of height) can be given as:

$$p^{linear}(z) = \frac{F}{W} + \frac{12M_y}{W^3} z \qquad (2)$$

where the origin is at the center of the load cell. If the bottom edge of a 125x125 mm load cell were at the center of the Part 581 zone, then the estimated force applied within the upper half of the Part 581 zone would be:

$$F^{Part581} = \int_{-62.5mm}^{-11.7mm} \left(\frac{F}{W} + \frac{12M_y}{W^3} z \right) dz \qquad (3)$$

TESTING PROGRAM

An enhanced load cell barrier with 125x125 mm load cells was constructed and used in six rigid barrier tests. There were nine rows of 16 load cells (a 9x16 array) for a total of 144 load cells. The nominal crash speed was 35 mph (56.3 kph). The vehicles tested were

- 2003 Honda Odyssey (Test 6945)
- 2005 Honda Odyssey (Test 6946)
- 2006 Ford F-250 (Test 6947)
- 2007 Chevrolet Silverado (Test 6948)
- 2006 Honda Ridgeline (Test 6982)
- 2002 Ford Focus (Test 6983)

The presence of moment data allows for an estimate of the load distribution across the barrier rows that is piecewise linear instead of a step function. Figures 4a through 4f show the load distribution along the z-axis at the maximum total force level for each test. Each data channel from the load cell barrier was filtered with a Society of Automotive Engineers (SAE) CFC 60 filter. The lowest row often experiences load only near the top edge, leading to apparently anomalous estimated tensile loads at the bottom edge. Note that an occasional data channel yielded anomalous data. In these cases, the data was simulated either by the average of the data channels to either side of it or by the symmetric channel on the opposite side (i.e., right vs. left) of the barrier.

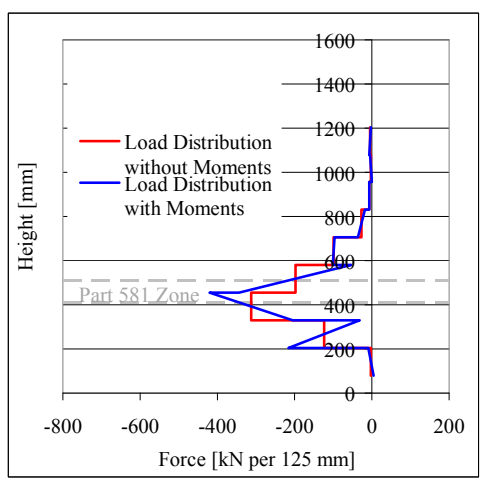

(a) 2003 Honda Odyssey (777 kN @31.4 msec).

[1] Some tests of vehicles with high ground clearance and high front hood height will forgo the lowest row or two of load cells in lieu of additional rows at the top of the barrier.

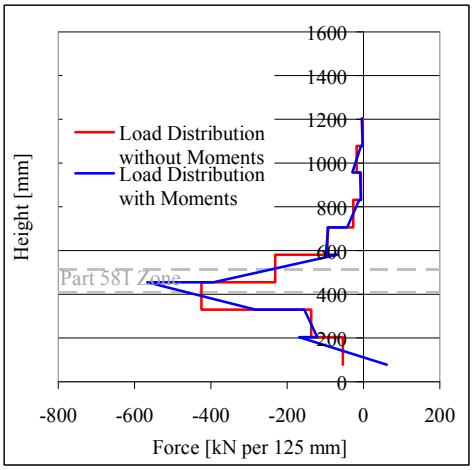

(b) 2005 Honda Odyssey (997 kN @28.2 msec).

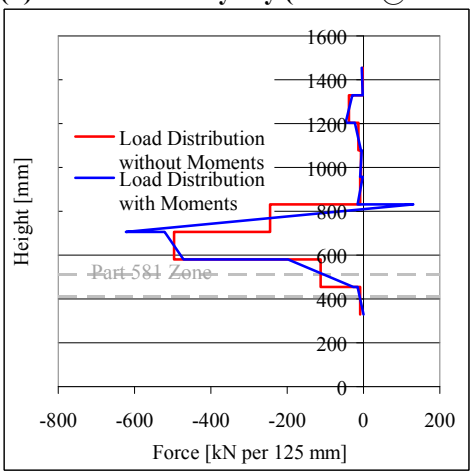

(c) 2006 Ford F-250 (937 kN @12.0 msec).

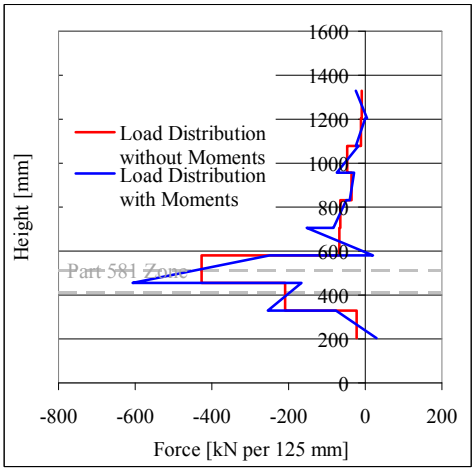

(d) 2007 Chevrolet Silverado (898 kN @48.2 msec).

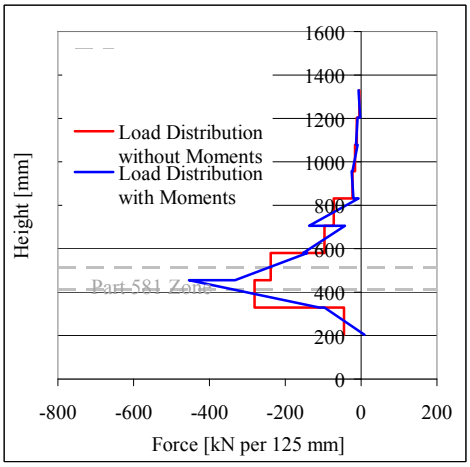

(e) 2006 Honda Ridgeline (787 kN @29.9 msec).

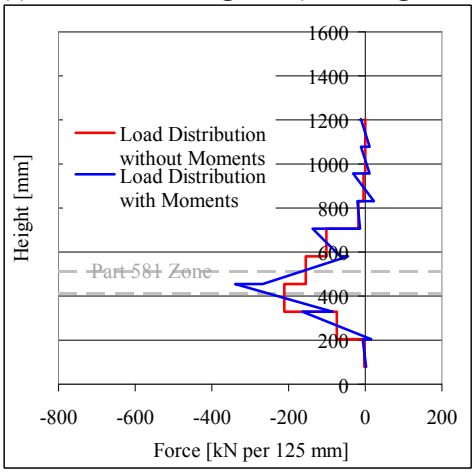

(f) 2002 Ford Focus (566 kN @39.2 msec).

Figure 4. Load distribution at maximum total load by vertical location with and without moments.

The force distributions at the time of maximum total load exhibit reasonably expected behavior in most cases, with most load being reacted in the third and fourth rows. Calculations with the moment data further imply that the load in those rows was primarily reacted in the Part 581 zone. A few anomalous negative loads are observed, but they are within the magnitude that might be expected if a major load path were temporarily aligned with the upper or lower half of a row of load cells.

The Ford F-250 and Chevrolet Silverado exhibited most of their crushing load above the Part 581 zone. This is indicative of potential problems with geometric compatibility. For this reason, these vehicles have been equipped by their manufacturers with Secondary Energy Absorbing Structures (SEAS). These components mounted below and behind the bumper structure provide a means for interaction between the vehicle and other lower

vehicles which may have begun to ride under their primary structure.

AVERAGE HEIGHT OF FORCE (AHOF400)

The height of force (HOF) can be computed at any instant by summing the product of applied force and the central height for all load cells and dividing by the total load. AHOF400 is the value of the instantaneous HOF for each data point weighted by the distance the occupant compartment travels over the associated data acquisition interval for the total displacement range 25 mm to 400 mm [1]. AHOF400 was first computed for the tests in the normal manner. It was then recomputed using the enhancement enabled by the moment data.

Figures 5(a) through 5(f) show the progression of HOF through the test for the two calculation methods. The calculated AHOF400 is also shown for reference.

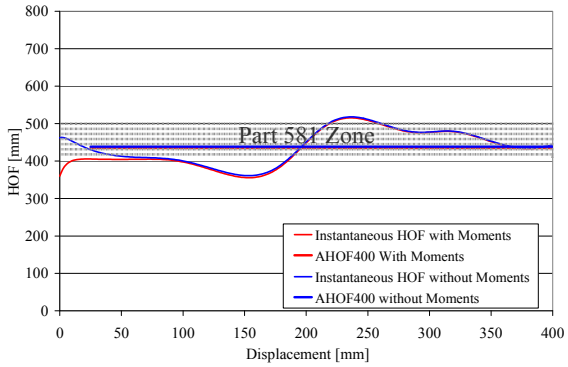

(a) 2003 Honda Odyssey.

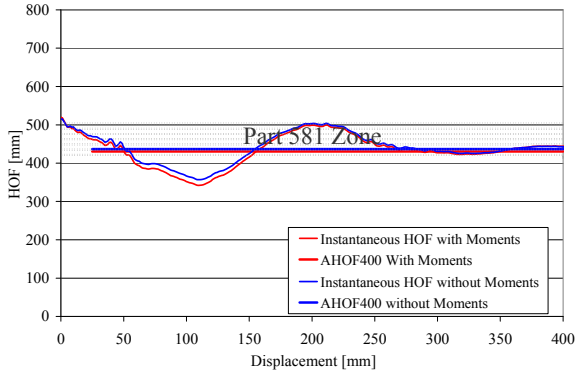

(b) 2005 Honda Odyssey.

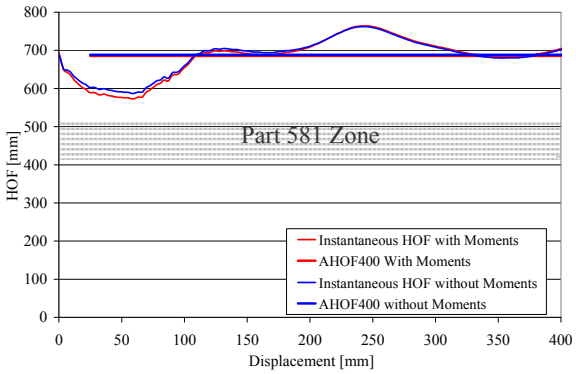

(c) 2006 Ford F-250.

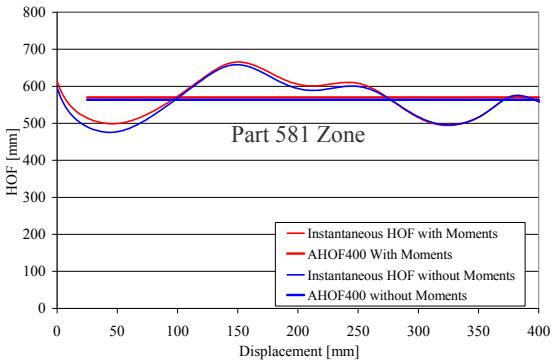

(d) 2007 Chevrolet Silverado.

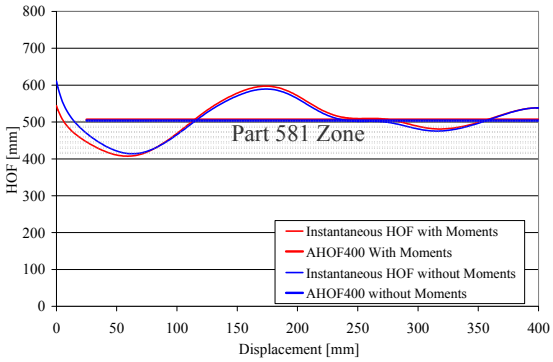

(e) 2006 Honda Ridgeline.

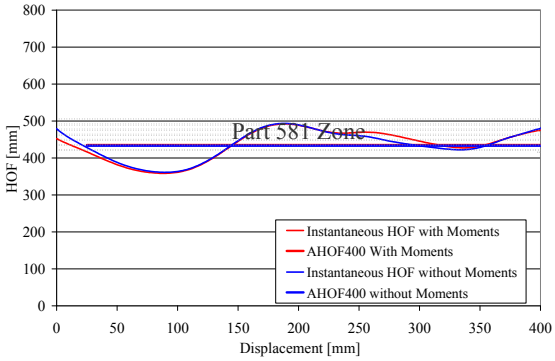

(f) 2002 Ford Focus.
Figure 5. HOF vs Displacement.

Table 1 gives the calculated AHOF400 of each test for the two computation methods, as well as the measured structural height (longitudinal bottom and top heights) at the test facility. In five of the six cases, the value of AHOF400 was comfortably in the range of heights of the bumper structure. For the Chevrolet Silverado, the AHOF400 was above the measured top of the bumper structure implying that significant load paths had developed above that structure during the first 400 mm of crush of the vehicle.

Note that the instantaneous HOF values are most disparate for low displacements. This might be expected, as the effects of minor noise in the moment channel or off-center load concentrations will be most visible in the HOF calculations when the overall force level is low. It is also notable that the AHOF400 changes by less than 10 mm with the inclusion of moment data. Recall that the maximum theoretical error in HOF is one half of the load cell size. The observed discrepancy is usually an order of magnitude lower. Despite significant load concentrations in the bumper regions (as evidenced by the force gradients visible in Figure 4), the net effect of the moments in opposite directions across the adjoining rows seems to be minimal.

Table 1: AHOF400 parameters by Calculation Method

Vehicle	AHOF400 without Moments	AHOF400 with Moments	Difference with Moments	Measured Structure Height
2003 Honda Odyssey	438.5 mm	434.9 mm	-3.6 mm	390 - 498 mm
2005 Honda Odyssey	436.7 mm	430.5 mm	-6.2 mm	400 - 500 mm
2006 Ford F-250	688.3 mm	685.7 mm	-2.6 mm	630 - 765 mm
2007 Chevrolet Silverado	563.3 mm	570.1 mm	+6.8 mm	444 - 544 mm
2006 Honda Ridgeline	503.8 mm	506.9 mm	+3.1 mm	487 - 578 mm
2002 Ford Focus	433.4 mm	435.0 mm	+1.6 mm	423 - 531 mm

For four of the six vehicles, the value of AHOF400 is within the Part 581 zone, mostly quite close to its center. Admittedly, the value for the Honda Ridgeline is close to the edge (within 5 mm). The values for the Chevrolet Silverado and Ford F-250 are again above the Part 581 zone. This is another indication that the vehicle structures may be too high to adequately engage the bumper structures of most vehicles in its early crush stages.

As mentioned, the Ford F-250 and Chevrolet Silverado (as well as the Honda Ridgeline) do have secondary energy absorbing structures (SEAS) which are intended to interact with a partner vehicle and share crash forces in the Part 581 zone. Nonetheless, due to their position in these vehicles (behind and below the bumper structure), the forces from these SEAS are arise only when the structure crushes to the point where load paths can develop at that height. In a deformable barrier test (and in a crash against a deformable vehicle), there is the possibility of a load path developing from these SEAS before the upper structure is fully crushed. In these rigid barrier crash tests, however, the development of a load path through the SEAS required significant crush of that structure.

As an example, evidence of the Ford F-250's SEAS structure can be seen later in its test. Although the total force in that test peaks at 937 kN at 12.0 msec after contact, the total force in the nominal third row does not exceed 15 kN until 46.8 msec, when the vehicle displacement is approximately 528 mm. After that load path is established however, the row load quickly passes 50 kN (53.4 msec /576 mm) on its way to a maximum of 78 kN (72.1 msec/650 mm). Even at the 100 msec point (while the vehicle still maintains contact with the barrier but after it has started its elastic rebound), the row load maintains a level of 41 kN. Figure 6 shows high-resolution force distribution plots at each of these times to illustrate this progression.

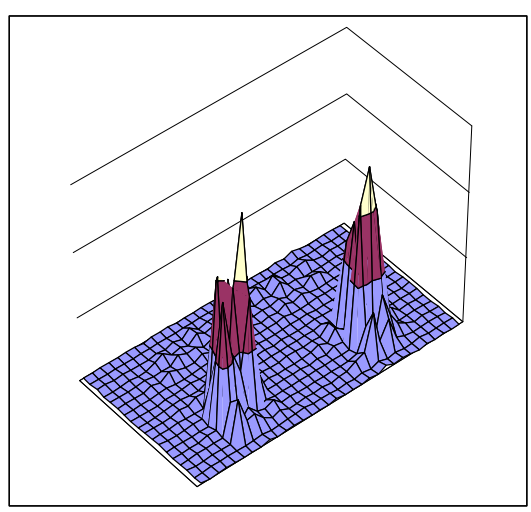

(a) Maximum Ftotal, t = 12.0 msec; d = 182 mm.

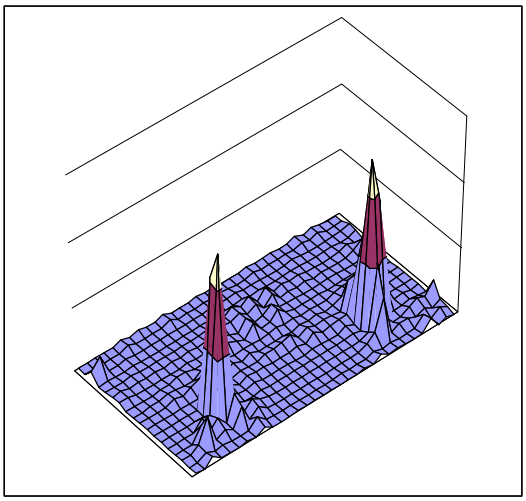

(b) F3 reaches 15 kN, t = 46.8 msec; d = 528 mm.

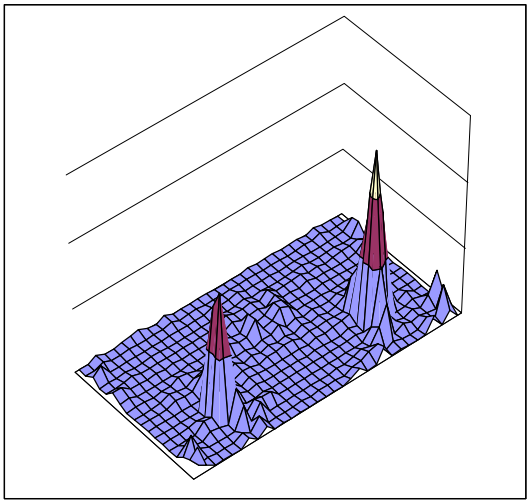

(c) F3 reaches 50 kN, t = 53.5 msec; d = 576 mm.

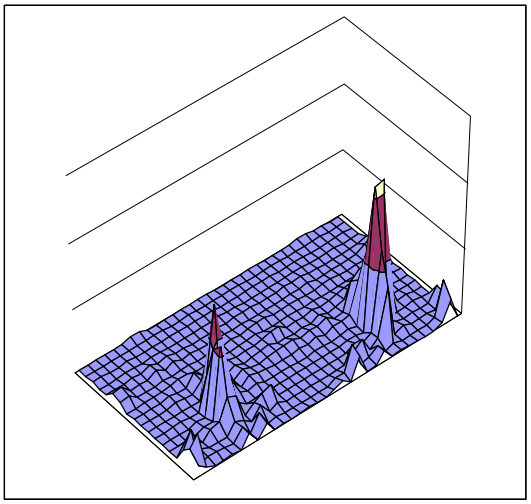

(d) Maximum F3, t = 72.1 msec; d = 650 mm.

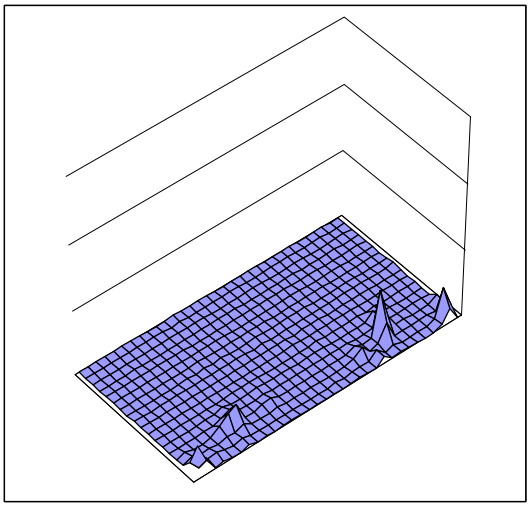

(e) During rebound, t = 100.0 msec; d = 638 mm.
Figure 6. Load distribution plots for test 6947 – 2006 Ford F-250.

GEOMETRIC COMPATIBILITY METRICS

There are several metrics other than AHOF400 that attempt to assess the geometric compatibility of automobile structures. There have been several developed that are based on a load cell barrier with 125x125 mm load cells with the boundary between two rows (nominally rows 3 and 4) set at the centerline of the Part 581 zone. The bottom of the 144 load cell array (nine rows by 16 columns) is nominally 80 mm above the ground surface. The criteria associated with these metrics usually dictate whether a secondary energy absorbing structure (SEAS) is recommended.

Nagoya Criterion

Nagoya University [3] proposed a compatibility criterion for the 144 load cell array. Under the assumption that the engine does not affect the distribution of impact forces until after the total force reaches 200 kN, the criterion evaluates the total load in the nominal third and fourth rows of the load cell barrier (F3 and F4) at the point when the total barrier load first reaches 200 kN. The criterion first requires that the sum of F3 and F4 exceed 80 kN. It then requires that the ratio of F3 to (F3+F4) be between 0.2 and 0.8, which nearly assures that the center of force for these rows is in the Part 581 zone. If these two conditions are met, the criterion indicates that the structure does not require a secondary energy absorbing structure (SEAS).

As part of the analysis of the tests with the enhanced load cell barrier, the load within the Part 581 zone (F581) was explicitly estimated using the method

described by Equation 3 above. Table 2 exhibits the calculated Nagoya Criterion parameters for the enhanced load cell barrier tests.

The main criterion (that F3+F4 is greater than 80 kN at the point when total load is 200 kN) is easily met for five of the six vehicles. Further, in four of these cases, the value is in fact more than 90% of the total load. In fact, in these four cases, moment calculations imply that more than half of the total load is reacted within the Part 581 zone itself. The Chevrolet Silverado exhibits a concentration of load in Row 4, indicating insufficient alignment of the load with the Part 581 zone.

Table 2. Nagoya Criterion Parameters for Enhance Load Cell Barrier Tests.

Test	6945	6946	6947	6948	6982	6983
Vehicle	2003 Honda Odyssey	2005 Honda Odyssey	2006 Ford F-250	2007 Chevrolet Silverado	2006 Honda Ridgeline	2002 Ford Focus
Time to 200 kN [sec]	0.01200	0.00984	0.00640	0.00672	0.00736	0.00848
Total Force [kN]	201.7	203.7	204.1	200.7	204.8	201.9
F3+F4 [kN]	193.4	184.4	45.9	97.9	187.0	199.3
F3/(F3+F4)	0.469	0.537	0.213	0.017	0.297	0.579
$F581^{total}$ [kN]	133.7	130.4	19.8	*	123.3	116.0
$F581^{lower}/F581^{total}$	0.410	0.409	0.291	*	0.437	0.550
SEAS needed?	No	No	Yes	Yes	No	No

*Moments at this point implied a small tensile value for $F581^{upper}$ for the Chevrolet Silverado, indicating a concentrated load just above the Part 581 zone.

The Nagoya criterion asserts that there is a necessity for a SEAS for the Ford F-250 and the Chevrolet Silverado. Only a small fraction of the load is reacted in Rows 3 and 4 or the Part 581 zone. A SEAS is necessary to provide some measure of compatibility between these models and most other vehicles. These vehicles do in fact have a SEAS, but, as mentioned earlier, it is difficult to evaluate the effectiveness of these SEAS structures through a rigid barrier crash test.

The Nagoya criterion could easily be modified for use with a moment-measuring load cell barrier. Rather than requiring a certain fraction of the total load (40%) to be in the measurable vicinity of the Part 581 zone and an indication that the geometric center of that load be within the Part 581 zone, the criterion could be simplified to require a specific fraction of the load to be reacted in that zone. Further research could be conducted to recommend a particular threshold, most likely in the 20% to 50% range.

Japanese Automobile Manufacturers Association (JAMA) Criterion

The Japanese Automobile Manufacturers Association (JAMA) also proposed a criterion [4] to evaluate the necessity of SEAS. The JAMA criterion evaluates the total force level in the nominal third and fourth rows (F3+F4) once the "central column force", F_c, reaches a critical value. F_c is defined as the sum of all forces in the four central columns of load cells. Once again, the F3+F4 quantity appears to be a proxy for the Part 581 load, which can be estimated far more accurately with a moment-measuring load cell barrier. JAMA did not propose a critical value for F_c.

In the crash tests, the value of F_c generally tracked the F3+F4 parameter closely until a certain load level and then stabilized or decreased while the F3+F4 rose substantially. The behavior observed for the Honda Ridgeline (Figure 7) is typical. The maximum value of F3+F4 at the critical value of F_c depended strongly on whether that critical value of F_c was greater than the local maximum of F_c experienced in the early segment of the test. For example, it can be seen in Figure 7 that F3+F4 would be close to F_c, if F_c were less than about 75 kN, but if a larger value of F_c were used, F3+F4 would be in the 400 to 500 kN range.

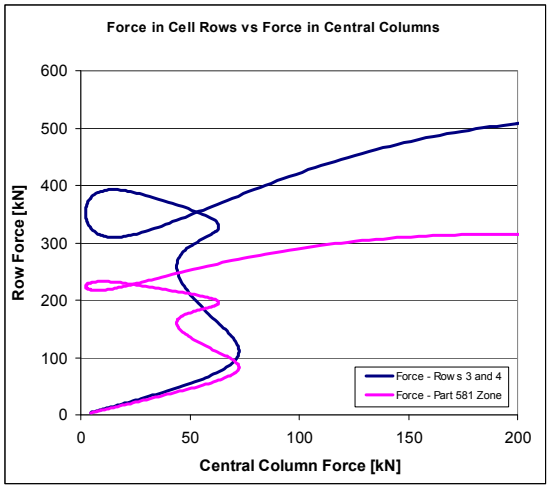

Figure 7. Row forces in the Part 581 region vs. central column force for the 2006 Honda Ridgeline.

The load-vs.-load curves in Figure 7 can be difficult to interpret. In general, the close correlation at low loads (less than about 50 kN) implies that the load in Rows 3 and 4 is primarily in the Part 581 zone. The fact that F581 and F3+F4 track F_c implies the load in the central columns above and below the considered rows is on the same order of magnitude as the load in those rows to either side of the center. This is not surprising, as one can imagine that at these low loads, the central section of the Part 581 structure reacts virtually all of the crushing loads. Eventually, significant loads are reacted by all components of the vehicle front structure. It is not surprising that during the intense crushing segment of the crash event, the load cells in the third and fourth rows pick up significant load outside the Part 581 zone (eventually including engine deceleration load) and therefore F3+F4 starts to exceed F581 by a significant factor. Nonetheless, even though the Part 581 zone is approximately 40% of the area of Rows 3 and 4, it is often calculated to react more than half of the F3+F4 load.

The stabilization or reduction of F_c is indicative of the transfer of load into the stiffer load paths through the vehicles side rail structure. Thus, the selection of a critical value of F_c implies an acceptable amount of central load that should be attained before this transition commences. The consequence of choosing a consistent value or a vehicle mass-specific value should be carefully considered.

CONSISTENCY OF AHOF400 RESULTS

Five of the six advanced load cell barrier tests were completed for virtually the same vehicles used in previous 125x125 mm single axis high resolution barrier cases. A 2007 Chevrolet Silverado was previously tested against a rigid barrier with 250x250 mm single axis load cells and yielded some anomalous data. Thus, no direct comparisons were possible for that model. The values of the AHOF400 for the remaining vehicles are given in Table 3. The two virtually identical high-resolution barrier test series provide an opportunity to evaluate the consistency of AHOF400.

Table 3. Comparison of AHOF400 in Similar Crash Tests.

Vehicle	Test No.	4x9 Single Axis 250x 250 mm Barrier AHOF 400	Test No.	9x16 Single Axis 125x 125 mm Barrier AHOF 400	Measured Height of Top and Bottom of Structure	Test No.	9x16 125x125 mm Barrier With Moments AHOF 400		Measured Height of Top and Bottom of Structure
							Without Moment	With Moment	
2002 Ford Focus	4216	436 mm	5712	448 mm	512-402 mm	6983	433.4 mm	435.0 mm	531-423 mm
2003* Honda Odyssey	4463	443 mm	5144	454 mm	508-388 mm	6945	438.5 mm	434.9 mm	498-390 mm
2005 Honda Odyssey	5273	450 mm	5714	451 mm	486-382 mm	6946	436.7 mm	430.5 mm	500-400 mm
2006 Honda Ridgeline	-	-	5715	548 mm	553-529 mm	6982	503.8 mm	506.9 mm	578-487 mm
2006 Ford F-250	-	-	5820	693 mm	742-611 mm	6947	688.3 mm	685.7 mm	765-630 mm
2007 Chevrolet Silverado	-	-	-	-	-	6948	563.3 mm	570.1 mm	544-444 mm

* Test 5144 was of a 2004 Honda Odyssey.

The AHOF400 values do not agree as closely as one might hope between the two sets of tests. In three of the five cases, the additional moment data reduces the discrepancy. The Honda Ridgeline experienced a difference in AHOF400 of 44 mm, which is a significant fraction of the height of the Part 581 zone (102 mm). In the remaining cases, the difference in (non-moment adjusted) AHOF400 between the two tests was 15 mm or less. This result leads to several questions. First, would the consistency have been enhanced if the moment adjustment had been available in all test series? Second, is 15 mm within the normal variability one can expect for AHOF400 in this type of test? And third, what factors can lead to the discrepancy on the order of magnitude observed for the Honda Ridgeline?

CONCLUSIONS

The addition of moment channels to the high resolution load cell barriers yields more information about the structural response of a vehicle in a vehicle-to-barrier crash test. In particular, it theoretically eliminates error in the AHOF400 calculation and it allows a more direct estimate of the forces directly in the Part 581 zone. The better representation of the Part 581 load could aid in the enhancement of the various compatibility criteria (e.g., Nagoya, JAMA, VNT) by the reduction of uncertainties from the non-Part 581 zone loads in the total row loads for the third and fourth rows (F3 and F4).

The ability to visualize an even higher resolution force pattern further aids assessment of the structural interaction during the crash event. In particular, it helped with the visualization of the effect of the SEAS late in some of the rigid barrier tests. Nonetheless, the effectiveness of SEAS devices that are displaced behind the primary energy absorbing structures may be easier to assess in vehicle-to-vehicle and vehicle-to-deformable barrier tests.

Other than visual enhancement and in the local region of the side rail impingement, the data for the moment about the vertical axis (M_z) does not significantly improve the understanding of the crash event and, in situations in which data acquisition resources are limited, might be comfortably sacrificed in lieu of redundancies for more important data channels.

In the analysis of the current tests, the calculated value of AHOF400 did not change substantially (less than 7 mm) as a result of the additional moment data.

Nonetheless, the 125x125 mm load cells do provide a smaller theoretical maximum error in computed AHOF400 than 250x250 mm load cells. Therefore, any further improvement is notable.

For all of the vehicles except the Chevrolet Silverado, the values of AHOF400 found with and without using the moment data were within the range of actual measured heights of the bumper structure.

When AHOF400 was evaluated over two sets of virtually identical tests, there was some lack of consistency. The discrepancies (on the order of 15 mm) may simply be the normal scatter in an assessment of this type. The additional accuracy derived from the moment data should minimize this test-to-test variation. Nonetheless, an improvement of 7 mm in measurement for which 15 mm of scatter is typical will be helpful but will not define system accuracy.

REFERENCES

[1] Patel S., Smith D., Prasad A., (NHTSA) and Mohan P., (The George Washington University), "NHTSA's recent vehicle crash test program on compatibility in front-to-front impacts". 20th ESV Conference, Paper No. 07-0231.

[2] Mohan, P., Marzougui, D., and Kan, C. D., "Modified Approach to Accurately Measure Height of Force (HOF)," Paper 2007-01-1182, SAE World Congress, Detroit, 2007.

[3]Evaluation Method of Ground Heights of Front Rail Based on Full Rigid Barrier Tests, Nagoya University presentation, September 2008.

[4] Japanese Automobile Manufacturers Association, "JAMA Stance on Compatibility Test Method," Mizuno, K., June 28, 2008.

[5] Mizuno, K., Yamazaki, K., Araia, Y., and Notsu, M., "Japan Research on Compatibility Improvement and Test Procedures," Paper 05-185, Nineteenth Enhanced Safety of Vehicles Conference, Washington, DC, 2005.

USE OF SECONDARY ENERGY ABSORBING STRUCTURES FOR IMPROVED SELF PROTECTION PERFORMANCE – EXPERIENCES DURING THE DEVELOPMENT OF A CHASSIS BASED VEHICLE

Ganesh Gadekar
Anil Kumar C
Ashok G Joshi
Makarand Takle
Tata Technologies Ltd. (Deputed to Tata Motors Ltd.)
India
Paper Number 11-0283

ABSTRACT

Secondary Energy Absorbing Structures (SEAS) have been discussed in literature in the context of improving geometric compatibility between larger vehicles like SUVs and cars. While compatibility related work is still in a research phase, development of the vehicles for self protection remains a priority. Vehicles also have to be designed to meet set targets against consumer group tests like Euro NCAP.

A Secondary Energy Absorbing Structure on a Crossover kind of vehicle was evaluated to see the effect on self protection. Through the evaluation it was realized the SEAS can actually be optimized for improving the self protection and lead to reduced weight of the chassis frame. This concept was optimized to achieve weight savings in EuroNCAP load case.

This paper presents the results of evaluations, analysis of the reasons why SEAS is expected to lead to weight savings in a typical offset frontal crash along with the optimization work carried out for achieving weight savings.

INTRODUCTION

In case of crash scenario for effective occupant protection, the structural crash behavior of the vehicle has to fulfill requirements like controlled energy absorption, structural integrity of the passenger compartment, limited intrusions in passenger cell and so on. These crash safety requirements resulted in significant weight addition on passenger car structures over last decade. Figure 1 show the weight spiral for European compact cars [1] where vehicle weight has significantly increased due to stringent legal/consumer group safety requirements and change in customer demands for growing vehicle size and comfort. However, this increased vehicle mass adversely impacted vehicle fuel efficiently and CO2 emissions due to increased energy consumption.

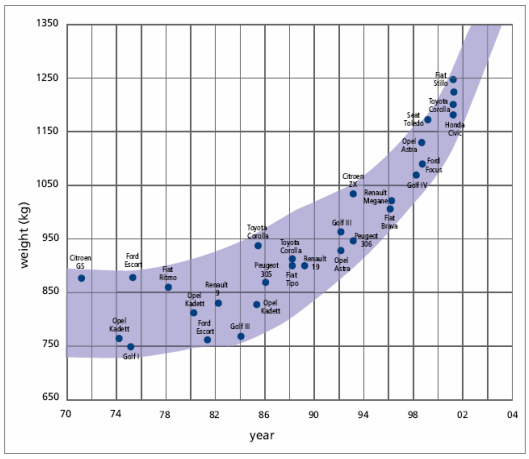

Figure 1. Weight spiral for European compact cars (Source: "Aluminium in Cars" Report by European Aluminium Association)

Today various light materials are being getting evaluated to reduce the weights of vehicle structures example include Aluminum, Magnesium Titanium etc. However the required weight reduction is not going to realized only through substitution of heavy materials by lighter ones unless it supported by appropriate new design and manufacturing design concepts. In this paper the concept of secondary energy absorbing device (SEAS) is being proposed which helped to achieve light weight design for chassis frame for body over chassis type crossover vehicle. In past Secondary Energy Absorbing Structures (SEAS) have been discussed in literature in the context of improving geometric compatibility between larger vehicles like SUVs and cars [3]. However no standard procedure has been defined yet to evaluate the compatibility aspects. The occupant protection in test conditions like ODB64 and FF56 is still area of focus for crash safety engineers. In this study emphasis was put on achieving weight reduction through introduction of new design concepts rather than using high strength steels and advanced

manufacturing techniques like laser welding. The vehicle design was evaluated against EuroNCAP ODB64 crash performance requirements. (Refer EuroNCAP Frontal Impact Testing Protocol Version 5 October 2009)

FRONTAL CRASH PERFORMANCE OF BODY OVER CHASSIS FRAME VEHICLES

In frontal crash accident scenario for body over chassis frame vehicle, chassis frame acts as main load bearing member. The front end of the chassis frame is designed to absorb significant amount of energy of impact (It is observed that in most cases chassis frame contributes up to 60% of energy by vehicle for vehicles providing reasonably good occupant protection). The general design strategy for chassis frame for crash application is depicted in Figure 2

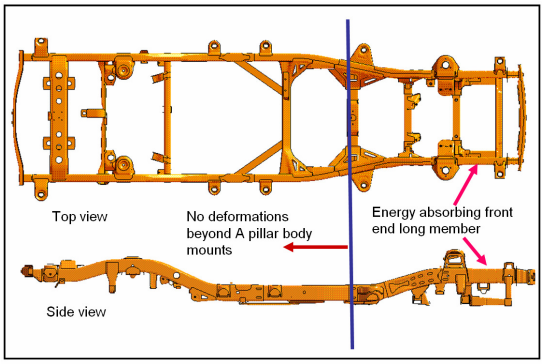

Figure 2. Chassis frame design strategy for offset frontal impact scenario

The chassis frame front long members are designed for optimum energy absorption targeting axial collapse mode. Once frame front end is collapsed during the early phase of crash, no deformations are intended beyond A pillar body mount area to ensure the structural integrity of passenger compartments without any significant structural intrusions. (Refer Figure 2) The special attention is required while designing frame stiffness in front crank area such that while frame front long member is deforming for energy absorption, front crank area should not deform. Second aspect is that frame should not interact with foot well or firewall area due to crank area deformations and struck side wheel should move straight rearward resting against side sill (rocker panel) rather interacting with weak footwell area.

CHASSIS FRAME DEFORMATIONS IN FRONT SWAN NECK AREA IN FRONTAL IMPACTS

While designing chassis frame for frontal crash applications especially for offset frontal impacts major challenge is to achieve required crash performance with minimum possible structural weight for chassis frame. While designing the chassis frame under consideration for frontal crash requirements large weight addition was resulted on chassis frame long members in front swan neck area. This was typically because while chassis frame front end is deforming, large bending moment (My) acts on frame front swan neck area leading to tendency of vertical frame bending of the frame in swan neck area. This is due to the vertical offset between frame long member part in frame front and in swan neck area (Refer Figure 3).

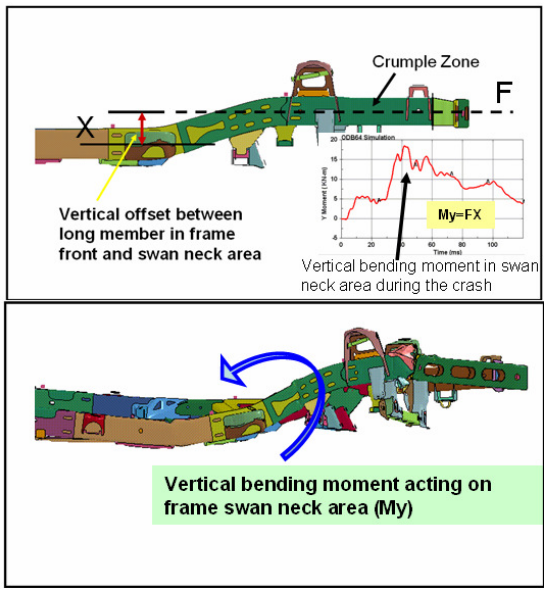

Figure 3. Frame deformations in front swan neck area due to vertical bending moments.

Apart from vertical bending in swan neck area, the chassis frame also deforms laterally in front swan neck area. This lateral bending of the chassis frame is due to moment Mz acting on the frame due to loads through front wheel as shown in the Figure 4.

Hence in order to reduce weight of the chassis frame in swan neck area the concept of SEAS was thought as a solution to this problem. It was expected that SEAS would reduce vertical bending moment acting on frame swan neck area thereby reducing reinforcement requirement in swan neck area. The proposed SEAS do not contribute to reduce lateral bending of the frame in swan neck area. The controlled lateral bending in swan neck area is desirable and helps to achieve energy absorption during the crash. However vertical bending of the frame is not at all desirable as it causes large loads on body structure leading to unstable passenger compartment of the vehicle during the crash.

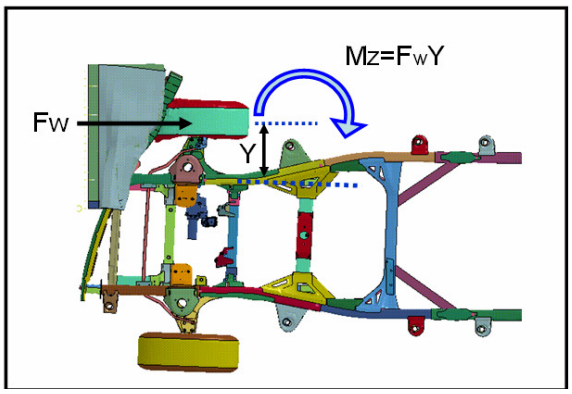

Figure 4. Lateral frame deformations in front swan neck area due to Mz bending moments.

SECONDARY ENERGY ABSORBING STRUCTURE (SEAS) FOR CHASSIS FRAME

Figure 5 shows schematic of SEAS concept which is expected to reduce vertical bending moment on chassis frame crank area by providing parallel load path for crash energy management.

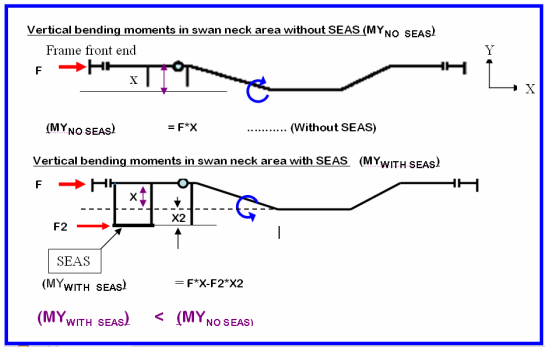

Figure 5. Effect of SEAS on reducing vertical bending moment in swan neck area.

In case of chassis frame design without SEAS, impact load (F) through long member results in vertical bending moments ($M_{Y\ NO\ SEAS}$) = F*X in frame crank area.
With introduction of SEAS, additional moment F_2*X2 acts in opposite direction resulting in ($M_{Y\ SEAS}$) < ($M_{Y\ NO\ SEAS}$) as shown in the Figure 5

As mentioned earlier the proposed SEAS do not affect lateral bending behavior of the frame in swan neck area

SIMULATION RESULTS FOR CHASSIS FRAME DESIGN WITH AND WITHOUT SEAS-VALIDATION OF SEAS CONCEPT

The chassis frame design which was analyzed as a part of this study is depicted in Figure 6.

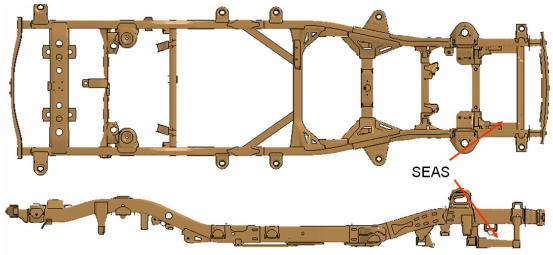

Figure 6. Chassis frame design studied for EuroNCAP ODB56 structural crash CAE.

This proposed design was analyzed in CAE for with and without SEAS (secondary energy absorbing structure) configurations. The forces and moments at long member, SEAS and front crank (swan neck) area (Refer Figure 7) were studied during the study in with and without SEAS configuration.

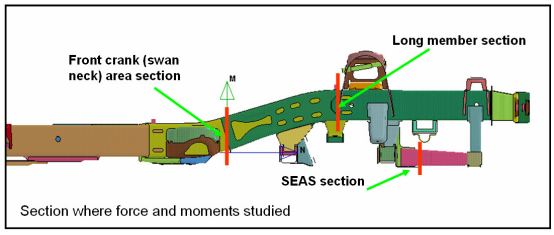

Figure 7. Frame front and crank (swan neck) area where forces and moments were studied.

The forces acting in longitudinal directions at long member and at SEAS cross section are shown in Figure 8.

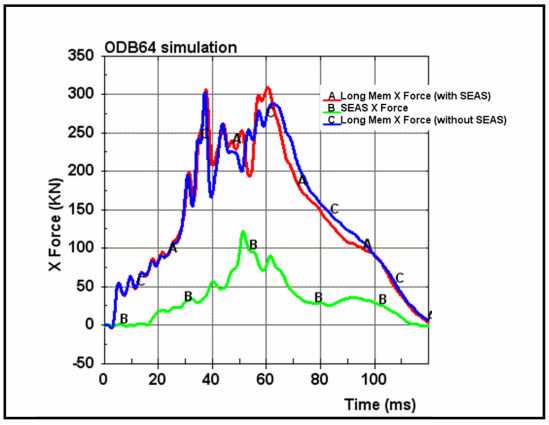

Figure 8. The forces acting in longitudinal directions at long member and at SEAS

It can be seen from the Figure 8 that current SEAS design offers average 70 KN resistance parallel to frame long member which offers average 250 KN resistance during this period. Thus SEAS acts as additional load path during early phase of crash, absorbing additional energy for chassis frame which is shown in Figure 9.

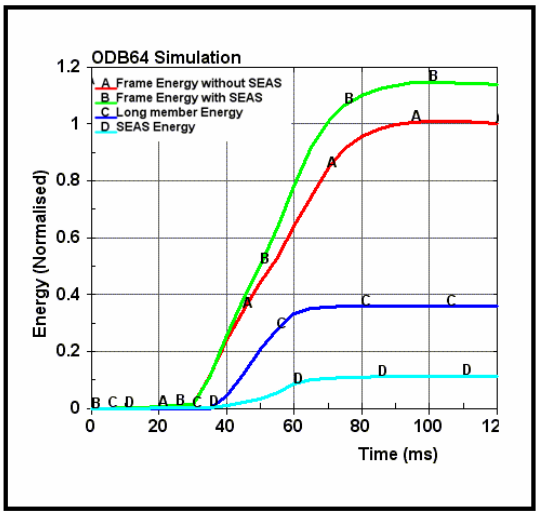

Figure 9. The Energy absorbed by chassis frame with and without SEAS design configurations

It can be seen that approximately 15% more energy absorption is observed for chassis frame with addition of SEAS. It helps to reduce inertia loading on the structure in later phase of crash.

Figure 10 shows the bending moments acting on chassis frame in front crank (swan neck area) area in with and without SEAS design configuration**.**

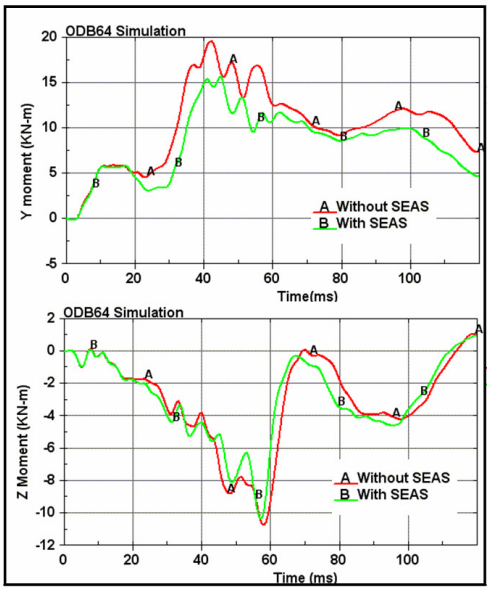

Figure 10. -Bending moments acting on chassis frame in front crank (swan neck area) area in with and without SEAS configuration.

It clearly seen that the bending moments about Y axis significantly reduces in case of design configuration with SEAS in place. This reduces the tendency for vertical bending of chassis frame in front crank (swan neck area). The vertical bending of the chassis frame is not desirable as it increases tendency of vehicle pitching leading to increased loading on BIW structure (risk of more intrusions passenger compartment.)

Figure 11 shows the comparison of vehicle deformation pattern in with and without SEAS design configuration along with frame Z bending measured at frame front swan neck area. It is clearly seen that without SEAS in place the Z bending in the swan neck area has increased by 10 % resulting in increased loading in Body structure causing high deformation in BIW cantrail area near C pillar (Refer Figure 11). More structural intrusions were observed in passenger compartment in without SEAS case. This difference in intrusion values is similar to order of difference that observed for Z bending of frame in swan neck area.

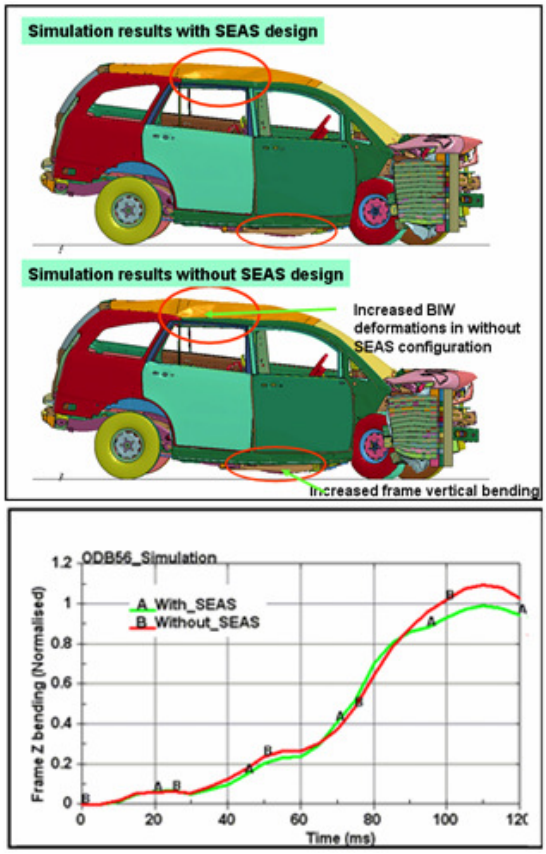

Figure 11. Comparison of vehicle deformation pattern in with and without SEAS design configuration.

The deceleration pulse of the vehicle measured at vehicle B pillar bottom is shown in Figure 12. The peak deceleration observed to be increased by approx. 10 g in case of design without SEAS configuration. This result clearly show that concept of SEAS definitely help to achieve better crash energy management of the vehicle leading to

reduced vehicle intrusions and shock levels transferred to occupants. Thus simulation results have clearly highlighted the benefits of SEAS concept and its potential for lighter weight design for crash energy management.

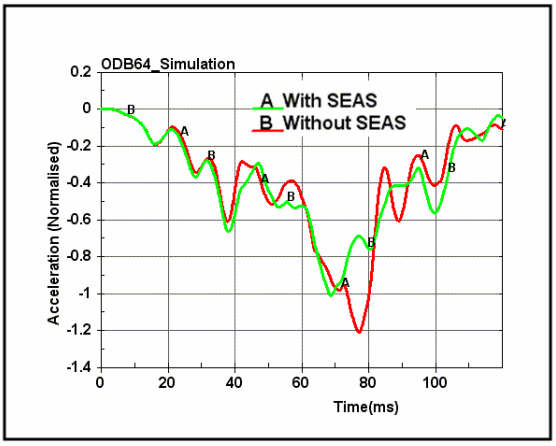

Figure 12. Comparison of vehicle deceleration pulse with and without SEAS design

WEIGHT SAVING ACHIEVED WITH SEAS CONCEPT

The concept of SEAS explained earlier helped to reduce chassis frame reinforcement's weight that were required around front swan neck area to meet structural targets for EuroNCAP offset frontal impact test at 64 kmph. Using proposed SEAS concept, through CAE based design optimization, almost 15 kg weight was saved in frame front swan neck area. The weight of the SEAS assembly in the final chassis frame design is 8 kg. Thus effectively 7 kg weight was saved in chassis frame design.

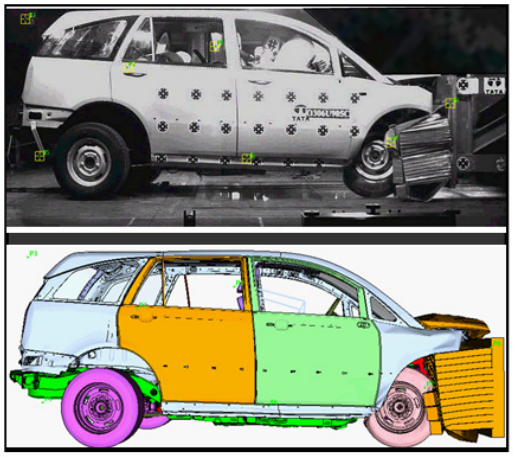

Figure 14. Comparison of vehicle structural deformation in EuroNCAP offset frontal impact test (test vs. CAE prediction).

The provision of SEAS device also helped to reduce 5 kg weight in BIW A pillar and cantrail area as SEAS helped to reduce impact loading on BIW as vertical bending deformations of chassis frame in front swan neck are controlled . Overall concept of SEAS saved 12 kg weight on complete vehicle to meet structural targets of EuroNCAP offset frontal test. The final vehicle design met target EuroNCAP crash performance as shown in Figure 14

CONCLUSIONS:

In the present study the concept of secondary energy absorbing device (SEAS) is proposed and it's benefits are demonstrated through full vehicle crash simulation results. The proposed SEAS concept reduces vertical bending moments in chassis frame swan neck area during the frontal impact scenario thus providing opportunities for light weight design concepts for chassis frame design. The proposed SEAS concept is implemented in Crossover vehicle program and approximately 12 kg weight reduction is achieved for complete vehicle for offset frontal crash requirements. The proposed SEAS concept also likely to improve the compatibility aspects of the vehicle crash performance which is not evaluated in this study.

REFERENCES

[1] Aluminium in Cars" Report by European Aluminium Association 2009, www.aluminium.org

[2] T Dutton, S Iregbu, R Sturt, A kellicut, B Cowell and K Kavikondala," The effect of forming on the crashworthiness of the vehicles with hydroformed frame siderails" SAE 1999

[3] Chung Kyu Park, Robert Thomson,Aleksandra Krusper, Cing Dao (steve) Kan,"The influence of subframe geometry on a vehicles frontal crash response ", ESV Paper 09-0403

[4]LSTC "LSDYNA User's manual version 971 May 2007, Livermore Software Technology Corporation.

FRONT AND SIDE CAR-TO-CAR CAE BASED CRASH ANALYSIS OF DIFFERENT CLASS VEHICLES

Jangho Shin
Advanced Safety CAE Team/Hyundai Motor Company
Republic of Korea
Haeng Kyeom Kim
Yun Chang Kim
Platform Development Team/Hyundai Motor Company
Republic of Korea
Paper Number 11-0073

ABSTRACT

In recent years, rapid-increasing market share of compact cars and SUVs has brought for both consumer and automaker to pay more attention on crash compatibility between the compact passenger vehicles and the light trucks (i.e., Pickups and SUVs). Vehicle compatibility regarding both self and partner protection in frontal crash of different class vehicles is one of hot issues in vehicle safety. Furthermore, it is expected that the amendment of UNECE-Regulation 94 to implement compatibility issues in couple of coming years. This paper presents front and side car-to-car CAE based crash of different class vehicles which describes a car accident in real field. Structural engagement and energy balance of different class vehicles in front and side car-to-car crash are identified. In this study, conceptual design of compatibility compliant frontal vehicle structure which subjects to improve the distribution of frontal crash loading and structural engagement between vehicles is introduced. The effects of proposed vehicle structure on possible candidates (i.e. FWRB, FWDB and PDB) for a compatibility evaluation test procedure and car-to-car crash are also investigated.

INTRODUCTION

SUVs and light trucks have a bad reputation as being incompatible with smaller vehicles in frontal crash. Indeed, those vehicles' aggressivity or incompatibility has been a thorny issue for many years and has been the subject of research both in Europe and the US. As well as protecting the occupants of a vehicle from the effects of a crash (self protection – i.e., NCAP), the protection of occupants in the colliding vehicles (partner protection) is on the Euro-NCAP road map and has been voluntarily committed to in the North American market.

Historically the most important factor for car crash compatibility was the vehicle mass ratio. Recently various studies and research have paid more attention on geometric alignments of vehicle front structure in car-to-car crash. To identify structural interaction of front structures and assess partner protection performance there is currently couple of test procedure candidates, which are expected to form the basis for future legislation and/or consumer testing to improve compatibility: proposed by EEVC WG15 [1] and NHTSA [2]. As well as evaluating the occupant injuries and compartmental deformation, the new compatibility metrics evaluate structural interaction and load distribution. For each of candidates a set of metrics has been proposed, defined and await finalization following the correlation between the proposed metrics and the added partner protection in the field.

This paper presents conceptual design of compatibility compliant frontal vehicle structure which subjects to improve the distribution of frontal crash loading and structural interactions between vehicles. The effects of proposed vehicle structure on possible candidates for a compatibility evaluation test procedure (i.e. FWRB, FWDB and PDB) are investigated by CAE simulation. In this study, Front and side car-to-car CAE based crash of different class vehicles which describes a car accident in real field has been conducted. The interactions of proposed frontal vehicle structure and energy balance in front and side car-to-car crash are also investigated.

COMPATIBILITY COMPLIANT VEHICLE STRUCTURE

Various studies show that frontal crash performance of a vehicle is significantly affected by interaction and stiffness of frontal structures [3]-[4]. In general the longitudinal members of large vehicles are inclined to higher than those of smaller vehicles. Additionally the horizontal misalignment of longitudinal members in frontal crash between different size vehicles can also occur because of their mismatch in design layout. When the crash members of vehicles miss each other, they fail to absorb enough crash load. Furthermore it could result in a severe deformation of passenger compartment or a penetration of smaller vehicle's cabin by missed longitudinal members [5].

Figure 1 shows baseline structure and concept design of

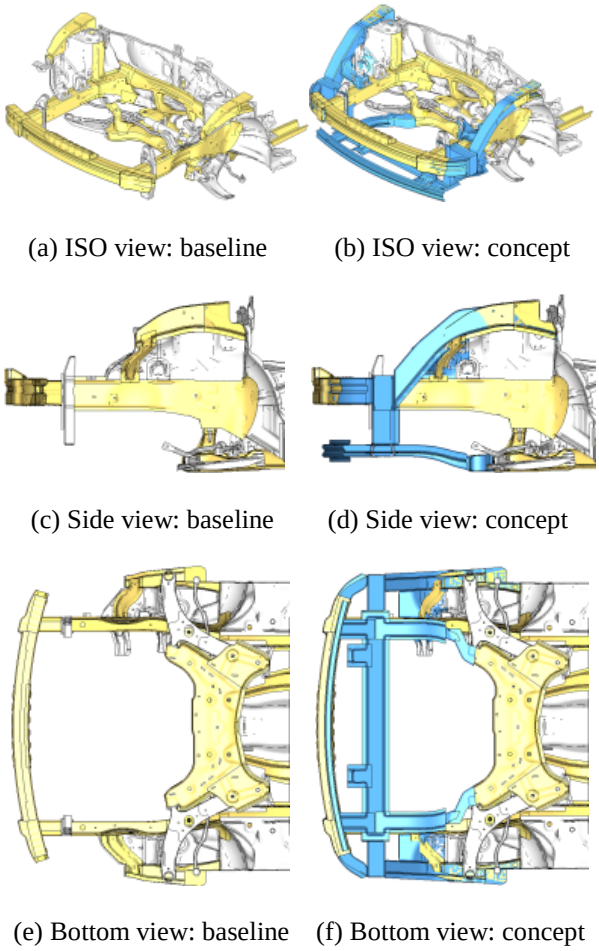

(a) ISO view: baseline (b) ISO view: concept

(c) Side view: baseline (d) Side view: concept

(e) Bottom view: baseline (f) Bottom view: concept

Figure 1. Baseline and concept design of compatibility compliant vehicle structure.

compatibility compliant vehicle structure. In concept structure, the connectivity of structure is improved as shown in the figure; lower members are added, front bumper rail is widen and coupled with fender. Lower members are elongated to front end as much as it can and also has its bumper rail to improve structural interactions at the initial crash stage.

In baseline, most of crash loadings are simply concentrated on the longitudinal members. By increasing loading path, the compatibility compliant vehicle structure has better uniform crash loading distribution characteristics than baseline vehicle structure which means the homogeneity of vehicle structure is improved. Another distinct feature of compatibility compliant vehicle structure is improving structural interactions between vehicles.

In order to clarify whether the presence of the lower member can be detected Full-Width Rigid Barrier test, Full-Width Deformable Barrier test and Progressive Deformable Barrier test have been conducted by CAE simulation [6]-[8].

Full-Width Rigid Barrier Test

In FWRB test, 125mm by 125mm high resolution load cells were used. The ground clearance of load cell barrier was 80mm as recommended by IHRA (International Harmonized Research Activities) Phase 1a [6]. The impact velocity of vehicles was set at 56km/h.

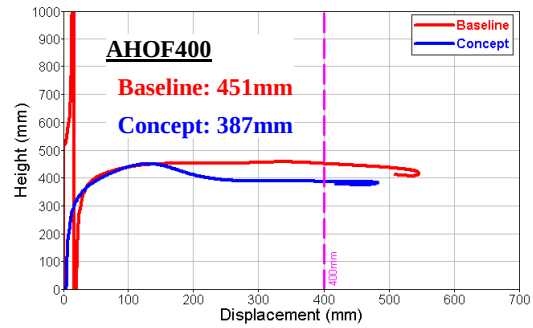

Figure 2. AHOF-displacement curves.

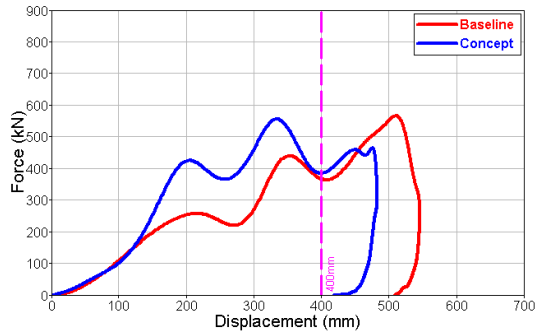

Figure 3. Total barrier force-displacement curves.

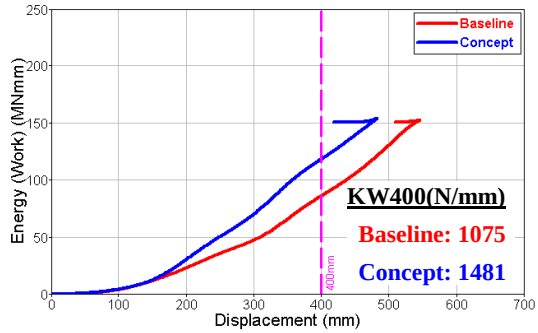

Figure 4. Energy-displacement curves.

Average Height of Force (AHOF)-displacement curve was shown in Figure 2. The AHOFs, which were calculated from displacement up to 400mm (AHOF400), was 451mm for baseline, and it decreased to 387mm for concept due to the presence of lower member. The coupling of bumper rail with fender apron

and elongated lower member which strengthen the stiffness of front end structure result in increasing of total barrier force up to 400mm and KW400 (Figure 3-4). This means better crash loading support at the early stage of impact.

Full-Width Deformable Barrier Test

The deformable barrier face used in FWDB test has two layers [7]. The first layer consists of a 0.34MPa aluminum honeycomb, and the second layer consists of a 1.71MPa element. The impact velocity was set at 56km/h.

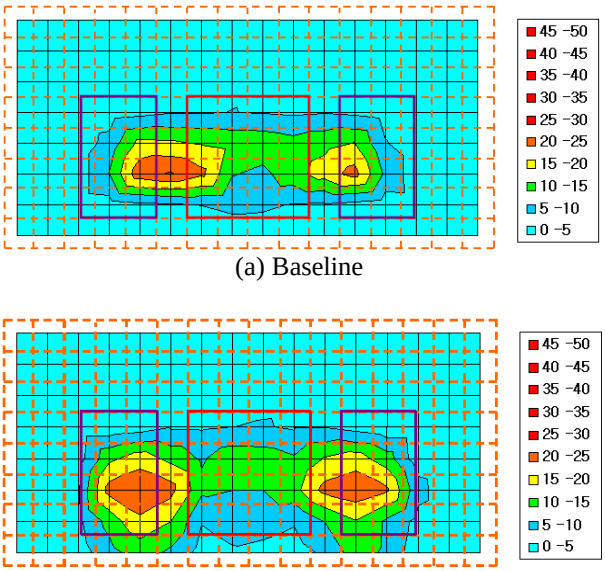

(a) Baseline

(b) Concept

Figure 5. Peak load cell distributions.

Figure 5 shows peak load cell force distributions of baseline and concept vehicle structures. It was observed that the force on the area of longitudinal members was large for both cases. As shown in figure, peak cell force for concept has wider area than that for baseline. This means concept vehicle structure has better homogeneity. Besides, the forces of 1st and 2nd rows for concept vehicle structure were generated by the lower member, which were not shown for baseline.

The Horizontal Structural Interaction (HSI) and Vertical Structural Interaction (VSI) in the assessment area for rows 2 to rows 5 are shown in Table 1-2. As shown in Table 1, outer support parameters of row 3 and row 4 for concept vehicle structure were lowered. This means concept vehicle structure has better horizontal homogeneity than baseline as above mentioned. In Table 2, minimum support of row 2 was lowered to zero which implies the presence of lower member and the force generation by the lower member are identified.

Table 1.
Structural interaction criteria
: horizontal structural interaction

	Baseline		Concept	
	Center Support	Outer Support	Center Support	Outer Support
Row 5	0.0	0.5	0.0	0.8
Row 4	0.0	2.5	0.3	1.0
Row 3	1.4	2.4	3.0	0.4
Row 2	0.0	0.6	2.6	0.1

Table 2.
Structural interaction criteria
: vertical structural interaction

	Baseline		Concept	
	Minimum Support	Load Balance	Minimum Support	Load Balance
Row 5	49.5	0.5	58.8	0.4
Row 4	0.0		0.0	
Row 3	0.0		0.0	
Row 2	42.8		0.0	

Here again, the presence of lower member on proposed conceptual design of compatibility compliant vehicle structure was clearly detected in FWDB test. Better crash loading support by the lower member is also demonstrated.

Progressive Deformable Barrier Test

Test conditions for PDB (60km/h, 50%) are used in this study [8]. The points that differed from the current ODB test conditions were the barrier structure, impact speed and overlap ratio.

The deformed shapes of barrier caused by each test vehicle are shown in Figure 6. It only shows a slight difference on PDB deformations. It is shown the results in these figures that the most of barrier deformations are caused by the engine and the transmission in both cases. It means that even though a lower member does play a great role on the early stage of crash, the existence of lower member was not detected.

The test results obtained for each vehicle in terms of the ADOD, AHOD and maximum barrier deformation are given in Table 3. The results show that AHOD is slightly lowered. The presence of a lower loading path is considered as an important factor with respect to compatibility. However, no significant difference is seen in AHODs. These results imply that it is difficult to detect or identify the presence of a lower member by AHOD alone. ADOD values also show no significant difference. The results indicate the ADOD is

dominantly influenced by the mass of vehicles rather than the characteristic of vehicle structure.
In PDB test, the effect of proposed conceptual vehicle structure is slightly shown. It is due to the final deformed shape of barrier is only considered in PDB test. It is required that other assessment parameters which can detect or identify the presence of member for improving structural interactions.

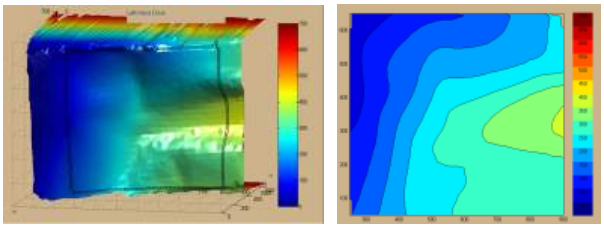

(a) Baseline

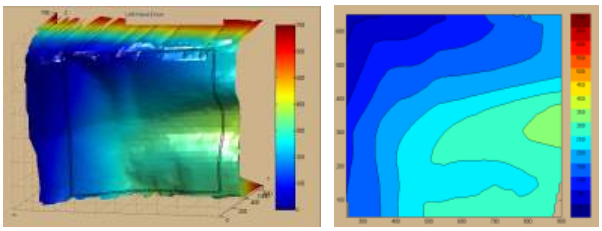

(b) Concept

Figure 6. PDB deformations.

Table 3.
Partner protection parameters for PDB

	Baseline	Concept
ADOD(mm)	246	227
AHOD(mm)	322	310
Dmax(mm)	407	372

FRONTAL CAR-TO-CAR CRASH

Frontal offset car-to-car crash test was performed as shown in figure 7: one is a midsize sedan (1465kg) and the other is a subcompact car (1060kg). The impact velocity was 56km/h for both vehicles and the overlap ratio was 50% of the smaller car (subcompact).
Figure 8 shows the front structural components for baseline vehicles and concept vehicles for respectively. In case of baseline vehicles, both midsize and compact cars have longitudinal members and bumper rail to absorb crash energy. For concept vehicles, lower members are added, front bumper rail is widen and coupled with fender to improve structural interactions. In the crash test, there existed geometric misalignments of the longitudinal members in the horizontal and vertical directions between vehicles. Consequently, the longitudinal members are vertically and horizontally missed each vehicles and the under ride of subcompact car was occurred in case of baseline vehicles (Figure 9-(a),(c),(e)). For concept vehicles, better structural interactions were shown than those of baseline vehicles. As shown in Figure 9-(b),(d),(f), vertical and horizontal mismatch of longitudinal members also exists. However, widen bumper rail and lower member result in better structural engagement in case of both lateral and vertical mismatch of longitudinal members. It is demonstrated that proposed concept vehicle structure is quite effective for structural interaction improvement at the early stage of car-to-car crash.

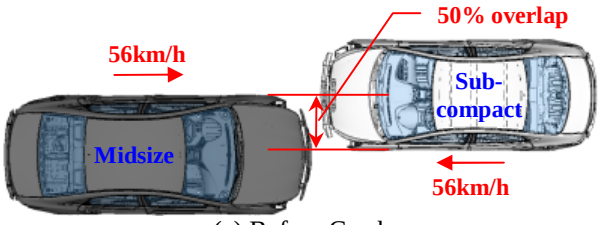

(a) Before Crash

(b) After Crash

Figure 7. Frontal car-to-car crash (both vehicles at 56km/h with 50% overlap of subcompact car).

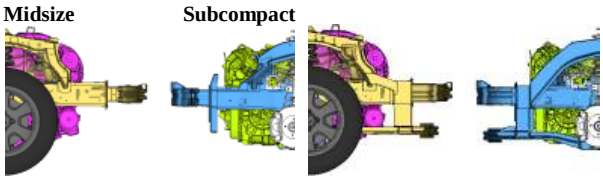

(a) Baseline (b) Concept

Figure 8. Geometric alignment of vehicles.

Figure 10 shows deformations of both vehicles in frontal car-to-car crash tests. For baseline vehicles, mismatch of longitudinal members results that lateral bending of member for midsize car occurred. In case of concept vehicles, the lower member and gusset of midsize car were engaged with the bumper rail of compact car which was vertically missed. The upper member of compact car which coupled with bumper rail was engaged with the bumper rail of midsize car as well. It is pointed that lower member of compact car was slightly deformed caused by the under ride of compact car.

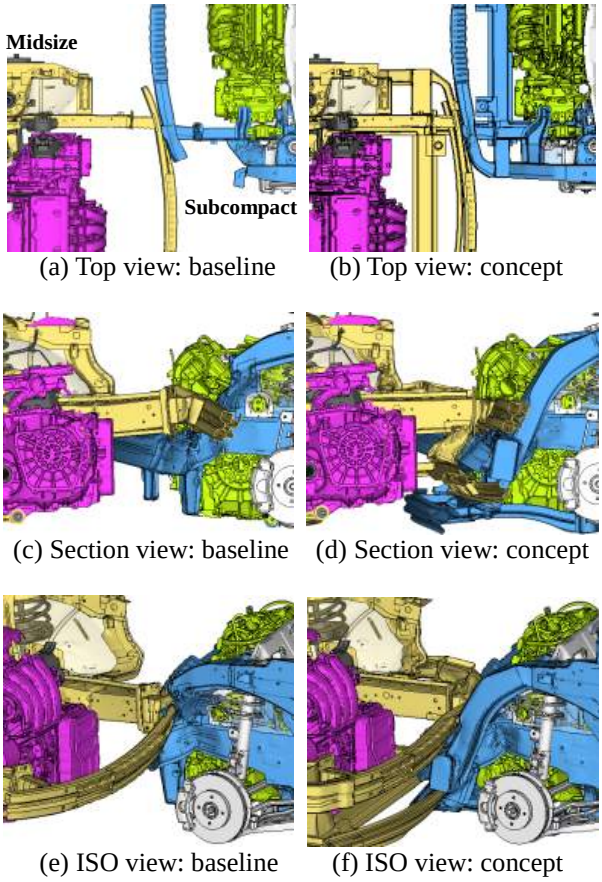

(a) Top view: baseline (b) Top view: concept

(c) Section view: baseline (d) Section view: concept

(e) ISO view: baseline (f) ISO view: concept

Figure 9. Structural engagements for frontal car-to-car crash.; (a)~(b): @10ms, and (c)~(f): @ 25ms

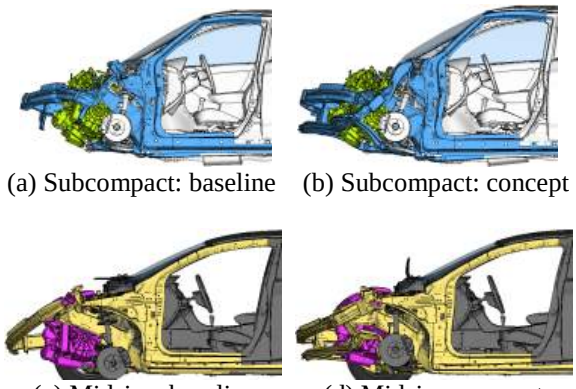

(a) Subcompact: baseline (b) Subcompact: concept

(c) Midsize: baseline (d) Midsize: concept

Figure 10. Deformations for frontal car-to-car crash.

Figure 11 shows deceleration curves for both midsize and compact cars. Due to the improvement of structural interactions at the early stage of crash for concept vehicles, not only initial deceleration values but also peak values were lowered for both midsize and compact cars.

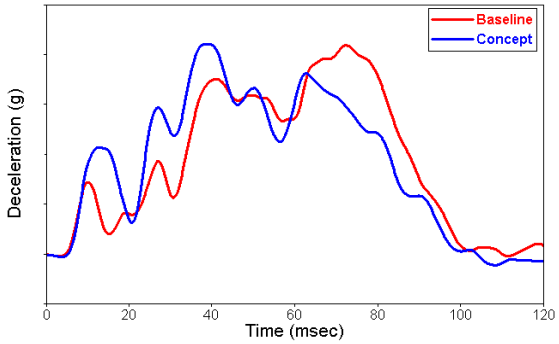

(a) Subcompact

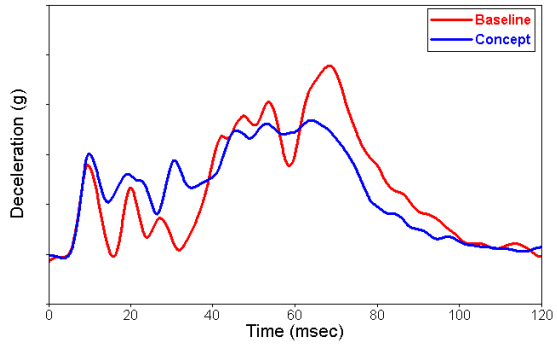

(b) Midsize

Figure 11. Deceleration curves for frontal car-to-car crash.

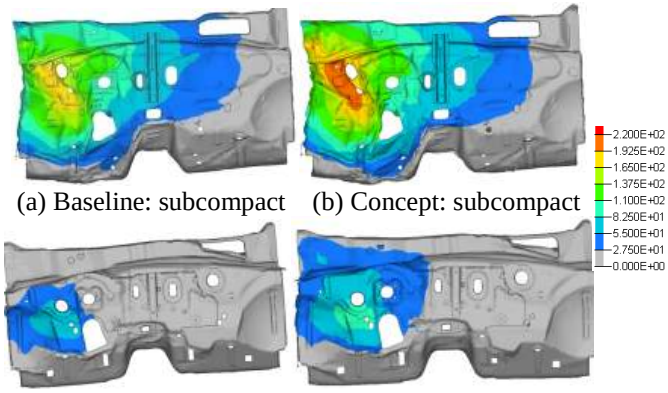

(a) Baseline: subcompact (b) Concept: subcompact

(c) Baseline: midsize (d) Concept: midsize

Figure 12. Dash intrusions for frontal car-to-car crash.

Figure 12-13 shows dash intrusions and vehicles deformations respectively. As shown in figure 12, dash local intrusions for both subcompact car and midsize car were slightly increased. The A-pillar deformation of the compact car was increased approximately 20mm caused by the under ride and increased stiffness of upper member. For midsize car, more intrusion at the brake pedal was occurred by the increased local intrusion of dash panel.

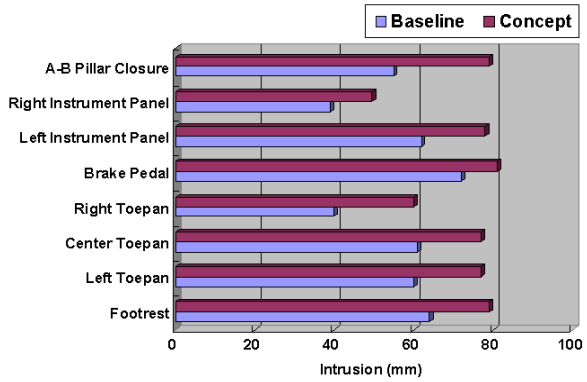

(a) Subcompact

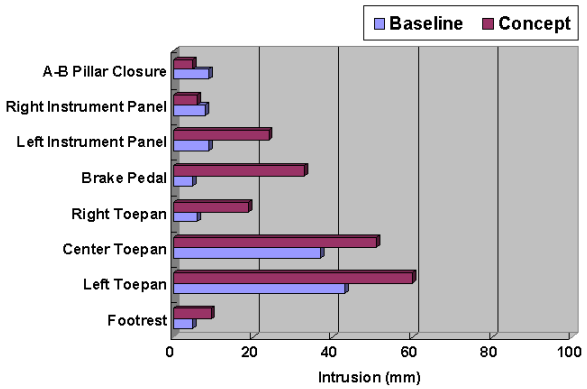

(b) Midsize

Figure 13. Vehicle deformations for frontal car-to-car crash.

The energy absorbed by both midsize car and subcompact car is distributed as shown in figure 14. For concept vehicles, added vehicle structures result that internal energy for each vehicles are increased. It is pointed that the ratio of absorbed energy was barely different. This means energy ratio is mainly influenced by mass ratio of vehicles even though both vehicles' stiffness is increased by concept vehicle structures.

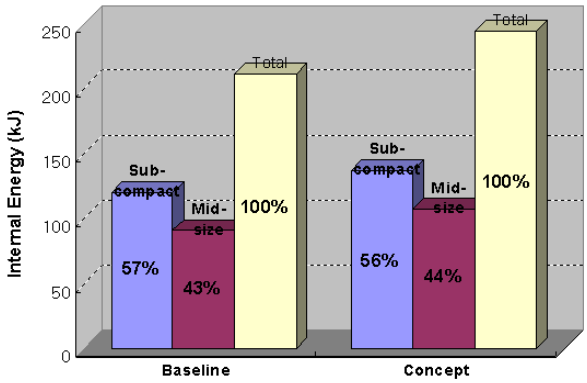

Figure 14. Internal energy distribution of frontal car-to-car crash.

SIDE CAR-TO-CAR CRASH

Side car-to-car crash test was performed as shown in figure 15: bullet (striking) vehicle is a midsize sedan (1465kg) and target (struck) vehicle is a subcompact car (1060kg). The velocity of target vehicle was 24km/h, and the bullet vehicle was travelling at 48km/h. The centerline of bullet vehicle was aimed at the R-point of target vehicle, with both vehicle centerlines perpendicular to each other. Test configuration is the same to that of the previous research performed by EEVC WG-13 [9]. Two tests have been performed using baseline and concept bullet vehicles.

(a) ISO view: before crash (b) ISO view: after crash

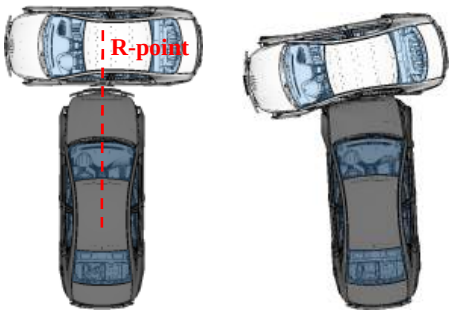

(c) Top view: before crash (d) Top view: after crash

Figure 15. Side car-to-car crash (bullet vehicle at 48km/h vs. target vehicle at 24km/h).

Figure 16 shows structural engagement between both bullet and target vehicles. In case of baseline vehicle, the structural engagement of longitudinal member of bullet vehicle with target vehicle's side impact beam was occurred at the early stage of crash. After that, the longitudinal member of bullet vehicle was laterally bent. As show in figure 16-17, it was observed that concentrated side intrusion of target vehicle at the area of passengers' femur by the longitudinal members of bullet vehicle. There was no structural engagement between the side-sill of target vehicle and the front structure of bullet vehicle due to the absence of lower member. For concept vehicle, front bumper rail of bullet vehicles was less bended. Less concentrated side intrusion occurred and the longitudinal members of bullet vehicle were slightly bent, because that homogeneity of bullet vehicle's frontal structure was

improved. It was clearly observed that structural engagement between the side-sill of target vehicle and the front structure of bullet vehicle by the presence of lower member.

Figure 18 shows b-pillar intrusions of target vehicle. For concept vehicle, maximum b-pillar intrusion was increased about 70mm caused by structural engagement between the side-sill of target vehicle and the lower member of bullet vehicle.

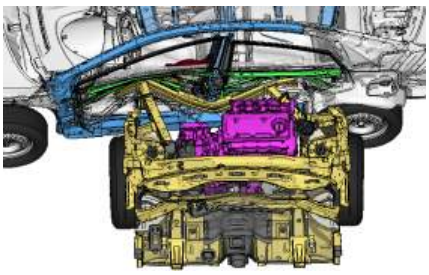

(a) Top view: baseline

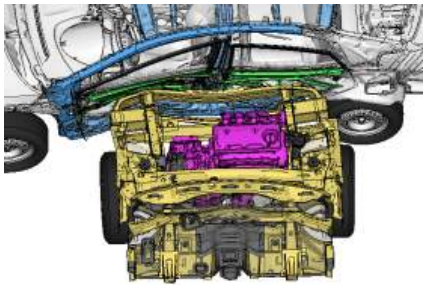

(b) Top view: concept

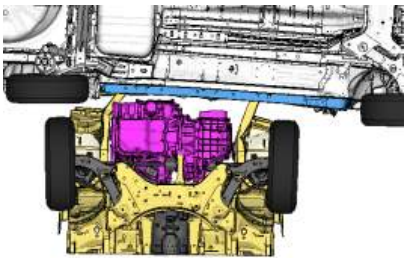

(c) Bottom view: baseline

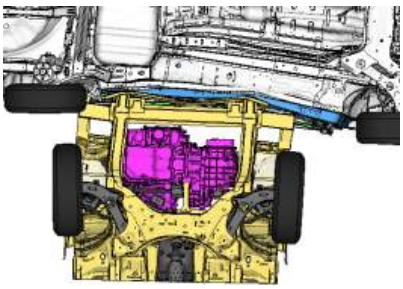

(d) Bottom view: concept

Figure 16. Structural engagements of side car-to-car crash. (@60ms)

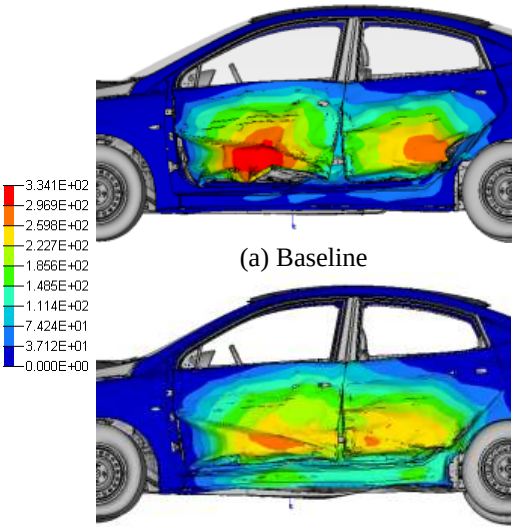

(a) Baseline

(b) Concept

Figure 17. Side intrusions of target vehicle.

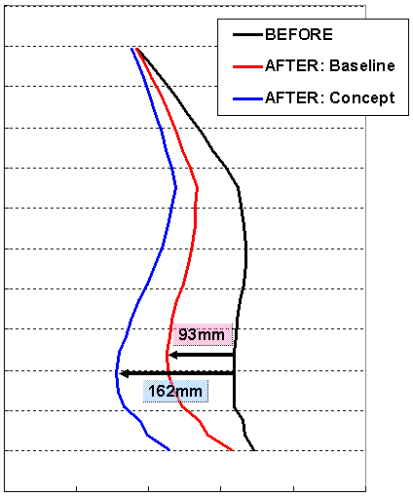

Figure 18. B-pillar intrusions of target vehicle.

The energy absorbed by both bullet vehicle and target vehicle is distributed as shown in figure 19. For concept vehicle structure the internal energy of target vehicle was highly increased 48% to 71% because of improved structural engagement of vehicles which results more increased deformation of target vehicle. On the contrary internal energy of bullet vehicle was decreased 52% to 23%. This means stiffness mismatch between the side structure of target vehicle and front structure of bullet vehicle.

In terms of side compatibility, it needs to be carefully examined that stiffness of front vehicle structure which subjects to improve structural interactions in frontal compatibility.

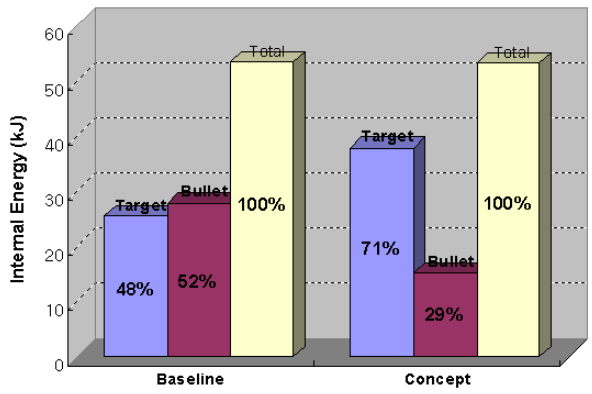

Figure 19. Internal energy distribution of side car-to-car crash.

CONCLUSIONS

For the improvement of structural interactions in front and side car-to-car crash a series of crash tests using midsize and subcompact vehicles was conducted. The results can be summarized as follows:

1. Conceptual design of compatibility compliant frontal vehicle structure which subjects to improve the distribution of frontal crash loading and structural interactions between vehicles is proposed.

2. In FWRB and FWDB test, the presence of lower member on proposed conceptual design of compatibility compliant vehicle structure was clearly detected. Better crash loading support by increased stiffness of front end structure is also demonstrated.

3. In PDB test, the effect of proposed conceptual vehicle structure is slightly shown. It is due to only the final deformation of barrier is measured in PDB test. It is required that other assessment parameters which can detect or identify the presence of member for improving structural interactions.

4. It is demonstrated that proposed concept vehicle structure results the improvement of structural interactions in front and side car-to-car crash. In terms of side compatibility, it needs to be carefully examined that the stiffness of front vehicle structure which subjects to improve structural interactions in frontal compatibility.

REFERENCES

[1] "Car Crash Compatibility and Frontal Impact," EEVC WG15 Final Report, 2007

[2] Patel, S., et al., "NHTSA's Recent Vehicle Crash Test Program on Compatibility in Front-to-Front Impacts," 20th International Technical Conference on the Enhanced Safety of Vehicles, Paper No. 07-0231, 2007

[3] Wykes, N., et al., "Compatibility Requirements for Cars in Frontal and Side Impact," 16th International Conference on the Enhanced Safety of Vehicles, Paper No. 98-S3-O-04, 1998

[4] Edwards, M., et al., "The Essential Requirements for Compatible Cars in Frontal Collisions," 17th International Conference on the Enhanced Safety of Vehicles, Paper No. 158, 2001

[5] Kleinwagen gegen Geländewagen: Audi Q7 vs. Fiat500 Crash Test, http://www.adac.de, 2008

[6] O'Reilly, P., "Status Report of IHRA Compatibility Working Group," 19th International Conference on the Enhanced Safety of Vehicles, Paper No. 365, 2005

[7] FWDB Test Protocol v3.0, 2007

[8] PDB Test Protocol v2.3, 2006

[9] "Development and Evaluation of the Advanced European Mobile Deformable Barrier (AE-MDB) Test Procedure," APROSYS Development Report, AP-SP11-0083, 2006

PROGRESSIVE DEFORMABLE BARRIER (PDB) – EVALUATION OF IT'S IMPACT ON SMALL CAR DESIGNS THROUGH CAE ANALYSIS.

Pratap Daphal
Anil Kumar C
Tata Technologies Ltd. (deputed to Tata Motors Ltd.) India.
Paper Number 11-0430

ABSTRACT

Progressive Deformable Barrier (PDB) based offset test method was recently proposed as an alternative to the existing regulatory test using Offset Deformable Barrier (ODB) as per ECE R94. Implications of this change on structural design of cars were studied through CAE simulations.

Comparative simulations were run with the two barriers for vehicles with different mass and effect of the barrier change was studied against the mass of the vehicle. Stiffness improvements required in car structures for similar intrusions when PDB was used were then studied. The study showed that PDB was able to absorb a lot more energy compared to ODB and this could essentially mean the car structures can be engineered with reduced energy absorbing capability while still meeting the requirements with PDB.

INTRODUCTION

A new test procedure using PDB was proposed vide GRSP/2007/17, in place of current ECE R94 offset frontal impact test procedure. The comparison of the proposal is as follows:

Parameter	ECE R94	French proposal
Barrier	EEVC	PDB
Test speed (kmph)	56	60
Overlap (%)	40	50

The implications of these changes are studied on structures of passenger cars and SUVs using CAE. The FE model of the PDB, used in study, was developed in Tata Motots. The FE model was validated with the test data available in the literature. (1) An overlay of the PDB and ODB is shown in Figure1. PDB is deeper and does not have the bumper elements.

PDB FE MODEL BUILD AND VALIDATION

The PDB FE model was built using a combination of brick and discrete elements. The stiffness of different cores of the barrier available in literature was used to define the stiffness of the FE model (Figure 2). The FE model of PDB was then validated with two physical tests. The test details and the physical test results were taken from the literature. (1)

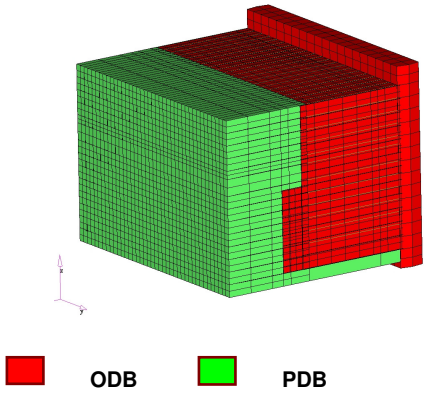

Figure 1. Overlay of ODB and PDB.

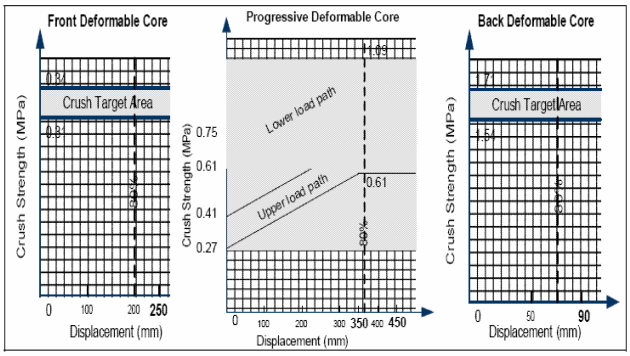

Figure 2. PDB core stiffness (1).

Test1: In This test a 1300kg offset flat rigid barrier impacts on the PDB at a speed of 60 kmph as shown in Figure 3. The requirement is that the resistance offered by PDB should lie in the corridor as sown in Figure 4.The performance of PDB Fe model in this test is given in Figure 4. The PDB FE model met the requirement of this test.

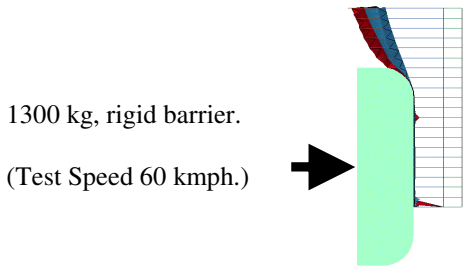

Figure 3. PDB validation Test1

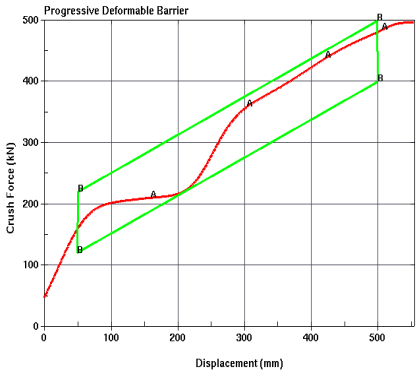

Figure 4. PDB resistance w.r.t. its Deformation.

Test 2: In this test a 1300 kg offset rigid tubular barrier impacts the PDB at a speed of 60kmph. The resistance offered by the PDB is required to lie within the corridor shown in the Figure 6. The FE model of PDB met this requirement.

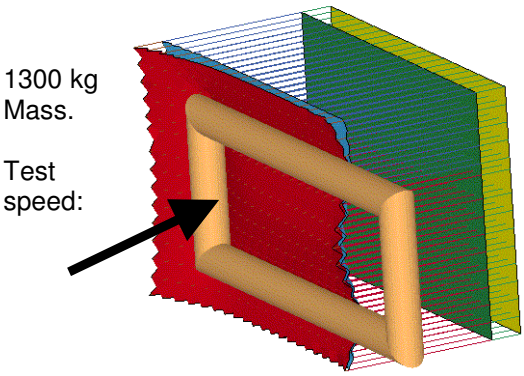

Figure 5. PDB FE model validation Test2.

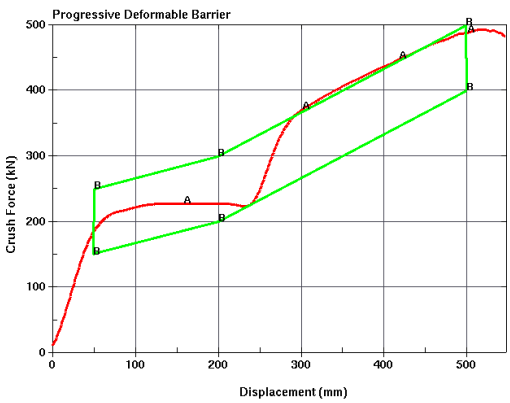

Figure 6. PDB resistance w.r.t. its Deformation.

ODB VS PDB stiffness comparison:

To compare the ODB and PDB stiffness, Simulations are carried out with flat rigid barrier. Following graph shows the comparison of PDB and ODB barrier stiffness upto 400 mm of crush. It was observed that as the crush increases the PDB has higher stiffness than ODB (Figure 7).

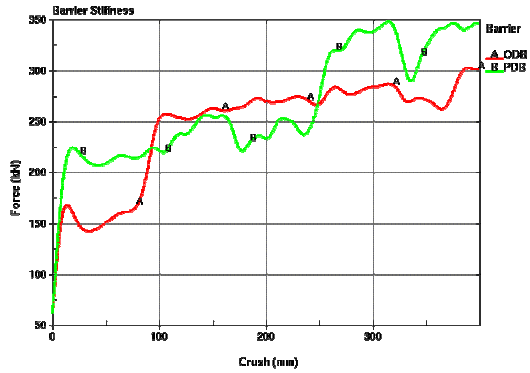

Figure 7. Stiffness comparison of ODB and PDB.

The validated PDB FE model was used for full vehicle crash simulations. Simulations were carried out for cars and for SUVs to study the structural crash performance with PDB and ODB.

- Passenger car with kerb wt of 750 kg.
- Car with kerb wt of 1100 kg.
- SUV with kerb wt of 2400 kg.

Passenger car with 750 kg kerb weight

The comparison of full vehicle ODB56 and PDB60 simulation results is given in the Table1 below. The critical parameters like energy absorption, intrusions and the crash pulse are used for comparison.

Table1. ODB56 VS PDB60 result comparison for small car.

Sr.no	Description	ODB 56	PDB 60
1	Initial Kinetic Energy (kJ)	119	131
2	Energy absorbed by the vehicle (kJ)	40	54.3
3	Energy absorbed by the barrier (kJ)	53	57.3
4	Residual kinetic energy (kJ)	11.5	10.8
5	Energy lost in Friction and Miscellaneous Energy (kJ)	14.5	8.6
6	Stopping distance X (mm)	645	550
7	Time to zero X velocity (ms)	76	58
Intrusion (Percentage change w.r.t ODB56))			
1	Peak steering column intrusion X		+45
2	Peak A pillar (Top) X-intrusion		+45

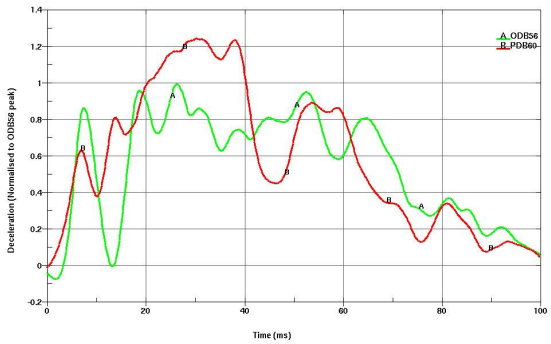

Figure 8.ODB56 Vs PDB60 crash pulse for small car.

The Effect of replacing ODB56 with PDB60 on small cars is summarized below.

- Overall deformation of vehicles structure increased.
- Resulting pulse is stiffer
- Resulting intrusions are higher

Passenger car with 1100 kg kerb weight

The comparison of structural crash performance of 1100 kg car with ODB56 and PDB60 is given in Table 2. The crash pulse comparison is given in Figure 9.

Table 2. ODB56 VS PDB60 result comparison for mid sized car.

Sr.no	Description	ODB 56	PDB 60
1	Initial Kinetic Energy (kJ)	177	196
2	Energy absorbed by the vehicle (kJ)	68	113
3	Energy absorbed by the barrier (kJ)	75	59
4	Residual kinetic energy (kJ)	13.2	7.8
5	Energy lost in Friction and Miscellaneous Energy (kJ)	20.8	16.2
6	Stopping distance X (mm)	880	815
7	Time to zero X velocity (ms)	90	80
Intrusion (Percentage increase w.r.t ODB56)			
1	Peak steering column intrusion X (mm)		+10
2	Peak A pillar (Top) intrusion X (mm)		-3

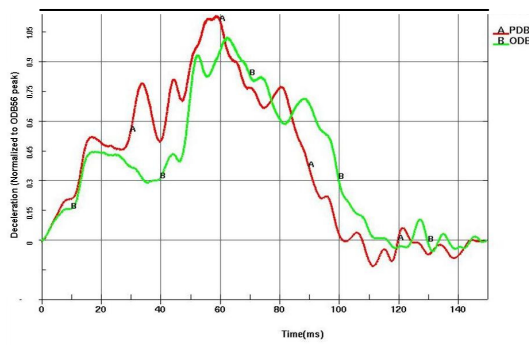

Figure 9. ODB56 Vs PDB60 crash pulse comparison for small car.

The Effect of replacing ODB56 with PDB60 on mid sized cars is summarized below.

- Overall deformation of vehicles structure increased.
- Resulting pulse is stiffer
- Resulting intrusions are higher

The crash pulse and the intrusion show that the crash severity of PDB on mid sized cars is less than the small cars.

From the results of 1100 kg car it was observed that the energy absorbed by vehicle with PDB60 has been increased by 14.3 kJ and 46 kJ respectively. In order to get similar vehicle intrusion with PDB, the vehicle stiffness has to be improved.

SUV with 2400 kg kerb weight

The effect on structural crash performance of SUVs by replacing the ODB56 by PDB60 is given in the Table 3. The crash pulse comparison is shown in Figure10.

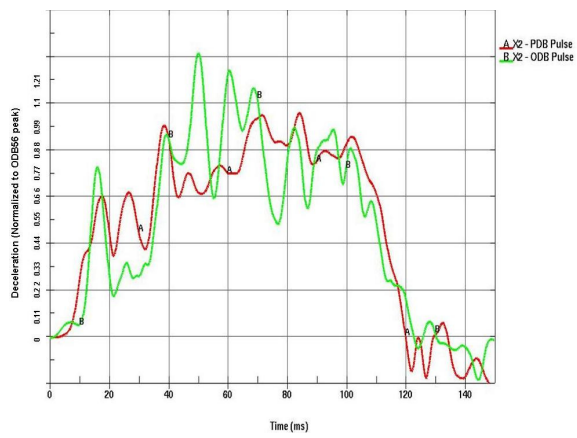

Figure10. ODB56 Vs PDB60 crash pulse comparison for SUV.

Table 3. ODB56 VS PDB60 result comparison for SUV.

Sr. no	Description	ODB 56	PDB 60
1	Initial Kinetic Energy (kJ)	285	329
2	Energy absorbed by the vehicle (kJ)	147	94.8
3	Energy absorbed by the barrier (kJ)	93.5	209
4	Residual kinetic energy (kJ)	19.2	14.5
5	Energy lost in Friction and Miscellaneous Energy (kJ)	25.3	10.7
6	Stopping distance X (mm)	930.9	1014.9
7	Time to zero X velocity (ms)	98.7	102.5
Intrusion (Percentage change w.r.t ODB56)			
1	Peak steering column intrusion X		-87
2	Peak A pillar (Top) X-intrusion		-90

The Effect of replacing ODB56 with PDB60 on SUVs cars is summarized below.

- Overall deformation of vehicles structure reduced.
- Resulting pulse is softer
- Resulting intrusions are lower

The crash pulse and the intrusion show that the crash severity of PDB60 on SUVs is lower than ODB56.

For vehicles that meet ODB56 test requirements, it is observed that impact of higher stiffness of PDB reduces with increasing mass of the vehicle. This is primarily because ODB56 forces the vehicle structure energy absorption capacity to be proportional to the mass.

The graph in Figure 11 shows the vehicle stiffness for 40 percentage of the barrier overlap for ODB56 case.
It was also observed from the simulations that PDB has higher energy absorbing capacity than ODB. It is possible for a stiffer vehicle to meet the PDB60 requirements without any energy absorbing zone at the front.

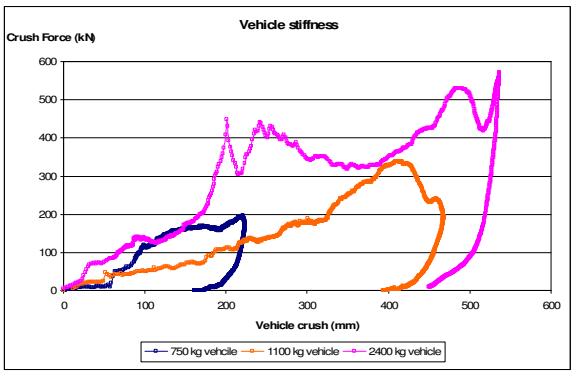

Figure 11. Vehicle stiffness with 40 % overlap.

To study this, simulations were carried out on a vehicle having stiff front end structure.
For this stiff vehicle the vehicle front end stiffness is further increased (over stiff) and one more PDB60 simulation is carried out. The results of these simulations are given in Figure 12 and Table 4.

Table 4. Comparison of ODB56, PDB60 simulation results for vehicles with stiff and over stiff front end.

Sr. No	Description	ODB56 (STIFF vehicle)	PDB60 (STIFF vehicle)	PDB60 (OVER STIFF vehicle)
1	Initial Kinetic Energy (kJ)	177	189	192
2	**Energy absorbed by the vehicle (kJ)**	**60**	**48**	**45**
3	**Energy absorbed by the barrier (kJ)**	**80**	**116**	**122**
4	Residual kinetic energy (kJ)	14	7	9
5	Energy lost in Friction and Miscellaneous Energy (kJ)	23	18	16
6	Stopping distance X (mm)	811	733	725
7	Time to zero X velocity (ms)	86	77	76
Intrusion (Percentage change w.r.t ODB56)				
1	Peak steering column intrusion X		-35	-58
2	Peak A pillar (Top) X-intrusion		-42	-48

The intrusion and the crash pulse for the above simulations show that for a vehicle with stiff front end the severity of PDB60 is less than ODB56. Even with further increase in the vehicle front stiffness it can meet the requirements in PDB60 test.

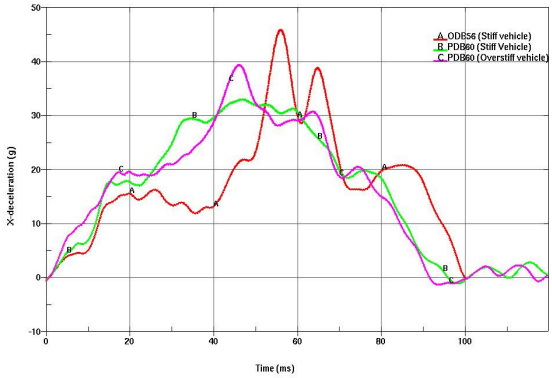

Figure 12. Comparison of crash pulse of ODB56, PDB60 simulation results for vehicles with stiff and over stiff front end.

CONCLUSIONS:

- The study showed that PDB has higher energy absorption capacity than ODB.
- Due to higher energy absorption capacity of the PDB, it is possible to engineer a vehicle structure with reduced energy absorption capacity while still meeting the requirements with PDB.

REFERENCES:

1. Economic and social council, Distr. General,TRANS,WP29,GRSP2007,17
2. Stephen Summers, “Overview of IHRA compatibility test development” NHTSA.
3. Pascal Delannoy , Tiphaine Martin, Pierre Castaing, “Comparative evaluation of offset test to control self and partner protection” 05-0010
4. Bernd Lorenz, “Mobile progressive deformable barrier and mobile rigid barrier tests- MPDB and MRB, IWG R94, Geneva, Dec 2008.
5. LSDYNA theory manual.

FRONTAL IMPACT IMPROVEMENTS – ENHANCED MODELLING OF THE IMPACT BARRIER

Loïc Grall,
Richard Zeitouni,
Céline Adalian
PSA Peugeot Citroën
France
Paper number 11-0435

ABSTRACT

The honeycomb barrier behaviour has a major influence on the vehicle structures designed to absorb a frontal crash, for ECE 94 or Euro NCAP and other NCAP frontal tests.
The increased use of modelling and the improvements made on numerical capacities forced us to be able to represent in a better and an in-depth manner the numerical behaviour of the honeycomb barrier in order to improve our prediction of the vehicle behaviour in a frontal crash test, especially on the load distribution in the car front-end.
PSA Peugeot Citroën launched a huge physical and numerical program on the behaviour of the regulatory honeycomb barrier in order to improve its numerical model available of the major crash software. This program focused on the instabilities generated by the industrial barrier that can lead to very different load distribution profiles.
Physical tests were performed from simple tests (honeycomb static compression) to more complex dynamic tests such as puncture tests, up to sub systems tests where a rigid car front end was propelled on a full ECE 94 barrier. This program highlighted new phenomena that were not represented up to now in the numerical barrier such as densification and effect of air pressure in the cells when high volume reduction and high velocities occurred. Other important scatterings due to bonding and cell wall thickness were also seen as major parameters to take into account.
All these mechanical characteristics as well as the aluminium mechanical behaviour are now included in the enhanced modelling developed in the crash software in order to represent all the simple tests performed up to the more complex ones. This led us to better predictive modelling of the honeycomb barrier.
The paper will conclude with a direct comparison between the standard barrier model and our enhanced model and their consequences on the prediction of the full car crash behaviour.
This brand new model is now used for the design of the new vehicle programs at PSA Peugeot Citroën.

INTRODUCTION - AIM OF THE STUDY

Several car programs face difficulties due to the honeycomb barrier behaviour in frontal impact. These difficulties are due to the change in the collapse of the structure and may induce significant differences in the load distribution of the car front end.
Considering the former problems vehicle have encountered, two phenomena have to been improved:

- Interaction between the 3rd load path and the barrier. This interaction precede the loading of the body-in-white and the loading of the doors
- Behaviour of the side members interacting with the frontal barrier bumper. The different behaviours lead to different energy absorption and various load paths to the base

For all the customer specifications, numerical modelling is taking a growing part of the vehicle development. It is the case for the passive safety specifications for which modelling help to reduce the cost of the industrial tools to manufacture the cars as well as reducing the number of physical prototypes needed for crash tests.

Therefore, PSA Peugeot Citroën decided to increase its knowledge and enhance the modelling of the current barrier face to prevent additional cost due to inaccurate modelling.

PRESENTATION OF THE HONEYCOMB BARRIER

As a short introduction, it is worth to present the EEVC barrier used in ECE 94 [1] or in the current Euro NCAP frontal impact protocol [2].

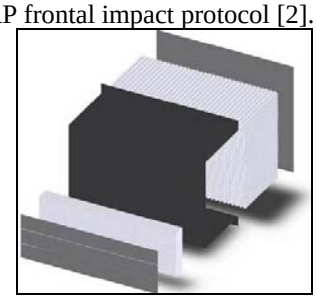

Figure 1. Exploded view of frontal barrier.

This barrier is made to represent another vehicle and consist of a main honeycomb block surrounded by a backing sheet and the cladding sheet. The honeycomb block is equipped with a bumper element made by three independent pieces and wrapped into the bumper facing sheet.
The whole barrier is made with aluminium and adhesive (familiarly called glue).

PROBLEM DEMONSTRATION

In a frontal ODB crash test, interactions between the vehicle and the frontal barrier lead to several unstable phenomena which are very problematic to reproduce in numerical modelling.

Problem 1

The load of the wheel and the front side-member cause the barrier front part to bend forward (see Figure 2).
This is strongly linked to the height of the 3rd load path which is an architectural parameter intrinsic to each vehicle project (determined by the wheel clearance volume).
In the current and standard numerical front barrier model (volumic model), this forward bending is not represented. This difference leads to a modification in the load path of the body side of the vehicle.

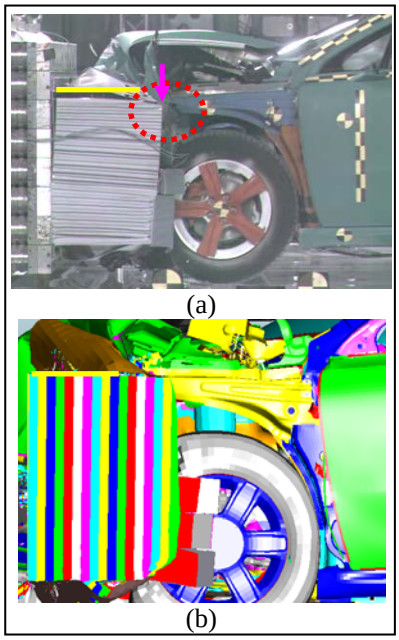

Figure 2. Forward bending of the barrier front which influence the interaction between the barrier and the vehicle
(a) Physical Behaviour
(b) Numerical modelling with a standard barrier model

The consequence of this forward bending leads to a significant difference on the 3rd load path in the end of the crash, as shown in Figure 3.

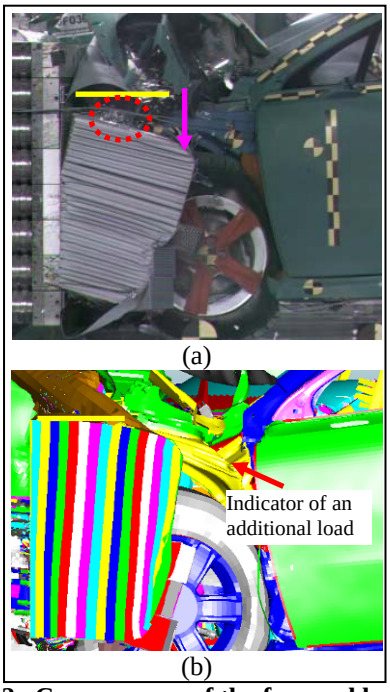

Figure 3. Consequence of the forward bending of the barrier front at the end of the crash
(a) Physical Behaviour
(b) Numerical modelling with a standard barrier model.

Problem 2

Rupture in the frontal barrier is also frequent and produced a reduction in the load wheel path (see Figure 4).
In modelling, the prediction of rupture in honeycomb is not represented.

Figure 4. Rupture in the barrier which modifies the load on the wheel.

Problem 3

Kinematics and deformation of front side members are sometimes affected. The different behaviours induce very different load distributions to the structure as presented in Figure 5.

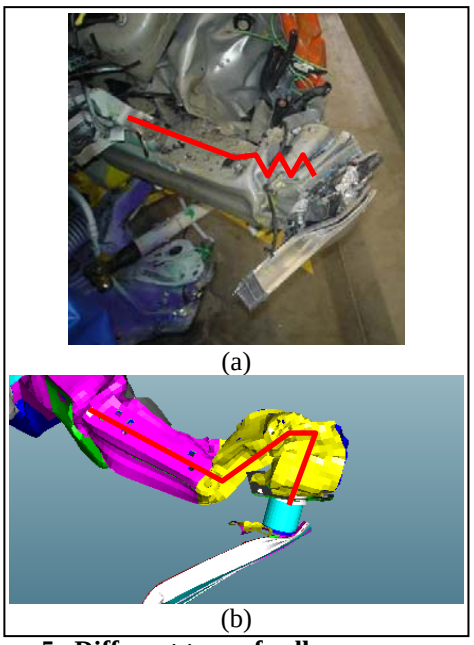

Figure 5. Different type of collapse
(a) Axial collapse of front side member
(b) Bending collapse in calculation.

These phenomena induce a lack of reproducibility that blurs the analysis and results of the crash-tests.

A PSA research program has therefore been launched to improve the modelling of the barrier face to get a more realistic behaviour of the interaction between the car front end and the barrier face. At this stage of the paper, it is wise to notice that these unrealistic effects we want to eradicate are purely due to the characteristics of the honeycomb barrier and are totally decoupled from the compatibility problem.

PRESENTATION OF THE RESEARCH PROGRAM

The guiding lines of the test campaign are:

- Use of rigid impactors (including a “rigid wheel” in order to simplify its modelling and therefore focus the modelling improvements on the honeycomb behaviour
- Impactors have to load the honeycomb barrier or the bumper in different global or local modes (compression, bending, shearing, puncture, etc.).
- Use progressive test complexity from the simple compression to a simplified rigid front side member to get a final model answering to all the requirements
- Use the maximum energy for each test in order to obtain the maximum information concerning the densification, and air effect if it is physically present.

This full test campaign did not have the aim to integrate the natural material scattering. This aspect has been previously performed through other internal specific researches conducted by PSA Peugeot Citroën..
The results of this scattering quantification have been introduced in this analysis and in the enhanced barrier modelling.

The different parameters and types of loading/behaviour identified in the barrier during an ODB frontal crash test are listed below:

- Stiffness modifications of the honeycomb and the bumper element
- Bumper element interaction into the honeycomb
- Perforation of the honeycomb cladding sheet
- Rupture in the honeycomb or in the bumper element
- Separation of the bumper and the honeycomb
- Absorbed energy

Different types of measurements were carried out:

- high speed videos
- load-cell wall
- accelerometers

To characterize the honeycomb barrier at the maximum energy possible, without creating any damage to the test rig, a safety layer of honeycomb was put between the rigid wall and the backing sheet. This honeycomb layer has been cut in block in order not to influence the load cell measurements.

The [3], [4], [5], [6] and [7] were used to identify the best sub-system test configurations.

The different types of test (sub-system tests) performed in this campaign are presented in Figure 6.

Test 1: Shear test XY et XZ of honeycomb	
Test 2: 100% compression of honeycomb	

Test 3: Load from a rigid wheel	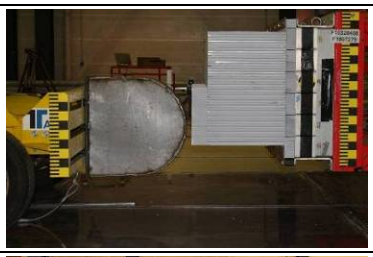
Test 4: 50% compression	
Tests 5 & 6: Local compression on honeycomb and complete barrier	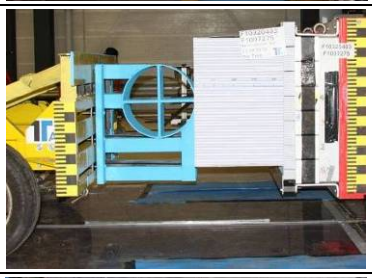
Tests 7 &8: Puncture of honeycomb and complete barrier	
Test 9 : Simplified side members	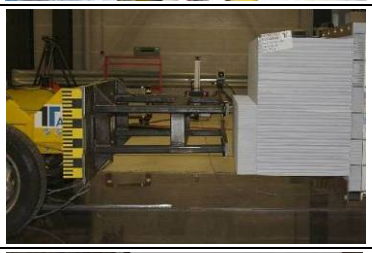
Test 10 : Simplified side members and rigid wheel	

Figure 6. Different test types performed in our test campaign.

Additional test campaigns have also been performed on:

- Traction on Aluminium tube samples to improve the material constitutive laws
- Local puncture on the honeycomb
- Local puncture on the bumper element
- Characteristic test on glue to define a corresponding model

RESULTS OF SUB-SYSTEMS TEST

The different physical phenomena reproduced in sub system tests help us to understand the different physical behaviour encountered during a vehicle-to-barrier test.

The numerical activity took place roughly during one year and led to two different models of barrier combining different hypothesis of rupture and global modelling (one or two thickness in honeycomb)

For this paper, we decided to present in details the three following tests:

1. Test 2:100% compression
2. Test 3: Load from a rigid wheel
3. Test 7: Puncture of honeycomb

For each test configuration, the physical results are presented first. In a second part, the modelling with different type of mesh or constitutive laws is presented and compared with the physical results.

Description of the different numerical models

Three different types of models were studied during this research.
The first one is a classical/standard honeycomb model which is often called “the initial model” in this paper. This initial model is a standard volumic model where each numerical element is associated to a standard honeycomb constitutive law.

The two new models are made through shell elements reproducing the actual walls of the aluminium constitutive element of the honeycomb barrier:

- “Type 1 model” is a shell element formulation with a first set of parameters representing rupture in the cladding sheet and the bumper facing sheet (same materialt ype).
- “Type 2 model” is a shell element formulation with different wall thicknesses and a second set of rupture parameters.

Results of Test 2: 100% compression

The test was performed with similar speed as the vehicle-to-barrier test. This speed is a key point to the physical phenomenon of air effect.
Figure 7 presents some images of the deformation during the test.

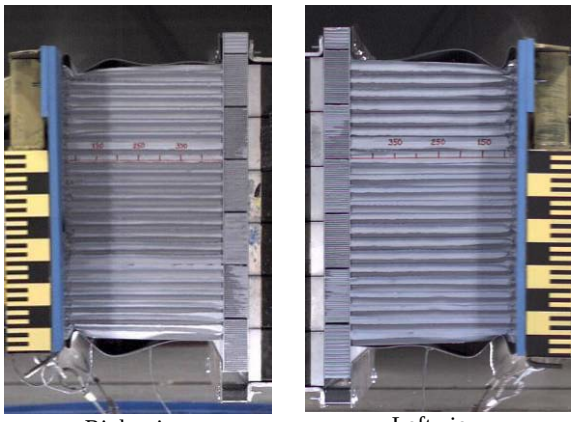

Right view Left view

5ms : honeycomb deforms from rear to front

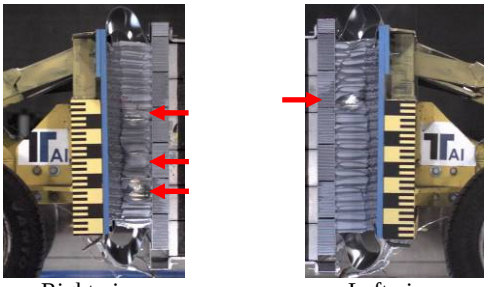

Right view Left view

25ms : 1 explosion on the left side due to the air containment in the honeycomb cells
3 explosions simultaneously on the right side

Figure 7. 100% compression test – Deformation at different times.

Despite the theoretical constant stiffness of the honeycomb, the video clearly shows that the deformation is not uniform but occurs from the front (impactor side) to the back (load cell wall side).
It is only at the end of the compression that the honeycomb starts to deform uniformly on the remaining thickness.

There is also a significant elastic recovery of the barrier. This phenomenon is illustrated in the following Figure (see red marks).

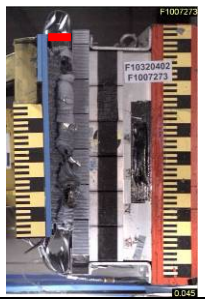

Right view at maximal displacement

Right view at final displacement

Figure 8. 100% compression test – Illustration of the elastic recovery between maximum deformation and barrier after impact.

After impact, the barrier shows a residual deformation between 75 and 80% of the dynamic global displacement.

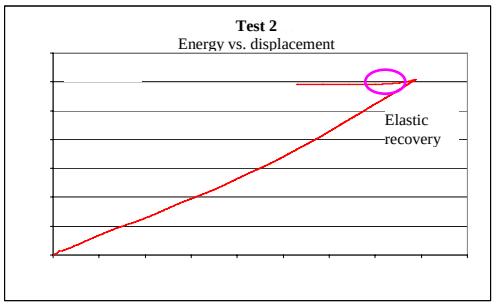

Figure 8. 100% compression test – Energy vs displacement and elastic recovery.

While the stiffness of the barrier is constant, there is however an increased effort from a quarter to the three quarters of the total displacement. It can be attributed to a phenomenon of confinement of the air inside the cells of the honeycomb barrier.

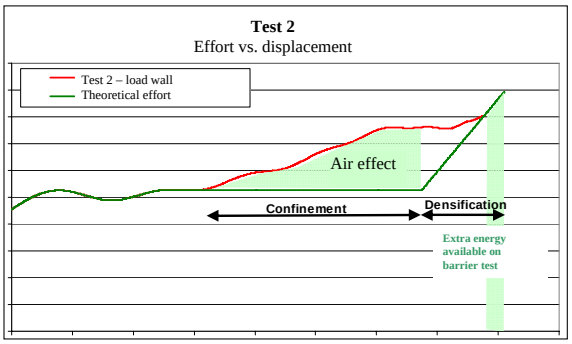

Figure 9. 100% compression test – Force vs displacement: theoretical behaviour (constant force) and force increase due to air confinement as measured through the load cell wall.

To quantify this phenomenon, an extrapolation of the theoretical curve without confinement was created, taking the following assumptions:

- Densification occurs at 75% of compression
- Maximum compression occurs at 90% of his displacement (without bumper part).

In this test, the energy absorption due to the confinement is assessed to approximately 13% of the total energy
In comparison, densification brings around 8% of total energy.

Therefore, this test shows that air confinement could be of the same importance as densification.

Without air containment or densification, the maximum potential energy of the barrier is about 90kJ (measured as the area under the curve of the theoretical effort).

Considering the two phenomena (densification and containment), the increase of energy is around 33%.

Test 2: 100% compression - Comparison with calculation

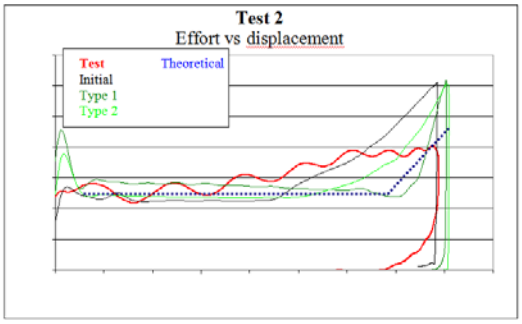

Figure 10. 100% compression test – Comparison of force vs displacement modelling and test result.

The main findings are:

- The initial numerical barrier does not present any spike as those found with the new ones. This effect has been improved recently via specific studies with good result for the enhanced modelling but they are not presented on this report neither on this graph.

- The type of shell model in "type 1" or "type 2" has the ability to take densification into account (to some extent). These barrier models present an improvement in numerical modelling with respect to the standard volumic model.

Additional numerical studies were carried out to understand the densification effect. The formulation of hourglass appears to be the main parameter of influence.

- None of the three barrier models is able to take into account the phenomenon of confinement. This explains why the final forces are overestimated in the 3 cases.

Results of Test 3: Load from a rigid wheel

Another type of test, more complex was conducted and analysed: the load from a rigid wheel.
Figure 11 shows the behaviour of the barrier at a specific time.

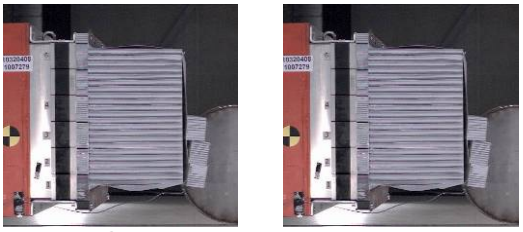

13ms 15ms

Early separation of the cladding sheet from the honeycomb block

Figure 11. Load from a rigid wheel – View of the cladding sheet separation from the honeycomb block.

As shown in the both views of Figure 11 it is interesting to notice that the bumper is not compressed during the test. The bumper is just bent by the impactor and forces the impactor to raise on the barrier body.

Figure 12 presents the load cell wall results at three different times.

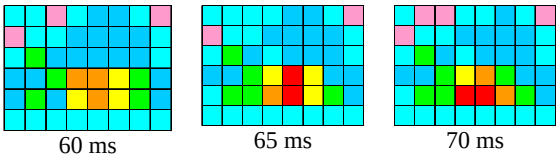

60 ms 65 ms 70 ms

Figure 12. Load from a rigid wheel – load cell wall at three different times.

The measurement of maximum force per cell on the load cell wall clearly shows the increase in the support surface horizontally through the bumpers. The load cells located directly in front on the rigid impactor (lines 6 and 7) only measure 50% of the total load. This means that the honeycomb barrier spread 50% of the localized input force.
Another important point in the deformation of barrier is the absence of rupture of the cladding sheet and the bumper element (see Figure 13).

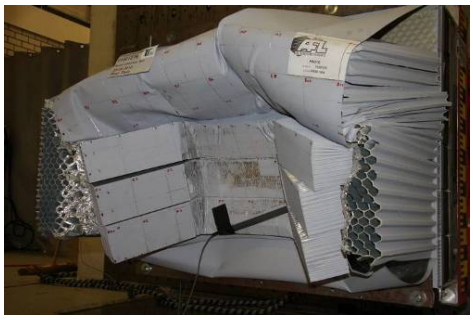

(a) ¾ front view

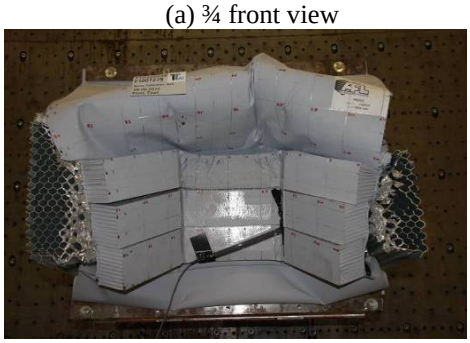

(b) Front view

Figure 13. Load from a rigid wheel – Post impact view of the cladding sheet sliding and the bumper non deformation.

The detachment and sliding of the cladding sheet from the honeycomb block of the barrier has contributed in limiting the work of the cladding sheet in traction.

Contrary to the previous test, we do not visually notice any elastic recovery of the barrier. This is probably due to the complex deformation of the barrier which is subject to very different internal constraints as in the initial test.

In summary:

- no rupture in the cladding sheet
- no shear in the bumper element.
- little or no compression in the bumper element
- no separation of the bumper element from the cladding sheet
- there is an important "peeling" (separation) of the cladding sheet from the barrier body which force it to slide into the centre of the barrier

Test 3: Load from a rigid wheel - Comparison with calculation

Here again, the modelling can be compared to the results of the physical test (see Figure 14).

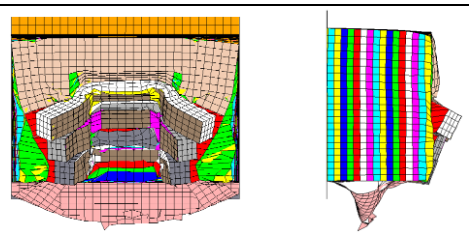

Front view Left view

(a) Initial barrier model

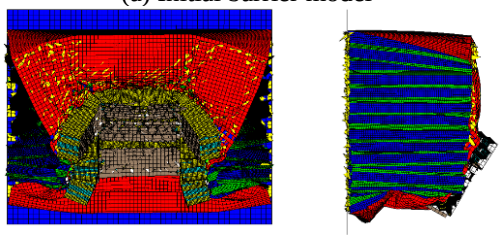

Front view Left view

(b) New shell barrier model: type 1

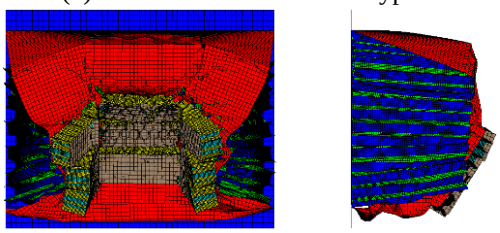

Front view Left view

(c) New shell barrier model: type 2

Figure 14. Load from a rigid wheel – Comparison of the three different models.

Figure 14 left view, clearly shows that with the new shell models, the forward bending of the top front of the barrier is well reproduced whereas the initial version of the barrier model is unable to make it, as mentioned in the introduction.

Figure 15 presents the comparison of the force-displacement curves between the three models and the physical test.

Figure 15. Load from a rigid wheel – Comparison of the force-displacement curves.

The main findings are:

- The "type 1" model is the only one presenting a small peak of initiation (that is even not present in the test). But, then it reproduces with a good accuracy the test curve even if a partial rupture of

the bumper facing sheet is present in the model but not in the physical test.

- The “type 2” model is very well correlated up to a quarter of the total displacement. The force is then somewhat underestimated while staying in the acceptable order of magnitude. It is interesting to notice the break in the cladding sheet and in the bumper that is not present in the test, and the insufficient separation of the cladding sheet from honeycomb block. This last point alone may explain the failure of the cladding sheet. This test shows that the different parameters are highly coupled: an adjustment in a rupture parameter of the cladding sheet will be linked to the rupture in the bumper and eventually will have an influence to the overall effort.

Results of Test 7: Puncture of honeycomb

Two different rigid impactors are used during the same test. One impactor has a rounded shape. The other presents a flat surface.

Figure 16 and 17 shows the behaviour of the barrier at different time and the final deformation of the barrier body.

1 ms: loading starts in the cladding sheet. | 10 ms: End of loading in the cladding sheet - Rupture in the cladding sheet at the centre. | 42 ms: Late side effects related to the folding of the cladding sheet inside the barrier body

Figure 16. Puncture of honeycomb – Three specific times during the test.

View onto the honeycomb deformed by square impactor | View onto the honeycomb deformed by round impactor

Figure 17. Puncture of honeycomb – Post impact deformation.

An interesting point to notice, as shown in Figure 17 is the pure shearing phenomenon induced by the square impactor, despite its small cross section of 100 x 100 mm. The honeycomb cells in contact with the square impactor have been fully compressed. Whereas, with the rounded shape impactor, the honeycomb cells have been deviated from their initial location and the impactor ends its journey on the backing sheet.

Results of Test 7: Puncture of honeycomb - Comparison with calculation

Comparing the test with the numerical models shows the following.
The rounded shape impactor shows that the rupture was first produced at the point of contact and spreads to the sides in the 4 perpendicular directions. The impression left in the cladding sheet looks more like a square than a cylinder. This is due to the mesh since it is the 4 "triangles" of the cladding sheet that were folded inward in the barrier.

Concerning the direct contact between the backing sheet and the rounded shape impactor, as previously mentioned, the phenomenon have been reproduced numerically on both barrier type 1 and type 2

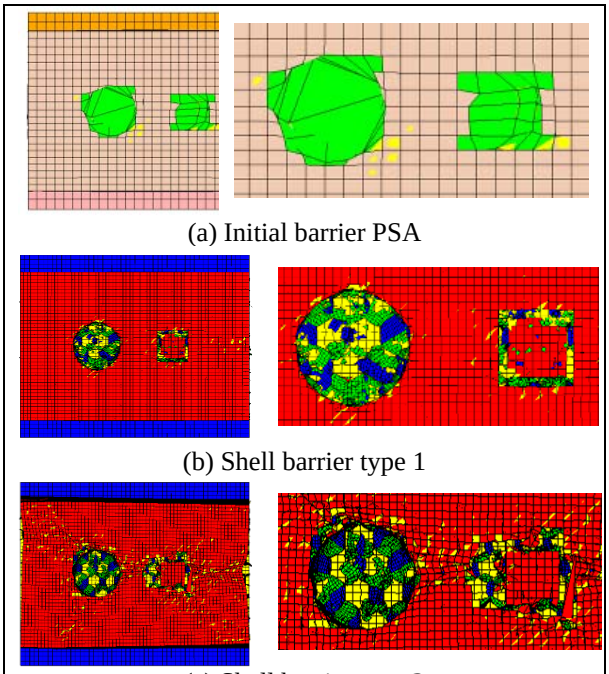

(a) Initial barrier PSA

(b) Shell barrier type 1

(c) Shell barrier type 2

Figure 18. Puncture of honeycomb – Results of the modelling.

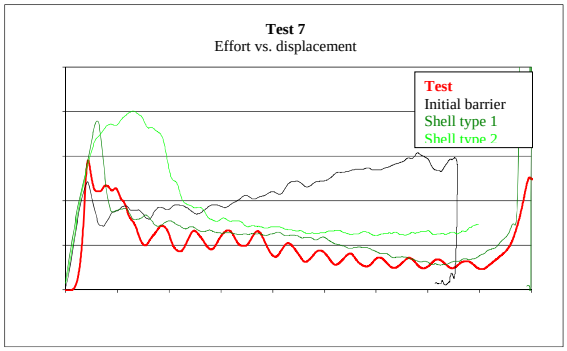

Figure 19. Puncture of honeycomb – Force – displacement comparison.

The main findings are:

- For the initial model, the first phase of the test is rather well reproduced. Indeed, the 2 ruptures occur simultaneously at 5 ms, in a force level very close to the test. However, the initial model then fails to predict the correct level of effort. It even increases with the displacement and eventually diverges completely from the test. It is likely that the absence of rupture of the honeycomb block during the perforation of the barrier associated with a work of pure compression volume elements are at the origin of this overestimation

- The "type 1" model also presents a rupture of the cladding sheet simultaneously at 7.5 ms. The 2 ruptures are relatively close to those observed in the test in terms of location and failure mode. The barrier then faithfully reproduces the decay of the effort during the next phase. The overall correlation is already at a good level.

- The "type 2" model breaks too late in the cladding sheet which results in an increase in effort that is kept for too long. It then reproduces with satisfaction the decay of the load even if it is somewhat overestimated compared to the test. In this test, the rupture parameter in the cladding sheet does not seem to be correctly tuned. However, in test 3, the same set of parameters gives good correlation. This shows the different way of rupture: traction-elongation, or tensile shear and the difficulty to model both with the same set of parameters.

- No barrier model at this stage of modelling is able to reproduce the separation of honeycomb from the barrier plate and its spread on the side as the impactor punctures into the barrier. Nevertheless, the prediction of effort is already at a good level for barrier type 2.

SOLVING OF NUMERICAL ISSUES ON QUASI-STATIC COMPRESSION

This part of the research was extremely complex and required many months of study and development.

As presented in the previous sections, there is a clear need to continue to improve the numerical models. This will be carried out via new parametric studies that have already been initiated. The aim is to represent more accurately some phenomena such as the glue rupture, the cladding sheet rupture or the peak load.

The plan of study focus on the following points:

- material laws for the various types of aluminium
- modelling of the honeycomb and the bumper
- modelling of the cladding sheet
- modelling of the glue

Each element of the barrier was characterized up to failure.

This report presents only part of the numerical difficulties: the ones considered as the most unexpected. The complexity in rupture analysis is well-known and therefore will not be presented in this paper.

The first simulation which was assessed is the static compression. This test was performed in order to verify the acceptability of the barrier model.

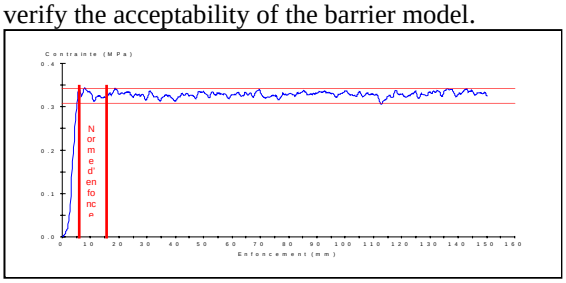

Figure 20. Test result of quasi-static compression.

The first difficulty encountered was the global effort of compression. The following parameter was studied:

- material law
- hourglass formulation

Several parameters in the Johnson-Cook material laws were studied, such as:
- perfect hardening
- low module of plasticity

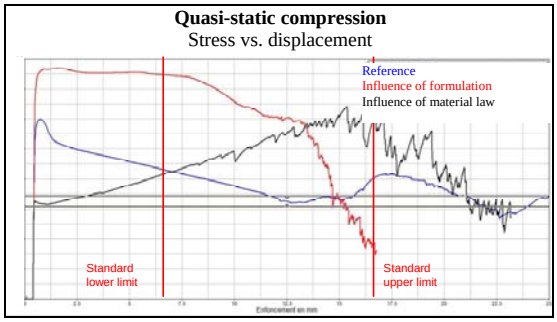

Figure 21. Quasi-Static compression - Influence of hourglass formulation and material law on stress/displacement response.

In this graph, either the constitutive law or the hourglass formulation modifies deeply the load of compression.

Although, the force level is drastically different, the behaviour is quite similar in terms of deformation between each honeycomb block.

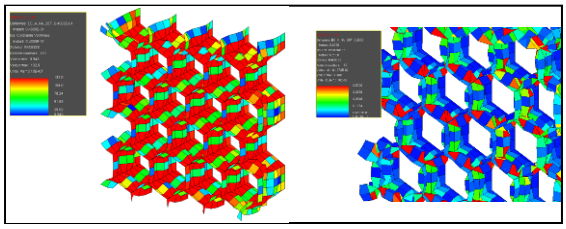

Figure 22. Quasi-static compression - Plastification of sample.

Finally, the major parameter in this test series was the global size of the honeycomb block. The side effect is much more important in the case of numerical calculation than in reality.

We decided to increase the size of the honeycomb block beyond its actual size as recommended by numerical modelling experts.
The results of simulation with a larger size of honeycomb block are encouraging concerning the load level, but the honeycomb deformations are not as progressive as expected.

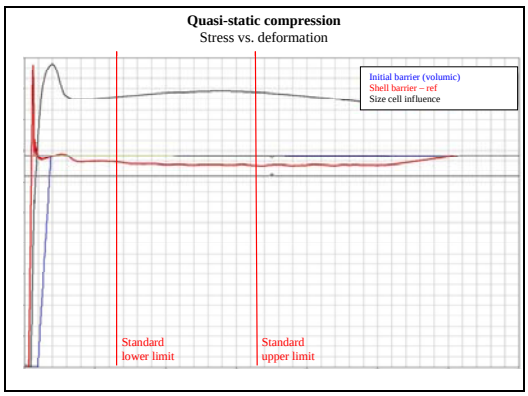

Figure 23. Quasi-static compression - Influence of cell in honeycomb block.

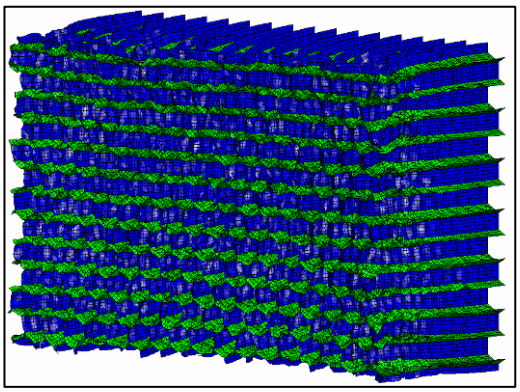

Figure 24. Quasi-static compression - Global crushing of honeycomb block.

In this modelling, the honeycomb block deforms uniformly as a whole, instead of getting a large deformation localized in the front part of the barrier.
To solve this problem of behaviour, a number of numerical parameters were studied:

- number of integration points
- type of deformation law for material
- shell plane stress plasticity (radial return or iterative projection)

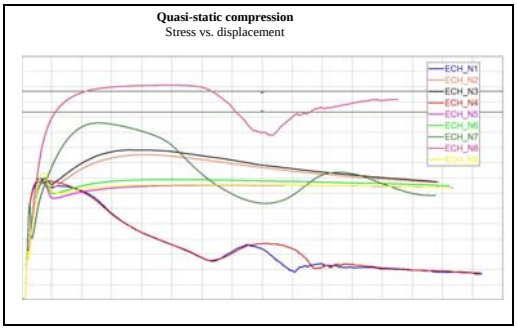

Figure 25. Quasi-static compression – influence of integration points in shell.

The results are inconclusive.
All characterizations in effort-displacement obtained are less stable than the reference configuration.

Even for smaller mesh sizes, the convergence of the deformation is not obtained.
An elementary study was then conducted: an isolated hexagon was studied to understand the numerical difficulties encountered.

The numerical structure appears to be too slender (even if the case does not appear in physical honeycomb). Thickness must then be artificially increased in the hexagon to find a satisfactory behaviour in terms of deformation.

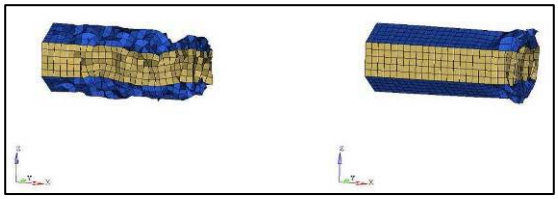

Figure 26. Quasi-static compression - Deformation of a honeycomb cell.

In conclusion, modelling the complete barrier in shell elements was very complex. Large numerical instabilities appeared and did not produce the expected improvement.
However, thanks to some trade-off we finally obtained a satisfactory modelling.
Some minor adjustments are still under study.

PROJECT APPLICATION

A first application was performed on vehicle projects.

Problem 1: Forward bending of frontal barrier

Even if the shell barrier presents some major improvements in deformation and kinematics of honeycomb, the project application is not satisfactory with the new barrier shell (see Figure 27).

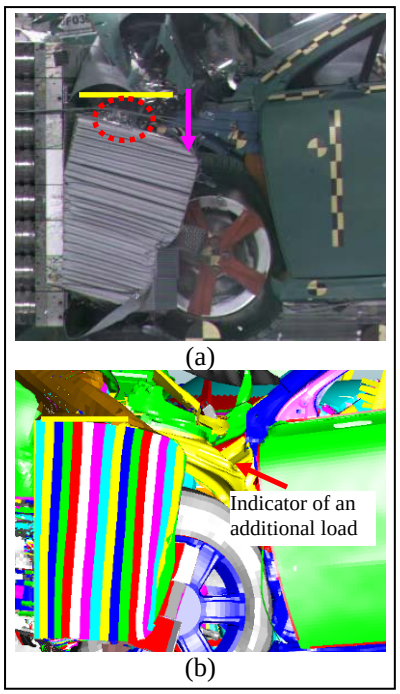

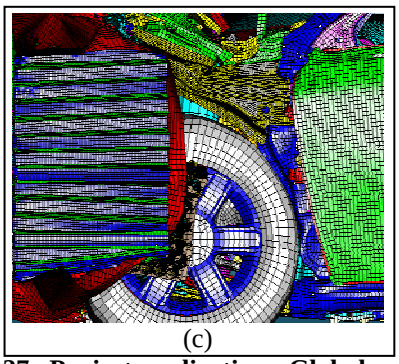

Figure 27. Project application - Global crushing of honeycomb block
(a) Physical Behaviour
(b) Numerical modelling with a standard barrier model
(c) Numerical modelling with a shell barrier.

However, the rupture in the honeycomb block and the cladding sheet allow minimising the additional load injected in the 3rd path load as seen in Figure 28.

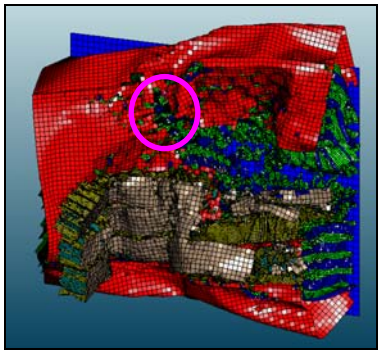

Figure 28. Project application – Deformed view of the barrier.

Problem 2: Rupture in the honeycomb block

Additional analysis show that the complete rupture is not far (see Figure 29)

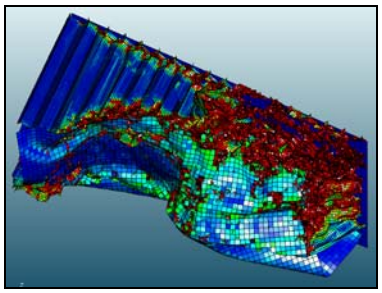

Figure 29. Project application – Side view of the barrier with plastic deformation.

Problem 3: Crush behaviour

The shell model presents an enhancement in the prediction of the side member deformation. The deformation is correctly reproduced.

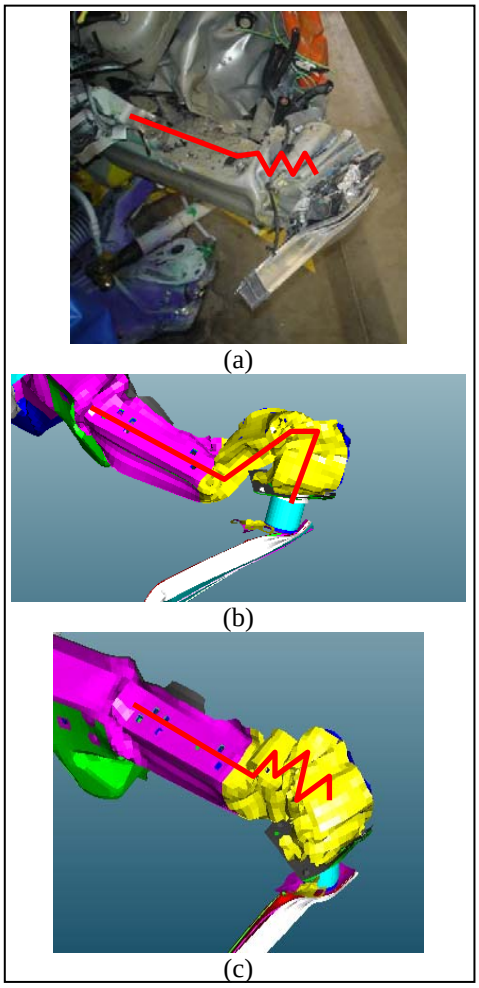

Figure 30. Project application –Different type of collapse
(a) Axial collapse of the front side member
(b) Bending collapse in calculation with the initial model
(c) Axial collapse with the shell model.

CONCLUSIONS

The study of the enhanced modelling of the frontal barrier led us to understand the physical phenomena which trigger the unstable behaviour of the barrier. Both the physical and numerical part enabled us to this understanding. These phenomena are mainly:

- forward bending of front barrier
- rupture in honeycomb

Their understanding and their enhanced modelling allow us to improve the interactions between the vehicle and the frontal barrier through its different load paths:

- side member
- wheel to sill
- upper load path

Numerically, the study permits to understand the influence of each parameter. The major parameters are highlighted are:

- material law
- hourglass formulation
- size and thickness of cell

However, some defaults of modelling are always under study for improvements:

- peak load (very important for calibration)
- rupture in glue
- adjustment/tuning of the rupture in the cladding sheet

The shell formulation of the barrier has shown is ability to improve the numerical behaviour of the overall crash of a full vehicle into the frontal ODB barrier.

The final enhanced model will be more faithful to physical phenomena and is now quite ready to be applied on projects in large dimensioning phase.

ACKNOWLEDGMENTS

The authors wish to thank the different labs (TNO/TTAI, the internal PSA Peugeot Citroën Crash Test Centre and the PSA Peugeot Citroën internal material Lab), the AFL honeycomb manufacturer and its directors Mr Poisson and then Mr Touratier and the PSA Peugeot Citroën research teams that were involved in this study (in the “SIMU” and “SGV” departments).

REFERENCE

[1] ECE94.01 Frontal Impact Regulation

[2] Euro NCAP Frontal Impact Testing Protocol - Version 5.0

[3] An investigation to compare the application of Shell and Solid Element Honeycomb Model in ODB, German LS-DYNA Forum October 2006, Brian Walker, Ian Bruce, Paul Tattersall, Mehrdad Asadi

[4] Development of the Advanced Finite Element Model for ODB Impact Barrier Mehrdad Asadi – Brian Walker – Hassan Shirvani, LS-Dyna 2009

[5] A New Generation of Crash Barrier Models for LS-DYNA, LS-Dyna Anwenderforum, Brian Walker – Ian Bruce – Paul Tattersall – Mehrdad Asadi, Ulm 2006

[6] A new Method to Model Aluminium Honeycomb Based Crash Barriers in Lateral and Frontal Crash Load Case, LS-Dyna Anwenderforum, Thomas Jost – Thomas Heubrandtner- Christian Ruff – Bernhard Fellner , Bamberg 2008

[7] A simplified model to simulate crash behaviour of honeycomb, Proceedings of International conference on Advanced Design and Manufacture, M. Asadi – Prof H. Shirvani – Prof E. Sanaei – Dr M. Ashmead,8-10th January, 2006, Harbin, China

INJURY ANALYSIS OF REAL-WORLD SMALL OVERLAP AND OBLIQUE FRONTAL CRASHES

Rodney W. Rudd, Mark Scarboro, James Saunders
National Highway Traffic Safety Administration
United States
Paper Number 11-0384

ABSTRACT

Recent research has indicated poor injury outcomes for front row occupants of passenger vehicles equipped with frontal air bags when the longitudinal frame rail(s) are missed by the struck object. The objective of this research was to establish key factors for injury causation from a uniform manual analysis of real world crashes where very limited or no engagement of the longitudinal structures occurred. A multidisciplinary team of experts at the National Highway Traffic Safety Administration was assembled to review the available real-world cases matching this crash profile. The NHTSA team utilized a uniform process to review all cases to ensure the same data points were evaluated by each team member. Regular meetings were held by the team to discuss cases and to keep the reviews uniform. More than 380 cases were extracted from the National Automotive Sampling System-Crashworthiness Data System (NASS-CDS) and the Crash Injury Research and Engineering Network (CIREN) for analysis.

Injuries to the thorax and pelvis were the most prevalent, and oblique loading played a role in thoracic and head injury causation. The cases reviewed demonstrated possible issues with air bag coverage of contact points, intrusion contributing to injury, and occupant lower extremity kinematics associated with crash obliquity influencing pelvic fractures. The final result of the reviews was to initiate a vehicle crash research plan to test the feasibility of recreating the real-world crash and kinematic responses seen during the case reviews. The results of these case reviews indicate opportunities for improved anthropomorphic test device (ATD) response to duplicate the crash outcomes seen in this research.

INTRODUCTION

Recent studies of frontal crashes identified several factors that are thought to lead to fatalities of restrained occupants in newer vehicles [Brumbelow and Zuby, 2009; Rudd *et al.*, 2009]. The authors in both studies identified concentrated or limited engagement of frontal structures as one of the factors associated with increased risk to the occupants. These findings were consistent with those by Lindquist *et al.* [2004] who associated small overlap frontal crashes with a large percentage of fatalities in a Swedish study. As a result of the NHTSA study published by Bean *et al.* [2009], NHTSA stated its intent to further analyze low-offset and oblique frontal crashes in its Vehicle Safety Rulemaking & Research Priority Plan 2009-2011 published in November 2009 [NHTSA, 2009].

Prior studies of field data related to frontal crashes and the amount of overlap have yielded varying results. Pintar *et al.* [2008] examined NASS-CDS and CIREN crashes meeting frontal crash criteria, and focused heavily on the injury outcome in crashes with small overlap based on the Collision Deformation Classification (CDC) [SAE, 1980]. They found that the lower extremities, thorax and head were the most common AIS 3+ injuries in nearside small overlap crashes as determined by those with specific classifications in the CDC (they used FLEE and FREE crashes, which represent frontal plane damage near either the left or right corner with everything below the beltline sustaining damage). They noted that the average Injury Severity Score (ISS) was greater for mismatched vehicle crashes (based on size and geometry) compared to pole/tree impacts or matched vehicle crashes, suggesting that crash partner size and geometry play a role in small overlap crashes. Of particular interest

was their finding, among the CIREN cases, that occupant injury tended to differ based on the CDC extent zone such that occupants in crashes with extent zone 2-5 had more severe spine and chest trauma than those in crashes with extent zone 6-9. The thought was that vehicle kinematics differed during later phases of the crash, and the occupants did not engage the air bag as effectively due to vehicle rotation in the cases with extent zone between 2 and 5. Scullion *et al.* [2010] also examined the small overlap crash problem, but did so using a slightly different approach. Cases were selected from NASS-CDS, and they used an adaptation of the Frontal Impact Taxonomy (FIT) developed by Sullivan *et al.* [2008] to segregate the crashes in a way that accounted for longitudinal rail location. They found that the AIS 2+ and AIS 3+ injury risk in the small overlap crashes was not higher than that in moderate offset or offset crashes. Results from both of these studies suggest that further investigation of the problem is needed.

In order to establish a more comprehensive method to identify small overlap and oblique crashes, in which the longitudinal rails are not optimally engaged, the Medical College of Wisconsin (MCW) examined the nature of the crash problem and developed a crash filter that uses vehicle class-specific geometry along with crush measures and the CDC to identify these crashes in NASS-CDS and similar databases [Halloway *et al.*, 2011]. Their method identifies the small overlap and oblique crashes from crashes that are considered frontal based on the CDC damage plane, but also includes those to the left or right side as long as certain other criteria are met. This approach extracts a larger number of cases that meet the small overlap and oblique crash criteria.

The objective of this effort was to identify injury causation in small overlap and oblique frontal crashes, and to support the development of a research program to investigate these types of crashes. Prior studies have evaluated prevalence and injury distribution [Pintar *et al.*, 2008; Scullion *et al.*, 2010], but a more in-depth review of injury causation and crash configuration was required. While case-by-case analysis is labor-intensive, a thorough assessment of the problem cannot be developed based on coded data alone. This paper represents the findings from an in-depth review of applicable small overlap and oblique frontal crashes.

METHODS

Cases for review were selected from NASS-CDS and CIREN. The following parameters were required for inclusion into the dataset:

- Passenger vehicles model year 1998 and newer
- General area of damage of most significant event (GAD1) is frontal (F) or left side (L) with frontal directions of force (PDOF1 between 320 and 0 degrees)
- Belt-restrained drivers only
- AIS 3+ injuries to the head, chest and knee/thigh/hip (KTH) of lower extremity; fatalities were excluded since they were reviewed in the study by Rudd *et al.* (2009) and are generally more severe
- Cases with over- or underride were removed

A preliminary filter was applied to the crashes to determine whether they were left offset or left small overlap type crashes. The filter was developed by MCW [Halloway *et al.*, 2011], and bases the crash type on the CDC code and the crush measurements. The distinction between an offset and small overlap impact (SOI) is based on whether the left longitudinal or frame rail was engaged in the crash based on generalized geometric measures.

The cases were divided among a multi-disciplinary team of engineers and crash investigators, and were reviewed, in-depth, to extract pertinent observations about the crash and injury causation beyond what is available in the coded data. A case review tool, similar to that described by NHTSA [2009b], was used by the reviewers to display case information and record reviewer feedback in a consistent, structured manner. The reviewers relied on coded variables, photographic, graphic, and supplementary data sources available within the NASS-CDS and CIREN data systems to reach the conclusions drawn for each case. The case review tool compiled the case-based and reviewer-entered data for analysis, and guided the reviewer through the case starting with the crash elements, then focusing on the occupant and injury causation, and ending with a narrative. Examples of

reviewer-coded variables include assessment of the obliquity of the crash, amount of offset, whether occupant anthropometry played a role in the injury causation, the advanced restraint features available on the vehicle, as well as an evaluation of the injury sourcing for the major head, chest and KTH injuries. The pelvic injuries were investigated further using the available radiology or mannequin diagrams, when possible, to determine the specific type of pelvic fracture(s) sustained by the occupant.

Given the case-review nature of this work, the NASS-CDS and CIREN cases have been combined for analysis and presentation purposes. No statistical analyses have been performed on the combined data, and no assessment of injury risk can be conducted since case weights were not used. Some cases were removed from the dataset by the reviewers if the nature of the crash was felt to be outside the area of interest.

RESULTS

A total of 387 cases were selected from the NASS and CIREN databases for inclusion in this study based on the inclusion criteria presented above. After removing the cases rejected by the reviewers, 276 remained. Cases were typically rejected due to the crash involving multiple impacts or catastrophic severity. Table 1 shows some summary information for the final dataset. There were 124 left small overlap cases and 152 left offset cases. Although the CIREN and NASS-CDS cases are separated in this table, they have been combined for the remainder of the analysis. Though the average ISS was slightly higher for CIREN for both crash types, the difference was not large enough to raise question about the similarity of the two sets of data in the context of this study. One larger difference in the data was that the CIREN left offset crashes consisted of a higher proportion of vehicle-to-vehicle crashes than NASS, with 82% compared to 70% for NASS.

Table 1.
Summary of case data

	CIREN	**NASS**	**CIREN**	**NASS**	**Total**
	Left Offset	*Left Offset*	*Small Overlap*	*Small Overlap*	
Case count	89	63	70	54	276
% male	53.9	47.6	48.6	53.7	51.1
Min age	17	15	16	17	15
Max age	83	79	83	80	83
Mean age	45	41	44	41	43
Min ISS	9	9	9	9	9
Max ISS	43	50	50	50	50
Mean ISS	19.7	18.2	19.9	18.2	19.1
% vehicle to vehicle	82	70	66	67	72
% oblique[1]	39	40	31	50	39
1. Reviewer-determined classification					

Figure 1 shows the percentage of cases for each crash type (SOI and offset) in which the occupant sustained AIS 3+ injuries to the indicated body regions (AIS 2+ for leg/foot) by crash type. The percentage of injuries for each body region was similar for both crash types, and Figure 1 shows that the knee-thigh-hip (KTH, which includes pelvis) body region was the most-injured for both crash conditions. AIS 2+ below-knee injuries occurred with nearly the same frequency as AIS 3+ chest injuries in both crash types.

Reviewers were tasked with identifying the crash angle as either co-linear or oblique, which affects occupant kinematics and interaction with the restraints and interior components. Figure 2 shows the percentage of cases in each crash category in which the occupant sustained AIS 3+ injuries to the indicated body regions (AIS 2+ for leg/foot) in co-linear or oblique left SOI crashes. The percentage of injuries for each body region was generally similar for both crash angles, and Figure 2 shows that the

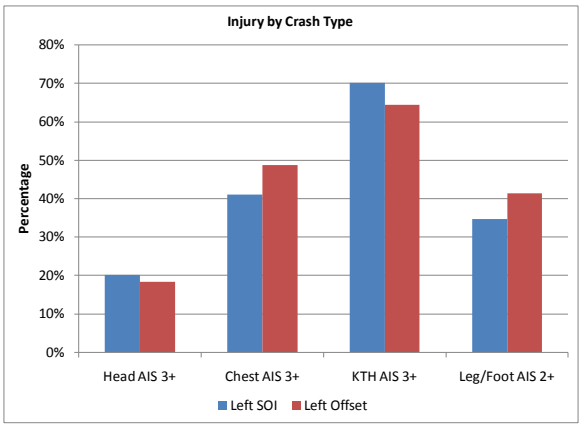

Figure 1. Percentage of cases sustaining injury to specified body regions for left small overlap and left offset crashes

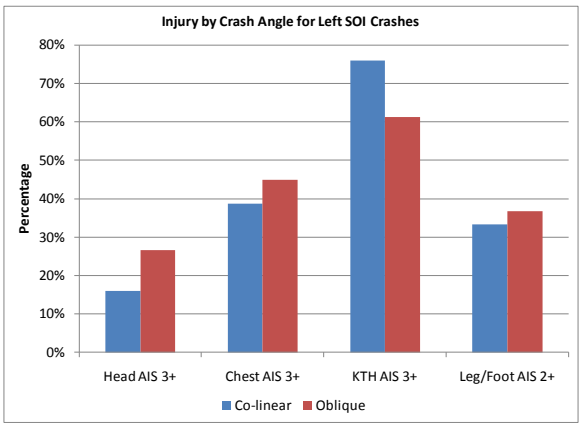

Figure 2. Percentage of cases sustaining injury to specified body regions for left SOI crashes by co-linear and oblique crash angle

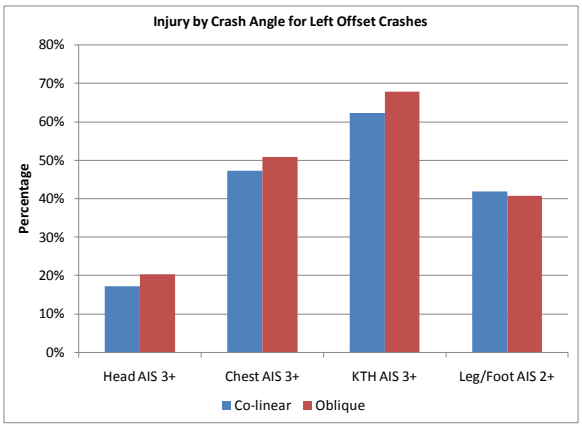

Figure 3. Percentage of cases sustaining injury to specified body regions for left offset crashes by co-linear and oblique crash angle

KTH body region showed the most difference between co-linear and oblique. Oblique crashes also showed a higher percentage of cases with AIS 3+ head injury. Figure 3 shows that crash angle has a relatively minor effect in the left offset crashes, with the various body regions seeing similar injury prevalence regardless of obliquity.

Figure 4 shows the assigned source for the most severe head injury for both left SOI and left offset crashes. For left SOI, the A-pillar and the steering wheel (SW) stand out as the most prominent injury sources for head injuries. For left offset crashes, the steering wheel and air bag were the most prominent, though the "other" category was cited frequently as well. Notable differences between the two crash types are seen with the air bag, A-pillar and instrument panel (IP), with the IP and A-pillar being more common in the small overlap crashes. Figure 5 shows the assigned source for the most severe chest injury for both left SOI and left offset crashes. There was a large difference in the number of chest injuries sourced to the door when comparing SOI to offset, which was offset by belt- and steering wheel-induced injuries. The KTH sources are shown in Figure 6, where it is evident that the instrument panel is the most frequent source in both SOI and offset crashes. There are more door-related KTH injuries in SOI crashes, but the proportion is small compared to the IP.

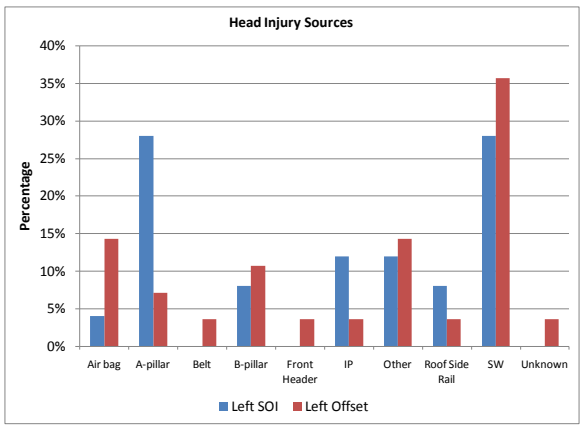

Figure 4. Injury source for most severe AIS 3+ head injuries for left SOI and left offset crashes

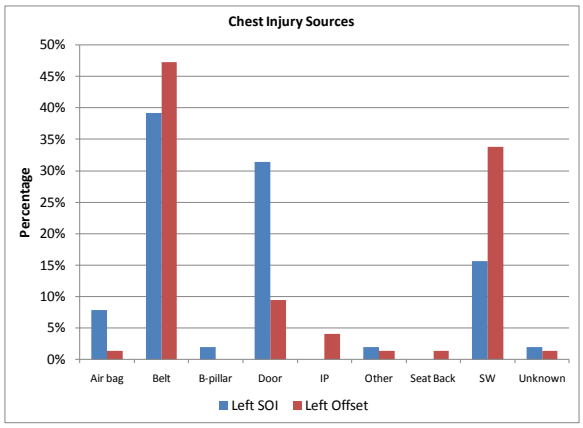

Figure 5. Injury source for most severe AIS 3+ chest injuries for left SOI and left offset crashes

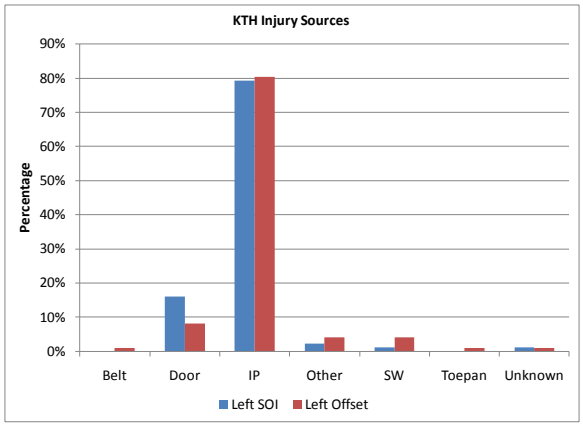

Figure 6. Injury source for most severe AIS 3+ KTH injuries for left SOI and left offset crashes

The next part of the analysis was to determine if crash angle has an effect on injury sources to the head, chest and KTH. Due to the number of cases for each crash type, the left SOI and left offset crashes were combined for this analysis so that the groups would not be too small. Figure 7 shows the head injury sources broken down by the reviewer-assessed obliqueness category. The most noticeable differences, other than for the "other" category, were the larger number of head injuries caused by the A- and B-pillars in oblique crashes. For the chest injury sources, only door showed a large difference for co-linear and oblique crashes (Figure 8). The belt was the most common source of chest injury, regardless of crash angle. The KTH sources are shown in Figure 9 for co-linear and oblique, but the differences are minor with only a slight increase in KTH injuries attributed to the door in the oblique crashes. Contact with the instrument panel is, by far, the most common cause of the KTH injuries.

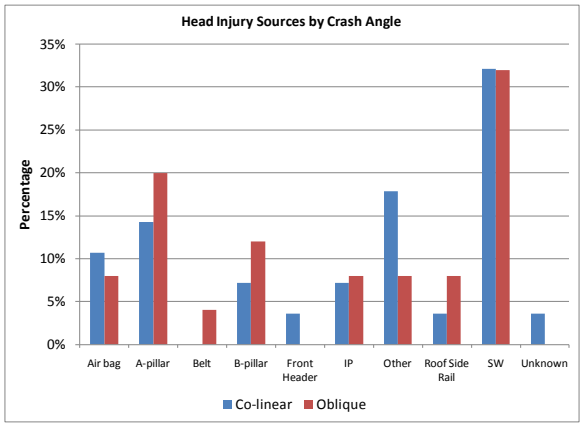

Figure 7. Injury source for most severe AIS 3+ head injuries for co-linear and oblique crashes

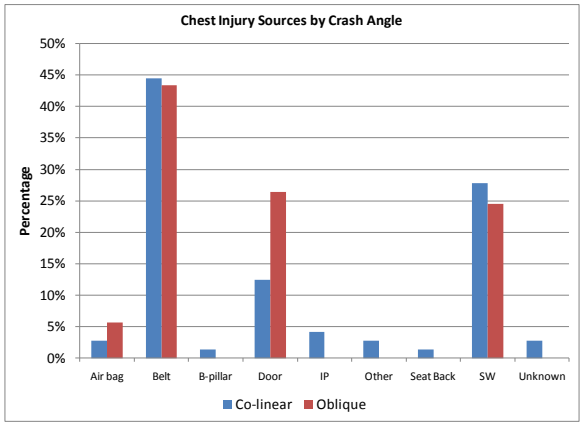

Figure 8. Injury source for most severe AIS 3+ chest injuries for co-linear and oblique crashes

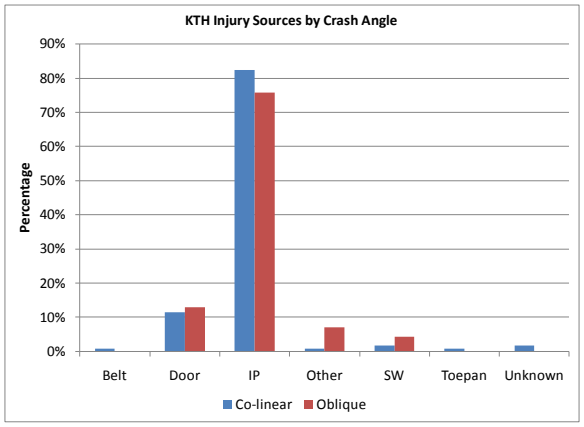

Figure 9. Injury source for most severe AIS 3+ KTH injuries for co-linear and oblique crashes

Since loading and intrusion of the footwell area is influenced by the motion of the left front wheel,

reviewers were asked to identify whether the wheel and tire assembly had engaged the rear portion of the wheel well and front door hinge pillar. Figure 10 and Figure 11 show the engagement of the tire for left SOI and left offset crashes. Tire engagement seemed to affect head injury most in the small overlap crashes. It can be seen from Figure 11 that left offset cases, in which the tire had engaged the structure near the occupant compartment, had a higher frequency of KTH injuries. There was less noticeable of a difference for the head and chest.

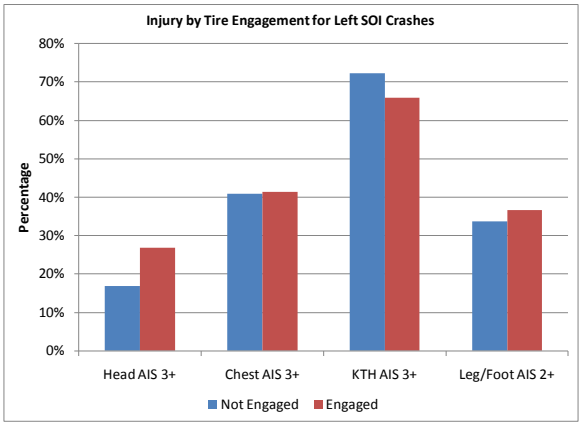

Figure 10. Injury prevalence per body region for wheel/tire engagement in left SOI crashes

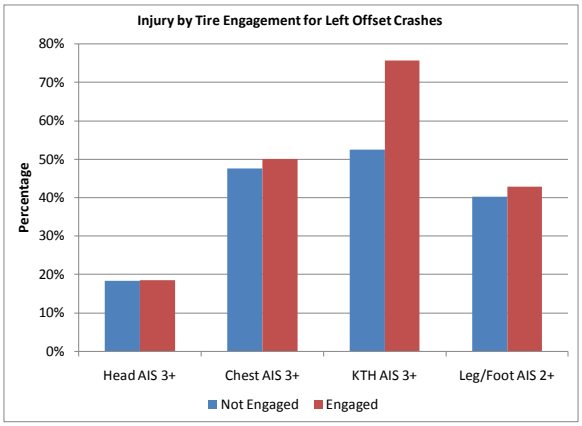

Figure 11. Injury prevalence per body region for wheel/tire engagement in left offset crashes

Since the KTH region stood out as the most injured body region, a more detailed analysis was conducted. Although there was a large number of thigh injuries (femur shaft, subtrochanteric and/or supracondylar fractures) captured in the KTH grouping, there was an interest in looking into the detail of the pelvic and hip injuries in the KTH group due to the clinical significance of these injuries. The types of fractures associated with thigh injuries do receive an AIS level 3 severity score indicating a serious threat to life, however, when treated promptly and appropriately these injuries, as a single-system insult, typically have shorter hospital stays and good outcomes. In contrast, injuries to the hip (especially injuries involving the articular surface of a joint) are well documented to be more complex to treat and have less optimal outcomes when compared to non-articular fractures of the KTH. Due to the non-specificity of the AIS coding system as it relates to hip injuries and the identification of articular involvement, it was necessary to review each case to document the level of pelvic and hip injury in greater detail. Since AIS severity coding is based on threat to life it was determined that hip and pelvic injuries at the AIS 2 level would be included in this analysis as well, since these codes include injuries to articular and weight-bearing structures. Along with capturing anatomical detail, the determination of loading conditions for injury causation was also pursued.

Figure 12 shows the breakdown of the locations of all coded KTH injuries with a severity of AIS 2 or higher among the 184 occupants who sustained AIS 3 and higher injury to the KTH region. There are a total of 384 AIS 2+ injuries coded for this group of occupants. The combination of pelvis and hip injuries makes up 44% of all AIS 2+ KTH injuries, while thigh injuries make up 37% of the injuries, and knee injuries account for the remaining 19%. There were 96 cases (52%) out of the 184 KTH cases where there was either a pelvic and/or hip injury.

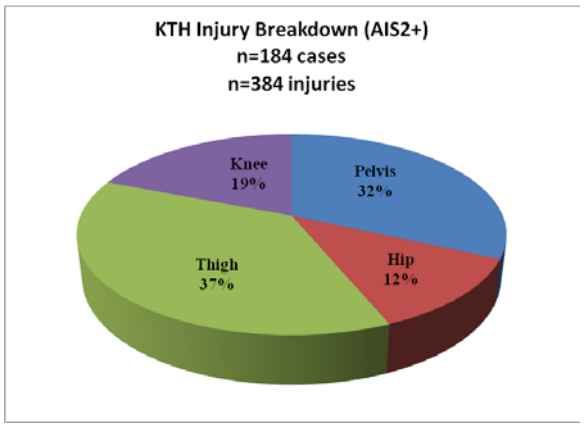

Figure 12. KTH injury breakdown for all injuries AIS 2 and higher

The breakdown of anatomical injury in the 96 cases where either a pelvic or hip injury was sustained, along with crash mode analysis, is displayed in Figure 13. Isolated acetabular fractures, pelvic ring fractures (sacrum, sacro-iliac joint(s), ilium or pubic rami) and proximal femur fractures are the highest frequency injuries. Acetabular fracture is present in 50% of all the cases, compared with only 36% of the cases having a pelvic ring fracture. The proximal femur (including fractures of the femoral head, neck, trochanter and hip dislocations) sustained injury in 32% of the pelvic/hip cases. The crash modes indicate minimal differences in the occurrence of acetabular fractures. Left offset crashes had the highest rate at 51% with the SOI crashes indicating 49%. The co-linear crashes had a rate of 52% with the oblique crashes demonstrating acetabular fractures 47% of the time.

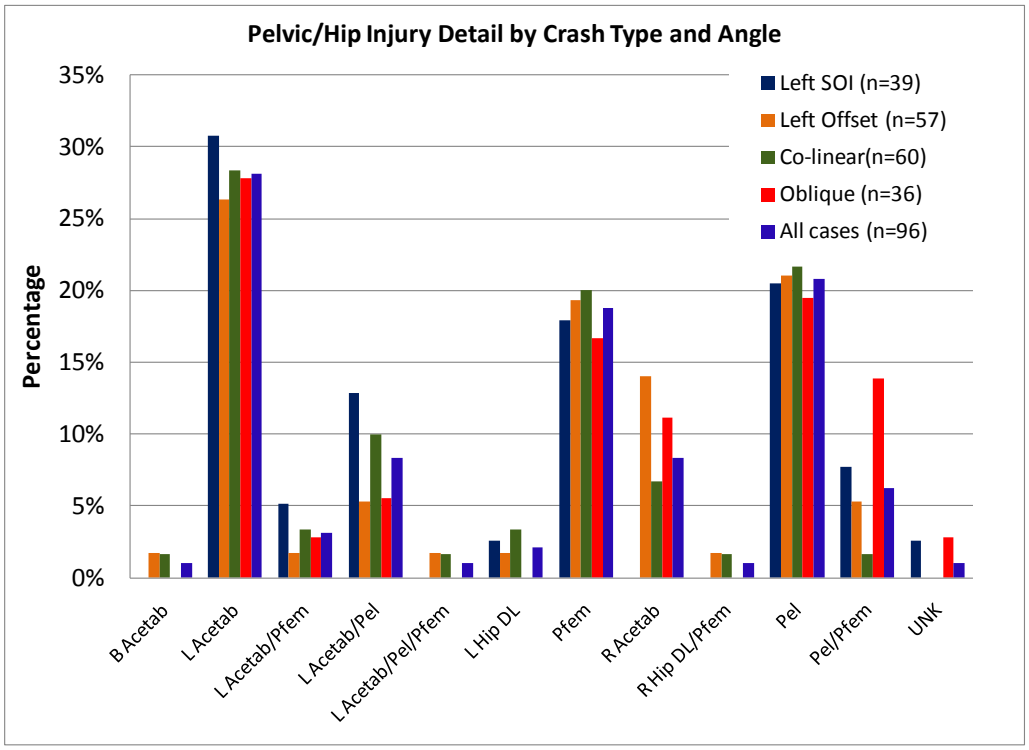

Figure 13. Anatomical detail of pelvic and hip injury for all study crash modes (B=bilateral, L=left, R=right, Pfem=proximal femur, Pel=pelvis, DL=dislocation)

In these two frontal crash modes, the femur shaft fractured less than 50% of the time, on average. However, the occupants in this group who sustained a pelvic and/or hip injury did so with the majority experiencing axial loading via the thigh. Figure 14 displays the incidence of femur shaft fracture in the subset of occupants sustaining pelvic and/or hip injury. Oblique crashes are the highest with a 50% incidence of femur shaft fracture concurrent with pelvic and/or hip injury. Left SOI and left offset both indicate the occurrence of femur shaft fracture with pelvic and/or hip injury slightly more than 40% of the time. Only 35% of the co-linear crashes resulting in pelvic and/or hip injury also sustained a femur shaft fracture.

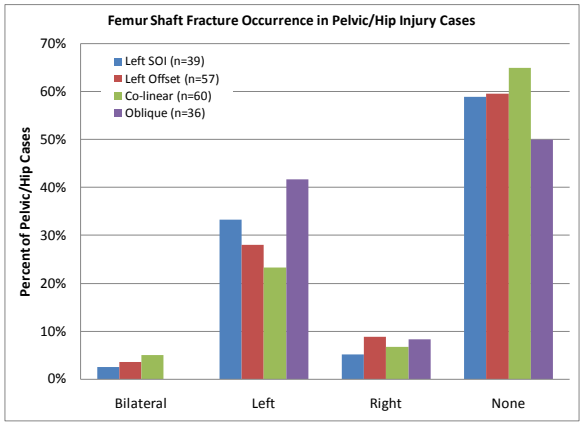

Figure 14. Pelvic/hip injury cases with associated femur shaft fractures

DISCUSSION

The differences in the incidence of injuries to the different body regions based on crash type and angle were not as large as was expected at the onset of this study. Regardless, in this subset of crashes, the results did show that the knee-thigh-hip was the body region sustaining the most AIS 3+ injuries. Overall, for the proportion of injury in the body regions, it seemed that crash angle had a greater influence than did crash type, especially when considering only left small overlap crashes (Figure 2). The oblique small overlap crashes saw a greater percentage of AIS 3+ head injury and a reduction in KTH injury compared to the co-linear crashes. For the head, as the crash angle deviates from co-linear, the kinematics of the occupant towards the left door results in less effective restraint by the air bag. A small increase in chest injury was also seen for the small overlap oblique crashes as well. It would be expected that the angle of the crash would play a role for left offset crashes as well, but there were only minor increases in injury prevalence compared to the co-linear crashes shown in Figure 3. In general, the findings of little distinction in injury between small overlap and offset are consistent with findings reported by Scullion *et al.* [2010] that injury risk was not higher in small overlap crashes.

Considering the source of the AIS 3+ head injuries, the steering wheel was the most common regardless of crash type or angle, though there were some differences worth noting. The A-pillar was more commonly cited in the small overlap than in the offset crashes, and it was responsible for a similar number of the AIS 3+ head injuries as the steering wheel in the small overlap group (Figure 4). There were also more head injuries associated with instrument panel contact in small overlap crashes, suggesting that the head was missing the air bag and steering wheel and moving slightly towards the side. This finding is corroborated by an increase in roof side rail contact and a decrease in air bag contact for the small overlap head injuries.

The changes in the chest injury source for small overlap crashes compared to left offset showed a similar trend of outboard movement, with SOI crashes having a larger percentage of AIS 3+ chest injuries associated with door contact and fewer with steering wheel contact (Figure 5). The proportion of chest injuries associated with belt contact were fairly similar for both crash types, and the belt was the most common source overall. Eighty percent of the knee-thigh-hip region injuries were associated with the lower instrument panel in both crash types, though there were slightly more KTH injuries associated with the door in the small overlap crashes (Figure 6). The overall tendency for more outboard injury sources in the small overlap crashes was expected due to the interaction of the struck and striking vehicle in these types of crashes, in which the striking object moves down the left side of the vehicle during the impact event. Figure 15 shows the crush of a vehicle in a co-linear small overlap crash, and Figure 16 shows the front left door of that vehicle, which is crushed due to continued interaction of the striking vehicle moving along the side. The vehicle position at, and after, impact is shown by the scene diagram in Figure 17, where it is evident that the case vehicle underwent rotation during the event. The rotation that occurred induced some lateral motion of the occupant towards the door, which was intruded by the crush caused by the striking vehicle moving along the side of the car. These factors lead to what appears to be a co-linear crash having injury sources that are more associated with an oblique crash. The driver in this case vehicle sustained chest injuries associated with contact to the interior door panel.

Figure 15. Front crush of vehicle in small overlap, co-linear crash

Figure 16. Crush of left front door of vehicle shown in Figure 15

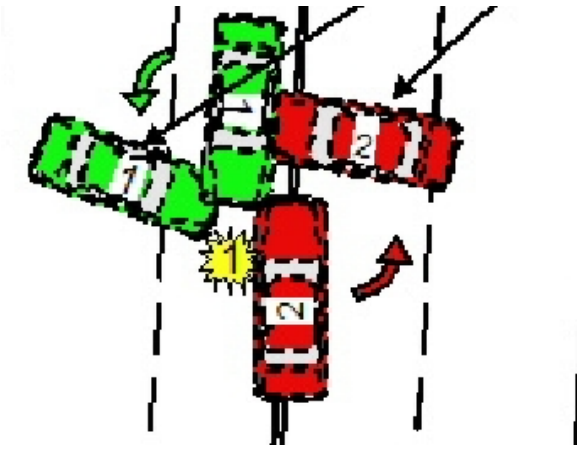

Figure 17. Vehicle rotation during crash indicated by position at impact and at rest (case vehicle, Vehicle 1, shown in green)

The injury source analysis was also conducted based on the reviewer-determined crash obliquity. As expected, the oblique crashes resulted in more A-pillar and roof side rail head injuries (Figure 7) and the chest had more of its AIS 3+ injuries sourced to the door than in the co-linear crashes (Figure 8). Chest injuries associated with the belt and steering wheel were about the same regardless of crash angle, which would be expected since these are all frontal crashes with a significant longitudinal loading vector. As with the crash type analysis, there wasn't much difference for the KTH injury source since most were attributed to contact with the lower instrument panel.

The knee-thigh-hip, which was the most frequently injured body region overall, was most often injured due to contact with the instrument panel in all crash types and angles. Because of the relatively small number of injuries associated with side components, it was not possible to discern any differences in causation based on crash type or angle. The detailed review of the pelvic and hip injuries indicates a large number of acetabular fractures within that group of injuries. Acetabular fractures typically involve disruption of the articular surface of the hip joint. This disruption often requires surgical repair, long-term recovery and can lead to artificial hip replacement, making this injury more life-altering than life-threatening. The pelvic and hip injury analysis also revealed over half of these injuries occurred in the absence of a femur shaft fracture, which suggests that more emphasis be placed on the evaluation of hip and pelvis loading in these types of crashes.

CONCLUSIONS

The detailed review of left offset and left small overlap frontal crashes in this study was conducted in order to identify distinct injury causation characteristics in each crash mode. The findings revealed that the crash angle influenced injury causation more than crash type, with oblique crashes demonstrating differences in head and chest injury sources. Small overlap crashes frequently produce oblique kinematics, and the interaction along the side of the struck vehicle increases chances for injuries from outboard components such as the door and A-pillar. A detailed review of the knee-thigh-hip injuries shows that hip and pelvis injuries frequently occur in the absence of femur fractures, especially in oblique crashes.

The findings of this work suggest that a test program to study occupant response in small overlap and oblique frontal crashes will need to be sensitive to the differences in occupant loading and injury causation that have been found in these cases. The ATD used in the testing should possess the biofidelity to replicate the real-world kinematics, and should be capable of measuring loads relevant to the dominant injuries. Appropriate biofidelity and injury measurement in the KTH complex is highly desirable due to the high number of injuries seen in this study.

Additional research is required to investigate the interaction and possible benefits of new safety technologies in these types of crashes. Technologies like side curtain air bags may be able to offer head

protection from A-pillar contact, striking vehicle contact or possibly upper door contact. Other improvements, such as chassis design, may minimize intrusion of components that frequently cause injury in crashes with small amounts of overlap.

ACKNOWLEDGEMENT

The authors would like to acknowledge the team members who assisted in the review of the NASS and CIREN cases and thank them for their contributions to this work: Matthew Craig, Mark Mynatt, Dan Parent, Michael Parsons, Jeff Suway and Chris Wiacek.

REFERENCES

Bean, J.D., Kahane, C.J., Mynatt, M., Rudd, R.W., Rush, C.J. and Wiacek, C. (2009) "Fatalities in frontal crashes despite seat belts and air bags – Review of all CDS cases – model and calendar years 2000-2007 – 122 fatalities." DOT HS 811 102, National Highway Traffic Safety Administration, Washington, DC.

Brumbelow, M.L. and Zuby, D.S. (2009) "Impact and injury patterns in frontal crashes of vehicles with good ratings for frontal crash protection." 21st International Technical Conference on the Enhanced Safety of Vehicles, paper number 09-0257.

Halloway, D.E., Saunders, J., Yoganandan, N. and Pintar, F. (2011) "An operational definition of small overlap impact for published NASS data." SAE World Congress, paper no. 2011-01-0543.

Lindquist, M., Hall, A. and Bjornstig, U. (2004) "Car structural characteristics of fatal frontal crashes in Sweden." ICrash 2004, 9(6), 587-597.

NHTSA (2009a) "Final vehicle safety rulemaking and research priority plan 2009-2011." Docket No. NHTSA-2009-0108.

NHTSA (2009b) "Problem definition for pre-crash sensing advanced restraints." DOT HS 811 114.

Pintar, F.A., Yoganandan, N. and Maiman, D.J. (2008) "Injury mechanisms and severity in narrow offset frontal impacts." Proceedings of the 52nd Annual Association for the Advancement of Automotive Medicine Conference.

Rudd, R.W., Bean, J., Cuentas, C., Kahane, C.J., Mynatt, M. and Wiacek, C. (2009) "A study of the factors affecting fatalities of air bag and belt-restrained occupants in frontal crashes." 21st International Technical Conference on the Enhanced Safety of Vehicles, paper number 09-0555.

SAE (1980) "Collision Deformation Classification." SAE Technical Standard J224, rev. MAR80.

Scullion, P., Morgan, R.M., Mohan, P., Kan, C., Shanks, K., Jin, W. and Tangirala, R. (2010) "A reexamination of the small overlap frontal crash." Proceedings of the 54th Annual Association for the Advancement of Automotive Medicine Conference.

Sullivan, K., Henry, S. and Laituri, T.R. (2008) "A frontal impact taxonomy for USA field data." SAE World Congress, paper no. 2008-01-0526.

FRONTAL CRASHES BETWEEN THE LONGITUDINAL RAILS

Paul Scullion
Richard M. Morgan
Kennerly Digges
Cing-Dao (Steve) Kan
George Washington University – National Crash Analysis Center
USA
Paper Number 11-0372

ABSTRACT

The *objective* of this study is to further investigate the injuries and injury mechanisms associated with belted front-row occupants in *Between Rail* frontal crashes. This study examines *real-world crash data from the NASS-CDS* between the years 1998-2009 with a focus on frontal crashes involving 1997 and later model year vehicles. This study expands upon a *methodology* developed by Ford Motor Co. for classifying frontal impacts based upon the Collision Deformation Classification (CDC) [SAE J224] and the location of direct damage relative to the estimated location of the underlying vehicle frame-rail structure. This Frontal Impact Taxonomy will be used to identify those crashes with damage localized between the vehicle frame-rails. In a recent study, it was identified that *Between Rail* impacts had a higher risk of front row occupants sustaining either an MAIS 2+, or MAIS 3+ injury, compared to all other frontal impact damage classifications (Full engagement, Offset, Moderate offset, Small Overlap, and so on). The extent of damage will be used as a measure of impact severity. This study will investigate a laboratory test by the Insurance Institute for Highway Safety. This laboratory test involves crashing the front of a passenger vehicle into a rigid pole along the longitudinal line of the vehicle. The laboratory test will be compared with real-world crash data.

INTRODUCTION

Arbelaez et al. (2006) analyzed real-world crash data to suggest that frontal collisions with narrow objects contribute significantly to occupant fatalities and injuries. He found that the fatality rate for this type of crash was declining less quickly than other types of frontal crashes. Arbelaez proposed that safety professionals for government regulation and consumer information should study with more concern the frontal collision with narrow objects.

Sullivan et al. [2008] of Ford Motor Company developed a methodology for defining the post-crash damage profile of vehicles in a frontal impact collision, using both vehicle crush measurements and elements of the CDC (National Automotive Sampling System - Crashworthiness Data System or NASS-CDS). This Sullivan classification method is based on the concept of identifying the location of the direct damage relative to the estimated location of the underlying vehicle structure, and the likely engagement of these primary structures (during the crash). The Ford study defined a *D, Y, Z No-Rail* crash. This classification involved direct damage to one of the larger frontal crash zones (SHL = D, Y, or Z; see SAE J224) and having none of the rails engaged. Sullivan reported that the *D, Y, Z No-Rail* crash had the highest risk of AIS ≥ 3 injury of any frontal crash type. The Ford paper did not specify that the stuck object had to be a narrow tree or pole, but did caution that some of the *D, Y, Z No-Rail* crashes involve a complex collision event.

Padmanaban and Okabe (2008) examined belted drivers of passenger vehicles in frontal crashes with narrow objects using US field data. As part of their study, they did a detailed examination of 400 NASS-CDS cases where the passenger vehicle impacts a narrow object in a frontal collision. Padmanaban and Okabe suggested that (1) frontal crashes with poles, posts, or trees are relatively infrequent and (2) the fatality risk is lower in narrow-object collisions than in other frontal crashes.

Hong et al. (2008) investigated the dynamic response of the structure of a passenger vehicle impacting (1) a full-frontal rigid barrier, (2) an offset frontal deformable barrier, and (3) a center pole. A finite element model of the vehicle was used for the study. The behavior of the frame rail was of key importance in understanding the structural behavior. It was found that the passenger vehicle well managed the full-frontal crash and 40% offset frontal crash by absorbing crash energy in the frame rails. In the center rigid pole impact, the pole avoided the side rails and caused detrimental intrusion into the occupant compartment. This study suggested the occupants in the *Between Rail* type of crash would

benefit by a transverse connection (or coupling) to the longitudinal frame rails.

At the IRCOBI Conference later in 2008, Hong et al. presented a step-by-step (and side by side) comparison of the (1) full-frontal impact, (2) 40% frontal offset impact, and (3) a center rigid pole impact. The graphical comparison (in 20-msec increments) illustrated the side rails crushed greatly in the full-frontal and the 40% offset crash. In the center pole impact, the pole misses the frame rails. While not shown in detail in the paper because of space limitation, compartment intrusion and dummy readings were high in the *Between Rail* type of crash.

The researchers of the Insurance Institute for Highway Safety (IIHS, 2009) analyzed case files from NASS. They found frontal crashes in which 116 drivers and right-front passengers were seriously traumatized or died despite using safety belts. Nineteen percent of the crashes were center impacts into a tree, pole, or post. IIHS noted that neither the government nor IIHS uses a frontal pole crash in their consumer information program. They had done center pole impacts with a 25.4-mm diameter pole in the laboratory. IIHS had concerns in matching the predicted injury risk from the laboratory tests with chest and abdominal trauma found in field data.

In 2010, Scullion et al. applied the Ford taxonomy (see Sullivan 2008) to classify real-world frontal-impact crashes based on the National Automotive Sampling System (NASS). Frontally-impacted vehicles were identified for 1985 – 2008 model year passenger vehicles with Collision Deformation Classification (CDC) data from the 1995 – 2008 years of NASS. Using the CDC-based information in NASS and using the methodology identifying the location of the longitudinal rail, he successfully grouped together the frontal impact crashes with common damage patterns. The Scullion findings suggested that the *Between Rail* crash—where the direct damage is between the two longitudinal rails—accounts for (1) 5.7% of all frontal crashes and (2) has a higher injury risk than any other crash type studied.

METHODOLOGY

This study incorporated the use of real-world crash data from the NASS-CDS to further investigate occupant injuries in *Between Rail* frontal crashes. The following case selection criteria were applied to the NASS-CDS data:

- NASS-CDS data 1997-2009
- Passenger cars or Light Trucks and Vans
- Vehicle model years 1997+
- Vehicles with a General Area of Damage to the Front of the vehicle
- Vehicles with a Direction of Force of 11, 12, or 1 o'clock
- Vehicles with a secondary impact where the extent of damage was greater than 2 were excluded.

Sullivan Frontal Impact Taxonomy

As previously mentioned Sullivan et al. (2008) developed a Frontal Impact Taxonomy (FIT) as a method for classifying vehicle damage based upon the post-crash damage profile and estimated location of the underlying vehicle frame rail structure.

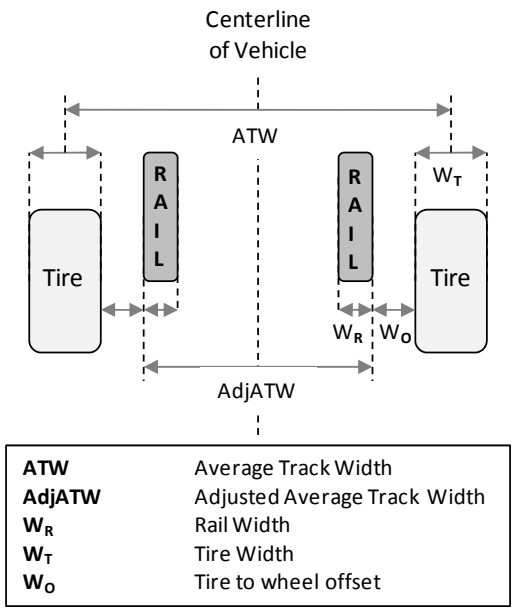

Figure 1. Estimated location of underlying vehicle structure (Sullivan, 2008).

In NASS-CDS there are no measurements that indicate the location of the vehicle frame rails relative to the centerline of the front-end of the vehicle. Sullivan used a sample of vehicles with known measurements to determine a ratio between the vehicle Average Track Width (ATW), which provided in NASS-CDS, and the width of the vehicle frame rails. The Adjusted Average Track Width (AdjATW) was calculated for both passenger cars and light trucks and vans (LTVs) using the formula shown in Equation 1.

$$\mathbf{AdjATW = ATW - WT - 2\ WO} \qquad \text{(Eq. 1).}$$

The AdjATW to ATW ratio was 0.7 for passenger cars and 0.6 for LTVs. The estimated location of the underlying frame rails for passenger cars in NASS-CDS was calculated using the formula shown in Equation 2.

Passenger Cars: **AdjATW = ATW * 0.7** (Eq. 2).
LTVs: **AdjATW = ATW * 0.6**

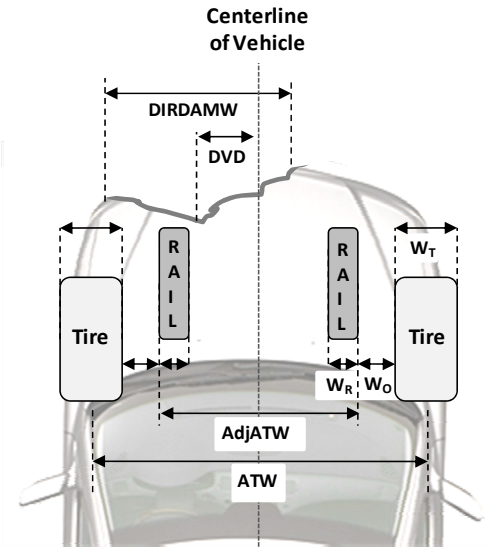

Figure 2. Direct damage location relative to estimated location of the underlying vehicle frame rails (Sullivan, 2008)

The Sullivan methodology is based upon the concept of classifying damage based on the engagement of the underlying frame-rail structure. In NASS-CDS the crash investigation report typically includes the direct damage width (DIRDAMW) as well as the location of the center of direct damage relative to the centerline of the vehicle (DVD). Assuming symmetry of the vehicle frame rails, if the location of direct damage was identified as having overlapped the location of a given frame rail, it was classified as having been engaged during the collision (Figure 2). Conversely, if the direct damage did not overlap the estimated location of a given frame rail it was classified as non-engaged.

In this study, the primary focus of analysis is on *Between Rail* crashes whereby it was determined that there was no rail engagement, with the direct damage located entirely between the vehicle frame rails.

The following additional selection criteria were applied to the data to ensure that vehicles could be classified based on post crash damage for the purpose of identifying *Between Rail* impacts in NASS-CDS:

- Known direct damage width
- Known direct and indirect damage width
- Known or non-missing average track width

The methods used in the Sullivan study were expanded to define a modified classification for frontal crashes designed to specifically address the *Between Rail* frontal crash. The taxonomy that was used in this study was comprised of seven distinct classification groups:

- Full Engagement
- Offset
- Moderate Offset
- Small Offset
- Between Rail
- Underride
- Other

RESULTS

Based on these NASS-CDS vehicle selection criteria, there were a total of 12,854 FIT classifiable vehicles (5,030,413 weighted) available for analysis. The graph in Figure 3 shows the distribution of frontal crashes by FIT classification. Further details of these classification groups are provided in Appendix A.

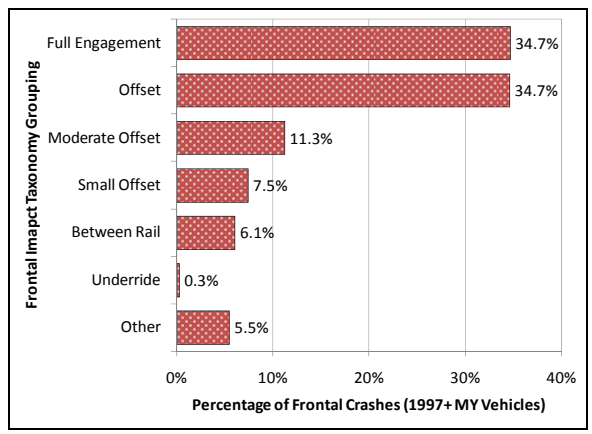

Figure 3. NASS-CDS 1997-2009 – Distribution of 1997+ MY Frontal Impact Taxonomy Classified Vehicles (weighted).

The highest distribution of frontal crashes involving 1997+ model year vehicles were attributable to *Full Engagement* and *Offset* crashes, in which each accounted for approximately 35% of the overall total. *Small Offset* crashes, where the direct damage occurred outside (with no engagement) of the vehicle frame rails were observed in 7.5% of frontal impact crashes (375,026).

Approximately one-in-twenty (6.1%) frontal crashes were classifiable as a being a *Between Rail* crash indicating that this type of impact damage is not an entirely uncommon occurrence with respect to frontal crashes occurring in the real-world.

Additional criteria were applied to the data for the analysis of occupant injury in 1997+ model year vehicles.

- Belted occupants aged 16 years old or older
- Occupants seated in the left-front (driver) or right-front (passenger) seat
- Vehicles were not involved in a rollover

Occupant injuries in NASS-CDS are recorded using the Abbreviated Injury Scale (AIS) developed by the Association for the Advancement of Automotive Medicine. This provides a measurement scale for assessing the severity of injuries to individual occupant body regions. This scale ranges from 1 (minor injury) to 6 (maximum injury). This analysis will provide crash injury data for both moderate or greater injuries (AIS 2+), and serious or greater injuries (AIS 3+). The highest severity injury sustained by an occupant is referred to as the Maximum AIS, or MAIS.

In Figure 4 the risk of MAIS 2+F and MAIS 3+F injuries to the nearside front-row occupant is displayed for each of the FIT groups.

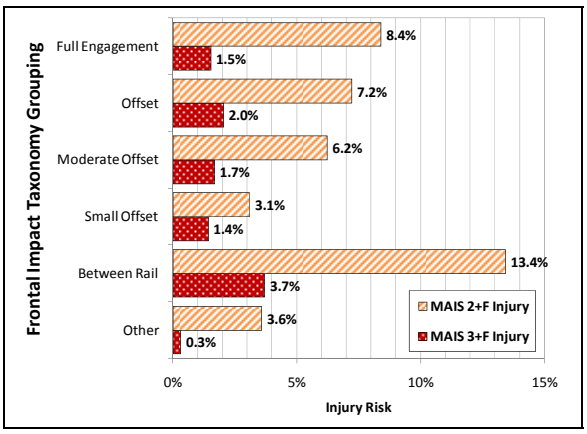

Figure 4. NASS-CDS 1997-2009 – Front row occupant injury risk in frontal impacts to 1997+ Model year vehicles (weighted).

The risk of an MAIS 2+ or MAIS 3+ injury was calculated by dividing the total number of injured occupants by the total number of front-seat occupants for each of the FIT groups. The risk of MAIS2+F and MAIS 3+F injury was greatest for those exposed to a Between Rails frontal crash compared to any other type of frontal crash, with risk values of 13.4% and 3.7% respectively. The risk of MAIS 3+F injury was similar among the Full Engagement, Offset, Moderate Offset, and Small Offset groups, with risks ranging between 1.4% and 2.0%. The weighted risk for underride crashes was not calculated due to small sample size.

The focus of this study is to assess the injuries associated with *Between Rail* frontal crashes. Based on the aforementioned case selection criteria there were a total of 903 occupants (274,458 weighted) in Between Rail frontal crashes that were available for analysis.

The Body Region AIS (BAIS) is the highest AIS severity injury sustained to each individual body region. Figure 5 show the weighted distribution of BAIS 2+ and BAIS 3+ injuries for each of the occupant involved in a *Between Rail* frontal crash.

The graph in Figure 5 provides an overview of the distribution of BAIS 2+ injuries in *Between Rail* frontal crashes. For the purposes of this study the following body regions were used in the classification of BAIS injuries: Head (including face), Neck (including C-Spine), Thorax, Abdomen, Spine (excluding C-Spine), Upper Extremity, Foot & Ankle, and Knee-Thigh-Hip (and other non-foot & ankle injuries).

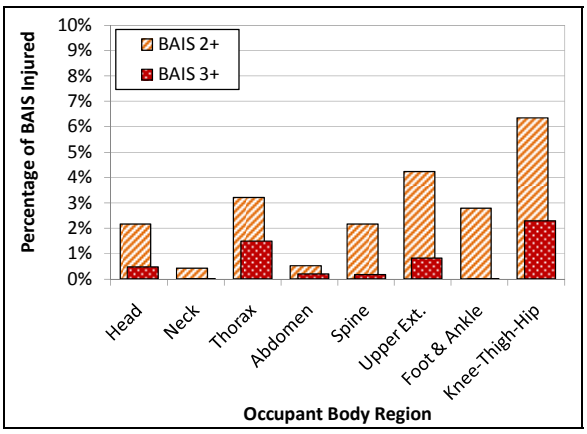

Figure 5. NASS-CDS 1997-2009 – Distribution of BAIS 2+ and BAIS 3+ Injured Occupants (weighted).

As well know in the safety community, the disability consequences of foot and ankle trauma can be severe. For example, Dischinger et al. (2005) found that 28% of patients with ankle/foot fractures in automotive collisions were unable to work one year post injury.

Parenteau et al. (1995) studied Swedish field data gathered by Folksam Insurance. She found that 76% of all the AIS = 2 or 3 foot-ankle injuries were produced in frontal car crashes. The graph in Figure 5 indicates that both BAIS 2+ and BAIS 3+ injuries for belted adult occupants in *Between Rail* crashes are strongly driven by trauma to the lower extremities.

IIHS Center Pole Frontal Impact Test Procedure

The authors considered the question of what sort of laboratory test might serve to represent the between rail frontal crash. One possible candidate is the center pole investigated by IIHS (IIHS Tech Data, 2011).

The Insurance Institute of Highway Safety crashed four recent passenger vehicles inducing direct damage between the longitudinal rails (Figure 6). Two Hybrid III 50th% dummies were positioned in the front-seat area. The test speed was 64-kph. The vehicles struck a rigid pole with a diameter of 25.4-centimeters.

Figure 6: IIHS Pole Impact Test Procedure – Test Number CF07003 (IIHS, 2011)

Assessing Injury Using Biomechanical Risk Curves

During the IIHS center pole tests, dynamic measurements were made in the Hybrid III dummies to approximate injury risk. The approximation of risk is done by using biomechanical risk curves for each body region. The risk to five body regions was calculated for:

<u>Head Injury</u> For the head, the authors used the injury curve proposed by NCAP (NHTSA 2008):

$$P_{head}\,(AIS \geq 3) = \Phi[(\ln(HIC_{15}) - 7.45231)/0.73998)],$$

where Φ = cumulative normal distribution (e.g., use NORMDIST(LN(cell),7.45231,0.73998,1) in Excel).

<u>Neck Tension</u> Assessing the neck, the authors used the tension risk curve proposed by NCAP (NHTSA 2008):

$$P_{neck}\,(AIS \geq 3) = 1/[1 + e^{(10.9745 - 2.375\,F)}],$$

where F = either axial tension or axial compression in kN.

<u>Thorax</u> Assessing the chest, the authors used the chest deformation risk curves proposed by NCAP (NHTSA 2008):

$$P_{chest}\,(AIS \geq 3) = [1 + \exp(12.597 - 0.5861*35 - 1.568\,\delta^{0.4612})]^{-1},$$

where δ is Hybrid III 50th% male chest deflection (mm).

<u>Knee-Thigh-Hip (KTH)</u> Assessing the knee-thigh-hip region, the authors used curve proposed by NCAP (NHTSA 2008):

$$P_{KTH}\,(AIS \geq 2) = [1 + e(5.7949 - 0.5196\,F_{femur})]^{-1},$$

where F = femur force in kN.

<u>Foot & Ankle Injuries</u> Assessing the foot-ankle region, the authors used the forefoot injury criteria develop by Smith (Smith 2003 and Murat 2007):

$$P_{foot}\,(AIS \geq 2) = [1 + e(4.25 - 0.01169875\,A_{foot})]^{-1},$$

where A_{foot} = acceleration in G's.

Comparison of IIHS Pole Impact Test Risks with Real-World Crash Data Risk

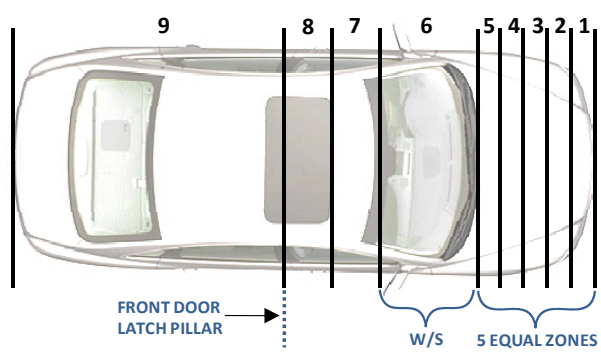

Figure 7. SAE Standard J224 – Extent of Damage

The diagram in Figure 7 provides an overview of the SAE Standard of classifying the extent of post-impact vehicle damage for crashes whereby the general area of damage was to the front of the vehicle. The vehicle is divided into nine cross-sections. The extent of damage classification is assigned based upon the vehicle cross-section where the highest residual deformation was observed to have extended.

Figure 8. IIHS Pole Impact Test CF07002 – Side and Oblique View of Post-Crash Damage (SAE J224 Extent of Damage – Zone 5) (IIHS).

The post-crash vehicle images in Figure 8 were provided by IIHS (2011). The graph in Figure 9 shows the results of logistic regression analysis of the weighted NASS-CDS data for *Between Rail* impacts by increasing extent of damage (as defined in SAE Standard J224). At an equivalent extent of damage observed to that of the IIHS frontal impact test (at the transition plane going from Zone 5 to Zone 6), the risk of sustaining an MAIS 2+F injury was 55.3% compared to 18.5% for an MAIS 3+F injury. As previously indicated, the injuries in the *Between Rail* frontal crash are primarily driven by the lower extremities. The risk of sustaining a BAIS 2+ injury is approximately 30% for the Knee-Thigh-Hip and 15% for the foot & ankle. The BAIS 3+ injury risk for chest injuries is over 7%, however the BAIS 3+ injury risks for the head, abdomen, and neck are all below 5%.

Table 1 provides a comparison of the occupant injury risks from the NASS-CDS *Between Rail* frontal impacts with those obtained from the series of IIHS pole tests. The injury risks for the head, neck, and chest are based on the risk of an AIS 3+ injury, and the KTH and foot & ankle injury are based on the risk of sustaining an AIS 2+ injury. The extent of damage for the vehicles tested in the IIHS test series approximately extended to the start of zone 6. The injury risks presented from the real-world data analysis include extent of damage zones between 4 and 6+.

The risk of sustaining a neck injury in the real world was found to be low (less than 1%) which agreed with the risks being predicted in the IIHS tests. The risk of average head injury risk was slightly over-predicted in the IIHS pole test compared to the risk observed in the real world. The risk of chest injury was similar for both the IIHS pole test and the real world when considering the risk of chest injury between Zone 5 and 6+. Using the Smith injury risk curves, a similar phenomenon was observed for injury risk for injuries sustained to the foot-ankle. The KTH risk derived from the IIHS pole test dummy readings indicated that the average risk was 3.7%. This was much lower than the injury risks observed in the real world that were found to range between 17.76% (extent 4) and 46.37% (extent 6+).

LIMITATIONS

Limitations of this study are that only vehicles with either (1) no secondary damage or (2) vehicles with the Extent of Damage for the secondary impact ≤ 2 were used for the analysis. This reduced the overall number of cases that were availble for analysis.

CONCLUSIONS

This study examined real-world crash data from the NASS-CDS between the years 1997-2009 with a focus on frontal crashes involving 1997 and later model year vehicles. It was found that *Between Rail* impacts had (1) a frequency of about 6.1% of all frontal crashes and (2) a higher risk of front row occupants sustaining either an MAIS ≥ 2, or MAIS ≥ 3 injury, compared to any other frontal impact studied.

In the NASS-CDS investigation of the *Between Rail* crash, a sample of 903 raw (un-weighted) crashes that corresponded to approximately 274,458 weighted crashes were investigated. While the *Between Rail* collision has the highest injury risk of any crash studied, the in-depth investigation suggests that this high risk may be due to exceeding numerous, lower-extremity trauma.

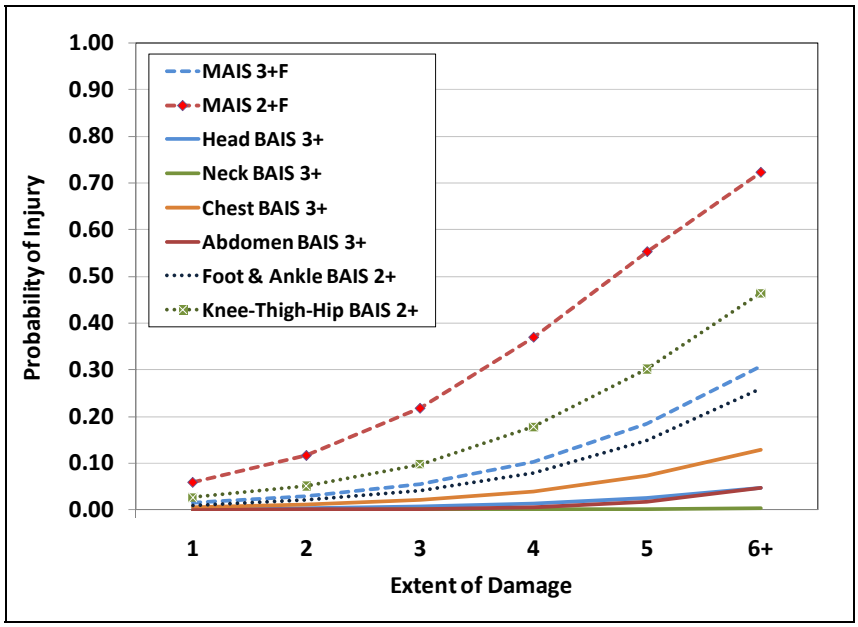

Figure 9. NASS-CDS 1997-2009 – Front Seat Occupant Injury Risk by Vehicle Extent of Damage (weighted).

Table 1.
Comparison of Injury Risks from NASS-CDS (weighted) and IIHS Center Pole Impacts

Body Region	Injury Rates (NASS-CDS)			Injury Rates IIHS Tests
	Extent of Damage 4	Extent of Damage 5	Extent of Damage 6	
Neck	0.09%	**0.18%**	0.38%	**0.14%**
Head	1.28%	**2.49%**	4.78%	**8.25%**
Chest	3.97%	**7.24%**	12.83%	**9.60%**
Foot-Ankle	7.92%	**14.82%**	26.03%	**25.50%**
KTH	17.76%	**30.17%**	46.37%	**3.70%**

The Insurance Institute of Highway Safety crashed four recent passenger vehicles inducing direct damage between the longitudinal rails. Two Hybrid III 50th% dummies were positioned in the front-seat area. The test speed was 64-kph. The vehicles struck a rigid pole with a diameter of 25.4-centimeters.

Using biomechanical risk curves to transform the dummy measure into injury risk, the IIHS center-pole laboratory test reasonably matched the field data, with one noteworthy exception. The exception is that the Knee-Thigh-Hip risk curves gave injury rates approximately one order of magnitude lower than the field data risk. Logically, the non-fidelity of the KTH risk curve and laboratory test combination would lead the safety community to bad design changes. The laboratory test would indicate a low risk for the lower extremities of the occupants. Consequently, the design engineer would fail to detect the high propensity for lower extremity trauma observed in the *Between Rail* field data.

While more research is needed to reconcile the wide difference between the KHT risk curve and the field data, this analysis suggests that other instrumentation in the laboratory test identifies the high risk of foot-ankle trauma. Using the risk curve developed by Smith (2003) and the bi-axial accelerometer on the foot of the Hybrid III dummy, ankle-foot injury risk rates approximate the field data although slightly higher. This finding suggests using both the existing KHT risk curve (until a better risk curve with fidelity is available) in combination with the foot-ankle risk curve. With the addition of the accelerometer instrumentation in the foot of the Hybrid III dummy, the authors suggest that a test along the design of the IIHS center-pole test might lead to design improvements for vehicle safety in the high-risk, *Between Rail* crash.

REFERENCES

AAAM, "Abbreviated Injury Scale — 1990 Revision," Association for the Advancement of Automotive Medicine, Des Plains, Illinois, 1990.

Arbelaez, R.A., Aylor,D., Nolan,J.M., Braitman, K.A., and Baker, B.C., "Crash Modes and Injury Patterns in Real-World Narrow Object Frontal Crashes," IRCOBI Conference, Madrid, Spain, September 2006.

Buyuk, M., Ozkan, D., Morgan, R.M., Digges, K.H., "Using Forefoot Acceleration to Predict Forefoot Trauma in Frontal Crashes," SAE World Congress, SAE Paper No. 2007-01-0704, 2007.

Dischinger, P.C., Read, K.M., Kufera, J.A., Kerns, T.J., Ho, S.M., Burch, C.A., and Burgess, A.R., "Consequences and Costs of Lower Extremity Injuries," U.S. Department of Transportation, National Highway Traffic Safety Administration, Report No. DOT HS 809 871, June 2005.

Hong, S.W., Park, C.K., Mohan, P., Morgan, R.M., Kan, C.D., Lee, K., Park, S., and Bae, H., "A Study of the IIHS Frontal Pole Impact Test, SAE World Congress," SAE Paper No. 2008-01-0507, Detroit, Michigan, April 2008.

Hong, S.W., Park, C.K., Mohan, P., Morgan, R.M., Kan, C.D., Lee, K., Park, S., and Bae, "Comparative Analysis of a Vehicle Impacting a Rigid Barrier, an Offset Deformable Barrier, and a Rigid Pole," IRCOBI Conference, Bern, Switzerland, September 2008.

Insurance Institute for Highway Safety, *Status Report*, Vol. 44, No. 2, March 7, 2009.

Insurance Institute for Highway Safety, TechData Website, http://techdata.iihs.org/ (Accessed February 2011).

NHTSA, "New Car Assessment Program," Docket No. NHTSA-2006-26555, 120 pp., July 11, 2008.

Padmanaban, J. and Okabe, T., "Real World Injury Patterns in Narrow Object Frontal Crashes: An Analysis of US Field Data," SAE Paper No. 2008-01-0527, Detroit, Michigan, April 2008.

Prasad P, Laituri, T.R., and Sullivan K, "Estimation of AIS3+ Thoracic Injury Risks of Belted Drivers in NASS Frontal Crashes," Journal of Automotive Engineering, 2004, Vol. 218, No. D6, IMechE, UK.

Parenteau, C.S., Viano, D.C., Lovsund, P., and Tingvail, C., "Foot-Ankle Injuries: Influence of Crash Location, Seating Position and Age," Association for the Advancement of Automotive Medicine, 1995.

SAE Standard J224. Collision Deformation Classification. Revised March 1980.

Scullion, P., Morgan, R.M., Mohan, P., Kan, C-D., Shanks, K., Jin, W., and Tangirala, R., "A Reexamination of the Small Overlap Frontal Crash," 54th Proceedings of the Association for the Advancement of Automotive Medicine, Las Vegas, Nevada, October 2010.

Smith, B., "A Mechanism of Injury to the Forefoot in Car Crashes," Wayne State University, Detroit, Michigan, Dissertation Doctoral Degree, 2003

Smith, B.R., Begeman, P.C., Leland, R., Levine, R.S., Yang, K.H., and King, A.I., "A Mechanism of Injury to the Forefoot in Car Crashes," IRCOBI Conference, Lisbon, Portugal, September 2003

Sullivan K, Henry S, Laituri TR. "A Frontal Impact Taxonomy for USA Field Data." Society of Automotive Engineers, SAE Paper No. 2008-01-0526, Detroit, Michigan, April 2008.

APPENDICES

Appendix A

The following section provides an overview description of the selection criteria used to classify frontal impacted vehicles. All classified vehicles had a general area of damage to the front of the vehicle, known damage and average track width, and were not subsequently involved in a rollover. With the exception of the 'other' group, all vehicles had a direction of force of 11, 12, or 1 o'clock.

Full Engagement Both vehicle frame rails were engaged as the result of collision.

Offset One vehicle frame rail was engaged as the result of collision, with the center of direct damage located inside the outer edge of the vehicle frame rail.

Moderate Offset One vehicle frame rail was engaged, with the center of direct damage located outside the outer edge of the vehicle frame rail.

Small Offset No vehicle frame rail engagement as the result of collision, with direct damage located entirely outside of the vehicle frame rails.

Between Rail No vehicle frame rail engagement as the result of collision, with direct damage located entirely between the vehicle frame rails.

Underride Type of damage distribution classified as an overhanging structure, or a specific vertical location of damage at the belt line or above.

Other Vehicles that with a direction of force of 9, 10, 2, or 3 o'clock, or not otherwise classifiable based on the aforementioned criteria.

Appendix B

The purpose of this appendix is to summarize the basic Hybrid III 50th% dummy readings for the crash of four make/models into a pole centered at the front of the vehicle. The tests were conducted by IIHS and the data were provided by IIHS (IIHS TechData). The test speed was 64-kph, and the rigid pole had a diameter of 25.4 cm.

TABLE 2.
Summary of Hybrid III Dummy Readings in IIHS Center Pole Tests

Measure	2006 Volkswagen Passat		2007 Chevrolet Malibu		2007 Subaru Legacy		2007 Toyota Camry	
	Driver	Passenger	Driver	Passenger	Driver	Passenger	Driver	Passenger
HIC_{15}	696	473	729	566	700	466	638	614
Axial tension neck (N)	1800	1000	1900	2000	2000	1400	2200	1500
Axial compress neck (N)	800	1000	1000	300	1500	200	600	1500
Chest deformation (mm)	38	30	43	43	39	34	32	31
Femur left (kN)	1.3	4.3	3.4	4.1	5.7	1.4	2.6	3.8
Femur right (kN)	2.1	1.9	7.7	2.8	4.4	0.8	2.6	0.1
Foot left (G's)	92	241	125	139	128	166	88	294
Foot right (G's)	309	127	297	174	250	90	357	288

The laboratory-derived probabilities of trauma (AIS ≥ 2 for the KTH and ankle/foot and AIS ≥ 3 for other body regions) based on these Hybrid III 50th% dummy readings are listed in TABLE 3. All probabilities are in percent.

TABLE 3.
Summary of Injury Risk Based on Hybrid III Dummy Readings and Biomechanical Curves

Body Region	2006 Volkswagen Passat		2007 Chevrolet Malibu		2007 Subaru Legacy		2007 Toyota Camry	
	Driver	Passenger	Driver	Passenger	Driver	Passenger	Driver	Passenger
Head	11	4	6.6	12.2	11.2	3.9	9	8.1
Neck	0.12	0.02	0.2	0.16	0.2	0.05	0.32	0.06
Chest	10.4	4.7	16	16	11.4	7.1	5.8	5.2
KTH left	0.6	2.8	2.5	1.7	5.6	0.6	1.2	2.1
KTH right	0.9	0.8	1.3	14.3	2.9	0.5	1.2	0.3
Foot left	4	19.3	6.8	5.8	6	9	3.8	30.8
Foot right	34.6	5.93	9.8	31.5	21	3.9	48.2	29.3

IMPROVING THE CRASH COMPATIBILITY OF CARS AND ROADSIDE POLES

Michael Griffiths
Road Safety Solutions
Australia
John Jarvie
Accountable Safe Innovations
Australia
Paper Number 11 - 0239

ABSTRACT

Car to pole impacts account for a large proportion of car occupant casualties in many motorized countries. Each year in Australia about 2000 vehicles crash into timber power poles resulting in approximately 100 fatalities and 1000 serious injuries at a community cost of about A$500 million. The estimates for North America are over 1000 fatalities and over 100,000 serious injuries each year, with an estimated 10-fold increase in costs. Historically the primary countermeasure used by road safety authorities has been to move utility/power poles away from the roadside. While this may reduce the risk of an impact, moving the position of the timber pole has little effect on the outcome if an impact occurs. To reduce the risk of injury there is a need to change the properties of the pole, so that the pole acts to stop the car while retaining integrity ensuring that neither becomes an unrestrained hazard.

This paper presents the results of a program aimed at developing a utility pole that absorbs energy and yields sufficiently to stop the vehicle in several metres at survivable decelerations with no intrusion into the occupant space. This has been achieved by using composite materials supplemented with built in energy management systems. To test the impact properties of the prototype, we conducted ten full-scale frontal crash tests using a variety of car sizes at impact speeds of 50, 80 and 100 km/hr. The performance of the poles during the tests was monitored using multiple high-speed cameras, and accelerometers were fitted to the vehicles on later tests.

The results demonstrate the superior impact performance of the composite poles and the ability of these poles to safely stop impacting vehicles even at high impact speeds, while retaining enough integrity to ensure cables carried by the poles remain intact and supported above the ground.

This superior impact performance carries substantial potential safety benefits. Furthermore, the projected whole of life costs of the composite pole are less than existing timber poles. The lighter weight and lower cost of the poles also assists the primary countermeasure of relocation away from the road. Limitations of the preliminary test program are the lack of instrumented test dummies that means that these results cannot be communicated directly in terms of injury criteria. However the reduced decelerations measured in the vehicle, and the retention of the occupant compartment even in the highest test speeds strongly indicates likely reduction in injury risk.

The composite pole used in these tests start as a standard production utility pole already in limited use in North America. It is then enhanced to absorb energy in a controlled manner, prevent unrestrained hazards and can keep the power/communication cables supported. Widespread use of these composite poles could prevent considerable serious injury, death and associated community cost.

INTRODUCTION

In one Australian state alone, between 2004 and 2008 there were 171 fatalities and 5,060 injuries following collisions with utility poles with an estimated annual cost of $178 million per year (RTA, 2009). Across Australia, these numbers would be expected to reach 100 fatalities per year, and many more serious injuries. Casualties resulting from collisions with utility poles are mainly an urban problem, and account for a large proportion of the fatality problem in at least Australia, North America and the ECU (RTA, 2009; TRB, 2004; Thomson et al, 2006).

The hazard created by robust timber utility poles arises from their usual close location to the roadway. To reduce this hazard the primary response has been to try to reduce the number of poles and ensure that those that remain are situated outside a designated safety zone i.e. set back a certain distance from the roadway. However, this measure does not address the severity of an impact should one still occur. Moreover, poles are used to provide necessary roadside utilities such as

lighting, and moving all poles a safe distance from the road side is not always possible.

Historically most roadside poles have been constructed from wood. Attempts to design safer poles have focused on using breakaway features and safety guards (Foedinger et al, 2003;TRB, 2004). Breakaway poles are designed to yield upon impact, and while this feature potentially reduces the severity of the initial pole impact, the broken away pole becomes a hazard as a secondary impact to the vehicle, or in impacts to other vehicles or road users. It also disrupts the utility being supplied by the pole. A better, more efficient approach would be to design a pole that absorbs energy to reduce the severity of the impact, but remains in place- so as to reduce any further hazard and a reduced possibility of disruption to services.

Modern composite technology presents the possibility of designing a new generation of energy-absorbing poles. This potential has been studied by Elmarakabi et al (2006, 2009) using finite element analysis who demonstrated the theoretical benefits to vehicle deformation and deceleration that might be achieved with this technology. Foedinger et al (2004) went further to develop a prototype energy-absorbing fibreglass-reinforced filiament wound tapered utility pole and demonstrated the ability of this device to mitigate crash severity in two frontal impacts at 50 and 70Km/h.

In our research program, we aimed to modify a standard production composite pole so that it would absorb energy and bring vehicles to a stop over a few metres in a controlled manner from speeds in the range of 50 to 100 km/hr, without the pole breaking away from its base in the ground. Standard production composite poles manufactured using protruded techniques are already in limited service in North America. Our aim was to add crash severity mitigating features to these poles that already provide an advantage in reduced weight, an improved strength-to-weight ratio, ease of installation, low maintenance, and environmental friendliness over wooden poles.

This paper reviews the development of the prototype design to achieve this, and results from preliminary testing demonstrating the ability of the safe system pole to reduce injury potential while maintaining integrity of the utilities being provided.

THE SAFE SYSTEMS POLE

The production pole that forms the foundation of the Safe Systems Pole was originally sighted in its use as a waterways channel marker. The information that the pole's structural characteristics could be relatively easily altered by changes in the mixes of binding resin and cloth led to the concept that such a pole could be developed to progressively yield and stop cars in a controlled manner.

TEST PROGRAM

The U.S. Department of Transportation's recommended procedures in the safety performance evaluation of highway features (NCHRP350) formed the basis of the test procedure.

All tests were conducted at the New South Wales RTA's Crashlab, external test facility suitable for the testing of roadside furniture located in Sydney, Australia. .

Initial tests assessed the base energy absorption properties of the composite poles with a variety of treatments of the standard base. Once a preliminary understanding was gained of how the fronts of vehicles relate with the base of the poles, a further round of tests reviewed the effect of various prototype enhancements to the poles to improve the control of the energy management systems in the pole.

All testing was conducted using two popular typical models of passenger cars at speeds of 50, 80 and 100 km/hrThe Hyundai Excel was used as a representative 'small car' and the 'large car' chosen was a Ford Falcon sedan.

Dimensional specifications for the Hyundai Excel were:-

- kerb weight of 967 kg
- overall length of 4.103 metres
- wheel base of 2.4 metres

Dimensional specifications for the Ford Falcon sedan were:-

- kerb weight of 1541 kg
- overall length of 4.906 metres
- wheel base of 2.791 metres

All tests were recorded using three high speed cameras, and one real time camera.

Some of the later tests included accelerometers fitted in the region of the "B" pillars of the vehicles.

Assessments of the rate of deceleration of the vehicle in the earlier tests were simple measurements of average deceleration based on the length that it took the vehicle to come to a stop.

Ten full-scale crash tests were conducted using popular typical models of passenger cars at speeds of 50, 80 and 100 km/hr.

Table 1
Pole Test Program

Test Number	Speed	Outcome
Assessment of minor modifications to basic pole		
Test 1 B09044	80 km/hr	
Test 2 B09045	80 km/hr	
Test 3 B09046	80 km/hr	
Test 4 B09048	80 km/hr	Vehicle brought to a stop in a distance of approximately 5 metres
Mark I Modified Poles		
Test 5 B10001	50 km/hr	Vehicle brought to a stop in a distance of approximately 1 metre
Test 6 B10002	80 km/hr	Vehicle brought to a stop in a distance of approximately 3 metres
Test 7 B10003	100 km/hr	Vehicle brought to a stop in a distance of approximately 4 metres
Mark II Modified Poles		
Test 8 B10014	100 km/hr	
Test 9 B10028	80 km/hr	Vehicle brought to a stop in a distance of approximately 3 metres
Test 10 B10029	100 km/hr	

RESULTS

The results of the individual tests can not be described in any detail for commercially in confidence/ intellectual property reasons

What can be said, and what can be shown here, is that the test program demonstrated proof of concept to the extent that:-

- at the NCHRP350 50 km/hr test, the pole deformed approximately a metre which with vehicle crush yielded an overall likely occupant average deceleration rate of 10g

- at the NCHRP350 80 km/hr test, the pole brought the vehicle to a stop in approximately 3 metres with an average deceleration rate in the order of 8 - 9g. There was no intrusion into any of the occupant compartments and the doors could be opened without extra force or the use of tools

- at the NCHRP350 100 km/hr test with a heavier vehicle, the vehicle was brought to a stop in approximately 5 metres. It had an average deceleration rate of 8g. The doors could be opened after the test without the use of additional force or tools.

Figure 2. Car about to impact pole at 80 km/hr

Figure 3. Pole yielding and car slowing

Figure 4. Pole continues to yield

Figure 5. Car nearly stopped

Figure 6. Some minor rebound

Figure 7. Car stopped, pole supporting cables above roadway

THE FUTURE

This concept has been demonstrated to meet our aims of developing a safe pole system that can mitigate crash severity while retaining integrity of services. The pole's energy management systems have been tuned to result in relatively gentle controlled deceleration for the vehicles in frontal impacts. Simultaneously during the program, systems for minimising the damage to the cables carrying power and communication have also been trialled.

The average deceleration for a stop from 80 km/hr over a distance of 3 metres was approximately 8.4g. As is well established from real world crashes and laboratory crash testing, occupant compartment accelerations in this range result do not cause injury to restrained vehicle occupants. At the same time, the energy managed stop can result in significantly reduced direct loads on the cables etc, so that the likelihood of damage to the power and communications systems (or utilities being carried by the pole) is reduced, or entirely prevented.

There is a need for a further test program before attempting to proceed to real world production (commercialization) of the product.

This next test program will have the aims of:-

- extending crash test scenarios to side on impacts,
- Further fine-tune energy management and pole retention systems
- Further fine-tune systems for minimising potential damage to the cables carrying power and communication

ACKNOWLEDGEMENTS

We thank Dr Julie Brown for assistance with advice and literature review.

REFERENCES

Elmarakabi, A, Sennah, K, Samaan, M, Siriya, P. (2006) Crashworthiness of Motor Vehicle and Traffic Light Pole in Frontal Collisions. Journal of Transportation Engineering 132(9):722-733.

Elmarakabi, A, Fielding, N. (2009) New Design of Roadside Pole Structure: Crash Analysis of Different Longitudinal Tubes using LS-Dyna. 7th European LS-Dyna Conference. 8 pgs

Foedinger, R, Boozer, JF, Bronstad, ME, Davidson JW. (2003) Development of Energy Absorbing Composite Utlity Pole. Transportation Research Record 1851, Paper No 03-2865:149-157.

NSW Roads and Traffic Authority (RTA) (2007) Road Safety Implictaions of utility pole placement. RTA. 66pgs.

NSW Roads and Traffic Authority (RTA) (2009) Reducing Trauma as a Result of Crashes Involving Utility Poles. NSW Centre for Road Safety, RTA 18 pgs

Thomson, R, Martinez, AV, Naing, C, Hill, J, Hoschopf, H, Dupre, G, Bisson, O, Kelkka, M, Van der Hort, R, Garcia, J. (2006) Roadside Infrastructure for Safer European Roads, RISER Consortium. 138pgs

Transportation Research Board (TRB)(2004) Utilities and Roadside Safety: State of the Art Report 9. National Academies. Washington DC. 68pgs.

CRASH TEST PERFORMANCE OF LARGE TRUCK REAR UNDERRIDE GUARDS

Matthew L. Brumbelow
Insurance Institute for Highway Safety
United States
Paper No. 11-0074

ABSTRACT

Large truck crashes account for a substantial portion of the fatalities and serious injuries occurring in modern passenger vehicles designed for good frontal crash protection. Incompatibilities in mass, stiffness, and ground clearance present challenges in improving crash outcomes for passenger vehicle occupants. A recent Insurance Institute for Highway Safety study of cases from the Large Truck Crash Causation Study (LTCCS) found that rear underride guards meeting US federal requirements still can allow severe passenger vehicle underride, often resulting in serious or fatal injury. The study identified patterns of real-world guard failure, but the impact speeds necessary to produce these failures could not be determined. Also, due to the LTCCS case selection requirement that each crash produce an injury, differences among the large number of guard designs and resulting crash performance and injury risk could not be compared. The current study used a series of six crash tests to investigate these issues.

Crash tests were conducted in which the front of a midsize sedan impacted the rear of a semi-trailer equipped with an underride guard. Three trailer/guard designs were evaluated in various conditions. Each guard design was certified to the US Federal Motor Vehicle Safety Standard (FMVSS) 223 requirements, and two also met the more stringent Canadian Motor Vehicle Safety Standard (CMVSS) 223 regulation. Quasi-static tests were conducted to determine the compliance margins.

In a full-width test at 56 km/h, the guard design built only to the US requirements failed catastrophically at the points of attachment to the trailer, allowing severe underride and trailer contact with the dummy's head. The second guard failed in 50 percent overlap tests at 40 and 56 km/h, producing underride to the base of the sedan's windshield in the first test and to the dummy's head in the second. The third guard was able to prevent underride in full-width and 50 percent overlap tests at 56 km/h but failed when the overlap was reduced to 30 percent.

The minimum force requirements of FMVSS 223 are too low to prevent guard failure in full-width crashes. CMVSS 223 is an improvement over the US regulation, but its requirements also should be strengthened because underride still can occur in offset crashes. Both standards should require quasi-static tests to be conducted with guards attached to a trailer. The current standards allow tests using a rigid fixture, so even well-designed guards could be attached to a trailer such that they fail to prevent underride due to weakness of the trailer chassis or attachment mechanism.

INTRODUCTION

According to the Fatality Analysis Reporting System (FARS), about 10 percent of passenger vehicle occupant fatalities occur in crashes involving large trucks. Two recent studies limited to frontal crashes of vehicles designed to perform well in crash test programs found that large truck crashes are a common source of fatality or serious injury for belted front-seat occupants [1,2]. The only US regulations addressing the structural incompatibility between passenger vehicles and large trucks are Federal Motor Vehicle Safety Standards (FMVSS) 223 and 224, which require rear underride guards on some tractor-trailers [3]. Both standards became effective in 1998, with FMVSS 224 outlining the types of trailers required to have underride guards as well as dimensional requirements for the guards, and FMVSS 223 describing strength and energy absorption requirements in quasi-static tests at three locations on the guard. The National Highway Traffic Safety Administration (NHTSA) issued this rule to "reduce the number of deaths and serious injuries occurring when light duty vehicles impact the rear of trailers and semitrailers with a gross vehicle weight rating of 4,536 kg or more" [4].

In setting the requirements for underride guards, NHTSA was concerned that "overly rigid guards could result in passenger compartment forces that would increase the risk of occupant injuries even in the absence of underride" (61 FR 2005). At the same time, the agency recognized the need for adequate guard strength because "the more the guard yields, the farther the colliding vehicle travels and the greater the likelihood of passenger compartment intrusion" (61 FR 2009). In the end, NHTSA believed the standards would produce guard designs that could be struck by passenger vehicles at speeds of 40-56 km/h and deform enough to prevent excessive deceleration

while not allowing the passenger compartment to strike the trailer.

The real-world performance of FMVSS-compliant underride guards had not been evaluated until a recent study by Brumbelow and Blanar [5]. The authors analyzed 115 cases from the Large Truck Crash Causation Study (LTCCS) in which a passenger vehicle struck the rear of a large truck. They identified that 30 of these trucks were equipped with guards that met one or both of the standards. In most of these cases, the guards failed to prevent severe passenger vehicle underride, defined as intrusion of the truck into the passenger compartment. An overall rate of guard failure could not be established because at least one injury was required for inclusion in LTCCS, but the authors were able to categorize the mode in which the guards failed. The most common failures were due to weakness in the attachment between the guard and trailer, deformation of the trailer chassis itself, or excessive bending of one outboard end of the guard in narrow overlap crashes.

Brumbelow and Blanar's [5] findings confirmed that the problems with FMVSS-compliant guards identified in a previous series of crash tests were indicative of field crash performance. The crash tests, conducted by NHTSA in support of the rulemaking, illustrated how an underride guard could meet all of the requirements of both standards yet still produce severe underride due to attachment failure or deformation of the trailer chassis [6]. The tested guard design was able to prevent severe underride of a 1992 Honda Civic in a 48 km/h full-width test only after the attachment hardware was upgraded and the trailer structure was reinforced. Elias and Monk [6] stated that compliance with FMVSS 223 was insufficient to ensure good crash performance if the "attachment hardware or the trailer sub-system to which the guard is attached is not of sufficient strength." However, the final rule that later was issued allowed guards to be tested independently of trailers and contained no provision for evaluating the strength of the trailer or attachment. NHTSA did state that adequate guard performance could not be assured at crash speeds above 45 km/h (61 FR 2010).

Transport Canada also conducted a series of full-width tests with guards meeting US requirements. A baseline guard design minimally compliant with FMVSS 223 was compared with a design equipped with "stoppers" to limit maximum guard deformation and with another guard that was strengthened to provide more resistance throughout the crash. Based on results of these tests, Transport Canada issued Canadian Motor Vehicle Safety Standard 223 [7]. Although this regulation contains substantially greater strength and energy absorption requirements than the US version for the main vertical supports of the guard, it does not require increased strength on the outboard ends of the guard nor does it directly address the potential for attachment or trailer weakness. In a follow-up test, a CMVSS 223-compliant guard mounted to a trailer prevented underride of a 1998 Honda Civic with an impact speed of 56 km/h, but damage to the trailer chassis allowed the guard to begin rotating upward.

The study of real-world guard performance raised some questions that previous crash tests did not address. Because delta Vs could not be calculated for the LTCCS cases, it was unknown what impact speeds would produce failure of production guards. The NHTSA and Transport Canada tests were conducted at speeds ranging from 48 to 64 km/h, but the guards were nonproduction designs developed specifically for research. Additionally, in 15 of the 18 previous tests, the guard was attached to a rigid test buck instead of a trailer, precluding the possibility of observing some of the failure modes present in the LTCCS sample and possibly exacerbating others. Brumbelow and Blanar [5] also identified several cases where the outboard end of the guard bent forward due to narrow overlap loading, but all of the previous crash tests were conducted with full overlap. Finally, due to the lack of cases without injury in LTCCS, it was unknown whether some production guard designs perform better than others. The current study evaluated these issues with a series of six crash tests conducted with production semi-trailers equipped with FMVSS-compliant underride guards.

METHODS

The 2007 Hyundai, 2007 Vanguard, and 2011 Wabash semi-trailers were selected for testing based on their availability through local dealers and the presence of major visible differences in the design of their underride guards. The most obvious differences pertained to the design of the guards' main vertical support members (Figure 1). The Hyundai's vertical supports were bolted directly to the lower rear cross-member of the trailer without any forward attachment points to the trailer's axle slide rails or other structure. The Vanguard and Wabash both had diagonal gussets to forward portions of the trailer chassis, but there also was a difference between the designs. The Vanguard relied on the shear strength of the attachment bolts as the only load path between the guard and trailer, whereas the Wabash was designed to transfer loads from the guard to the chassis through overlapping steel plates.

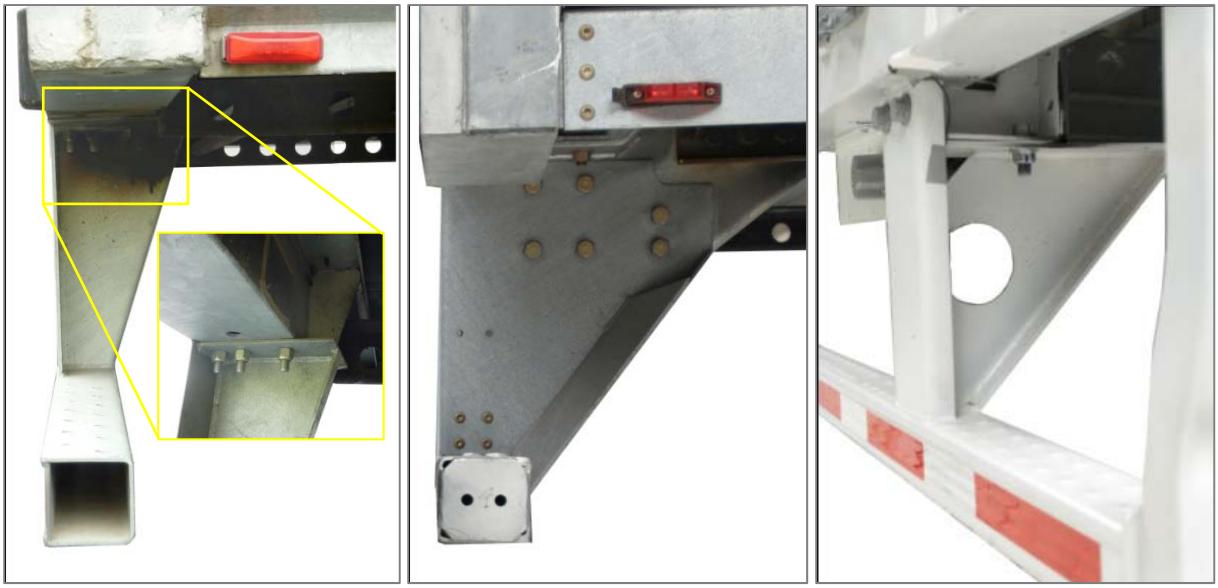

Figure 1. Vertical underride guard support members of 2007 Hyundai (left), 2007 Vanguard (middle), and 2011 Wabash (right) semi-trailers.

The certification labels on the Vanguard and Wabash trailers indicated they complied with CMVSS 223 as well as FMVSS 223. However, the Vanguard's production date corresponded with a time period when CMVSS compliance still could be achieved by testing to the US requirements. To verify compliance with both rules and enable comparison of crash test outcomes with the margin of compliance, quasi-static tests of all three guard designs were conducted. Both FMVSS 223 and CMVSS 223 specify three test locations on the underride guard, designated P1, P2, and P3 (Figure 2). Each location is loaded with a rigid force application device measuring 203 mm square. For the current study, the guards were tested at locations P1 and P3 but not P2. Each guard design was tested twice at P3 because CMVSS 223 requires cutting the guard in half to prevent any strength contribution from the nontested side of the guard. The tests were conducted according to NHTSA and Transport Canada test procedures [8,9] with a loading rate of 1.3 mm/sec. Tests were conducted with a rigid fixture, and a new guard was mounted for each test.

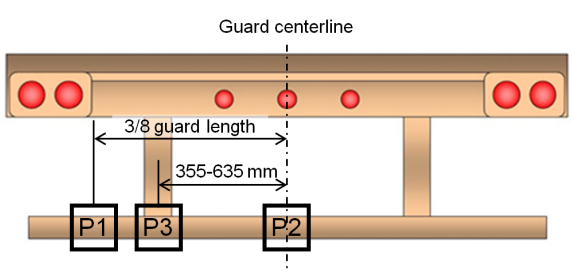

Figure 2. FMVSS 223 and CMVSS 223 test locations. The CMVSS P3 test is conducted with the guard cut in half.

Conditions for each of the six crash tests are listed in Table 1. Despite model year differences, all trailers were new, and none had corrosion or other damage that could have affected the test results. The 2010 Chevrolet Malibu midsize sedan was selected as the test passenger vehicle based on its Top Safety Pick designation by IIHS and five-star frontal scores for both the driver and front passenger in NHTSA's New Car Assessment Program (1990-2010 test format).

Table 1.
2010 Chevrolet Malibu front into trailer rear crash tests

Trailer	Speed (km/h)	Malibu overlap with guard	Guard ground clearance (cm)
2007 Hyundai	56	Full-width	47.6
2007 Vanguard	40	50%	42.2
2007 Vanguard	56	50%	42.7
2011 Wabash	56	Full-width	44.5
2011 Wabash	56	50%	44.3
2011 Wabash	56	30%	45.3

The trailers were loaded with 11 concrete blocks totaling 18,700 kg for the 53-foot (16.2-m) Vanguard and Wabash trailers, and 9 blocks totaling 15,300 kg for the 48-foot (14.6-m) Hyundai trailer. The ground clearances listed in Table 1 were measured with the

trailers loaded and the air suspensions pressurized. All of the guards were closer to the ground than the 56-cm maximum allowed by FMVSS 224. The trailers' sliding rear axles were placed in a position that resulted in a setback of about 200 cm from the rear surface of the rear tires to the rear of the trailer. When tested, each trailer was attached to a 2001 Kenworth tractor, and the trailer's brakes were pressurized to 40 psi to simulate being stopped in traffic. Injury measures were recorded from Hybrid III 50th percentile male dummies positioned in the driver seat of each Malibu and in the right front passenger seat for the two full-width tests. High-speed film and digital cameras were used to document the dynamic performance of the underride guards. Precrash and post-crash measures were taken of the Malibu A-pillars and roof header.

RESULTS

When tested quasi-statically on a rigid fixture, all three guard designs met FMVSS 223 requirements at the P1 and P3 test locations by large margins. The Vanguard and Wabash trailers also met the CMVSS 223 requirements. Performance of the Wabash was especially notable, as it sustained a higher force level throughout the test and absorbed much more energy than the Vanguard. Table 2 lists results of the quasi-static testing. Two of the tests had to be stopped early due to yielding of the test fixture.

Deformation patterns of the underride guards varied substantially in the quasi-static tests. For example, in the FMVSS 223 P3 test, the vertical support member of the Hyundai guard was pulled slowly from some of the bolts attaching it to the fixture, whereas the vertical member itself deformed only minimally. In the same test, the Vanguard's vertical member flexed for the first 50 mm of loading and then the attachment bolts began to shear, causing the measured force to drop below that measured for the Hyundai later in the test. The Wabash guard reached its peak force earliest, and then the vertical member began buckling near its attachment to the horizontal member. As the buckling continued, the rear surface of the guard eventually bottomed out against the diagonal gusset, causing the load to increase again late in the test. Figure 3 shows the force-displacement curves for all three guards in the FMVSS 223 P3 test.

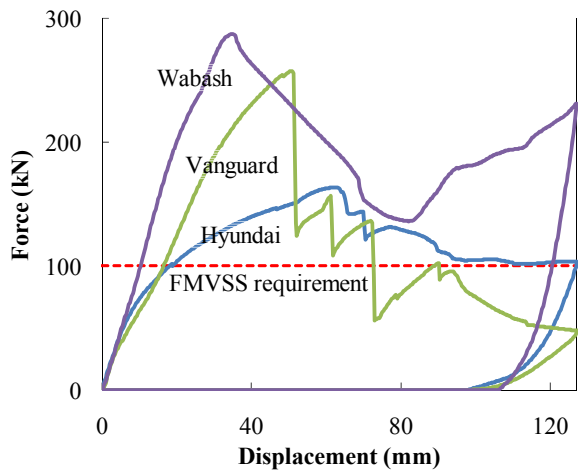

Figure 3. FMVSS 223 P3 test results.

Table 3 summarizes results of the six crash tests, and Figures 4-6 show the 2010 Chevrolet Malibus at the times of maximum forward excursion. In the first 56 km/h full-width test, the 2007 Hyundai guard was ripped from the trailer's rear crossmember early in the crash, allowing the Malibu to underride the trailer almost to the B-pillar. The heads of both dummies were struck by the hood of the Malibu as it deformed against the rear surface of the trailer. Under the same test conditions, the main horizontal member of the 2011 Wabash guard bent forward in the center but remained attached to the vertical support members, which showed no signs of separating from the trailer chassis. The Malibu rebounded rearward from the trailer without underride.

Table 2.
Quasi-static test results

	FMVSS/CMVSS P1 peak force (kN)	FMVSS P3 peak force (kN)	FMVSS P3 energy absorbed (kJ)	CMVSS P3 peak force (kN)	CMVSS P3 energy absorbed (kJ)
Requirement	**50**	**100**	**5.6**	**175**	**10**
2007 Hyundai	109	163	13.9	135	11.8
2007 Vanguard	143*	257	14.0	209	11.8
2011 Wabash	162	287	22.1	297*	21.5*

*Test was stopped prior to 125 mm (49 mm for Vanguard, 116 mm for Wabash).

Table 3.
2010 Chevrolet Malibu front into trailer rear crash test results

Conditions	Trailer	Guard performance	Underride	Max. longitudinal A-pillar deformation (cm)
56 km/h, full-width	2007 Hyundai	Attachments failed	Catastrophic	80
	2011 Wabash	Good	None	0
40 km/h, 50% overlap	2007 Vanguard	Attachments failed	Moderate	0
56 km/h, 50% overlap	2007 Vanguard	Attachments failed	Severe	27
	2011 Wabash	End bent forward	None	6
56 km/h, 30% overlap	2011 Wabash	End bent forward	Catastrophic	87

Figure 4. 56 km/h, full-width tests with 2007 Hyundai trailer (left) and 2011 Wabash trailer (right).

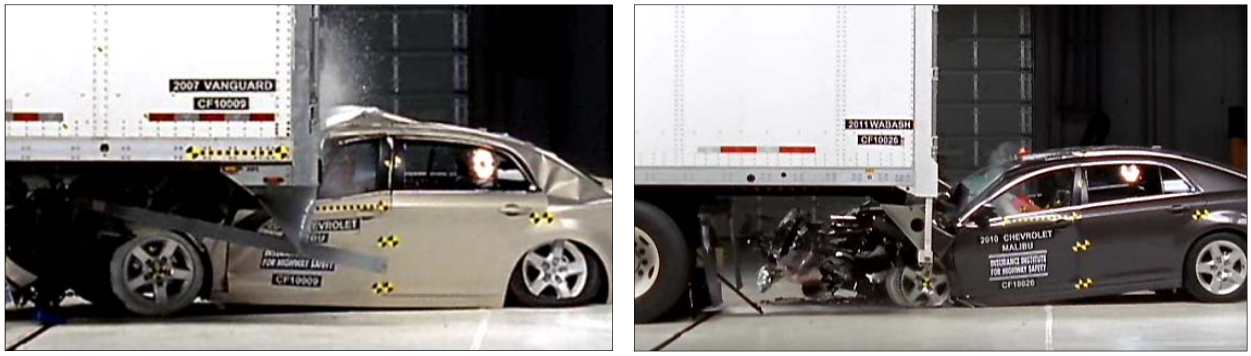

Figure 5. 56 km/h, 50 percent overlap tests with 2007 Vanguard trailer (left) and 2011 Wabash trailer (right).

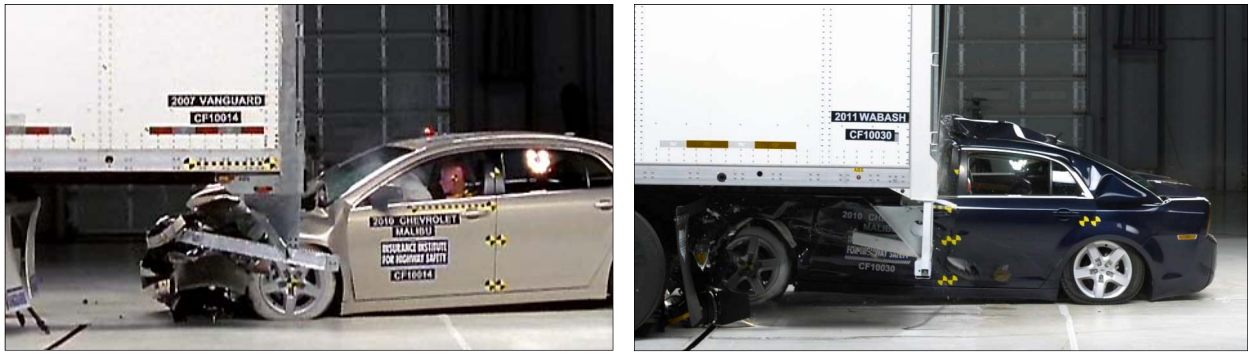

Figure 6. 40 km/h, 50 percent overlap with 2007 Vanguard trailer (left); 56 km/h, 30 percent overlap test with 2011 Wabash trailer (right).

In the 50 percent overlap tests at 40 and 56 km/h, several of the bolts attaching the Vanguard guard to the trailer failed in shear, allowing the Malibu to underride the trailer. At the lower test speed, the Malibu's hood was pushed into the base of the windshield, but the trailer itself did not cross the plane of the windshield into the passenger compartment. When struck at 56 km/h, the trailer loaded the driverside A-pillar and roof, and the driver dummy's head struck the trailer's rear crossmember. In contrast, the Wabash guard was able to prevent underride in the 56 km/h, 50 percent overlap test. The outboard end of the guard's horizontal member bent forward early in the test, but the right vertical support remained engaged with the Malibu's left wheel and shock tower, and stopped the car without any indication of separating from the trailer.

In the 30 percent overlap test, the Malibu's left wheel was aligned just outboard of the Wabash guard's right vertical support. When struck at 56 km/h, the outboard end of the guard bent forward early in the test, and the Malibu underrode the trailer until the front of the car struck the trailer's right rear tires, with the longitudinal extent of the underride damage stopping just short of the B-pillar. The driver dummy's head struck the rear of the trailer.

Peak injury measures recorded by the dummies during the tests are listed in Table 4. Resultant head accelerations ranged from 107 to 130 g for the four dummies that struck the rear of the trailer or the hood of the Malibu as it was pushed through the windshield by the trailer. Loading durations for these impacts were very short; maximum head injury criterion (HIC) values were calculated during 4-7 ms intervals, with values ranging from 254 to 880.

DISCUSSION

The current study supports the analysis of real-world cases from LTCCS that found underride guards compliant with FMVSS 223 and 224 could fail catastrophically and allow severe underride of the passenger compartments of striking vehicles [5]. Although the impact speeds at which these failures occurred could not be determined from the previous study, the lack of cases with serious injuries due to overly stiff guards suggested that the benefits of strengthening the requirements would outweigh any potential increased risk of deceleration-based injuries in lower-speed crashes. The current study confirms this by showing that production guard designs fail at speeds used in consumer information tests where low injury risk is an industry-accepted target. The underride resulting from these guard failures essentially nullifies the frontal crashworthiness built into modern passenger vehicles. As shown in Table 4, head injury measures recorded by the dummies in the tests with severe underride were much higher than those reported for the Malibu's NCAP rigid wall test at the same speed. Although measures of chest acceleration and deflection were greater in tests without underride than in those with guard failure, they still were comparable with or lower than the peak levels recorded in the NCAP test.

Table 4.
Peak dummy injury measures

		Head resultant acceleration (g)	Head injury criterion (36 ms)	Chest resultant acceleration (3 ms clip, g)	Chest displacement (mm)	Left femur force (kN)	Right femur force (kN)
Hyundai							
Full overlap, 56 km/h	Driver	128	754	21	-19	-0.3	-0.3
	Passenger	107	557	14	-20	-0.1	-0.1
Vanguard							
50% overlap, 40 km/h	Driver	15	24	16	-25	-0.1	-0.1
50% overlap, 56 km/h	Driver	109	254	14	-20	-2.2	0.0
Wabash							
Full overlap, 56 km/h	Driver	54	328	36	-38	-2.2	-1.2
	Passenger	50	319	36	-37	-2.3	-1.8
50% overlap, 56 km/h	Driver	36	160	25	-33	-3.7	-0.9
30% overlap, 56 km/h	Driver	130	880	37	-16	-0.6	-0.1
NCAP							
Rigid wall, full	Driver	49	330	43	-40	-2.0	-1.2
overlap, 56 km/h	Passenger	55	389	42	-32	-0.5	-0.8

The requirements of both FMVSS 223 and CMVSS 223 are insufficient to produce underride guards with adequate crash performance. The current study indicates several changes are needed. Force requirements should be increased for the P1 and P3 test locations, the P1 test should be moved farther outboard, and all tests should be conducted with the guard attached to a trailer. These changes also would address all the failure modes observed in the study of LTCCS cases.

Both the Hyundai and Vanguard guards met the US requirements, with the Vanguard also passing the more stringent CMVSS P3 test. Yet both guards exhibited at least partial failure of their attachments in the quasi-static tests that were similar to those observed in the crash tests with disastrous results. Figure 7 shows how the rearmost edge of the top of the Hyundai's vertical guard support ripped away from two attachment bolts in the FMVSS 223 test and in the crash test. In the crash test, the forward bolts remained attached to the guard but were ripped from the trailer's rear crossmember. The force requirements of both standards at the P3 location are not high enough to guarantee robust attachment designs that can hold the underride guard in place during a crash. In the FMVSS P3 test, the Vanguard achieved a force 157 percent greater than the requirement before its attachment bolts began to fail. Yet some of the bolts fractured in the 50 percent overlap crash at 40 km/h, and when the test speed was increased to 56 km/h, the right half of the guard completely detached from the trailer.

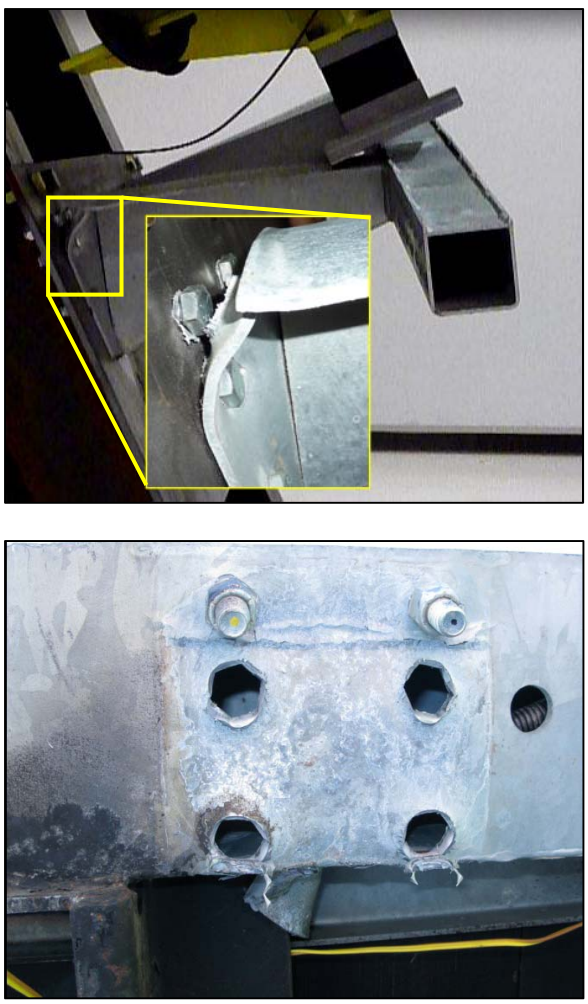

Figure 7. Hyundai underride guard after FMVSS P3 test (left) and Hyundai trailer rear crossmember after crash test, from below (right).

The Wabash guard was the only design that showed no sign of attachment failure in the quasi-static and dynamic conditions. It exceeded the FMVSS 223 and CMVSS 223 P3 force requirements by 187 and 70 percent, respectively. Crucially, its design did not rely on the attachment hardware itself to transfer loads from the guard to the trailer chassis. To encourage such designs, the regulations could be further improved with a stipulation that all attachment hardware must remain intact for the duration of the test or until an even higher force threshold is reached.

To extend protection to the full width of the trailer, the P1 test also needs to be upgraded. The Wabash guard was able to prevent underride in the 50 percent overlap condition, but this almost entirely was due to the vertical support member's interaction with the Malibu's wheel and other outboard structure. When the overlap with the guard was reduced to 30 percent (36 percent overlap with the trailer), the strength of the guard's horizontal member was insufficient to prevent catastrophic underride despite exceeding the FMVSS 223 and CMVSS 223 P1 force requirement by 224 percent. This means that even the strongest guard tested was able to prevent underride only when the Malibu overlapped some portion of the center 49 percent of the trailer's width. Protecting the full width of the trailer from underride does not seem unrealistic because the main longitudinal structures of many semi-trailers are the side rails on the lateral ends of the trailer. Strong vertical support members attached to the side rails would be beneficial in narrow and some wider overlap crashes by allowing the main horizontal portion of the guard to distribute the load across more of the passenger vehicle's structure. Flatbeds and other trailers with their main structures farther inboard may require different design strategies, but this should not preclude extending protection where already possible. Brumbelow and Blanar [5] found that van trailers were the most common type of truck unit involved in fatal rear-end crashes (36 vs. 13 percent for flatbeds).

Even large increases in the FMVSS 223 and CMVSS 223 minimum force levels will not guarantee real-world improvements unless they are accompanied by a requirement that the certification tests be conducted with underride guards attached to the trailer design for which they are intended. Some of the crash tests produced deformation to various portions of the trailer, suggesting the total resistance of the guard-attachment-trailer system was lower than that of the guard alone when tested on a rigid fixture. As shown in the inset of Figure 1, the Hyundai's rear crossmember did not fully overlap the top mounting plate of the guard. A narrow metal tab was welded to the front surface of the crossmember to engage with the portion of the guard that was otherwise unsupported. During the crash test, however, the tabs on both sides were crushed as the guard rotated upward. Certifying such designs on a rigid fixture does not assess the guard's true ability to prevent underride.

NHTSA's compliance test reports show the agency has used a range of fixtures [10]. The standard states the guard should be attached to either "a rigid test fixture" or "a complete trailer," but most guards appear to have been tested on partial sections of the rear of a trailer. Although some of these configurations may be more realistic than the rigid fixture specified in the standard, the sections are fixed at locations that would be free to deform in real-world crashes. Ideally, the regulation would require guards to be certified while attached to complete trailers. At a minimum, they should be attached to sections of the trailer rear that include all the major structural components and that are constrained far enough forward that the load paths near the guard are not changed.

CONCLUSIONS

Tests of semi-trailers equipped with FMVSS 223 compliant underride guards demonstrate that guard failure and severe passenger vehicle underride can result from impact speeds and overlap conditions that passenger vehicles are designed to manage in crashes with stiffer objects. CMVSS 223 requirements are an improvement over US regulations but still are insufficient to produce good performance in offset crashes. Both standards should be upgraded to promote trailer and guard designs that are strong enough across their full widths to remain engaged with the frontal structures of striking passenger vehicles.

ACKNOWLEDGMENT

This work was supported by the Insurance Institute for Highway Safety.

REFERENCES

[1] Brumbelow ML, Zuby DS. 2009. Impact and injury patterns in frontal crashes of vehicles with good ratings for frontal crash protection. *Proceedings of the 21st ESV Conference* (CD-ROM). Washington, DC: National Highway Traffic Safety Administration.

[2] Rudd RW, Bean J, Cuentas C, Kahane CJ, Mynatt M, Wiacek C. 2009. A study of the factors affecting fatalities of air bag and belt-restrained occupants in frontal crashes. *Proceedings of the 21st ESV Conference* (CD-ROM). Washington, DC: National Highway Traffic Safety Administration.

[3] Office of the Federal Register. 1996. Federal Register, vol. 61, no. 16, pp. 2004-2036. NHTSA – Final rule. Docket no. 1-11, Notice 11; 49 CFR Part 571 – FMVSS, Rear Impact Guards, Rear Impact Protection. Washington, DC: National Archives and Records Administration.

[4] National Highway Traffic Safety Administration. 2009. Title 49 Code of Federal Regulations (CFR) Part 571, rear impact protection. Washington, DC: Office of the Federal Register.

[5] Brumbelow ML, Blanar L. 2010. Evaluation of US rear underride guard regulation for large trucks using real-world crashes. *Proceedings of the 54th Stapp Car Crash Conference*, 119-31. Warrendale, PA: Society of Automotive Engineers.

[6] Elias JC, Monk MW. 1993. Heavy truck rear underride protection. Report no. DOT-HS-808-081. Washington, DC: National Highway Traffic Safety Administration.

[7] Canada Gazette Directorate. 2004. Canada Gazette, Part II, vol. 138, no. 20. Motor Vehicle Safety Act; Regulations amending the motor vehicle safety regulations (rear impact guards). Ottawa, Ontario.

[8] Office of Vehicle Safety Compliance. 1997. Laboratory test procedure for FMVSS 223, rear impact guards. Report no. TP-223-00. Washington, DC: National Highway Traffic Safety Administration.

[9] Transport Canada. 2003. Test method 223, rear impact guard. Ottawa, Ontario.

[10] Office of Vehicle Safety Compliance. 2011. OVSC compliance database. http://www.nhtsa.gov/cars/problems/comply/. Washington, DC: National Highway Traffic Safety Administration.

ANALYSIS OF COMPATIBILITY AND OCCUPANT INJURY MECHANISMS IN FRONTAL COLLISIONS INVOLVING BUSES IN SPAIN

Francisco Javier, Páez Ayuso
Arturo, Furones Crespo
Alexandro, Badea Romero
Enrique, Alcalá Fazio
Francisco, Aparicio Izquierdo
University Institute of Automobile Research (INSIA) – Technical University of Madrid (UPM)
Spain
Paper Number 11-0288

ABSTRACT

The European Regulations introduced over the last years on the enhancement of secondary safety of buses and coaches are proving to be efficient, reducing accident seriousness and their consequences, as real accident data can show. However these measures seem to be insufficient, especially in certain impact configurations such as frontal collisions in which not only the driver and the crew are the most prone to casualty but also the rest of the occupants who often suffer severe or fatal injuries.

The aim of the study presented in this paper is to identify the main characteristics of large passenger vehicles (LPVs) frontal collisions that have occurred in Spain over the last years, and to analyse the compatibility of these vehicles with their collision partners or obstacles in frontal impacts.

The study has two main parts: a statistical analysis based on the Spanish Accident Database that includes bus accidents occurred in Spain between 1993 and 2008 investigated by the Police Forces with at least one injured person as consequence of the accident; and an in-depth study using a LPV accident database including highly detailed information, retrospective investigation, reconstruction, police reports and medical records with injury description and mechanisms. A total of 28 real-world accidents were considered, in depth-analysed by the Accident Research Unit of INSIA and investigated in collaboration with the Police Forces, Paramedics and Hospitals.

It is expected that the results obtained in this research will help to gauge the extent of the problem in the Spanish roads and to understand the influence of compatibility on the injury severity of the occupants of both vehicles and their mechanisms.

The statistical analysis revealed that interurban frontal bus accidents represent around 50% of the total Spanish interurban bus accidents with killed or severe injuries. The in-depth analysis based on the injury mechanisms most commonly found suggests that new structural solutions in the frontal design of the bus should be considered to enhance occupant protection and to improve the compatibility between the vehicles involved.

There are not many research works about LPVs frontal collisions up to day, so the potential enhancement of secondary safety is still high. This study is based on Spanish data and its conclusions reflect the situation in the Spanish roads, however it should be extended and considered as guidelines for future research works.

INTRODUCTION

Large passenger vehicles (LPVs) are rarely involved in road accidents compared in proportion to other vehicles. The casualties registered each year in these accidents are quite few; making buses and coaches one of the safest means of mass transportation. In Europe, bus and coach accidents represent less than 1% of all traffic fatalities [1], whilst in the United States an average of 200 occupants are killed in a year from which 40 are occupants of the bus [2]. The ratio of these fatalities by the number of passengers and travelled kilometres is often compared to the one obtained in trains and planes [3]. Nevertheless, the media impact when a bus or coach accident occurs is stunning. The outcomes in terms of injury severity for occupants of both the bus and its collision partners, when involved, suggest that issues like compatibility and occupant protection, in certain accident configurations, still have a large potential of enhancement.

Substantial efforts have been undertaken as regards the rollover protections for occupants of LPVs. In Europe, real accident data are proving the effectiveness of the Regulations enforced over the last years on the enhancement of secondary safety of buses and coaches. However, there is still a potential to reduce furthermore the casualties, especially on compatibility issues when head-on collisions are considered.

Compatibility is a complex issue, and it has been recognised by many research teams during the last decades. Although the issue of compatibility has been highlighted since the 1960s, little systematic research has been performed until recently.

The International Harmonised Research Activity (IHRA) on compatibility was one of the six Working Groups set up following the Melbourne ESV (May 1996), as it was recognised that international co-ordination of research programmes would be beneficial.

The European Union and the European Enhanced Vehicle-safety Committee (EEVC – WG15) were asked to be the lead for compatibility. The first meeting was held on 1997. Its main objective has been to develop a test procedure for car frontal impact compatibility.

However the major research effort has been focused on car compatibility. LPVs compatibility is an issue that needs to be addressed in order to reduce the number of fatalities and injuries among occupants of both the LPV and its collision partner.

The present research study, based on real-world accident data of accidents involving at least one LPV in a frontal collisions with an obstacle or other vehicles, aims to identify specific characteristics of this scenario, which could serve to find new efficient protections measures. This work should lead to improve the LPV frontal compatibility for both the opposite vehicle and self protection.

SOURCES AND METHODS

Statistics from the National Accident Database

A sample of accidents involving LPVs in head-on collisions was extracted from the Spanish Accident Database. This database is compiled by the Road Traffic Directorate (DGT) and includes all road accidents occurred in the Spanish public roads, with at least one injury person as consequence and one motor vehicle involved, all reported by the Police Forces. It contains an average of 93000 accidents per year.

The available information about LPVs does not allow splitting into categories M2 and M3 according to European Directive [4]. So, “LPVs” includes indistinctively both “buses” and “coaches”.

A descriptive statistical analysis of the derived dataset has been performed. Records related to compatibility issues were extracted for this purpose. First the crashworthiness of the collision partner was studied; smaller vehicles with less mass like cars and vans were considered and their behaviour was compared. Then the impact on the LPV was analysed separately, considering for this a wide range of collision partners from cars to heavy goods vehicles (HGVs). Finally the crashworthiness of bus and coaches was contrasted with other large vehicles that have a different frontal geometry and structural behaviour, such as lorries, comparing the consequences for occupants.

Only the consequences for the occupants of the first row were considered for this analysis, for both the LPV and its collision partner.

In-depth analysis of real LPV accidents

The second part of this study uses fully detailed information of real-world LPV accidents to identify the main characteristics of frontal collision involving buses and coaches. Only M3 category vehicles have been analysed during this phase.

The aim was to depict the injury mechanisms and to study the frontal damage of the LPV and the collision partner in head-on impacts.

Representative cases were selected from an in-depth survey of real-world bus and coach accidents (SIRABUS database), which are gathered in a dataset of 28 accidents. These are serious accidents with killed or severely injured occupants as consequence, collected between 1996 and 2009. Detailed information from scene, vehicle and human records is available in the dataset.

The SIRABUS database was commissioned to INSIA by the DGT and includes retrospective investigations, accident reconstructions through computer simulations, police reports and medical records with injury descriptions and mechanisms.

Kinematic parameters were estimated from the in-depth analysis and derived from the simulations, all presented in the next section.

Representative cases that stand out due to their particular characteristics and consequences are summarized in this paper, and their most interesting aspects are contrasted with the patterns found from the statistical analysis.

RESULTS

Statistical research

First part of the research is a statistical analysis of accidents with LPVs involved occurred in Spanish roads. They make a 2% average share of annual road accidents across Spain.

The aim is the analysis of compatibility between LPVs and their collision partners in frontal collisions, and comparatively with the equivalent cases with HGV involved.

The period of analysis covers from 1993 to 2008. Two samples were selected from the Spanish Accidents Database in which the cases that fit the following criteria were included:

- First sample collects accidents with at least one LPV involved, and second sample includes accidents with at least one HGV involved. The rest of the criteria are the same for both samples.
- Only frontal collisions have been selected, and with two vehicles involved in the accident. In case of obstacle crashes, it was not possible to identify the bus impact area.
- Accidents must have occurred in interurban areas.
- The injury severity analysis has been performed only for drivers and front seat occupants (they have been called "front row occupants").

The selection of these two samples is justified by several reasons. First, it has been considered interesting the comparison of compatibility features of two types of heavy vehicles: LPVs and HGVs. Secondly, only interurban accidents have been included, to assess the accidents features at high speed. Thirdly, the injury severity analysis has been performed only for the occupants of the front row of the vehicles due to the accident configuration and its relation with compatibility.

When considering two-vehicle accidents it is possible to identify the opposite vehicle. Three different categories have been considered to evaluate their compatibility when crashed with a heavy vehicle: a) passenger cars; b) light goods vehicles (LGVs), with a gross vehicle weight under 3.5 tones, e.g. vans; c) large vehicles like HGVs or other LPVs.

First, the evolution of the number of accidents of each category in the samples selected is presented (in Figure 1).

There is a greater number of accidents with HGV than with LPVs involved. Also the accidents with cars as collision partners are the most frequent for both HGV and LPVs.

The injury severity distributions shown below are based in the ratio of KSI among the front row occupants by the total number of front row occupants, for each kind of vehicle involved and its collision partner.

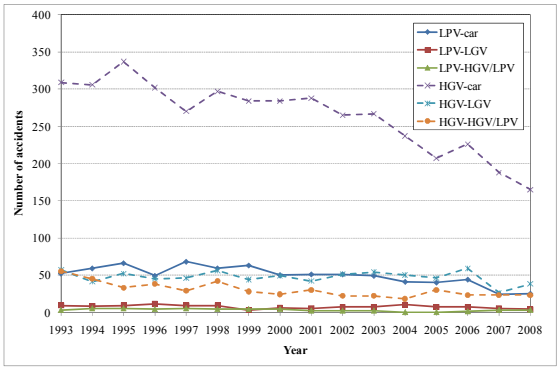

Figure 1. Number of accidents per year.

The following graph (Figure 2) shows the evolution of the ratios for the accidents of the samples selected and in which the collision partner for the LPV or HGV is a car or a LGV.

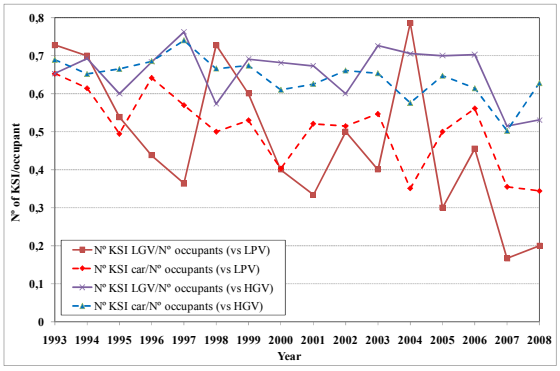

Figure 2. Evolution of the KSI/occupant ratio for cars and LGVs, in frontal collisions with LPVs and HGVs.

Among the front row occupants of cars and LGV in accidents with LPVSs and HGV as collision partners the trends are decreasing along the period of analysis. However the decreasing rate is higher when the opposite vehicle is a LPV whilst when it is a HGV the rate is much lower. The reasons for these facts may be multiple. In the last 10 years, and due to the introduction of the EuroNCAP tests, the car manufacturers have improved greatly the structural behaviour of those vehicles, making them safer in case of frontal collision, and this can explain the downward trends of ratios for passenger cars front row occupants.

Regarding the fact that HGVs are more aggressive than LPVs for the front row occupants of the opposite vehicles, it can be explained by the structural design of the frontal of both kinds of large vehicles. Whilst the frontal underrun

protection in HGV has not been compulsory in Spain until 2003 (and only in new vehicles registered from this year), the low floor design in LPVs has been very common since long time; this design presents resistant structures at a low level of the front of the LPV which prevents from underrun, improving the compatibility of these vehicles.

When comparing the ratios of injury distributions among the front row occupants of cars and LGV (for each category of opposite vehicle, bus and HGV), great differences cannot be found. Though the weight of LGV is greater, passenger cars (as stated previously) have experienced an improvement of their structural design in the last years, increasing their crashworthiness.

Among the front row occupants of LPVs and HGVs (Figure 3), the injury severity ratios are greater when the collision partner is a LGV than when it is a car (LGV are heavier and geometrically different than cars).

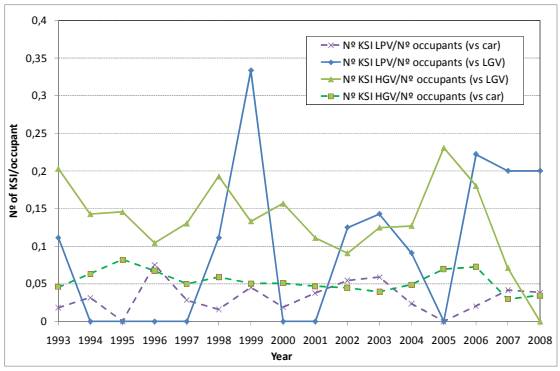

Figure 3. Evolution of the KSI/occupant ratio for LPVs and HGVs, in frontal collisions with cars and other LPVs.

Next (in Figure 4) it is shown the evolution of the ratio selected for front row occupants of LPVs and HGV when having an accident with a LPV or a HGV as collision partner.

The severity levels are lower for LPV front occupants than for HGV front occupants, when having a collision with large vehicles (LPVs or HGVs). It can be explained partly due to the low number of cases of frontal accidents between buses and HGV/buses. But as the figure shows, despite it is thought that the driver position in LPVs is particularly exposed when having a frontal collision (due to the low distance from the driver position to both the front edge of the vehicle and to the floor), in the case of HGV this problem is not still solved.

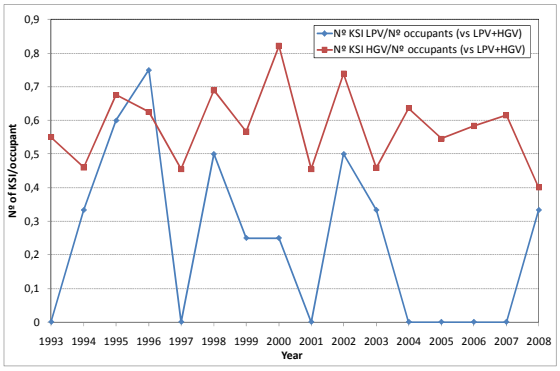

Figure 4. Evolution of the KSI/occupant ratio for LPVs and HGVs, in collisions with HGVs and LPVs.

Overview of frontal collisions included in the in-depth analysis

The revision of all cases included in the SIRABUS database revealed that in 14 out of 28 LPV accidents, one of the most important events of the accident was a frontal impact; this means another vehicle or an obstacle is hit by the frontal of the LPV. The distribution of all the 28 accidents on the Spanish territory is presented in (Figure 5). Frontal accidents are marked distinctively.

As shown on the map, the collected sample covers a wide spread area of the Spanish territory. However, the representativeness of this sample is limited due to the reduced number of cases.

Figure 5. Spread of frontal accidents from SIRABUS.

The vehicle type and the collision partner or struck obstacles for the 14 frontal accidents selected from SIRABUS are listed in (Table 1).

There is only one bus (vehicle designed for urban transport) included in the list, the rest were different sort of coaches (vehicles designed for interurban transport). This is due to the high

seriousness of the selected accidents, according to the sampling criteria of SIRABUS, which come about more often out of urban areas, where the driving speed is higher and more suitable for coaches rather than buses.

Table 1. Vehicle type and collision partner or stroke object

Accident ID	Type of LPV	Collision partner/obstacle	Event order
IN1001	Coach	Car	1st
IN1002	Double Decker coach	Mountain wall	2nd
IN1004	Scholar coach	Lorry	1st
IN1007	Coach	Lorry	1St
IN1008	Coach	Lorry	1st
IN1010	Coach	Articulated lorry	1st
IN1013	Coach	Lorry	1st
IN1014	Scholar Coach	Car	1st
IN1016	Coach	Bridge pillar	2nd
IN1017	Coach	Car	1st
IN1018	Coach	Articulated lorry	1st
IN1019	Coach	Sewer siphon	2nd
IN1024	Coach	Articulated lorry	1st
IN1027	Suburban Bus	Mobile crane	1st

All these cases can be classified in three typical scenarios: S1) Head-on collision with a passenger car; S2) Collision with a HGV (which has a considerable mass and a flat surface); S3) LPV crashes into a rigid obstacle.

For all scenarios, the accident took place in conventional roads or highways. The overlap varies from 5 to 100% of the frontal surface.

Whilst in the third scenario the LPV is the only vehicle involved, in the other two scenarios the number of vehicles involved in the accident varies from 2 (most frequently) to 5.

Vehicle damage and impact kinematics

Scenario 1 The damage suffered by both the LPV and the car is clearly illustrated (in Figure 6). Some parameters of the collision like velocity change (ΔV), overlap and maximum depth of the deformation are also specified for the LPV.

In one accident (IN1001) the coach caught fire after the collision, resulting most of the vehicle burnt; however damages from the direct impact were clearly differentiated.

By regarding the damages of all vehicles it can be noticed that the coach structure resulted almost unharmed compared to the car. Nevertheless, important deformations were produced at the lower frontal.

The frontal of the passenger car was completely crushed, absorbing most of the plastic deformation energy of the impact.

ID	LPV	Car
IN1001	ΔV = 31 km/h Contact overlap: 48% Max. depth: 1 m	
IN1014	ΔV = 11.8 km/h Contact overlap: 10% Max. depth: 1 m	
IN1017	ΔV = 3.27 km/h Contact overlap: 10% Max. depth: 0.1 m	

Figure 6. Vehicle damage. Scenario 1.

Within this scenario, neither ΔV nor overlap seems to affect directly on the deformation of the LPV and its extent. It is rather an issue of mass, geometric and stiffness compatibility, as shown in previous studies [2].

Scenario 2 Eight out of the 28 accidents are included in this scenario. In these frontal collisions against HGVs it was observed that, when directly impacted, the frontal of both vehicles is seriously harmed, and the windscreen is blasted.

Two rear-ends were included in this scenario due to the characteristics of the impact, which from the LPV's point of view were similar to other frontal collisions. In these cases the frontal of the LPV hits the back of a HGV which is a flat and rigid surface and the velocity change is comparable to the rest of head-on collisions of this scenario.

There were intrusions at different heights at the driver and crew positions, affecting especially the

leg room. The maximum depth of the deformations depends not only on the velocity change, but on the contact overlap, as shown (in Figure 7), where 4 representative collisions are presented showing the vehicle damage.

It is noticeable that the deformation energy is divided between both vehicles, but the absorption capacity is clearly limited due to the stiffness of the frontal structures.

ID	LPV	HGV
IN1007	ΔV = 32 km/h Contact overlap: 15% Max. depth: 9 m	
IN1008	ΔV = 31 km/h Contact overlap: 65% Max. depth: 0.9 m	
IN1027	ΔV = 32 km/h Contact overlap: 80% Max. depth: 0.8 m	
IN1024	ΔV = 45 km/h Contact overlap: 100% Max. depth: 1 m	

Figure 7. Vehicle damage. Scenario 2

Comparing the first three out of the four collisions included (in Figure 7), the influence of overlapping on the deformation of the vehicle can be clearly assessed. Thus for similar ΔVs, the deformation of the LPV can vary from almost the entire vehicle length to 0.8m. In the first case (IN1007), the longitudinal frame member absorbs very few impact energy due to the offset with the collision partner at the impact point. In the second (IN1008) one longitudinal frame member is clearly more collapsed than the other, and the maximum longitudinal deformation is 0.9m. In the third case (IN1027), both longitudinals collapse together and the deformation depth is reduced to 0.8m.

The influence of ΔV on the vehicle damage can be observed by comparing the last two cases (IN1027 and IN1024). It can be noticed that in similar conditions and the same overlap, a difference of 13 km/h of the delta velocity can be translated in 20 cm or so of deformation of the entire frontal.

Due to the limited space available, the deformation depth is almost equal to the intrusion, especially for the driver and crew positions.

Scenario 3 The influence of both overlapping and ΔV on the vehicle deformation is also manifested in this scenario. Images from the scene are presented together with the vehicle damage (see Figure 8).

In the first collision (IN1002) a double-decker coach crashes into a mountain wall. The deformation affects the entire frontal, causing intrusions into the driver and crew positions, and into the first seat row of the upper deck. Despite the high collision speed, the deformation energy is absorbed by the entire frontal structure limiting the maximum deformation depth. However the deformations are comparable to the intrusions, due to the lack of space available for deformation.

In the second case (IN1016), a high ΔV combined with small overlap results into a tremendous intrusion on the right half of the coach. The deformation is totally unsymmetrical; the left half was almost unaffected. This particular profile of damage suggests that the structural design of the frontal should be improved in order to enhance the force distribution across the entire frontal and thus the absorption capacity, as has been previously proved in smaller vehicles [5], with beneficial results.

By comparing the collision described above with the last collision (IN1019), the influence of ΔV when impacting a rigid object can be assessed. The overlapping is similar in both cases, but in the last case, the coach impacts the sewer siphon at a much lower speed. The vehicle had a previous rollover,

sliding along the ditch on its right side, and loosing momentum.

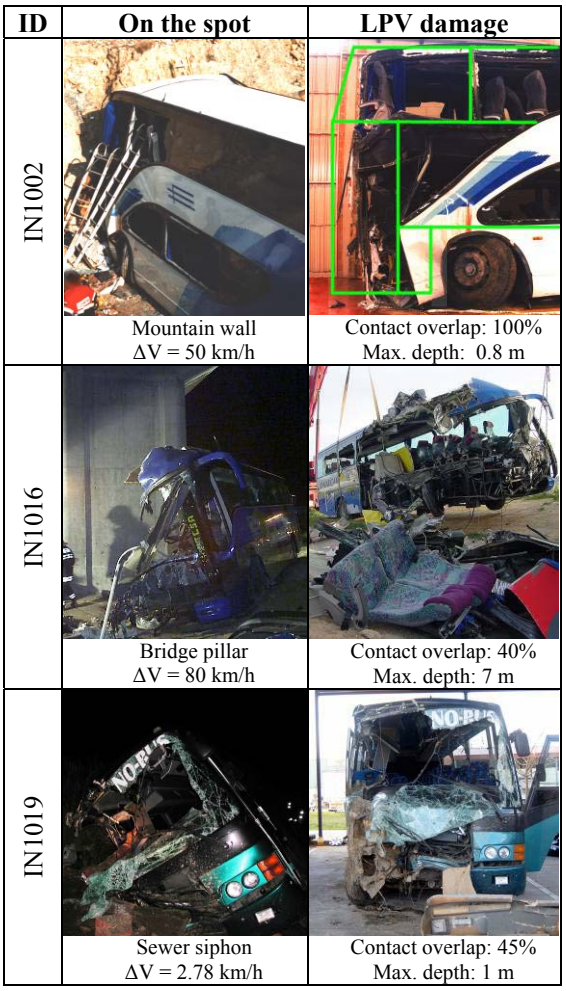

Figure 8. Vehicle damage. Scenario 3

Although the high collision velocity, when the entire frontal structure absorbs the deformation energy (IN1002), the depth results similar to the one obtained at a lower speed and smaller overlap (IN1019).

Injury mechanisms

A brief revision of the injury severity is summarised in Table 2. This shows the occupancy of the LPV at the moment of the accident, the resulted injury severity and, separately, the injury severity of the driver.

The distributions show that 20% of the occupants were killed in the accident, 26% were severely injured, 46% were slightly injured and only 8% of the occupants were unharmed. Within the drivers, the resulted distribution is: 28% were killed, 50% were severely injured, 14% slightly injured and only 7% unharmed.

Table 2. Injury outputs

Accident ID	Nr. of Occupants	Fatalities	Severely injured	Slight injured	Driver Severity
IN1001	58	31	5	15	Fatal
IN1002	48	11	31	4	Severe
IN1004	46	7	14	25	Severe
IN1007	38	27	5	6	Fatal
IN1008	30	0	1	27	Severe
IN1010	18	1	5	8	Severe
IN1013	23	1	5	15	Severe
IN1014	15	0	0	7	Slight
IN1016	43	6	18	17	Severe
IN1017	46	1	15	30	Slight
IN1018	32	0	4	24	Severe
IN1019	12	2	5	4	Uninjured
IN1024	5	1	2	2	Fatal
IN1027	28	3	3	22	Fatal
Total	442	91	115	206	

The drivers suffered the most severe injuries followed by the second row occupants.

A classification of the occupants by the injury mechanism cause of the most severe injuries has been done (see Table 3); the rate from the total number of occupants of the vehicle is included in round brackets. Projection was the most common for all occupants; intrusion for the first and second row; some partial and complete ejections were also registered, but these were caused by a previous or subsequent rollover, when the case. Some occupants were also entrapped between seats and some few died by asphyxia.

In projected passengers impacted against the backrest of the front seat or bulkhead and the most common injuries were contusions and fractures affecting the face, head, chest, abdomen and both upper and lower limbs. Intrusions provoke lacerations and fractures.

Table 3. Injury mechanisms

Accident ID	Intrusion	Projection	Ejection	Driver Mechanism
IN1001	Unknown	Unknown	Unknown	Unknown
IN1002	4 (8.3%)	30 (62.5%)	0	Intrusion
IN1004	10 (21.7%)	16 (34.7%)	Unknown	Intrusion
IN1007	14 (36.8%)	18 (47.6%)	6 (15.7%)	Intrusion
IN1008	1 (3.3%)	27 (90.0%)	0	Intrusion
IN1010	2 (11.1%)	11 (61.1%)	1 (5.5%)	Intrusion
IN1013	1 (43.4%)	19 (82.6%)	1 (43.4%)	Intrusion
IN1014	0	7 (46.6%)	0	Projection
IN1016	20 (46.5%)	21 (48.8%)	0	Projection
IN1017	Unknown	Unknown	Unknown	Unknown
IN1018	1 (3.1%)	28 (8.7%)	0	Intrusion
IN1019	0	11 (91.6%)	0	–
IN1024	1 (20.0%)	4 (80.0%)	0	Intrusion
IN1027	1 (3.5%)	20 (71.4%)	0	Intrusion

DISCUSSION

The representativeness of the data included in this study and thus the results and conclusions are

limited due the available information for the statistical analysis, and the number of cases for the in-depth analysis respectively. However, the complementary results of both methodologies may represent the situation on the Spanish roads, but can not be directly extrapolated.

Although serious accidents involving LPVs occur rarely, making this a safe means of transportation, this study shows that compatibility is still an issue that must be further improved. The connectivity across the frontal should be enhanced so both longitudinal frame member will deform in the event of a frontal collision despite the offset of longitudinal axis of both vehicles.

It was concluded that the space available for the vehicle deformation is almost inexistent; this may generate intrusions in the vehicle making their occupants prone to injury, especially in the front seats.

New solutions should be adopted to improve the frontal of buses and coaches, considering the shortcomings on the structural behaviour presented in this paper. In this sense, the solution described by Steinmetz [6] should be highlighted. Other solutions – [7] and [8] – regarding the absorption capacity of large vehicles should be also considered.

CONCLUSIONS

Accidents involving LPVS do not happen very often in the Spanish roads in comparison to other vehicles. However, the media impact generated around them motivates the interest of having a clear picture of the issue.

The statistical analysis performed in this study reveals that in Spain, interurban accidents are the most serious, and among this group, frontal collisions represent a half of the cases. Nevertheless it was found that the rates of killed and severely injured per occupant within this accidents are not especially high compared to other large vehicles. The crashworthiness of the LPV depends on the collision partner, and especially on its size and mass.

The in-depth analysis revealed that on head-on collisions with passenger cars, the absorption capacity of the LPV is very low, so the car absorbs most of the deformation energy.

In collisions in which the LPV frontal hits a rigid obstacle or another large vehicle, the deformations and the intrusions suffered by the vehicle depend directly on both overlapping and velocity change.

The findings suggest that the frontal design of buses and coaches could be improved to enhance the connectivity across the frontal and thus the occupant protection.

ACKNOWLEDEGEMENTS

The SIRABUS database was performed by INSIA on the behalf of the Spanish Road Traffic Directorate (DGT). This research was partially supported by the Madrid Regional Ministry of Education and the European Social Fund (ESF) through the Research Personnel Support Program of Madrid Autonomous Community.

REFERENCES

[1] Niewöhner, W., Berg, F.A. and Vorgerd, D. (2004). Accident Overview and a Selection of Scenarios. *Proc. 4th DEKRA/VDI Symposium Safety of Commercial Vehicles.* Neumünster.

[2] Olivares, G., Yadav, V. (2007). Mass transit bus-vehicle compatibility evaluations during frontal and rear collisions. *Proc. 20th Int. Technical Conf. Enhanced Safety of Vehicles*. Lyon.

[3] Australian Transport Safety Bureau. (2005). *Cross Modal Safety Comparisons: Discussion Paper* [online]. Available at: http://www.atsb.gov.au/media/36229/cross_modal_safety_comparisons.pdf. [accessed at 21th September 2010].

[4] Commission of the European Communities (2001). *Commission Directive 2001/116/EC on the Approximation of the Laws of the Member States Relating to the Type-approval of Motor Vehicles and their Trailers. Annex II – Definition of Vehicle Categories and Vehicle Types.* Brussels.

[5] Zobel, R., Schwartz, T. and Thomas, G. (2005). Towards a Beneficial, Scientifically Meaningful, and Applicable Compatibility-Testing. *Proc. 19th Int. Technical Conf. Enhanced Safety of Vehicles*. Washington DC.

[6] Steinmetz, G. (2010). A New Front Structure for Coaches to Improve their Crashworthiness. *Proc. FISITA 2008 World Automotive Congress*. Budapest.

[7] Forsberg, J. and Nilsson, L. (2008). The Optimisation Process of an Energy Absorbing Frontal Underrun Protection Device. *International Journal of Vehicle Design* **46, 3,** 271 – 379.

[8] TRL and TNO. (2007). Improvement of Vehicle Crash Compatibility through the Development of Crash Test Procedures. VC-COMPAT project Report [online]. Available at: http://ec.europa.eu/transport/roadsafety_library/publications/vc-compat_final_report.pdf. [accessed at 21th September 2010].